Low-energy effective models for two-flavor quantum chromodynamics and the universality hypothesis

Dissertation

zur Erlangung des Doktorgrades

der Naturwissenschaften

vorgelegt beim Fachbereich Physik

der Johann Wolfgang Goethe-Universität

in Frankfurt am Main

von

Mara Grahl

aus Frankfurt am Main

Frankfurt (Januar 2014)

(D 30)

vom Fachbereich Physik der

Johann Wolfgang Goethe-Universität als Dissertation angenommen.

Dekan: Prof. Dr. Joachim Stroth
1. Gutachter: Prof. Dr. Dirk-Hermann Rischke
2. Gutachter: Prof. Dr. Bengt Friman

Datum der Disputation: voraussichtlich 12.03.2014

Eidesstattliche Versicherung

Ich erkläre hiermit an Eides Statt, dass ich die vorliegende Dissertation selbständig angefertigt und mich anderer Hilfsmittel als der in ihr angegebenen nicht bedient habe, insbesondere, dass alle Entlehnungen aus anderen Schriften mit Angabe der betreffenden Schrift gekennzeichnet sind. Auf Textpassagen und Abbildungen, die aus eigenen Publikationen [1, 2] stammen, wird lediglich zu Beginn des entsprechenden Abschnitts entsprechend hingewiesen.
Ich versichere, nicht die Hilfe einer kommerziellen Promotionsvermittlung in Anspruch genommen zu haben.
Frankfurt a.M., den 14.01.2014

Contents

Notation

We use natural units where $\hbar = c = k_B = 1$.
D denotes the spatial dimension.
Finite groups are denoted in Schoenflies notation.

Alles Gescheite ist schon gedacht worden, man muß nur versuchen, es noch einmal zu denken.
(Johann Wolfgang von Goethe)

Chapter 1

Introduction

Exploring nature at more and more extreme distance scales, both microscopic and macroscopic, has always triggered groundbreaking scientific insights and innovations. This path has lead to our current understanding that nucleons (protons and neutrons) are composed of quarks kept together due to the strong interaction which is mediated by gluons. With the advent of the quark model developed by Gell-Mann, quantum chromodynamics (QCD) soon became successful in describing many features of the strong interactions observed in experiment. Using the words of Goethe, with the modern high-energy collider experiments physicists all around the world try to improve our understanding of whatever holds the world together in its inmost folds. At the Large Hadron Collider (LHC) in Geneva, for example, protons are accelerated and collided with each other such that energy densities occur which have never been measured before. Whereas the highest reachable collision energy of 14 TeV merely corresponds to the energy released when clapping ones hands [3], the energy densities reached are incredibly high when compared to those encountered in every-day life. Due to the high energy density, the temperature, T, and the baryonic chemical potential, μ_B, reach values as in the early stages of the universe. There is theoretical as well as experimental evidence that hadronic matter undergoes a transition to an exotic state of matter, called quark-gluon plasma, when increasing T and/or μ_B. This transition is accompanied by a so-called chiral transition. It is an important question whether this chiral transition involves latent heat or not, i.e., whether it is of first order or continuous. Many results indicate the chiral transition to be crossover (i.e., not a real phase transition) for vanishing chemical potential and of first order for vanishing temperature. It is, however, still under debate whether this is true. If so, it is natural to assume that there exists a critical endpoint, $(T_c \neq 0, \mu_B \neq 0)$, where the chiral transition is of second order, which can be regarded as the border case between first order and crossover. Indeed, a critical endpoint exists in several theoretical approaches describing the chiral phase transition, the predictive power of which are lively discussed. A main goal of the future CBM experiment [4] at GSI in Darmstadt is to shed light on the existence of the critical endpoint.
Near the QCD (phase) transition, the strongly coupled nature of QCD together with the absence of any small expansion parameter is what makes analytical calculations from first principle almost impossible. The same is true for realistic effective models for QCD, which share this difficulty. Hence the investigation of the QCD phase diagram indispensably depends on nonperturbative

methods. The most popular among such are lattice calculations, resummation theory, the Dyson-Schwinger formalism, and the functional renormalization group (FRG). All of these approaches are used complementary, and are sometimes even combined. One of the strengths of the FRG method is that it can be successfully applied not only to effective models, but also to QCD itself (see Sec. 4.4). In order to guide these first-principle calculations, however, results from effective models for QCD are very helpful.

Our thesis is centered around the question of which order the chiral phase transition of two-flavor QCD is. Clarifying the conditions for the possible existence of a second-order transition, determining the universality class to which it belongs, etc., are tasks which require knowledge and techniques from several areas. First of all, in chapter 2 we want to outline several general aspects of phase transitions which are of central importance for the understanding of the RG approach towards them. Our focus lies on reviewing the universality hypothesis, a crucial ingredient when it comes to the construction of effective theories for order parameters, the credibility of which often heavily depends on universality arguments. We finish the chapter with an attempt to formulate the latter more precisely than usually done. Chapter 3 discusses the chiral phase transition from a general point of view. We supplement well-known facts with a detailed discussion of the so-called $O(4)$ conjecture. In chapter 4 we introduce the nonperturbative method we use, the FRG method. Furthermore, we discuss the relation between effective models for QCD and the underlying fundamental theory making use of the FRG perspective. Chapter 5 is concerned with a mathematical subject indispensable for our approach towards the study of phase transitions, namely the systematic construction of polynomial invariants characterizing a given symmetry. We want to emphasize that this topic is of very general interest in any field of research where symmetry considerations play a role. With this thesis we point out its relevance in the context of high-energy physics and hope to reinforce the interest in systematic methods for the derivation of invariants associated with continuous symmetry groups. We present a simple, but novel, brute-force algorithm to effectively construct invariants of a given polynomial order. Chapter 6 is devoted to RG studies of several dimensionally reduced theories which are capable to either predict or to rule out the possible existence of a second-order phase transition. Of main interest for us is the linear sigma model, particularly in presence of the axial anomaly. It turns out that the fixed-point structure of the latter is rather complicated, requiring a deeper understanding of the underlying method and its preconditions. This leads us to a careful analysis of the fixed-point structure of several models, which is of great benefit for our review of the universality hypothesis and has several spin-off effects. For example, in the course of studying the influence of vector and axial-vector mesons we encounter a new universality class, which might be more relevant in other areas where chirality plays a role. Some important questions, however, cannot be addressed in the framework of dimensionally reduced theories where the explicit dependence of temperature has been eliminated. We are therefore pushed towards FRG studies where the temperature is kept as an explicit variable. We note that a great part of our work consisted in finding our own implementations of suitable algorithms to solve the encountered partial differential equations numerically. Our routines (which entirely use well-known methods) are provided in an appendix. Our main goal, the application to effective models for QCD, is discussed in chapter 7. In chapter 8 we state our conclusions and give an outlook. The appendices A–D provide several routines utilized in this work and contain other material to which we refer in the main chapters.

Chapter 2

Phase transitions and the renormalization group

2.1 Basic aspects

A *phase transition* is defined as a thermodynamic process in which a system changes from one *phase* to another at a transition point where a thermodynamic potential is non-analytic. Often one considers either the grand-canonical potential, Ω, or the Helmholtz free energy, F, whose definitions in terms of the grand-canonical partition function, $\mathcal{Z}$, and the partition function, Z, respectively, are given by

$$\Omega = -T \ln \mathcal{Z} \ , \tag{2.1}$$

$$F = -T \ln Z \ . \tag{2.2}$$

Both quantities are related by

$$F = \Omega + \sum_i \mu_i Q_i \ , \tag{2.3}$$

where the μ_i denote the chemical potentials associated with the conserved net-charges Q_i.
According to the modern classification, one defines the order of a phase transition using the notion of *latent heat* which is the amount of heat a system absorbes or releases, respectively, without changing its temperature. A *first-order* phase transition involves latent heat whereas a *continuous* phase transition does not. Continuous phase transitions are of *second order* if there exist discontinuities in second derivatives of the free energy with respect to certain thermodynamic variables, and of *infinite order* if not. Right at a first-order phase transition one observes the coexistence of clusters of both phases. At a second-order phase transition there are clusters of any size giving rise to self-similarity on all length scales. This is equivalent to a diverging *correlation length* (which can be defined as the largest size of the clusters) which is the deeper reason for the existence of universal power laws (see Sec. 2.2). The divergence in the correlation length is caused by long-range fluctuations of a so-called *soft mode*. The nature of this mode can be quite different and depends on the physical context. For example it can be a phonon

of vanishing frequency at the transition point, or it can be a particle becoming massless. Very often, but not necessarily, the different phases are associated with different symmetries and the corresponding phase transition is accompanied by symmetry breaking (SB). A symmetry can be explicitly broken when changing from one phase to the other, or the phase transition can go along with a *spontaneous breaking* of a symmetry (which can be either continuous or discrete). One speaks of spontaneous symmetry breaking (SSB) if a system as a whole (for example the Lagrangian for this system) is symmetric under a certain symmetry transformation, whereas there exists an *order parameter* which is not invariant under the full symmetry group in the so-called spontaneously broken phase[1]. In a first-order phase transition, the order parameter changes discontinuously from a nonzero value in the spontaneously broken phase to zero in the restored phase, when a certain variable (for example temperature) is varied. In a second-order phase transition the change is continuous. Plotting two thermodynamic variables of state against each other one obtains a phase diagram. Points where the phase transition is of second-order (*critical points*) are associated to SB with one exception: a line of first-order phase transitions not associated to any symmetry can end in a so-called *critical endpoint* which is not associated to SB [2]. This is a major difference in comparison with infinite-order phase transitions which are never accompanied by SB. Since critical points are associated with SB, explicit breaking of symmetry usually turns the transition into a *crossover*. In a crossover transition (which is not a true phase transition) the order parameter continuously approaches, but never reaches zero. For first-order phase transitions accompanied by SB, there remains a discontinuous jump in the order parameter also in case of (small) explicit breaking of symmetry. Redefining the order parameter ϕ by subtracting its value at the transition point, $\phi \to \phi - \phi_c$, one still has a well-defined order parameter and a first-order phase transition.

The partition function can be always expressed as a path integral over field variables which undergo thermal and quantum fluctuations [5]. Models which are defined on a lattice can be usually translated into field theories in the limit of a large number of lattice points (for the Ising model see Ref. [6]). In case of QCD, at the microscopical level the fields consist of the quark fields, Ψ and $\bar{\Psi}$, the ghost fields, c and $\bar{c}$, and the gauge fields, A. Commonly one tries to translate the formulation in terms of entirely microscopic degrees of freedom into one involving the order parameter which is usually of composite nature arising dynamically from the interaction between the microscopical constituents. In general the order parameter is a scalar quantity constructed from the components Φ_i of a so-called order-parameter field Φ. For example, in case of the $O(4)$ symmetric linear sigma model for the chiral phase transition, the order-parameter field has four real-valued components, $\Phi \equiv (\sigma, \pi_1, \pi_2, \pi_3)$. The order parameter, however, is given by the vacuum expectation value of the sigma field, $\langle\sigma\rangle$, that is the value of the field at the global minimum of the potential describing the system. As an analytic treatment of the path integral is

[1] We note that the massless Goldstone modes arising in the spontaneously broken phase if the symmetry is a continuous one are not be confused with a soft mode, which is only massless right at the transition point.

[2] The conjectured critical endpoint of QCD is an example (see also Sec. I.2.2.4.5. in Ref. [4]). Chiral symmetry is explicitly broken due to nonvanishing quark masses. One can argue that only right at the critical endpoint a $Z(2)$ symmetry is effectively realized. This gives rise to Ising universality with $Z(2)$-noninvariant scaling corrections (see Sec. 3.3.1) but there do not exist two phases of distinct symmetry. More generally, a d-dimensional hypersurface of first-order phase transitions can be bordered by a $d-1$ dimensional *critical boundary*. Fig. 3.2 contains examples for such critical boundaries.

only possible in exceptional cases, one depends on approximations and simplifying assumptions. Using such simplifications, in Sec. 4.4 we sketch a systematical derivation of an effective theory for the order parameter of the chiral phase transition starting from QCD itself. In this derivation order-parameter degrees of freedom (mesonic fields) are introduced using the technique of bosonization. Fermions can be effectively integrated out giving rise to a fermion determinant. Instead of deriving the effective mesonic potential by explicitly calculating this determinant, we use chiral symmetry to make an expansion in terms of group-theoretic invariants.

In case of phase transitions accompanied by spontaneous symmetry breaking, an expansion of the free energy in terms of group-theoretic invariants constructed from the order parameter components is a natural thing to do. Landau's approach towards second-order phase transitions is based on such an expansion. Also the renormalization group approach still relies on a truncation of the free energy and Landau's expansion in terms of invariants is still the best choice when treating second-order transitions. Accordingly one often speaks of a Landau-Wilson (or Landau-Ginzburg-Wilson) ansatz. Although originally intended for second-order phase transitions, it is also quite successfully applied to first-order phase transitions where a group-subgroup relation exists between the phases [7]. Whereas in the former case the free energy can be truncated at fourth order in the order parameter, in the latter case it is necessary to go to sixth order. Landau theory is a *mean-field theory*, i.e., the order parameter is replaced by its average value and fluctuations about this mean-field value are not taken into account. From the path-integral perspective it constitutes a *saddle-point approximation*, where the partition function is approximated by the integrand at a constant value for the order-parameter field minimizing the free energy [6]. A consequent improvement of the mean-field approximation is the so-called *Gaussian approximation* where quadratic fluctuations are taken into account. This approximation is possible because Gaussian integrals are analytically solvable. Further improvement can be achieved by taking account of higher-order fluctuations in a perturbative expansion. The basic idea underlying the renormalization group (RG) approach towards phase transitions is nonperturbative and consists of separating fluctuations into fast and slow modes in momentum space and absorbing the effect of fast modes successively into the parameters of an ansatz for the free energy. One can write down an explicit differential equation for the free energy, which is exact and implements this idea. Earliest examples for such so-called *exact renormalization group* (ERG) equations are those of Wegner and Houghton [8] and Wilson and Kogut [9]. Expanding the free energy in powers of the field, these equations lead to an infinite tower of coupled differential equations for the expansion parameters, which are difficult to handle. Later, other, equivalent exact renormalization group equations, namely those of Wetterich [10] and Morris [11], turned out to be more practical and are referred to as *functional renormalization group* (FRG) equations. The latter can be successfully applied to describe second-order as well as first-order phase transitions. In the early days however, the renormalization group method gained its popularity in the field of phase transitions from the celebrated ϵ-expansion of Wilson and Fisher [12]. Their approach combined the renormalization group idea with both, a perturbative expansion, and an expansion in $\epsilon \equiv 4 - D$, where D is the spatial dimension of the system under consideration. The ϵ-expansion is designed to describe critical phenomena characteristic of second-order phase transitions and is a practical tool to calculate critical exponents. Large parts of our understanding about critical behavior and universality were facilitated by investigating different models in the ϵ-expansion and comparing

the results to experiments. We will discuss aspects of critical phenomena, critical exponents, universality, and the ϵ-expansion in the following sections.

2.2 Universality - an experimental fact

Close to the critical point of a second-order phase transition certain thermodynamic quantities show a power-law behavior involving critical exponents. For example, near the critical temperature T_c of a transition, the order parameter vanishes according to the power law

$$\phi \propto |T - T_c|^{\beta} \ . \tag{2.4}$$

Another example is the correlation length, ξ, which diverges as

$$\xi \propto |T - T_c|^{-\nu} \ . \tag{2.5}$$

The explicit definition of the order parameter depends on the specific system under consideration, and the same is true for the other thermodynamic quantities showing a power-law behavior. Usually one can define the specific heat, C, and the corresponding critical exponent, α, according to

$$C \sim \frac{\partial^2 F}{\partial T^2} \propto |T - T_c|^{-\alpha} \ , \tag{2.6}$$

and the susceptibility, χ_h, for a certain external field, h, according to

$$\chi_h \sim \frac{\partial \phi}{\partial h} \propto |T - T_c|^{-\gamma} \ . \tag{2.7}$$

Further one can define a power law for the two-point correlation

$$\langle \phi(\vec{r}) \phi(\vec{r}\,') \rangle \propto |\vec{r} - \vec{r}\,'|^{2-D-\eta} \ , \tag{2.8}$$

where $\phi(\vec{r})$ is the local value of the order parameter, the brackets denote the vacuum expectation value, D is the spatial dimension, and η is called *anomalous dimension*. For a comparison between liquid-gas systems, magnets, and QCD we refer to Ref. [13]. We also recommend chapter I.2 of Ref. [4].
Critical behavior can be universal in the sense that different systems can share the same values for the critical exponents. Such systems are said to belong to the same *static universality class*. It is a fascinating observation that systems which are very different at the microscopical level can fall into the same universality class. A lot of examples can be found in the modern review of Pelissetto and Vicari [14]. Furthermore, universal scaling relations exist between the critical exponents:

$$\alpha = 2 - \nu D \ , \quad \beta = \frac{\nu}{2} \left(D - 2 + \eta \right) \ , \quad \gamma = \nu \left(2 - \eta \right) \ . \tag{2.9}$$

We note that in order to observe the nontrivial critical exponents characteristic of a certain universality class one has to be sufficiently close to the critical point, namely in the so-called *critical region*. Outside of this region, but still close to the critical point, one finds mean-field critical exponents irrespective of the universality class to which the model belongs. The size of

the critical region is not universal but depends on the microscopical details of the model [15], i.e., in the framework of the RG, which will be discussed in the next section, it depends on the values for the couplings involved in the potential defining the model at the microscopical cutoff scale (UV scale).
So far we discussed *static* universality classes, which refer to systems which are in local thermal equilibrium. This means that if we tune the system from temperature T_1 to temperature T_2 in a time interval Δt, the equilibration time, τ, has to be small compared to Δt. In contrast, *dynamic universality classes* refer to the behavior of systems out of equilibrium. One usually distinguishes these classes with respect to the dynamic critical exponent z involved in the universal power law

$$\tau \sim \xi^z \sim (T - T_c)^{-\nu z} \ . \tag{2.10}$$

Different models belonging to the same static universality class can give rise to different dynamic critical exponents z, i.e., usually static universality classes split into several dynamic universality classes. This is due to the fact that the dynamical behavior depends on the equation of motion and certain conserved densities in addition to the order parameter (which can be a conserved density itself). For more details we refer to the seminal work of Hohenberg and Halperin [16], which provides a classification of the most important (but clearly not of all possible) dynamic universality classes.

2.3 Explaining universality using the RG

Finding a more macroscopic description for a system initially defined at some microscopic scale is a very general problem in physics. In such an effective model, the detailed structure is averaged out, retaining only the desired relevant information. Renormalization group equations exactly serve this purpose. The general idea behind the renormalization group approach towards phase transitions was already discussed in Sec. 2.1. We now proceed with this discussion, focusing on universality encountered for second-order phase transitions.
The partition function written as a path integral over order-parameter component fields Φ_i reads

$$Z = \prod_i \int \mathcal{D}\Phi_i e^{-S[\Phi;\vec{\lambda}]} \ , \tag{2.11}$$

where S denotes the Euclidean action which involves the couplings λ_i mediating the interactions between the field components. Denoting temperature by T and spatial dimension by D, S is given by

$$S = \int_0^{1/T} d\tau \int d^D\vec{x}\mathcal{L} \ , \tag{2.12}$$

where the Euclidean Lagrangian is the sum of a kinetic term K and a potential U,

$$\mathcal{L} = K + U. \tag{2.13}$$

In momentum space the action S is a functional of the Fourier components $\Phi(\omega_n, \vec{p})$ and involves sums over Matsubara frequencies, ω_n, and integrations over the momenta, $\vec{p}$. It is physically meaningful to impose a high momentum (ultraviolet) cutoff Λ on the momentum integrations,

that is, only fluctuations $\Phi(|\vec{p}| < \Lambda)$ are taken into account.
In order to investigate second-order phase transitions near the critical point it it sufficient to study the so-called *dimensionally reduced* theory, at least if fermions are absent. Dimensional reduction is a mechanism first proposed by Appelquist and Pisarski [17] and is based on the idea that the nonzero bosonic Matsubara modes, $\omega_{n\neq 0} = 2n\pi T$, act like heavy masses for large T, leading to a decoupling of these modes in analogy to the Appelquist-Carazzone theorem [18]. The generalization to fermions is not obvious because the smallest fermionic Matsubara modes are given by $\pm\pi T \neq 0$. Whereas in general dimensional reduction only sets in at sufficiently high temperature, near the critical point of a second-order phase transition it takes place due to the diverging correlation length [19]. In order to investigate critical phenomena it is therefore justified to consider the dimensionally reduced theory, neglecting the τ-dependence of the fields:

$$S = \frac{1}{T}\int d^D\vec{x}\mathcal{L} \ . \tag{2.14}$$

The averaging process mentioned above can be implemented iteratively by integrating out momentum modes and absorbing their effect into the couplings λ_i (for details we refer to Ref. [6]). In each iteration step, the functional integral over modes $\Phi(\Lambda/b < |\vec{p}| < \Lambda)$, where $b > 1$, can be performed using perturbation theory. The result can be absorbed into a redefinition of the couplings if momentum is rescaled by

$$\vec{p}^{\ '} = b\vec{p} \ , \tag{2.15}$$

and the field components by an appropriate factor, $\Phi'(\vec{p}') = f(b)\Phi(b\vec{p})$. This procedure results in recursion relations for the couplings, which, for b infinitesimally close to 1, turn into differential flow equations,

$$k\frac{\partial}{\partial k}\lambda_i = F_i(\Lambda, \vec{\lambda}) \ , \tag{2.16}$$

where the momentum scale k separates modes which already have been taken into account, $\Phi(|\vec{p}| > k)$, and modes which remain to be integrated out. The explicit dependence on the cutoff Λ on the r.h.s. of Eq. (2.16) can be eliminated by introducing dimensionless couplings, $\bar{\lambda}_i$, by multiplying the couplings λ_i by appropriate powers of Λ,

$$\bar{\lambda}_i = \lambda_i\Lambda^{-[\lambda_i]} \ , \tag{2.17}$$

where $[\lambda_i]$ denotes the dimension of λ_i. Eq. (2.16) with Eq. (2.17) yields the flow equations for the dimensionless couplings,

$$k\frac{\partial}{\partial k}\bar{\lambda}_i = F_i(\vec{\bar{\lambda}}) \ . \tag{2.18}$$

The flow equations (2.18) can be used to determine if a second-order phase transition exists for the model defined by the action (2.12). This is due to the fact that the correlation length (2.5) diverges at the critical point of a second-order phase transition. Since Eq. (2.15) implies that every quantity of dimension length is rescaled by the factor b^{-1} in a RG step, this implies for the correlation length

$$\xi' = \xi/b \ . \tag{2.19}$$

At a fixed point of the flow equations (2.18),

$$k\frac{\partial}{\partial k}\bar{\lambda}_i^* = 0 \ , \tag{2.20}$$

this implies for the fixed-point value of the correlation length:

$$\xi^* = \xi^*/b \ , \tag{2.21}$$

which can be only satisfied for either $\xi^* = 0$ or $\xi^* = \infty$. Indeed it turns out that critical exponents can be calculated from the RG flow close to fixed points, and that the stability properties of the fixed points determine if a second-order phase transition can be associated with one of them. Another argument which explains the correspondence between the existence of a second-order phase transition and an infrared fixed point is the following. Every point in coupling space corresponds to a certain bare action $\bar{S}_{k=1}[\bar{\Phi}, \bar{\lambda}_{k=1}]$. Whereas in Landau theory no fluctuations are taken into account, this is the case in the RG approach. Integrating out fluctuations, one obtains an effective action, $\bar{S}_k[\bar{\Phi}, \bar{\lambda}_k]$, describing the system where fluctuations with momenta $p > k$ have been taken into account. An infrared fixed point is special in the following sense: starting in the UV with the fixed-point action, the effective action remains equal to the fixed-point action under the RG flow, i.e., irrespective of the fluctuations which are taken into account or not. This is exactly the physical picture of scale invariance which is characteristic for second-order phase transitions. No matter at which resolution scale one looks at the system (i.e., which momentum fluctuations one is able to resolve), one always sees qualitatively the same picture. The question whether a system can be practically tuned to the critical point by varying a certain number of physical parameters (such as for instance the reduced temperature $(T - T_c)/T_c$, which is an example for a so-called relevant scaling variable introduced later) can be answered by a stability analysis of the fixed point. In the following we summarize the important facts concerning such investigations. In App. E we provide several graphs illustrating the abstract discussion. These examples show the RG flow in the vicinity of two fixed points calculated in Sec. 6.6.

It is a reasonable assumption that the potential U in expression (2.13) is a functional of the order-parameter field and its derivatives, $U = U[\Phi, \partial_\mu\Phi\partial_\mu\Phi, \dots]$. Note that we work in Euclidean space, where $\partial_0 = \partial/\partial\tau$. Usually one further assumes that Φ is independent of τ, i.e., $U = U[\Phi, \partial_i\Phi\partial_i\Phi, \dots]$. In general, an expansion of the potential U in terms of order-parameter components reads

$$U_{\mathrm{LP}} = \sum_i c_i^{(1)}\Phi_i + \sum_{i,j} c_{i,j}^{(2)}\Phi_i\Phi_j + (...) \ , \tag{2.22}$$

where the coefficients as well the order-parameter components are real-valued variables. The local-potential approximation (2.22) neglects terms involving derivatives. Derivatives are only present in the kinetic term, which is usually of the form

$$K = \frac{1}{2}\sum_i \partial_\mu\Phi_i\partial^\mu\Phi_i \ . \tag{2.23}$$

All statements in this thesis are made under the assumption that the kinetic term is of this form. The more refined derivative expansion (compare with Eq. (4.7)) keeps such terms,

$$U_{\mathrm{D}} = U_{\mathrm{LP}} + \sum_{i,j} d_{i,j}^{(2)}(\Phi)\partial_\mu\Phi_i\partial^\mu\Phi_j + (...) \ . \tag{2.24}$$

In momentum space the derivatives translate into four-momenta,

$$\partial_\mu \Phi_i \partial^\mu \Phi_j \to (\omega^2 + \vec{q}^{\,2}) \Phi_i \Phi_j \ , \tag{2.25}$$

so that it becomes obvious that the local-potential approximation becomes problematic if high-momentum fluctuations dominate the system. As in Landau theory, an expansion of U in terms of group-theoretic invariants constructed from the order-parameter components is a natural truncation. In local-potential approximation this expansion has the general form

$$U = \sum_i \lambda_i^{(1)} I_i^{(1)} + \sum_i \lambda_i^{(2)} I_i^{(2)} + \sum_i \lambda_i^{(3)} I_i^{(3)} + \sum_i \lambda_i^{(4)} I_i^{(4)} + (...) \ , \tag{2.26}$$

where $I_i^{(n)}$ denotes the group-theoretic invariants constructed from the order-parameter components, which are polynomials of n-th order. Truncating the expansion at the n-th order we speak of the local-potential approximation at naive scaling dimension n. This approximation will be discussed later. At this point we only want to mention that according to rules stated by Landau [20, 21], the existence of a second-order phase transition requires $\lambda_i^{(1)} = \lambda_i^{(3)} = 0$, which rules out certain potentials from the beginning (compare with the discussion in Sec. 2.4). The decision whether the model defined by Eqs. (2.14) or (2.26), respectively, allows for a second-order phase transition can be inferred from the eigenvalues of the stability matrix S, which have to be evaluated for each of the fixed points $\{\bar{\lambda}_i^*\}$:

$$(S_{ij}) \equiv \left(\frac{\partial \beta_i}{\partial \bar{\lambda}_j} \right) \Big|_{\vec{\bar{\lambda}} = \vec{\bar{\lambda}}^*} \ , \tag{2.27}$$

where the beta functions are defined by

$$\beta_i \equiv k \partial_k \bar{\lambda}_i \ . \tag{2.28}$$

The classification of fixed points according to their stability-matrix eigenvalues is a well-known task in stability theory of differential equations. Integrating Eq. (2.18) from the ultraviolet (UV) limit ($k = \Lambda$, which corresponds to $k = 1$ after rescaling) down to the infrared (IR) limit ($k = 0$), the values for the couplings $\bar{\lambda}_i(k)$ change along flow lines in coupling space. Examples can be found in chapter 6. Also the following general statements are illustrated by these examples. Note that in our notation the arrows in the flow diagrams always point from the UV to the IR.
In general, for each infrared fixed point, there exists a so-called critical manifold in coupling space: starting in the UV on the critical manifold, the flow ends in the infrared fixed point in the IR limit. Every point on the critical manifold represents a system at criticality because, due to Eq. (2.21), the correlation length is divergent on the whole critical manifold. In the dimensionally reduced theory (2.14) the couplings do not carry any implicit dependence on scaling fields. In order to tune the system through a phase transition, one hence has to assume an explicit dependence of the initial UV couplings on the relevant scaling fields u_i. A trajectory $\bar{\lambda}_i(\vec{u})$ which crosses the critical manifold describes a second-order phase transition at the point of intersection. Whether a certain UV action can be tuned towards the critical line by varying a certain number of relevant scaling fields depends on the location in coupling space of both, the UV couplings and the critical manifold. At a fixed point, directions in coupling space in which the flow is repelled from the fixed point are called *relevant* directions. Accordingly, directions in which the flow is

attracted towards the fixed point are called *irrelevant* directions. In general, the $\bar{\lambda}_i$-directions are neither purely relevant, nor purely irrelevant. Instead, such directions in coupling space are associated in the following way with the scaling fields u_i.
Consider first a fixed point associated with entirely real eigenvalues. In this case the left eigenvectors $\vec{v}_i$ of the stability matrix (2.27),

$$\vec{v}_i^T \mathbf{S} = y_i \vec{v}_i^T \tag{2.29}$$

determine directions perpendicular to purely irrelevant directions[3]. Of course the exact definition of such directions is only possible right at a fixed point and becomes less precise when moving a little bit away from it. In the close vicinity, however, the definition still constitutes a satisfying approximation (see for example Fig. 6.1). The scaling fields can be defined by

$$u_i(k) = \vec{v}_i^T \cdot (\vec{\bar{\lambda}}_k - \vec{\bar{\lambda}}^*) \ , \tag{2.30}$$

and it is possible to derive the following flow equations for them [6]:

$$k \frac{\partial u_i(k)}{\partial k} = -y_i u_i(k) \ . \tag{2.31}$$

Obviously, a scaling field u_i associated with a positive (negative) eigenvalue, $y_i > 0$ ($y_i < 0$), becomes smaller (larger) under the RG flow towards the IR. Starting in the UV with a point $\vec{\bar{\lambda}}_{k=\Lambda}$ in the close vicinity of the fixed point, we conclude that in the IR limit $\delta\vec{\bar{\lambda}}_k \equiv (\vec{\bar{\lambda}}_k - \vec{\bar{\lambda}}^*)$ becomes more and more perpendicular to $\vec{v}_i^T$ if $y_i > 0$, which means that it becomes more and more parallel to a purely irrelevant direction. Likewise, if $y_i < 0$ and $u_i > 0$, the difference $\delta\vec{\bar{\lambda}}_k$ necessarily increases with the flow towards the IR. Hence, in order to arrive at the fixed point in the IR limit, the scaling fields associated with negative eigenvalues, say u_i with $i = 1, \ldots, n_c$, must vanish in the UV, i.e. $u_i(k = \Lambda) = 0$ for $i = 1, \ldots, n_c$. Accordingly, one refers to them as *relevant scaling fields* and one can identify their UV values with the physical variables which are to be tuned to zero in order to arrive at a second-order phase transition. An example is given by the reduced temperature, $u_1(k = \Lambda) = (T - T_c)/T_c$. Obviously, the number n_c determines the nature of the second-order transition associated with the fixed point. For $n_c = 1$ one has an IR-stable fixed point associated to an ordinary critical point in experiment. For $n_c > 1$ the fixed point is n_c-fold IR unstable and can be associated with a multi-critical point ($n_c = 2$: bicritical, $n_c = 3$: tricritical, etc.). Furthermore, it can be shown that the critical exponent ν in the power law (2.5) for the correlation length can be identified with the inverse of the negative eigenvalue associated to the reduced temperature,

$$\nu = -\frac{1}{y_1} \ . \tag{2.32}$$

The outline of a proof can be found in Ref. [6].
If $y_i = 0$ one speaks of a *marginal* eigenvalue, and one cannot decide whether the associated scaling field is relevant or irrelevant. In this case one has to go beyond the utilized polynomial order in the Landau potential.

[3] We note that the stability-matrix eigenvalues y_i are the same irrespective whether determined from the left or from the right eigenvectors.

For the above discussion we assumed entirely real eigenvalues. The stability matrix can, however, exhibit complex eigenvalues, too. Such eigenvalues indicate the existence of planes in coupling space where the flow describes spirals in the vicinity of the fixed point. Refraining from an interpretation of the eigenvectors associated with the complex eigenvalues, we only want to state that if the real part of the eigenvalue is positive (negative), the spiral is directed towards (away from) the fixed point in the IR. A fixed point with n_c negative eigenvalues, whereas all other eigenvalues have positive real parts, is hence associated to an ordinary critical point for $n_c = 1$ and to a multi-critical point for $n_c > 1$.
Assuming a single quadratic invariant, $\sum_{i=1}^{N} \phi_i^2$, the anomalous dimension η involved in the power law (2.8) can be calculated from the flow equation for a field-independent coupling

$$d_{ij}^{(2)}(\Phi) \equiv \frac{1}{2}\delta_{ij}\left(Z_k^{-1} - 1\right) \tag{2.33}$$

in front of a corresponding term in the derivative expansion (2.24), which is determined by [6]

$$\eta_k = k Z_k^{-1} \frac{\partial Z_k}{\partial k} \tag{2.34}$$

with $\eta = \eta_{k=0}$. The assumption of a single quadratic invariant will be discussed in detail later.

2.4 Universality hypothesis

Setting the stage

In the preceding sections we have already discussed the theoretical framework which is capable to describe static universal critical behavior. Starting from a potential of the form (2.26), one can derive the fixed points under the RG flow and calculate the stability-matrix eigenvalues associated to each of them. Fixed points with a single negative eigenvalue are called IR stable and correspond to second-order phase transitions. The critical exponent ν can be inferred from the stability matrix via Eq. (2.32). Knowing in addition to ν also the anomalous dimension η, one can infer all other critical exponents from the scaling relations (2.9), if one has trust in their validity. For lattice models a field-theoretic treatment is necessarily constrained to those which can be rewritten as field theories in the continuum limit. Other models have to be addressed for example in a real-space RG approach or by Monte-Carlo RG simulations (see for example Refs. [14, 22]). Usually a rewriting is possible, but some models are intrinsically related to the structure of the lattice (compare with Ref. [23]). For an important lattice model, the infamous (exactly solvable) eight-vertex model of Baxter in $D = 2$ dimensions [24], we cannot state a field-theoretic formulation. It is of relevance, however, since it spoils the original form of the universality hypothesis in that the critical exponents continuously depend on coupling constants of the action. This is found also for several other lattice models (see [25] and references therein). We want to emphasize that this phenomenon is not restricted to low-dimensional systems. In particular, there is evidence that the critical exponents of the eight-vertex model continuously vary in any dimension [26]. For a three-dimensional Ising model with continuously varying exponent γ see Ref. [27]. It has been shown, however, that the phenomenon is caused by "marginal couplings" in the action which defines the theory (see Sec. 5.12 of the review [22]). In the following we exclude this case in a systematic way by restricting the discussion to models

without such marginal couplings, which should take account of the majority of physically relevant systems.
Obviously, the critical exponents that can arise in the framework summarized above only depend on

1. the properties of the potential U (assuming the kinetic term to be of the form (2.23)),

2. the spatial dimension D.

The interesting question is now what are the properties of two different Lagrangians falling into the same static universality class. Which conditions have to be necessarily fulfilled, and can one state sufficient criterions? We review this question in detail in this section. A notion closely related is that of "the" *universality hypothesis*, which actually appears in slightly varying scope and content in the literature. We can distinguish between different versions with rising ambition. First one can define as universality hypothesis simply an enumeration of (partially loosely defined) features on which the critical exponents predominantly depend. These features are (compare for example with Ref. [28])

- the spatial dimension D,
- the number of components of the order parameter,
- the 'symmetry properties' of the order parameter,
- the (non-)existence of long-range interactions,
- maybe other (unknown) ones.

One of the earliest versions of the universality hypothesis was given by Griffiths in 1970 and was based on results for a very limited amount of lattice models [29]. Also Kadanoff pointed out the essential features in a rather qualitative form in 1971 (compare the quotation given in Ref. [30]). In a more ambitious sense, one can define the universality hypothesis as a set of criteria which are hypothesized to be necessarily or sufficiently fulfilled for two models falling into the same universality class (i.e., in RG language, being attracted by the same infrared stable fixed point). Section 4.6. of Ref. [7] discusses the progress in this direction. Unfortunately, in the literature often many highly questionable assumptions are made *between the lines* when claiming that two models fall into the same universality class "according to the universality hypothesis". The following discussion will give an impression how subtle the issue can be.
Instead of considering all possible potentials of the form (2.22), we can restrict the discussion to potentials which are expected to arise as order-parameter theories in the real world. All phase transitions involving spontaneous symmetry breaking are covered by taking into account all the most general potentials invariant under symmetry groups in their particular representations. But also the most prominent second-order phase transitions which are not related to spontaneous symmetry breaking can be successfully described on this basis. The famous Kosterlitz-Thouless phase transition for example occurs in a system of spatial dimension $D = 2$. According to the Mermin-Wagner theorem there cannot exist spontaneous breaking of symmetry in two spatial dimensions. Nevertheless, the Kosterlitz-Thouless transition falls into the $O(2)$ universality class.

Another example is the critical endpoint of the liquid-gas phase transition. Although both phases are not distinguished by any symmetry at the critical endpoint the phase transition falls into the $Z(2)$ universality class. Therefore we restrict the discussion to most general potentials invariant under symmetry groups in their particular representations, which are of the form (2.26).
For convenience we introduce the following notation.

- We denote the set of n potentials of the form (2.26) by $\{U_1^P, U_2^P, \ldots, U_n^P\}$ if the same fixed point P exists in all of the n models.

- For a potential U of the form (2.26) we denote the subspace spanned by the linearly independent invariants of order m by $\{I_i^{(m)}\}$.

- An *integrity basis* for a certain representation $\Gamma(G)$ of a group G is defined by a set of invariants (basic invariants) from which all other invariants can be constructed by summation and multiplication.

First of all we distinguish between those static universality classes which have been observed in experiment (EUV's), and those static universality classes which are defined by IR-stable fixed points associated with fixed-point potentials (i.e., the potentials at the fixed points) of a certain symmetry (SUV's). We note that the same fixed point can exist in different models of the form (2.26). A necessary condition for this situation is of course that the fixed-point potential is a special case of the potentials defining the models. Since different fixed points have different characteristic stability-matrix eigenvalues, every EUV should be in one-to-one correspondence with a specific infrared fixed point. Indeed, most of the EUV's have been very successfully identified with certain SUV's with (see Refs. [7, 14, 21] for comprehensive reviews). For example, the Ising universality class encompasses a large variety of experimentally well-accessible systems, and the agreement between theory and experiment (including high-precision studies in microgravity environment [14]) is convincing. In other cases, however, such a mapping has not yet been achieved in a satisfactory manner. In the following we point out three examples for such cases. First of all we point to Tab. X in Ref. [31] for an example where a second-order transition is seen experimentally, whereas no stable infrared fixed point is found in the ϵ-expansion. Second, it is also well-known that the standard ϵ-expansion is only an asymptotical expansion and not convergent [32], i.e., there is an optimal loop order from which on the results for the critical exponents become worse. Although it has been demonstrated in the context of $O(N)$ models that this problem can be cured by using resummation techniques yielding high-precision critical exponents which agree astonishingly well with experiments and lattice simulations, to our knowledge this program has not been carried out for all universality classes involving anisotropic symmetries. One might find unexpected deviations between theory and experiment here. Another problem of the low-loop ϵ-expansion is the extension of the results to $D = 3$ by setting $\epsilon = 1$ in the end. There exist examples where this extrapolation clearly fails [33], one of which is of great relevance for two-flavor QCD, namely the $U(2)_L \times U(2)_R$-symmetric model (see Sec. 3.3.2). Third, the stability of certain fixed points for potentials with anisotropic symmetry is still under debate. An example is the cubic anisotropy model which will be discussed in Sec. 6.3.

Polynomial order

One important property of the potential U is its polynomial order (or naive scaling dimension). As far as we can tell from the above references, every EUV can be defined via the value for ν. Calculating the value of ν for a certain SUV from the FRG method, the precision dramatically depends on the truncation order. In local-potential approximation at a certain naive scaling dimension, however, the value is universal in the following sense. Consider a fixed point P and a set $\{U_1^P, U_2^P\}$. Let the fixed-point potential involve m linearly independent couplings (including mass terms in the counting). Then m of the stability-matrix eigenvalues calculated with respect to U_1^P coincide with m of the stability-matrix eigenvalues calculated with respect to U_2^P. Usually, in local-potential approximation it is therefore possible to unambiguously identify each universality class associated with a fixed point from the universal stability-matrix eigenvalues, and in particular from ν. For the identification of the SUV's known to the author the value for η is not needed. Special attention, however, has to be paid to the following cases. First, in presence of fixed points with marginal eigenvalues the truncation order has to be increased in order to decide on the stability properties. The second case is subtle. One can ask whether there could exist different universality classes which correspond to the same fixed-point potential at a certain truncation order. Only beyond this order the fixed-point potentials would be distinguishable. We are, however, neither aware of an argument ruling out this possibility, nor of universality classes of this type.

Symmetry and the number of order-parameter components

Another crucial property of the potential U is its symmetry, i.e., under which symmetry transformations of the fields it is left invariant. In order to uniquely determine the invariants it is not sufficient to specify only a symmetry group G. Fixing in addition the representation $\Gamma(G)$ of the group, however, uniquely determines the potential. As we outline in App. A.1, in general the N real order-parameter components Φ_i are involved in a tensor φ, the form of which depends on the particular choice for $\Gamma(G)$. From the transformation law of φ under the action of the group one can infer how the fields Φ_i transform, and from this one can derive the subspaces $\{I_i^{(m)}\}$, where the representation $\Gamma(G)$ leaves simultaneously invariant all the invariants $I_i^{(m)}$ (see Sec. 5).

In terms of a potential a phase transition is described by a minimum which changes from a nonzero value to zero. In Landau theory this is achieved by tuning a single coupling in front of the quadratic invariant $\lambda_0^{(2)} = \sum_{i=1}^N \phi_i^2$ from a negative value to zero while it is assumed that the higher-order invariants assure stability. Landau and Lifshitz introduced the following necessary conditions for the existence of a second-order phase transition associated with a single relevant variable [20, 21, 34]:

1. necessary condition: the potential does not involve invariants of odd polynomial order,

2. necessary condition: the potential involves exactly one quadratic invariant: $\lambda_0^{(2)} = \sum_{i=1}^N \phi_i^2$.

In the following we refer to these conditions as *Landau-Lifshitz criteria*. It is stated in the literature that the above conditions imply that the symmetry of the potential must correspond

to an irreducible representation [21, 34, 35, 36]. However, they rigorously hold true only in mean-field approximation but not necessarily beyond mean-field level [37]. Ref. [38] clearly emphasizes that irreducibility of the representation is not a necessary condition. Nevertheless, for $D = 3$ spatial dimensions the Landau-Lifshitz criteria are usually reliable. Interesting in this respect is our investigation of the $SU(2) \times U(2)$-symmetric model belonging to a reducible representation and involving two quadratic invariants.

Impressive investigations have been performed for order parameters with $N \leq 2$ [21, 39], $N = 3$ [21, 39], $N = 4$ [31, 40, 41], $N = 6$ [42, 43], and $N = 8$ [44] components, respectively. Some general features have been discussed in Ref. [45] (see also Ref. [46]) for arbitrary N at one-loop order in the ϵ-expansion. The main result of Ref. [45] is that for $N < 4$ the only stable IR fixed point is the $O(N)$-symmetric one, whereas for $N > 4$ it is always unstable. Refs. [21, 31, 39, 40, 41, 42, 43, 44] consider vector representations which are irreducible on the real numbers and involve N order-parameter components. Irreducibility on the real numbers means that the representation is either real, or an irreducible representation can be obtained by taking the direct sum of the representation and its complex conjugate [47]. We note that there is a one-to-one correspondence between $N/2$-dimensional complex vector representations (represented by complex-valued matrices $\mathbf{M}$ acting on complex-valued vectors $\vec{z}$) and N-dimensional real vector representations due to the isomorphism [48]

$$\mathbf{M}\vec{z} \simeq \begin{pmatrix} \mathrm{Re}\,\mathbf{M} & -\mathrm{Im}\,\mathbf{M} \\ \mathrm{Re}\,\mathbf{M} & \mathrm{Im}\,\mathbf{M} \end{pmatrix} \begin{pmatrix} \mathrm{Re}\,\vec{z} \\ \mathrm{Im}\,\vec{z} \end{pmatrix} . \tag{2.35}$$

The chosen restrictions are obviously compatible with the Landau-Lifshitz criteria. The set of distinct matrices of an irreducible vector representation $\Gamma(G)$ is a group called the *image of* G *under* Γ and is denoted by $I_\Gamma(G)$ in the following. According to Ref. [21] $I_\Gamma(G)$ completely determines the Landau potential associated with $\Gamma(G)$ and all of the irreducible representations exhibit a single quadratic invariant. In case of an N-component order parameter we are only interested in images where this quadratic invariant is given by $\sum_{i=1}^N \phi_i^2$. Since $(\sum_{i=1}^N \phi_i^2)^2$ is necessarily an invariant if $\sum_{i=1}^N \phi_i^2$ is one, we conclude that we can restrict the relevant G's to subgroups of $O(N)$. Different irreducible representations of the same group G can be associated to different images and hence different Landau potentials. For instance, the irreducible representations W_1, W_2, W_3, and W_3, respectively, of the group O_h^5 are associated with the image L_1, whereas the irreducible representation X_5^- of O_h^5 is associated with the image L_7 (see Tab. I of Ref. [43]). Further, different groups can have irreducible representations corresponding to the same image (see again Tab. I of the above reference). It is also possible that the subspace $E \equiv \{I_i^{(4)}\}$ coincides for different images. This is for example the case for the images L_1, L_2, L_3, and L_5 in Tab. I of the above reference. Distinct Landau polynomials can be labeled by the largest image group (i.e., the group of highest symmetry) which is also known as *centralizer* E_c *of* E. We speak of most general E_c-invariant Landau potentials. The largest group leaving invariant the fixed-point potential found for the most general E_c-invariant Landau potential is a subgroup of E_c and is called *little group of* E_c, which we denote by E_c^*. Another group relevant for the discussion is the *normalizer* E_N defined as the largest group leaving invariant the space E as a whole, which in general contains the centralizer as a subgroup.

We note that at least in the study for $N = 6$ another group-theoretical criterion (proposed by

Michel and Toledano) has been used, which rules out certain irreducible representations. Furthermore, in all of the Refs. [21, 39, 31, 40, 41, 42, 43, 44] calculations are finally restricted to discrete subgroups of $O(N)$ (point groups). For the remaining irreducible representations the images are calculated, from which the most general potentials up to fourth order are constructed and the RG flow is studied in an $n \leq 2$ loop-order ϵ-expansion. According to Ref. [41], in spite of the restriction to discrete subgroups of $O(N)$, the following enumeration covers *all* possible Landau potentials (up to polynomial-order four) for the respective numbers of order-parameter components N, which are consistent with the Landau-Lifshitz criteria, i.e., *all* possible groups and representations of relevance. We can confirm this statement, however, only for the cases $N = 1$ and $N = 2$. For $N \leq 3$ we have the following objections. Whereas the restriction to discrete subgroups is clearly appropriate in the context of phase transitions in crystals, we doubt its validity in the general case, however. As pointed out in Section 3.1. of Ref. [7], in case of liquid crystals for instance continuous groups in real space have to be taken into account. Apart from this, only vector representations are taken into account. However, also tensor representations[4] should be taken into account (compare with App. A). Tensor representations are of particular importance when considering gauge theories, i.e., local symmetries which the above references do not take into account. In case of gauge theories one usually (but not necessarily) speaks of *Ginzburg-Landau* potentials, whereas we confined the discussion to Landau potentials in absence of couplings to gauge fields. We will continue with the discussion of gauge fields in Sec. 4.4. In the following we summarize the most important results inferred from the above references.

For $N = 1$ the Landau-Lifshitz criteria restrict the form of the potential to

$$U_{\mathrm{O}(1)} = r\phi^2 + \lambda\phi^4 \ , \tag{2.36}$$

which corresponds to the fundamental representation of $O(1)$. Also when taking into account all possible groups and representations this is obviously the only possibility consistent with the criterions of Landau and Lifshitz. The potential exhibits the infamous Ising fixed point, which is IR stable (see Sec. 6.1).

For $N = 2$ only the groups C_n and C_{nv} are potentially consistent with the Landau-Lifshitz criteria. The corresponding vector representations with carrier space $\vec{\phi} = (\phi_1, \phi_2)^T$ give rise to the following integrity bases [21, 39]:

$$C_{nv}: \quad I_1 = \phi_1^2 + \phi_2^2 \ , \quad I_2 = (\phi_1^2 + \phi_2^2)^{n/2} \cos(n\theta) \ , \tag{2.37}$$

$$C_n: \quad I_1 = \phi_1^2 + \phi_2^2 \ , \quad I_2 = (\phi_1^2 + \phi_2^2)^{n/2} \cos(n\theta) \ , \quad I_3 = (\phi_1^2 + \phi_2^2)^{n/2} \sin(n\theta) \ , \tag{2.38}$$

with $\tan\theta = \frac{\phi_1}{\phi_2}$. For $n = 4$ we obtain:

$$I_2 = \phi_1^4 - 6\phi_1^2\phi_2^2 + \phi_2^4 \ , \quad I_3 = 4\left(\phi_1\phi_2^3 - \phi_1^3\phi_2\right) \ , \tag{2.39}$$

from which one determines the most general C_{4v}-potential,

$$U_{\mathrm{C}_{4\mathrm{v}}} = rI_1 + aI_1^2 + bI_2 = r\left(\phi_1^2 + \phi_2^2\right) + g_1\left(\phi_1^4 + \phi_2^4\right) + g_2\phi_1^2\phi_2^2 \tag{2.40}$$

(where $g_1 \equiv a + b$, and $g_2 \equiv 2a - 6b$), and the most general C_4-potential,

$$U_{\mathrm{C}_4} = U_{C_{4v}} + g_3\left(\phi_1\phi_2^3 - \phi_1^3\phi_2\right) \ . \tag{2.41}$$

[4] For potentials associated to tensor representations see for instance [49, 50, 51, 52, 53] and Sec. 6.5.

For $n = 1$ one obtains two linear invariants, $I_2 = \phi_2$ and $I_3 = \phi_1$, which is not compatible with the Landau-Lifshitz criteria. For $n = 2$ one obtains the additional quadratic invariants, $I_2 = \phi_2^2 - \phi_1^2$ and $I_3 = 2\phi_1\phi_2$, which is incompatible as well. Also the case $n = 3$ spoils the conditions of Landau and Lifshitz due to the two cubic invariants, $|I_2| = \phi_2^3 - 3\phi_1^2\phi_2$ and $|I_3| = 3\phi_2^2\phi_1 - \phi_1^3$. For $n > 4$ no fourth-order potentials different from the potentials (2.40) and (2.41), respectively, are generated. Hence, the only candidates for stable IR fixed points are the latter potentials. At one-loop order in the ϵ-expansion the only stable IR fixed point is the isotropic $O(2)$-symmetric one [45]. We reinvestigate the fixed points in Sec. 6.2 from the FRG method. We find an IR-stable $O(2)$ fixed point in case of the C_{4v}-potential, whereas the investigation of the C_4-potential remains inconclusive even at naive scaling dimension six.
Using Brezin's rule [45] (also known as trace condition), which states that

$$\sum_k^N c_{ijkk}^{(4)} = \delta_{ij} c \tag{2.42}$$

if the potential (2.22) exhibits a single quadratic invariant, we conclude that the potential (2.41) is in fact the most general Landau potential for $N = 2$ consistent with the Landau-Lifshitz criteria. That is, any representation of any group is associated with a special case of this potential.
For $N = 3$ only the groups O, O_h, T_h, Y, and Y_h are consistent with the Landau-Lifshitz criteria [21, 39]. The corresponding vector representations with carrier space $\vec{\phi} = (\phi_1, \phi_2, \phi_3)^T$ are all associated with the same most general fourth-order Landau potential:

$$U_{\mathrm{C}} = r\left(\phi_1^2 + \phi_2^2 + \phi_3^2\right) + g_1\left(\phi_1^2 + \phi_2^2 + \phi_3^2\right)^2 + g_2\left(\phi_1^4 + \phi_2^4 + \phi_3^4\right) \ . \tag{2.43}$$

For the groups Y and Y_h, however, the degeneracy in the potential is lost at higher order. The potential U_{C}, which is said to possess a cubic symmetry, will be studied in Sec. 6.3 from the FRG method. We confirm the one-loop order ϵ-expansion result that the only stable IR fixed point is the isotropic $O(3)$-symmetric one [45].
For $N = 4$ the number of distinct potentials consistent with the Landau-Lifshitz criteria is significantly larger. According to Refs. [21, 31, 41], there are 22 nonequivalent centralizers labeling 22 distinct Landau potentials. The group-subgroup relationship between the 22 groups together with the associated polynomials is shown in Fig. 1 of Ref. [31]. Only six of the Landau potentials exhibit a stable IR fixed point, namely those associated with the centralizers $O(4)$, $\left(\frac{Y}{C_2}; \frac{Y^*}{C_2}\right)^*$, $(D_\infty \times D_\infty)^*$, $\left(\frac{O}{D_2}; \frac{O}{D_2}\right)^*$, $\left(\frac{C_8}{C_4}; \frac{D_4}{D_2}\right)$ and $\left(\frac{D_4}{D_2}; \frac{D_4}{D_2}\right)^*$, respectively. In total there are only four distinct stable IR fixed points which are listed in Tab. 6.2. We note that Ref. [40] discards the $\left(\frac{Y}{C_2}; \frac{Y^*}{C_2}\right)^*$-symmetric potential since it is not associated to a representation of a point group, i.e., is not relevant for crystals. Accordingly, in their counting there are, apart from the isotropic case, only four physically relevant Landau potentials with anisotropic symmetry exhibiting a stable IR fixed point. Since we are not only interested in point groups we regard all of the five Landau potentials with anisotropic symmetry as physically relevant. We reinvestigate the five anisotropic Landau potentials from FRG in Sec. 6.4 where the $\left(\frac{C_8}{C_4}; \frac{D_4}{D_2}\right)$-symmetric potential is of particular interest. In Ref. [31] the fixed-point structure for this potential was derived not from an explicit calculation but from an elegant group-theoretical analysis. Since the centralizer $\left(\frac{C_8}{C_4}; \frac{D_4}{D_2}\right)$ is not a little group, the RG flow consists of trajectories characterized by several little groups, giving rise to manifolds of different symmetry. The fixed-point structure, further discussed in Sec. 6.4,

can then be inferred from the Landau potentials associated to these little groups [31]. Nevertheless, it is quite interesting how this complicated fixed-point structure appears in an explicit FRG calculation. We were able to verify at least part of it.

For $N = 6$ there have been found 11 different images giving rise to six distinct Landau potentials consistent with the Landau-Lifshitz criteria [42, 43]. Only two of them exhibit a stable IR fixed point, namely

$$U_1 = r\sum_{i=1}^{6}\phi_i^2 + g_1\left(\sum_{i=1}^{6}\phi_i^2\right)^2 + g_2\sum_{i=1}^{6}\phi_i^4 + g_3\left(\phi_1^2\phi_4^2 + \phi_2^2\phi_5^2 + \phi_3^2\phi_6^2\right) \ . \tag{2.44}$$

and

$$U_6 = U_1 + g_4\left[\phi_1\phi_4\left(\phi_1^2 - \phi_4^2\right) + \phi_2\phi_5\left(\phi_2^2 - \phi_5^2\right) + \phi_3\phi_6\left(\phi_3^2 - \phi_6^2\right)\right] \ . \tag{2.45}$$

The Landau potential U_1 is associated to certain irreducible representations of the groups O_h^5, O^3, T_d^2, and O^8, respectively. The Landau potential U_6 is associated to the irreducible representation $M_2 \oplus M_3$ of the group O^6, and to the irreducible representation $M_2 \oplus M_3$ of the group O^7, respectively. We reinvestigated these two Landau potentials from FRG but found the quartic truncation order inconclusive due to the occurrence of marginal eigenvalues. We refrained from further studies in this case. Instead, we found a new Landau potential exhibiting a stable IR fixed point. It is associated with the $[3,1] \oplus [1,3]$ representation of $SU(2)_V \times SU(2)_A$. Apparently it does not appear in Refs. [42, 43] because it is not a representation of a point group. It will be discussed in Sec. 6.8.1.

Utilizing the same strategy also for $N = 8$, no IR stable fixed points have been found for models other than the isotropic $O(8)$ model [44]. In Sec. 6.8.3, however, we present a potential exhibiting a stable IR fixed point. Unfortunately, we are not able to determine the symmetry group to which it corresponds.

For $N = 5$, $N = 7$, and $N > 8$ we are not aware of similarly systematical investigations.

Range of interaction

Also the range of interaction of the terms involved in the potential U is a relevant property. In local-potential approximation (2.22), and also in simple forms of the derivative expansion (2.24), only local interactions (short-range interactions) are taken into account, i.e., the fields involved in the interaction terms are localized at the same point in space. Non-local interactions (long-range interactions), however, cannot be excluded by the symmetry constraints discussed above and can have an effect on the critical exponents [28]. Probably the simplest non-local interaction is of the isotropic form

$$\sim \int d^D\vec{x} \int d^D\vec{x}\,'\Phi_i(\vec{x})\Phi_i(\vec{x}\,')\frac{1}{|\vec{x} - \vec{x}\,'|^{D+d_\sigma}} \ , \tag{2.46}$$

which has been mainly studied in the framework of $O(N)$ models, in particular for the Ising model (see Ref. [54]). At least in this context, in local-potential approximation (where $\eta \equiv 0$), for $-D \le d_\sigma \le 0$ one can speak of strong long-range interactions, and for $0 < d_\sigma \le d_c(D)$, where $d_c(D) = D/2$ for $D < 4$, one can still speak of weak long-range interactions. In this case the range of interaction, as well as the angular dependence, indeed has influence on the critical exponents or

even on the order of the phase transition. We are not aware of systematic investigations studying the influence of non-local interactions on the anisotropic models discussed above, however.

Attempts in stating a more precise universality hypothesis

In the following we consider only systems in which long-range interactions are either absent or can be neglected, respectively. Furthermore we restrict the hypothesis to models which can be formulated as a field theory and whose phase transition is associated to a spontaneous breaking of symmetry. Note further that we excluded models exhibiting marginal couplings giving rise to critical exponents varying continuously with these couplings. Then a universality hypothesis (UH1) can be stated as follows:
Two models A and B exhibiting a second-order phase transition associated to a single relevant variable (e.g. temperature or any other quantity) necessarily fall into the same universality class if the following conditions are fulfilled:

1. The spatial dimension D is the same.

2. The order parameters are associated with equivalent irreducible representations, i.e., the representations are related by a similarity transformation.

This version is rather restrictive as it leaves not much room for differences between A and B. Based on systematic investigations is also the following restricted universality hypothesis (UH2):
Two models A and B exhibiting a second-order phase transition associated to a single relevant variable necessarily fall into the $O(N)$ universality class if the following conditions are fulfilled:

1. The spatial dimension D is the same.

2. The order parameters have the same number $N \leq 3$ of components.

We propose a further universality hypothesis (UH3) on the basis of the rule that a stable IR fixed point implies the coincidence of the centralizer and the normalizer associated to it, for which a proof was presented in Ref. [31]. If we understand the implications of this rule correctly (which needs to be checked) one can formulate the following universality hypothesis:
Consider two models A and B with N-component order parameters defined by potentials associated to normalizers G_A and G_B, respectively, both exhibiting a second-order phase transition associated to a single relevant variable. Let us denote all possible normalizers (of potentials) which are identical to subgroups of $O(N)$ giving rise to a real irreducible N-dimensional representation by G_i, $i = 1, \ldots, l$. Then, A and B belong to the same universality class if $G_A \subseteq G_i$ and $G_B \subseteq G_i$ holds exactly for one of the G_i. This G_i is the normalizer associated to the fixed-point potential.
The above formulations have the premise that two models exhibit a second-order phase transition (and therefore IR-stable fixed point(s)) and state sufficient conditions for them to fall into the same universality class. A closely related problem is the identification of sufficient/necessary conditions for the existence of a stable IR fixed point in a certain class of models. Several efforts have been made in topological studies (see for instance Refs. [55, 56]). We are optimistic that further investigations in this direction will lead to more refined versions of the universality hypothesis.

Finally we want to state several points which challenge the universality hypothesis. Ref. [57] conjectures the existence of two simultaneously stable fixed points. Ref. [58] gives an example where critical exponents change along the second-order phase boundary. These examples illustrate that even version (UH1) of the universality hypothesis remains unproven in a general setting (on the other hand, so far, no definitely confirmed violations exist). In particular the possible existence of two (or even more) IR-stable fixed points of distinct symmetry in a model cannot be ruled out a priori (compare with Sec. 6.4.3). Very recently we found two IR-stable fixed points in a most general $U(2)_A \times U(2)_V$-symmetric Landau potential up to sixth polynomial order, which seem to be associated with the same symmetry but with different ν (see Sec. 6.5). So far, their existence does not constitute a violation of the universality hypothesis, however, because the Gaussian fixed point aquires marginal stability-matrix eigenvalues at this truncation order. Also the studies at higher truncation order remain inconclusive due to the occurence of marginal eigenvalues. Further investigations are in progress. We further note that, at least in principle, there could exist models involving N order-parameter components which, nevertheless, fall into a universality class associated with $M < N$ order-parameter components. In the cubic anisotropy model (which involves an arbitrary number of order-parameter components), for instance, there exists a fixed point associated with the Ising universality class (see Sec. 6.3). Although it turns out to be unstable in explicit calculations, we are not aware of a general reason why this must be the case.

Ref. [59] is of particular interest for us as it concerns QCD. The authors of the latter reference study a dimensionally reduced Gross-Neveu model at finite temperature which, according to the universality hypothesis, should fall into the same universality class as the Ising model. Lattice calculations, however, suggest that the critical exponents are different. More precisely, the numerical data for the Gross-Neveu model is in agreement with mean-field behavior. We suspect that this has to do with the large-N expansion which has been performed, since one finds mean-field exponents for the Ising model in the large-N limit. The authors, however, argue against this asserting that their result is not an artifact of their approximation. Also the range of the interactions involved should be checked. Further investigations are desired in order to verify the violation and to understand the underlying reasons. A confirmation of the results would also question the applicability of the universality hypothesis (but maybe only that of dimensional reduction) to two-flavor QCD (compare with Sec. 3.3.2).

Die Farben sind Taten des Lichts, Taten und Leiden.
(Johann Wolfgang von Goethe, Zur Farbenlehre)

Chapter 3

Quantum chromodynamics

3.1 Phase transitions in quantum chromodynamics

Originally, the quark model, and later QCD, was constructed to explain the existence and properties of hadrons (mesons and baryons). One of the features of QCD is *asymptotic freedom*, meaning that the coupling strength between quarks becomes smaller with increasing momentum transfer involved in the interaction[1]. Deep-inelastic scattering of leptons by nucleons confirmed this prediction (see for example Ref. [61] for a detailed discussion and the history of such experiments). On this basis another state of matter was predicted for high temperature and/or baryonic chemical potential, which is now known as *quark-gluon plasma*. One of the earliest references to this exotic phase is that of Collins and Perry [62] who spoke of a 'quark soup'. Their idea was that at high densities, as observed in neutron stars, one must expect the hadrons to overlap. Due to asymptotic freedom, quarks should interact weakly in this phase which motivated the authors to consider the 'quark soup' as a relativistic gas of free quarks. For high temperature, the existence of a quark-gluon plasma phase was confirmed from first principles in Ref. [63] using perturbation theory, which is justified due to asymptotic freedom.
An important question is whether the transition from hadronic matter to the quark-gluon plasma phase goes along with a true phase transition. So far, the answer is not complete. QCD possesses two kinds of symmetry which can be broken spontaneously, namely chiral symmetry and the center of the color gauge group, respectively, both of which are only approximate in case of physical quark masses causing explicit symmetry breaking. Consequently the spontaneous breaking of symmetry associated with the corresponding phase transitions is only of approximate nature. In case of chiral symmetry and the chiral phase transition this is mirrored in the experimental fact that the would-be Goldstone particles have a (small) mass due to explicit symmetry breaking. Nevertheless, as discussed in Sec. 2.1, also in case of physical quark masses one can still speak of an exact first-order chiral phase transition and an exact critical endpoint. Second-order lines and ordinary critical points encountered for vanishing quark masses, however, will be turned into crossover. It is a nontrivial question to which extent the transition from hadronic matter to the QGP is determined by descriptions based on (explicitly broken) chiral and/or center symmetry.

[1] For a proof from first principle that asymptotic freedom also exists with respect to high baryon density and/or temperature see Ref. [60].

Although the associated order parameters, which will be introduced in the following, should play an important role, it is rather likely that other degrees of freedom are relevant, too. This will be discussed for the critical endpoint in Sec. 3.3.1.

First, there is a discrete $Z(N_c)$ symmetry, the center of the gauge group $SU(N_c)$, where N_c is the number of colors. This center symmetry is only exact in the limit of infinite (static) quark masses and approximate in the case of finite (dynamical) quark masses. Correspondingly, the spontaneous center symmetry breaking is of approximate nature in presence of dynamical quarks as well. An order parameter can be defined as the vacuum expectation value of a quantity called Polyakov loop, L, named after A.M. Polyakov, who discovered its relation to the free energy F of a single quark [64] in case of infinite quark masses:

$$\langle L \rangle = \exp\left(-F/T\right) , \tag{3.1}$$

where T denotes temperature. The free energy of a single quark is linked to confinement. At small temperatures quarks are confined in hadrons, that is no free single quarks exist (i.e., $F = \infty$), and hence $\langle L \rangle = 0$ in the so-called confined phase. Due to asymptotic freedom, at high temperature one expects quarks to be liberated (i.e., F finite) so that $\langle L \rangle \neq 0$ in the so-called deconfined phase. Since $\langle L \rangle$ is not invariant under $Z(N_c)$, the center symmetry is spontaneously broken in the deconfined phase. In presence of dynamical quarks one can still speak of an exact first-order phase transition if one redefines the order parameter by subtracting its value at the transition point: $\langle L \rangle \to \langle L \rangle - \langle L \rangle_c$. A second-order phase transition is only possible at a critical endpoint in case of dynamical quark masses. Unfortunately, the analogue to Eq. (3.1) for dynamical quark masses fails to describe confinement in a strict sense. The transition described on the basis of explicitly broken center symmetry, which is still called deconfinement transition, can therefore only be an approximate description of the expected hadron-QGP transition in the real world. A second-order phase transition with respect to the Polyakov loop in case of static quark masses will be turned into a crossover in presence of sufficiently light quarks.

Second, there is chiral symmetry, $U(N_f)_R \times U(N_f)_L$, which is defined by the following unitary transformations:

$$\psi_{R,L} \longrightarrow U_{R,L}\psi_{R,L} \quad , \qquad U_{R,L} \equiv \exp\left(i \sum_{a=0}^{N_f^2-1} \alpha_{R,L}^a T_a \right) \in U(N_f) , \tag{3.2}$$

where N_f is the number of flavors, $U_{R,L}$ acts on the right-handed or left-handed fermionic quark spinor $\psi_{R,L}$, respectively, given by

$$\psi_{R,L} \equiv P_{R,L}\psi \quad , \quad P_{R,L} \equiv \frac{1 \pm \gamma_5}{2} \quad , \quad \psi = \psi_R + \psi_L , \tag{3.3}$$

the T^a denote the generators of $U(N_f)$, and ψ is the fermionic quark spinor appearing in the QCD Lagrangian. $U(N_f)_R \times U(N_f)_L$ can be rewritten in terms of axial and vector transformations,

$$\psi \longrightarrow U_{V,A}\psi \quad , \qquad U_V \equiv \exp\left(\mathrm{i} \sum_{a=0}^{N_f^2-1} \alpha_V^a T_a \right) \quad , \qquad U_A \equiv \exp\left(\mathrm{i}\,\gamma_5 \sum_{a=0}^{N_f^2-1} \alpha_A^a T_a \right) , \tag{3.4}$$

due to the group isomorphism [65]

$$\begin{aligned} G &\equiv U(N_f)_V \times U(N_f)_A \simeq U(N_f)_R \times U(N_f)_L \\ &\simeq U(1)_V \times U(1)_A \times \left[SU(N_f)/Z(N_f)\right]_L \times \left[SU(N_f)/Z(N_f)\right]_R . \end{aligned} \tag{3.5}$$

However, chiral symmetry is only an exact symmetry of QCD for vanishing quark masses $m_q = 0$. In consequence, spontaneous chiral symmetry breaking is only of approximate nature in case of physical quark masses. The associated order parameter is given by the so-called quark condensate, which is defined by the following vacuum expectation value:

$$\langle \overline{\psi}_p \psi_q \rangle = \langle \overline{\psi}_{L,p} \psi_{R,q} \rangle + \langle \overline{\psi}_{R,p} \psi_{L,q} \rangle \ , \tag{3.6}$$

where p, q are flavor indices. Obviously, a (non-)vanishing quark condensate, $\langle \overline{\psi}_p \psi_q \rangle$, is equivalent to (non-)vanishing chiral condensates, $\langle \overline{\psi}_{L,p} \psi_{R,q} \rangle$ and $\langle \overline{\psi}_{R,p} \psi_{L,q} \rangle$, respectively. For $m = 0$, all quark flavors are equivalent, and hence $\Phi_{pq} \equiv \langle \overline{\psi}_{L,p} \psi_{R,q} \rangle = \varphi \delta_{pq}$. Whereas the QCD Lagrangian is invariant under full chiral symmetry in the case $m_q = 0$, a non-vanishing chiral condensate is only invariant under the subgroup $U(N_f)_V$, $\Phi \longrightarrow U_V \Phi U_V^\dagger = \Phi$ (compare with App. A.2), but not under $U(N_f)_A$. Chiral symmetry is hence broken by a non-vanishing chiral condensate following the pattern

$$U(N_f)_R \times U(N_f)_L \to U(N_f)_V \ . \tag{3.7}$$

Again, in presence of dynamical quarks one can speak of an exact first-order phase transition if one redefines the order parameter by subtracting its value at the transition point: $\langle \overline{\psi}_p \psi_q \rangle \to \langle \overline{\psi}_p \psi_q \rangle - \langle \overline{\psi}_p \psi_q \rangle_c$. A second-order phase transition is only possible at a critical endpoint in case of dynamical quark masses. Otherwise a second-order phase transition found for vanishing quark masses will be turned into a crossover.

A sketch of the QCD phase diagram consistent with the current results from different approaches towards QCD is shown in Fig. 3.1. In the so-called Columbia plot (compare Fig. 3.2), the

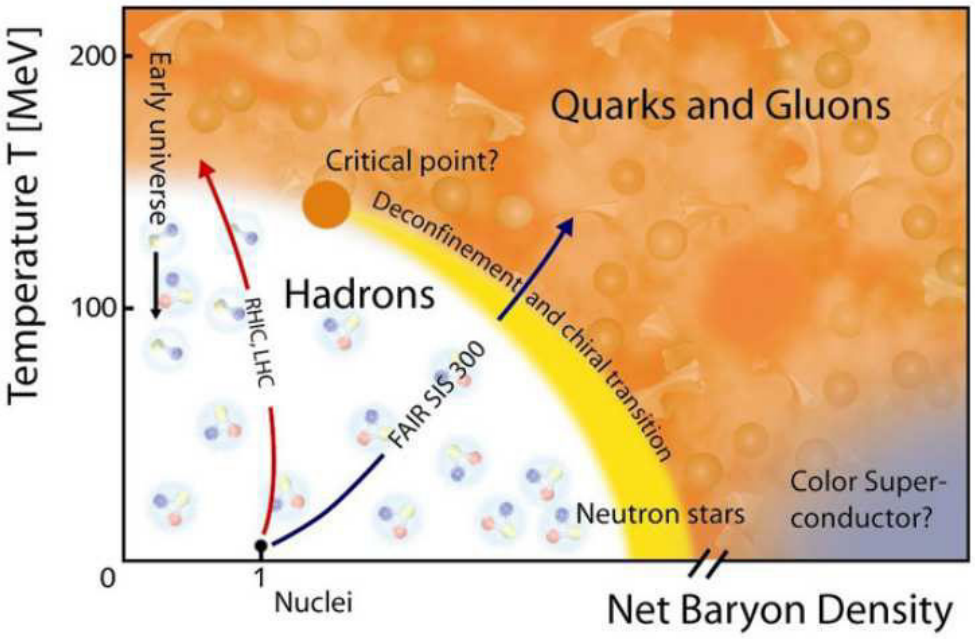

Figure 3.1: Conjectured QCD phase diagram. Taken from Ref. [66].

QCD phase diagram in the $m_{u,d}$-m_s plane for vanishing chemical potential, the order of the

QCD phase transitions is summarized. Originally its form was based on lattice calculations at

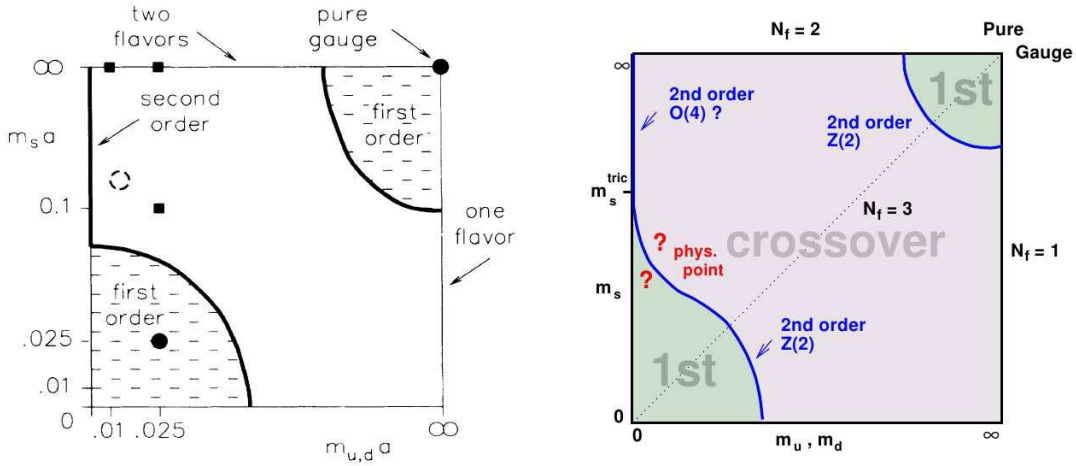

Figure 3.2: Conjectured QCD phase diagram for vanishing baryonic chemical potential. The left panel shows the original Columbia plot of the Columbia group [67], where filled dots mark points where lattice calculations were performed, and the dashed circle indicates the point of physical quark masses. The right panel shows a modern, more refined version [68].

only a few points in the different regimes [67]. The plot is schematic in two ways. First, it is only the simplest possible form consistent with the results so far. In particular, the shape of the second-order boundaries is simply a sketch. The existence of merely two points, randomly picked, one associated to a first-order phase transition and another associated to a crossover transition, already give rise to the conclusion that a second-order boundary should exist in between (compare with the discussion in Sec. 2.1). Second, the lower left corner corresponds to the chiral transition, whereas the upper right corner is associated with the deconfinement transition. Both transitions are no real phase transitions in between the limit of small and large quark masses, respectively, and hence the label 'crossover' in the plot refers to both, either the chiral transition or the deconfinement transition. We emphasize however that both transitions have to be distinguished from each other.

Later, the form of the phase diagram was verified from other approaches towards QCD. Fig. 1.2. in chapter I.1. of Ref. [4] (and the discussion thereof) comprises an enlightening summary of their applicability in different regions of the diagram. It provides as well an insight from which sources our information about the QCD phase diagram stems. A question still under debate is whether the point associated to the real quark masses falls into the crossover or into the first-order region. Further, efforts were made to determine the universality class of the second-order lines (see Sec. 3.3 for details). The possibility of $O(4)$ criticality for infinitely high strange quark mass (i.e., effectively $N_f = 2$) on the one hand, and indication for $Z(2)$ universality along the second-order boundaries on the other hand gives rise to the prediction of a tricritical point at some critical value m_s^{tric}, where the universality class changes from $Z(2)$ to $O(4)$. Until very recently, it has been assumed that the phase transition can only be of second-order in presence of the axial anomaly, and if so, it should belong to the $O(4)$ universality class. However, as

demonstrated in Ref. [33] (see also Sec. 6.5), a second-order phase transition can also exist in absence of the anomaly. Consistent with Refs. [1, 33] we do not expect a second-order phase transition for finite anomaly strength, but also this statement should be thoroughly checked. For a detailed discussion we refer to Sec. 3.3.2.

3.2 Instantons and the axial anomaly

Although the explicit breaking of the $U(1)_A$ symmetry contained in Eq. (3.5) plays a major role in this work, our investigations did not require a deeper knowledge of the circumstances causing the anomalous breaking. Within the scope of this thesis we are only concerned with the implications for the order of the chiral phase transition. Nevertheless, we want to briefly discuss some central aspects concerning the general background.

Instantons are solutions to the Euclidean classical equations of motion of quantum mechanics or of quantum field theory, for which the action takes a finite value [69]. A prominent example for an instanton solution is the one in the gauge sector of QCD, encountered by Polyakov and collaborators [70]. These gauge-field configurations are also of relevance for light quark dynamics, for example in the case of the axial anomaly. It was shown by t'Hooft that instantons explicitly break the axial $U(1)_A$ symmetry of QCD, which explains why the η' meson is not an (approximate) Goldstone particle in the real world [71]. Whereas the QCD Lagrangian is invariant under $U(1)_A$ transformations in the chiral limit at the classical level, quantum corrections lead to a non-conservation of the associated Noether current. This is an example of a general situation to which one refers to as an anomaly, in this special case called *axial anomaly*. Whereas the breaking pattern (3.7) would yield N_f^2 (approximate) Goldstone particles (in presence of nonzero quark masses), which equals the number of generators of the broken $U(N_f)_A$, there remain only $N_f^2 - 1$ of them if the explicit breaking of $U(1)_A$ is taken into account. As already mentioned, this explains why the η' is significantly heavier than the members of the pseudoscalar $SU(N_f = 3)$ octet (the approximate Goldstone particles). More precisely, the axial $U(1)_A$ is not completely broken but a discrete $Z(N_f)$ symmetry remains, which is related in a certain way with the speculative possibility of CP violation in QCD [72]. And this is only one of many examples illustrating how far-reaching the implications of the anomalous breaking actually are (or could be, respectively).

Our next remark concerns the notion *anomaly strength*. We were already concerned with an explicit breaking of symmetry in the case of nonzero quark masses breaking chiral symmetry. In this context the *strength* of the explicit breaking is determined by the quark masses. Light quarks break chiral symmetry only *weakly*. In this sense, a large number of instantons breaks $U(1)_A$ *stronger* than a small number. Accordingly, the instanton density is a measure for the strength of the anomaly. Correspondingly, in the framework of the linear sigma model one can quantify the anomaly strength by the coefficient in front of the $U(1)_A$-breaking term (compare with Sec. 3.3.2).

Finally, we want to state an expression for the instanton density n which was derived by the authors of Ref. [73]:

$$n(Q,T) = n(Q,0)\exp\left[-\frac{1}{3}\lambda^2(2N_c+N_f) - 12A(\lambda)\left(1+\frac{1}{6}\left[N_c-N_f\right]\right)\right]. \tag{3.8}$$

In the following we list the quantities entering the above equation:

$$n(Q,0) = C_{N_c} Q^5 \left(\frac{4\pi^2}{g^2}\right)^{2N_c} \mathrm{e}^{-8\pi^2/g^2}\, \zeta Q^{-1} \prod_i m_i \ , \tag{3.9}$$

$$A(\lambda) \simeq -\frac{1}{12}\ln\left(1+\frac{\lambda^2}{3}\right) + \alpha\left(1+\gamma\lambda^{-3/2}\right)^{-8} \ , \tag{3.10}$$

$$\frac{4\pi}{g^2(Q)} = \frac{4\pi}{g^2(Q_0)} - \frac{1}{6\pi}(33-2N_f)\ln\frac{Q_0}{Q} \ , \tag{3.11}$$

$$C_{N_c} = 0.260156\zeta^{-(N_c-2)}/(N_c-1)!(N_c-2)! \ , \tag{3.12}$$

$$\lambda = \pi T/Q \ , \tag{3.13}$$

where Q denotes the inverse of the instanton scale size $\rho = Q^{-1}$. Eq. (3.11) is the perturbative one-loop renormalization group equation for the running coupling constant of QCD, g, with Q_0 denoting an arbitrary reference scale, at which the value of g is known. A common choice for Q_0 is the mass of the Z-boson, for which $g^2(M_Z)/4\pi = 0.1184 \pm 0.00007$ [74]. The light quark masses are denoted by m_i, N_c denotes the number of colors, and N_f the number of flavors. Finally, $\zeta = 1.33876$, $\alpha = 0.01289764$, and $\gamma = 0.15858$.

3.3 Critical behavior in QCD

In this chapter we want to discuss aspects which are of importance for the current understanding of critical behavior in QCD.

3.3.1 Ising universality in QCD

The boundary in the lower left corresponding to a second-order chiral phase transition is commonly claimed to inevitably fall into the Ising universality class. This statement is often founded on a mean-field analysis of the linear sigma model [75] where the dynamical quark masses are taken into account by an explicit symmetry breaking term. In a strict sense the universality hypothesis is only applicable in case of exact chiral symmetry. In order to determine the universality class for QCD with physical quark masses from the linear sigma model one has to make the nontrivial assumption that the universality hypothesis is also valid in presence of (small) explicit symmetry breaking for critical endpoints. Ref. [75] demonstrates that only the sigma particle becomes massless when tuning the mass parameter of the model towards the critical value. According to group-theoretic arguments the Ising universality class is believed to be the only one possible in case of a single-component order parameter (see the discussion of the Ising model (2.36) in Sec. 2.4). Further assuming the number of massless modes not to change beyond mean-field one arrives at the above statement. The same arguments can be used to justify that the critical endpoint at nonzero chemical potential should belong to the Ising universality class as well.

Ref. [15] has been seminal in the case of the critical endpoint of QCD. The authors apply the CJT formalism in ladder approximation directly to QCD extending the work of Ref. [76]. Investigating the behavior of the chiral condensate in the chiral limit for $N_f = 2$, they find a second-order line (SOL) and a first-order line (FOL) joining in a tricritical point (TCP). The critical behavior at

the TCP should belong instead to another universality class. In contrast to Ref. [76], the authors also study the influence of nonvanishing quark masses. As expected, they find that the quark condensate decreases with increasing temperature and/or chemical potential, however, it never vanishes. This is a consequence of the explicitly broken chiral symmetry. One can still speak of a first-order phase transition by considering the quark condensate minus its value at the transition point where the condensate shows a discontinuous jump (to a nonvanishing value). A first-order line ends in a critical endpoint (CEP), where the discontinuity vanishes and the transition becomes crossover. At the CEP the condensate drops down from a rather high to a very small value and its temperature gradient is infinite. Consequently, the transition is hard to distinguish from a second-order phase transition at the CEP. The distance between the CEP and the TCP becomes larger with increasing quark mass. Now the authors calculate quark-number and chiral susceptibilities which are expected to diverge at a second-order phase transition (compare with Sec. 2.2) in the neighborhood of the TCP and determine critical exponents. For very large quark masses, $m_q > 100$ MeV, one observes a mean-field critical exponent of 2/3. This is explained by the fact that the TCP does not lie in the critical region of the CEP (i.e., the region where nontrivial critical exponents associated to the CEP are observed) in this case. Accordingly one finds mean-field exponents associated to the CEP. For nearly vanishing quark mass, $m_q = 0.1$ MeV, one finds critical exponents significantly distinct from mean-field values, which indicates that the TCP has influence. The influence becomes weaker with increasing quark mass, however, it is still significant for realistic quark mass $m_q = 5$ MeV.

Apart from certain peculiarities involved in the ladder approximation (for example only a QCD-like running coupling is used), the results mentioned so far can be regarded as derived from first principles. One can conclude as follows. Although the TCP is only of exact nature for $m_q = 0$, it still affects the critical exponents significantly at physical quark mass m_q where it is only of approximate character. Also the CEP gives rise to critical behavior in the susceptibilities. However, it remains an open question to which extent Ising universality exists close to the CEP. It should be possible to derive scaling corrections in dependence of m_q in analogy to those for the critical endpoint of the liquid-gas transition. In this case there does not exist an exact symmetry either, nevertheless one observes $Z(2)$ (Ising) critical behavior[2] with $Z(2)$-noninvariant corrections to the power laws [14]. Another critical endpoint which should correspond to the Ising universality class is the one of nuclear matter. In comparison with the critical endpoint of QCD it is experimentally much better accessible. In fact, it has been stated in Sec. I.2.2.3.4 of Ref. [4] that actually measured critical behavior is in agreement with Ising universality.

Another part of Ref. [15] consists of partly courageous universality considerations complementary to their study in the framework of the CJT formalism. We address these points in the following. First of all, the authors speculate that the second-order line SOL corresponds to a sequence of $O(4)$ critical points. This extends the original $O(4)$ conjecture, which predicts an $O(4)$ critical point for $\mu = 0$ and $m_q = 0$ if the strength of the axial anomaly is sufficiently high (see Sec. 3.3.2). Unfortunately we are not familiar enough with the assumptions involved in the ladder approximation in order to judge their interesting proposal.

Our second remark concerns the role of the sigma particle. According to the authors of Ref. [15]

[2]For a first-principle derivation (not assuming an effective Landau potential) of the $Z(2)$-symmetric critical endpoint present in a microscopic liquid-gas model we refer to Ref. [77].

(and in consistence with Ref. [75]) the sigma field is the soft mode for both the TCP and the CEP, i.e. drives the divergence in the susceptibilities. There is evidence that this is not true for the CEP. Due to the far-reaching implications of this point, in the following we explain in large detail why. The authors themselves mention the similarity with the situation in the NJL model by citing Ref. [78]. Qualitatively the same phase diagram, containing a tricritical point and a critical endpoint, is found in a simple NJL model,

$$\mathcal{L} = \bar{\Psi}(i\gamma^\mu\partial_\mu - m_q)\Psi + G_1\left([\bar{\Psi}\Psi]^2 - [\bar{\Psi}\gamma_5\vec{\tau}\Psi]^2\right) , \tag{3.14}$$

which can be derived as an effective theory for QCD from first principles neglecting explicit gluonic degrees of freedom and most of the hadronic degrees of freedom. Such a derivation becomes obvious from the discussion in Sec. 4.4, more precisely from expression (4.36), which for $G_2 = G_3 = G_4 = 0$ yields the Lagrangian (3.14) if the gluonic part is neglected. See also Ref. [79] for a more explicit derivation. We note that at least to some extent, gluon dynamics effectively hides in the four-fermion couplings. As pointed out by Fujii in Refs. [80, 81], the sigma particle remains massive at the critical endpoint of the NJL model (see also Ref. [82]) while certain susceptibilities diverge. The phase transition associated with such a significant divergence can not be driven by the massive sigma particle. Again, the situation is similar to the Ising-like continuous transition at the critical endpoint of the liquid-gas transition. According to Fujii, at the CEP the soft mode driving the divergences in the susceptibilities is given by a scalar density fluctuation. At the TCP, i.e. in the chiral limit, the soft mode is the sigma field instead. We note that, although the (tri)critical endpoint is a feature of the chiral phase transition, its location might be affected by the deconfinement transition. The interplay with the Polyakov loop is taken into account in PQM (Polyakov-Quark-Meson) and PNJL (Polyakov-Nambu-Jona-Lasinio) models.
Due to the strongly-coupled nature of QCD near the chiral and the deconfinement phase transition, nonperturbative methods are indispensable. First of all there is lattice QCD which at nonvanishing baryonic chemical potential suffers from the infamous sign problem: the fermion determinant is complex valued with vanishing average phase factor in the thermodynamic limit, which rules out standard Monte-Carlo techniques. Fortunately so-called reweighting methods have been recently developed allowing to study QCD at nonvanishing chemical potential. For example in Ref. [83] the existence of a critical endpoint is inferred for semi-realistic quark masses (whereas the strange quark mass is reasonable, the up and down quark mass are four times heavier than in reality) from the so-called Lee-Yang zeros of the partition function. On the other hand, the computation time rises with decreasing quark masses, for vanishing as well as for nonvanishing chemical potential, which still hampers a reliable answer to the $O(4)$ conjecture. The latter is the main subject of this thesis and will be introduced in the following section.

3.3.2 From the linear sigma model to the $O(4)$ conjecture

In this section we address the upper left corner of the Columbia plot (Fig. 3.2), i.e., the two-flavor case, $N_f = 2$. An effective theory for the order parameter, the chiral condensate, is given by the linear sigma model. In Sec. 4.4 we discuss how such an effective theory could in principle be derived starting from QCD and imposing approximations in successive stages.

The final step in this approach would consist in an approximate calculation of the fermion determinant, stated in Eq. (4.45), which is a major contribution to the action of the effective theory. Instead of explicitly calculating the fermion determinant one can perform an expansion guided by symmetry. Consistent with Sec. 4.4 we assume that the relevant degrees of freedom are mesons, i.e., the expansion should be in terms of mesonic fields. On the other hand, consistent with Landau theory, it should be an expansion in terms of the order parameter. This is actually in perfect agreement because, as shown in App. A.2, in flavor space the chiral condensate can be parameterized by the mesonic fields. In the following we assume that the relevant degrees of freedom are the scalar mesons σ and $\vec{a}_0$ on the one hand, and the pseudoscalar mesons η and $\vec{\pi}$ on the other hand. In the representation $[2,\overline{2}]\oplus[\overline{2},2]$ of $SU(2)\times SU(2)$, the chiral condensate, Φ, can be parameterized in terms of these mesonic fields [compare with Tab. A.1 and Eq. (A.50)]:

$$\Phi = \frac{1}{\sqrt{2}}\left[(\sigma + \mathrm{i}\,\eta)\mathbf{1}_2 + (\vec{a}_0 + \mathrm{i}\,\vec{\pi})\cdot\vec{\tau}\right] \ . \tag{3.15}$$

We further assume that long-range interactions between the mesons can be neglected. In addition we neglect explicit contributions of quarks and gluons. Their effect is, of course, to a certain extent contained in the effective mesonic degrees of freedom and the effective interactions between them. As far as it concerns the critical behavior, taking into account quarks explicitly should not turn a second-order phase transition into a first-order one since the lowest fermionic Matsubara frequency, $\nu_0 = 2\pi T$, adds a thermal contribution to the effective quark mass (compare also with the discussion of dimensional reduction in Sec. 2.3). Since only light degrees of freedom play a role at a second-order phase transition, quarks should not wash out critical behavior if it exists in their absence. The situation is different for the gauge fields. Following Ref. [84], it is even very likely that gauge-field contributions lead to a fluctuation-induced first-order transition (compare with Sec. 4.4). Taking account of gauge-field fluctuations is a task for future investigations. We proceed with the construction of the most general Lagrangian invariant under chiral symmetry in the representation $[2,\overline{2}]\oplus[\overline{2},2]$. We note that most of the following has been taken from our publication [1].

The most general perturbatively renormalizable Lagrangian for $D = 3$ (neglecting the anomalous dimension) which is invariant under the chiral $U(N_f)_V \times U(N_f)_A$ symmetry of QCD, where N_f denotes the number of quark flavors, was investigated by Pisarski and Wilczek [85] regarding the order of the chiral phase transition. Choosing the $[\bar{N}_f, N_f]\oplus[N_f,\bar{N}_f]$ representation of $SU(N_f)_A \times SU(N_f)_A$, in Euclidean space this Lagrangian reads

$$\mathscr{L}_\Phi = \frac{1}{2}\mathrm{Tr}(\partial_\mu\Phi^\dagger)(\partial_\mu\Phi) + \frac{1}{2}m_\Phi^2\mathrm{Tr}\Phi^\dagger\Phi + \frac{\pi^2}{3}g_1(\mathrm{Tr}\Phi^\dagger\Phi)^2 + \frac{\pi^2}{3}g_2\mathrm{Tr}(\Phi^\dagger\Phi)^2 \ . \tag{3.16}$$

We note that the ϵ-expansion is a perturbative method and hence one neglects perturbatively nonrenormalizable terms in this approach. Instead, in nonperturbative approaches (such as FRG) one has to consider their influence (compare with the discussion of the polynomial order in Sec. 2.4). The invariance under axial and vector transformations (A.51) can be easily confirmed from the invariance of the trace under cyclic permutations. The circumstance that instantons explicitly break the $U(1)_A$ [71] (see also Ref. [86]) is known as $U(1)_A$ anomaly. The authors of Ref. [85] conjectured that, for $N_f = 2$, the chiral phase transition of QCD can be of second order in the presence of the $U(1)_A$ anomaly. In this case, it would fall into the $O(4)$ universality class. This

is the already mentioned $O(4)$ conjecture.
The term commonly introduced into Eq. (3.16) in order to explicitly break the $U(1)_A$ symmetry is

$$\det\Phi^\dagger + \det\Phi \,. \tag{3.17}$$

In Sec. 5.3 we show that, for $N_f = 2$, the most general form of the anomaly including terms up to naive scaling dimension four is [65]

$$\mathcal{L}_A = c\left(\det\Phi^\dagger + \det\Phi\right) + y\left(\det\Phi^\dagger + \det\Phi\right)\mathrm{Tr}\Phi^\dagger\Phi + z\left[\left(\det\Phi^\dagger\right)^2 + \left(\det\Phi\right)^2\right] . \tag{3.18}$$

These terms must be added to Eq. (3.16),

$$\mathcal{L} = \mathcal{L}_\Phi + \mathcal{L}_A \,, \tag{3.19}$$

if one wants to study the impact of the $U(1)_A$ anomaly on the chiral phase transition. For $N_f = 2$ and including terms up to naive scaling dimension four, the Lagrangian (3.19) is the most general Lagrangian invariant under $SU(2)_A \times U(2)_V$ and respecting parity symmetry. We note that the terms $\sim y, z$ are always induced by the RG flow if $c \neq 0$. Therefore, in the following we shall use the notion "in the presence of the anomaly", whenever $c \neq 0$. Note also that

$$\left(\det\Phi^\dagger + \det\Phi\right)^2 = -\mathrm{Tr}(\Phi^\dagger\Phi)^2 + (\mathrm{Tr}\Phi^\dagger\Phi)^2 + \left[\left(\det\Phi^\dagger\right)^2 + \left(\det\Phi\right)^2\right] , \tag{3.20}$$

so that the square of the term (3.17) is not linearly independent from the other invariants contained in Eq. (3.18). Finally note that

$$i\left(\det\Phi^\dagger - \det\Phi\right) \tag{3.21}$$

is not invariant under CP transformations [85].
In this work, we consider the case $N_f = 2$. The Lagrangian (3.19) can be rewritten as [87]

$$\mathscr{L} = \frac{1}{2}\left(\partial_\mu\sigma\partial_\mu\sigma + \partial_\mu\vec{\pi}\cdot\partial_\mu\vec{\pi} + \partial_\mu\eta\partial_\mu\eta + \partial_\mu\vec{a}_0\cdot\partial_\mu\vec{a}_0\right) + U \,, \tag{3.22}$$

$$\begin{aligned} U = {} & \frac{1}{2}\mu^2\left(\sigma^2 + \vec{\pi}^2 + \eta^2 + \vec{a}_0^2\right) + \frac{\lambda_1}{4!}\left(\sigma^2 + \vec{\pi}^2 + \eta^2 + \vec{a}_0^2\right)^2 \\ & + \lambda_2\left[\left(\sigma^2 + \vec{\pi}^2\right)\left(\eta^2 + \vec{a}_0^2\right) - \left(\sigma\eta - \vec{\pi}\cdot\vec{a}_0\right)^2\right] \\ & + c\left(\sigma^2 - \eta^2 + \vec{\pi}^2 - \vec{a}_0^2\right) + y\left(\sigma^2 + \vec{\pi}^2 + \eta^2 + \vec{a}_0^2\right)\left(\sigma^2 - \eta^2 + \vec{\pi}^2 - \vec{a}_0^2\right) \\ & + z\frac{1}{2}\left(\eta^2 + \vec{a}_0^2 - \sigma^2 - \vec{\pi}^2 - 2\vec{a}_0\cdot\vec{\pi} + 2\eta\sigma\right)\left(\eta^2 + \vec{a}_0^2 - \sigma^2 - \vec{\pi}^2 + 2\vec{a}_0\cdot\vec{\pi} - 2\eta\sigma\right) \,, \end{aligned} \tag{3.23}$$

where $\lambda_1 \equiv 4!\frac{\pi^2}{3}\left(g_1 + \frac{1}{2}g_2\right)$, $\lambda_2 \equiv 2\frac{\pi^2}{3}g_2$, $\mu^2 \equiv m_\Phi^2$. For $c = 0$, $y = 0$, and $z = 0$ Eq. (3.22) reduces to the $U(2)_L \times U(2)_R$-symmetric Lagrangian (3.16).
The RG flow for the Lagrangian (3.16) was analyzed for different values of N_f. The results from the ϵ-expansion [65, 88] prove that for $N_f = 2$ the $O(8)$-symmetric infrared (IR) fixed point is unstable, which is confirmed from FRG studies [87] as well as from lattice calculations [89]. The absence of a IR-stable fixed point is a sufficient criterion for the phase transition to be of first order. Very recently, however, the existence of an IR-stable $U(2)_A \times U(2)_V$-symmetric fixed point has been confirmed in a RG approach similar to the ϵ-expansion [33]. The authors convincingly

explain this surprising finding by a failure of the low-loop ϵ-expansion, which only finds fixed points that also exist near $D = 4 - \epsilon$. Their perturbative field theoretic RG approaches (MZM scheme and $3D\overline{MS}$ scheme, respectively) circumvent an expansion in ϵ. Instead, the perturbative expansion is directly performed for $D = 3$. Their results pushed us to a FRG investigation of the most general $U(2)_A \times U(2)_V$-potential in higher truncation order (see Sec. 6.5). The FRG approach is perfectly fine with $D = 3$ as well, and due to its nonperturbative nature it goes beyond the one-loop ϵ-expansion, the results of which can be reproduced using a quartic truncation in the limit of vanishing mass term. Going to sixth order in the canonical scaling dimension we can indeed confirm the existence of two IR-stable $U(2)_A \times U(2)_V$-symmetric fixed points (see Sec. 6.5). The results at this (and higher) truncation order, however, are inconclusive because the Gaussian fixed point aquires marginal stability-matrix eigenvalues. Further investigations are in progress.

Apart from our publication [1] we are not aware of other explicit RG calculations for the Lagrangian (3.22) in the presence of anomaly terms. The FRG study presented in Refs. [90, 91] neglects the fields η and $\vec{a}_0$ from the beginning. A very recent qualitative discussion can be found in Ref. [33]. Other RG results in the presence of the anomaly can be found in the literature only for cases where the anomaly term acts as a coupling of order higher than two [see for example Refs. [92, 93, 94, 95, 96]]. Also, studying how c approaches ∞ has not yet been investigated explicitly on the level of RG flow equations. In Sec. 6.6 we want to fill these gaps by appropriately extending the study presented in Ref. [87].

The $U(1)_A$ anomaly explicitly breaks the $U(1)_A$ symmetry contained in $G \equiv U(N_f)_V \times U(N_f)_A \simeq U(1)_V \times U(1)_A \times [SU(N_f)/Z(N_f)]_L \times [SU(N_f)/Z(N_f)]_R$ down to $Z(N_f)_A$, where $\simeq$ symbolizes group isomorphy. The group $U(1)_V$ is associated with baryon number conservation and should not be broken (spontaneously) during the phase transition. Thus one usually argues that one can neglect it when studying the chiral phase transition, leaving $[SU(N_f)_L \times SU(N_f)_R]/Z(N_f)_V \to SU(N_f)_V/Z(N_f)_V$ for the symmetry breaking pattern relevant for the chiral phase transition in the presence of the anomaly [65]. The spontaneous breaking of a discrete symmetry does not yield Goldstone modes, such that it is sufficient to consider the breaking of the continuous group $G' \equiv SU(N_f)_L \times SU(N_f)_R$ in the chiral phase transition in the presence of the anomaly. In Sec. 6.6 we nevertheless consider the effective theory for the order parameter invariant under $U(1)_V \times G'$ in the search for the IR fixed point associated to spontaneous breaking of $SU(N_f)_L \times SU(N_f)_R$. We can now substantiate the $O(4)$ conjecture. We neglected (a) the possible existence of long-range interactions between the mesons, (b) gluonic contributions, and (c) other than the lightest scalar and pseudoscalar mesons. Assuming in addition (d) the validity of the universality hypothesis (see Sec. 2.4), we conclude that if the chiral phase transition of two-flavor QCD in the presence of the anomaly is of second order, then the Lagrangian (3.22) falls into the same universality class as QCD. The Lagrangian (3.19) has eight degrees of freedom, whereas the $O(4)$ model has only four. It is therefore a priori not clear that the Lagrangian (3.19) has an IR-stable $O(4)$ fixed point. Due to the existence of two mass terms one expects two relevant directions instead. This corresponds to the fact that the representation of the Lagrangian (3.22), or (3.19), respectively, is reducible. It consists of the sum of two equivalent $O(4)$ representations [65, 97, 98] (see Sec. A.2), $\Phi_1 = \sigma t_0 + i\vec{t} \cdot \vec{\pi}$ and $\Phi_2 = i\eta t_0 + \vec{t} \cdot \vec{a}$, which are both irreducible, but not faithful,

representations of $SU(2) \times SU(2)$. This circumstance is due to the isomorphism

$$SU(2) \times SU(2)/Z(2) \simeq SO(4) \,, \tag{3.24}$$

which means that $SU(2) \times SU(2)$ is locally isomorphic to $O(4)$. Therefore, the symmetry of QCD allows for an $O(4)$ representation, if only the sigma and pion are light particles. At mean-field level this can be confirmed. The analysis in Refs. [99, 100] shows that if we identify $\vec{\pi}$ with the Goldstone modes[3], the fields η and $\vec{a}_0$ are massive at the critical point, whereas the field σ is as light as the pions (and can be interpreted as the chiral partner[4] of the pion). Since at the critical point only the modes with smallest mass are relevant (i.e., which count as components of the order parameter), we conclude that, if the mean-field approximation were justified, the IR fixed point would indeed be the stable Wilson-Fisher fixed point of the $O(4)$ model.
Of course, the mean-field approximation neglects quantum fluctuations (such as instantons), which might change the universality class or might lead to the instability of the fixed point. For this reason we study the FRG flow for the Lagrangian (3.22) in Sec. 6.6. One could argue that for very large anomaly strength, $c \to -\infty$, η- and $\vec{a}$-loop diagrams should be suppressed according to the Appelquist-Carazzone decoupling theorem [18] due to the very high tree-level mass for the corresponding fields. Since the ϵ-expansion deals only with loop diagrams, one can indeed expect to find the $O(4)$ fixed point [5]. However, this argument says nothing about (a) the stability of the $O(4)$ fixed point and (b) the cases of small and intermediate anomaly strength.

3.3.3 A few words on experiments

According to Ref. [101] "the discovery of the critical point would in a stroke transform the map of the QCD phase diagram from one based only on reasonable inference from universality, lattice gauge theory and models into one with a solid experimental basis." So far, apart from vague evidence, a reliable experimental detection has not happened yet. This might change with the upcoming CBM experiment [4, 102] which will study for example event-by-event (ebye) fluctuations of observables indicating the existence of a critical point. In particular, the CBM detector will be able to detect ebye fluctuations in the kaon-pion and the proton-pion ratio using the time of flight method.
Although there exist ideas how one could (in principle) measure static critical exponents near the QCD critical endpoint (see for instance Ref. [103]), in reality this is rather unrealistic. A severe problem is the short duration of a heavy-ion collision. Together with relation (2.10) the growth of the correlation length is severely limited (see Ref. [101] for details). This makes it extremely hard to observe a signal in the correlation length when the system cools through the critical point.
There is even less hope to find (remnants of) $O(4)$ critical behavior in experiment, however,

[3] The spontaneous breaking of $SU(2)_A$ gives rise to $N_f^2 - 1 = 3$ Goldstone bosons, the pions, which in reality acquire a (small) mass due to the explicit breaking of chiral symmetry caused by the (small) quark masses m_q. One can take account of this small mass by the introduction of an explicit symmetry breaking term. We restrict our investigation, however, to the chiral limit where $m_q \equiv 0$.

[4] Chiral partners should become degenerate in mass in the chirally restored phase.

[5] Note that in the limit $c \to -\infty$ the $O(4)$ fixed point corresponds to the above mentioned $O(4)$ representation $\Phi_1 = \sigma t_0 + i\vec{t} \cdot \vec{\pi}$. The limit $c \to \infty$ would in turn correspond to the equivalent $O(4)$ representation $\Phi_2 = i\eta t_0 + \vec{t} \cdot \vec{a}$ with σ and $\vec{\pi}$ simply exchanging roles with η and $\vec{a}$.

it is not ruled out completely (compare with Ref. [104]). A basic requirement is of course a medium with baryonic chemical potential as small as possible. This is the case for the early universe which went through the QCD phase transition. Unfortunately, we are not aware of any measurable consequences of a second-order phase transition in this case. Another possibility are observables at mid-rapidity in heavy-ion collisions since this regime is rather free of baryons [4]. The further restrictions are obvious. First of all it is questionable if the strange quark mass is high enough to allow for an effective two-flavor scenario where a second-order phase transition is possible. Second, physical quark masses explicitly break chiral symmetry turning the second-order phase transition into a crossover, so that only remnants of criticality might be observable. On top of this, as in the case of the critical endpoint, there is the problem of finite-size effects and critical slowing down which drastically limits the correlation length. Apart from these limitations one could look at similar observables as in the search for the critical endpoint (certain ebye correlations, enhancement of particles interacting strongly with the sigma and/or the pions, etc.).

Chapter 4

FRG

4.1 Wetterich equation

Before we begin our discussion, let us note that a large amount of our understanding about the Functional Renormalization Group (FRG) method was gained from the excellent textbook of Peter Kopietz, Lorenz Bartosch, and Florian Schütz [6]. For an introduction to the subject from scratch, we refer to this detailed work. Their textbook also provides a prescription of Functional Methods in general, which allows for a self-contained introduction to the FRG approach, as well as the derivation of what lies at heart of the latter, the *Wetterich equation*. Our discussion sets in at that point, explaining the meaning behind this powerful tool.
The basic idea lying at heart of the FRG approach is the same as the one discussed in Sec. 2.3, namely averaging out fluctuations and absorbing their effect into the parameters of the theory. In the context of a theory which can be described by an effective action Γ, the *Wetterich equation*

$$\partial_k \Gamma_k = \frac{1}{2} \mathrm{STr}\left[(\partial_k \mathbf{R}_k) \left(\mathbf{\Gamma}_k^{(2)} + \mathbf{R}_k \right)^{-1} \right] \tag{4.1}$$

implements such an averaging, where the average effective action, $\Gamma_k[\Phi]$, is a functional of field components Φ_α and depends on the momentum scale k. The superfield label α may contain continuous as well as discrete components. For example, in case of an N-component scalar field theory in D-dimensional space, the superfield label reads $\alpha = (i, \vec{p})$, so that $\Phi_\alpha = \Phi_i(\vec{p})$, where $\vec{p}$ is a D-dimensional momentum vector, and $i = 1, ..., N$. In the following we denote $p = |\vec{p}|$. The supertrace $\mathrm{STr}[...] \equiv \mathrm{Tr}[\mathbf{Z}...]$ involves the statistics matrix $\mathbf{Z}$, which implies a minus sign in case of fermionic (i.e., Grassmann-valued) field components:

$$\mathbf{Z}_{\alpha\alpha'} = \delta_{\alpha\alpha'} \zeta_\alpha \ , \tag{4.2}$$

where $\zeta_\alpha = (-)1$ if Φ_α is a bosonic (fermionic) field component. The statistics matrix enters due to the anticommutation of Grassmann numbers and appears also in the matrix $\mathbf{\Gamma}_k^{(2)}$:

$$\left(\mathbf{\Gamma}_k^{(2)} \right)_{\alpha\alpha'} = \frac{\delta^2 \Gamma_k}{\delta\Phi_\alpha \delta\Phi_\beta} \mathbf{Z}_{\beta\alpha'} \ . \tag{4.3}$$

Aside from the field components, the average effective action, $\Gamma_k\left[\Phi(p); \lambda_k\right]$, contains couplings λ_k mediating the interaction between them. In D-dimensional space, apart from other parameters,

the degrees of freedom always carry momenta p, i.e., occur in various momentum modes. However, the momenta p are restricted to values smaller than k. Consistent with Sec. 2.3, let us assume that the system is described at a certain microscopical level by an effective action $\Gamma_{k=\Lambda}[\Phi(p);\lambda_\Lambda]$, where the degrees of freedom Φ carry momenta p smaller than some ultraviolet (UV) cutoff Λ. Integrating Eq. (4.1) down from Λ to some momentum k_0, one obtains in result the average effective action $\Gamma_{k=k_0}[\Phi(p);\lambda_{k_0}]$, where modes $\Phi(p > k_0)$ have been eliminated. However, due to averaging process involved, the degrees of freedom still feel the presence of these modes. As in Sec. 2.3, their effect simply has been absorbed into the couplings λ_{k_0}. Integrating the flow equation down to the *infrared* (IR) limit, $k = 0$, one effectively takes account of all possible momentum modes, i.e., all fluctuations allowed in the system. In the derivation of Eq. (4.1), a k-dependent inverse free propagator is introduced by adding a regulator $\mathbf{R}_k(p)$ to the inverse free propagator for the field $\Phi(p)$,

$$\mathbf{G}_{0,k}^{-1}(p) = \mathbf{G}_0^{-1}(p) - \mathbf{R}_k(p) \ , \tag{4.4}$$

where the regulator is necessarily defined such that

1. only modes $\Phi(p \approx k)$ contribute to $\partial_k \Gamma_k$ at the scale k, which assures that the modes are successively integrated out,
2. $|(\mathbf{R}_{k\to 0})_{\alpha\alpha'}| = 0$, which assures that all modes have been taken into account in the IR limit,
3. $|(\mathbf{R}_{k\to\Lambda})_{\alpha\alpha'}| = \infty$, which assures that the ultraviolet (UV) limit is obtained at $k = \Lambda$.

If these conditions are fulfilled, the results in the IR limit should be independent from the particular definition for the regulator. The form of the flow equations derived from Eq. (4.1), however, depends on the definition, and hence the choice of the regulator is of great practical importance. Finally, we note that Eq. (4.1) is an *exact* equation, i.e., no approximation is involved. In the following section we discuss the approximation which is used throughout this thesis.

4.2 Local-Potential Approximation

For simplicity, and since we are concerned with fermions only in Sec. 7.3, we restrict the discussion to bosonic fields, i.e. N scalar fields Φ_i, for the rest of this chapter. At nonzero temperature a scalar field theory is defined by the action

$$S = \int_0^{1/T} d\tau \int d^D\mathbf{x} \left(\frac{1}{2} \partial_\mu \Phi(\tau,\mathbf{x}) \cdot \partial_\mu \Phi(\tau,\mathbf{x}) + U(\Phi(\tau,\mathbf{x})) \right) \ , \tag{4.5}$$

where the metric is Euclidean,

$$\partial_\mu \Phi(\tau,\mathbf{x}) \cdot \partial_\mu \Phi(\tau,\mathbf{x}) = \frac{d\Phi}{d\tau} \cdot \frac{d\Phi}{d\tau} + \frac{d\Phi}{dx_1} \cdot \frac{d\Phi}{dx_1} + (\cdots) + \frac{d\Phi}{dx_D} \cdot \frac{d\Phi}{dx_D} \ , \tag{4.6}$$

and periodic boundary conditions, $\Phi(\tau,\vec{x}) \stackrel{!}{=} \Phi(\tau + \frac{1}{T},\vec{x})$, are implied.
The effective action can be expanded in terms of gradients of the field [6, 105],

$$\Gamma[\Phi] = \int_0^{1/T} d\tau \int d^D\mathbf{x} \left[U(\Phi(\tau,\mathbf{x})) + Z(\Phi) \partial_\mu \Phi(\tau,\mathbf{x}) \cdot \partial_\mu \Phi(\tau,\mathbf{x}) + (\cdots) \right] \ , \tag{4.7}$$

which is known as *derivative expansion* (compare with Eq. (2.24)). Setting $Z(\Phi) \equiv 1$ and ignoring higher-order terms in the expansion defines the so-called *local-potential approximation* (LPA). In momentum space, at nonzero temperature T, and in absence of fermions the Wetterich equation (4.1) reads

$$\partial_k \Gamma[\Phi] = \frac{1}{2} \sum_{i,j}^{N} \sum_{\omega,\vec{q}} \sum_{\omega',\vec{q}'} [\partial_k \mathbf{R}_k]_{i,\omega,\vec{q};j,\omega',\vec{q}'} \left[\left(\mathbf{\Gamma}_k^{(2)} + \mathbf{R}_k \right)^{-1} \right]_{j,\omega',\vec{q}';i,\omega,\vec{q}} , \tag{4.8}$$

where the superlabels i and j correspond to the field components, and the indices ω and ω' denote the bosonic Matsubara frequencies $2n\pi T$. We note that the notation we use [6] implies

$$\frac{1}{V} \sum_{\vec{q}} \xrightarrow{V\to\infty} \int \frac{d^D \vec{q}}{(2\pi)^D} \tag{4.9}$$

in the limit of infinite volume V. The regulator can be chosen in diagonal form [10],

$$[\mathbf{R}_k]_{i,\omega,\vec{q};j,\omega',\vec{q}'} = \delta_{ij} \delta_{\omega\omega'} \delta_{\vec{q}\vec{q}'} R_k(\vec{q}) . \tag{4.10}$$

Assuming $\Phi(\tau, \vec{x}) \equiv \Phi$, Eq. (4.7) implies $\Gamma_k \equiv (V/T) U_k$, and hence, in the limit (4.9), we obtain for Eq. (4.8)

$$\partial_k U_k(\Phi) = \frac{1}{2} T \sum_{\omega} \sum_{i}^{N} \int \frac{d^D \vec{q}}{(2\pi)^D} \partial_k R_k(\vec{q}) \left[\left(\mathbf{\Gamma}_k^{(2)}(\omega, \vec{q}) + \mathbf{R}_k(\vec{q}) \right)^{-1} \right]_{ii} . \tag{4.11}$$

In momentum space $\partial_\mu \Phi \cdot \partial_\mu \Phi \to (\omega^2 + \vec{q}^{\,2}) \Phi \cdot \Phi$, and hence

$$[\mathbf{\Gamma}_k^{(2)}(\omega, \vec{q})]_{ij} = (\omega^2 + \vec{q}^{\,2}) \delta_{ij} + \frac{\delta^2 U_k}{\delta \Phi_i \delta \Phi_j} . \tag{4.12}$$

Using the optimized regulator introduced by Litim [106],

$$R_k(\vec{q}^{\,2}) = (k^2 - \vec{q}^{\,2}) \theta(k^2 - \vec{q}^{\,2}) , \tag{4.13}$$

we obtain

$$\partial_k R_k(\vec{q}^{\,2}) = 2k \theta(k^2 - \vec{q}^{\,2}) . \tag{4.14}$$

Since the integrand in Eq. (4.11) only depends on $q \equiv |\vec{q}|$, one can perform the integration over the angular part leaving

$$\partial_k U_k(\Phi) = \frac{1}{2} \left(\frac{2^{1-D} \pi^{-D/2}}{\Gamma(D/2)} \right) T \sum_{\omega} \sum_{i}^{N} \int_0^\infty dq q^{D-1} \partial_k R_k(q^2) \left[\left(\mathbf{\Gamma}_k^{(2)}(\omega, q^2) + \mathbf{R}_k(q^2) \right)^{-1} \right]_{ii} . \tag{4.15}$$

Due to (4.14), the integral in Eq. (4.15) can be restricted to $\int_0^k$, and further:

$$\partial_k R_k(q^2) \left[\left(\mathbf{\Gamma}_k^{(2)}(\omega, q^2) + \mathbf{R}_k(q^2) \right)^{-1} \right]_{ii} = \begin{cases} 0 & \text{for } q^2 > k^2 , \\ 2k \left[\left((\omega^2 + k^2) \delta_{ij} + \frac{\delta^2 U_k}{\delta \Phi_i \delta \Phi_j} \right)^{-1} \right]_{ii} & \text{for } q^2 \le k^2 . \end{cases} \tag{4.16}$$

This results in

$$\partial_k U_k(\Phi) = K_D k^{D+1} T \sum_{\omega} \sum_{i}^{N} \left[\left((\omega^2 + k^2) \delta_{ij} + \frac{\delta^2 U_k}{\delta \Phi_i \delta \Phi_j} \right)^{-1} \right]_{ii} , \tag{4.17}$$

where we denoted

$$K_D \equiv \frac{2^{1-D}\pi^{-D/2}}{\Gamma(D/2)D} \ . \tag{4.18}$$

Using the fact that the trace of the inverse of a matrix equals the sum of its inverse eigenvalues, Eq. (4.17) can be rewritten as

$$\partial_k U_k(\Phi) = K_D k^{D+1} T \sum_{\omega} \sum_{i}^{N} \frac{1}{\omega^2 + k^2 + M_i^2} \ , \tag{4.19}$$

where M_i^2 denotes the N eigenvalues of the mass matrix

$$M_{ij} = \frac{\delta^2 U_k}{\delta\Phi_i \delta\Phi_j}. \tag{4.20}$$

Finally, carrying out the sum over the Matsubara frequencies $\omega = 2n\pi T$, where the sum runs from $n = -\infty$ to $n = \infty$, we obtain

$$\partial_k U_k(\Phi) = \frac{1}{2} K_D k^{D+1} \sum_{i}^{N} \frac{1}{E_i} \coth\left(\frac{E_i}{2T}\right) \ , \quad E_i = \sqrt{k^2 + M_i^2} \ . \tag{4.21}$$

Due to $\lim_{x\to\infty} \coth x = 1$, at zero temperature the flow equation (4.21) becomes

$$\partial_k U_k(\Phi) \overset{T=0}{=} \frac{1}{2} K_D k^{D+1} \sum_{i}^{N} \frac{1}{E_i} \ . \tag{4.22}$$

Another important limit is that of high temperature, where the flow is dominated by thermal fluctuations. Expanding the hyperbolic cotangent around zero,

$$\coth\left(\frac{E_i}{2T}\right) \simeq \frac{2T}{E_i} + \mathcal{O}\left(\frac{1}{T}\right) \ , \tag{4.23}$$

we obtain the flow equation for the case where thermal fluctuations are dominant:

$$\partial_k U_k^{DR}(\Phi) = K_D k^{D+1} \sum_{i}^{N} \frac{1}{E_i^2} \ , \tag{4.24}$$

where we defined the dimensionally reduced potential by

$$U_k^{DR}(\Phi) \equiv \frac{U_k(\Phi)}{T} \ . \tag{4.25}$$

Comparing Eq. (4.24) with Eq. (4.21) we observe that taking into account only the zeroth Matsubara mode, $n = 0$, in the latter equation results in the former one. This is an example of *dimensional reduction*, which we already discussed in Sec. 2.3.

4.3 FRG investigation of phase transitions

4.3.1 Evolution of the potential

One possibility to study the phase transition of a model is to solve the Wetterich equation numerically. In a finite-temperature study one aims at solving Eq. (4.21) for different values of T. One

makes an ansatz for $U_{k=\Lambda}(\Phi)$ in the UV limit where one starts the integration down towards the IR limit. The IR limit, $k = 0$, corresponds to the solution where all fluctuations have been taken into account, i.e., to the physical solution. The ansatz $U_{k=\Lambda}(\Phi)$ is chosen such that one obtains the desired values for certain physical observables (such as for example the pion decay constant, physical masses, etc.). The order of the phase transition, as well as the critical temperature T_c, can be inferred from the dependence of the IR value for the global minimum on the temperature, $\Phi_0(T)$. The integration can be stopped at a certain k_f from which on the value Φ_0 does not change significantly anymore. Whereas $\Phi_0(T)$ continuously decreases towards zero for a second-order transition, it shows a discontinuous jump in case of a first-order transition. Characteristic of a first-order transition is also the occurrence of a maximum separating two minima during the evolution of the potential in k. Studies at nonzero temperature can be found in chapter 7. We describe the numerical algorithms we used in App. C and provide example routines implemented in *Mathematica*.

One can also study the evolution of the dimensionally reduced potential from Eq. (4.24). Dimensional reduction corresponds to a high-temperature approximation and temperature is not available anymore as an explicit parameter. Nevertheless, because the diverging correlation length near a second-order phase transition leads to dimensional reduction, one can decide about the order of the transition in the framework of the dimensionally reduced theory. Here, consistent with Landau's approach towards phase transitions, the UV parameters involved in $U^{DR}_{k=\Lambda}(\Phi)$ have to be regarded as temperature-dependent parameters. The explicit dependence can be calculated in a perturbative expansion in T^{-1}. For our purposes this is not necessary, however, since we are interested in the whole coupling space and any phase transition which can be achieved by tuning the mass term[1] in the UV potential $U^{DR}_{k=\Lambda}(\Phi)$. More practical in the case of the dimensionally reduced theory, however, is a fixed-point analysis for the rescaled parameters of the potential as described in Sec. 4.3.2.

4.3.2 Fixed-point analysis

The general framework underlying a fixed-point analysis was already described in Sec. 2.3. It remains to explain how we extract the flow equations (2.18) from Eq. (4.24). The large amount of examples presented in Sec. 6 makes this step rather obvious. Nevertheless we want to give a general description.

We discuss models defined by potentials U of the form (2.22) or (2.26), respectively. Plugging U into the flow equation (4.24), we perform a Taylor expansion of the r.h.s. in terms of the fields Φ_i and read off the flow equations for the couplings by comparison of coefficients. The calculation can be simplified by setting certain fields Φ_i to zero after having determined the mass matrix M_{ij} stated in Eq. (4.20). Hereby, with the corresponding fields set to zero, the potential U must still contain the same number of linearly independent terms, so that one obtains a flow equation for each of the couplings. We emphasize that no approximation is involved in setting the respective fields to zero since the coefficients in the Taylor expansion are of course independent of the fields. Working with a potential of the form (2.26) one has to rewrite the remaining

[1] In general a transition can also be described by tuning other couplings. Consistent with Landau theory, however, we assume that the mass term is the relevant parameter to tune.

fields Φ_i in terms of the basic invariants (those invariants from which all others are constructed) after having calculated M_{ij}. In order to obtain the correct flow equations this mapping has to be unambiguous. We further note that ambiguous flow equations can arise, depending on the monomial in the Taylor expansion from which one infers the flow, if U is not a most general polynomial (at the given order) invariant under some group.

4.4 Towards the chiral phase transition from first principles - On the relationship between QCD and effective models for QCD

In order to investigate the order of the chiral phase transition and the possibility of a second-order phase transition one requires a framework which is capable of describing the behavior of the order parameter. An approach which derives the behavior of the order parameter from first principle, without imposing restrictive assumptions and invoking approximations, is out of reach. In our opinion, however, it is still justified to speak of an approach *from first principle* if it starts from QCD, and if the assumptions and approximations made are systematically improvable. In the following we try to outline a way towards this goal, which remains of course incomplete.
In general, the effective action, $\Gamma[\Phi]$, is a functional of field components Φ_α, which can be either bosonic or fermionic, where α is a superfield label containing continuous and/or discrete variables. It can be written in the following form [6]:

$$\Gamma[\Phi] = \sum_{n=0}^{\infty} \frac{1}{n!} \int\!\!\!\!\!\!\int_{\alpha_1} \cdots \int\!\!\!\!\!\!\int_{\alpha_n} \Gamma^{(n)}_{\alpha_1 \cdots \alpha_n} \Phi_{\alpha_1} \cdots \Phi_{\alpha_n} \ . \tag{4.26}$$

The irreducible vertices herein can be expressed in terms of the infinitely many one-particle irreducible Feynman diagrams without external legs (usually called vacuum diagrams), $G_i^{(n)}$:

$$\Gamma^{(n)}_{\alpha_1 \cdots \alpha_n} = \sum_i^{\infty} a_i G_i^{(n)} \ , \tag{4.27}$$

where the coefficients a_i contain combinatorial factors and factors of i, depending on notational conventions. We note that the quadratic contribution in Eq. (4.26) can be decomposed into kinetic and mass terms for the fields. Furthermore we remark that one can prove that the Wetterich average effective action at $k = \Lambda$ equals the bare (or classical) action [6].
In practice, in order to apply the Wetterich equation (4.1) to QCD, one has to choose a reasonable truncation for Γ, i.e., to pick out the relevant terms out of the infinitely many ones. For a practical truncation certain assumptions are indispensable. To which extent these preconditions are justified has to be tested by comparison to lattice results or experiments. Depending on the scope of application the required assumptions differ. In this work we are interested in the order of the chiral phase transition, and we make the assumption that mesons are the degrees of freedom which have the strongest influence on the order of the chiral phase transition. The simplest Feynman diagrams with one meson in the initial and one in the final state, respectively, are the so-called box diagrams [107]. A few examples are depicted in Fig. 4.1. Note that the first diagram on the left is not one-particle irreducible and consequently does not contribute to the

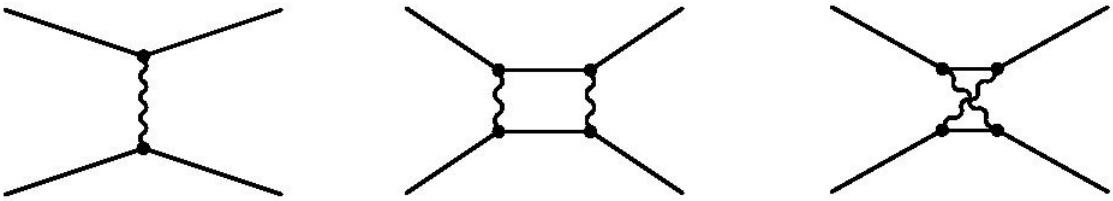

Figure 4.1: Examples for four-fermion box diagrams of QCD. Solid lines denote the quark propagator, curly lines the gluon propagator.

effective action. The interactions between mesons are obviously mediated by gluons. Although not possible analytically, one could absorb the influence of gluons into effective n-point fermion couplings by integrating out the gluonic fields in the partition function. Instead, in order to keep at least some explicit gluonic influence, we keep the classical QCD interactions in our truncation, but we substitute the box-diagrams by all possible four-quark interactions (neglecting higher-order interactions as well as ghost contributions). Actually the four-quark interactions should automatically arise in an expansion of the right hand side of the FRG flow equation when the classical QCD interactions are present. According to Ref. [108] these interactions can be classified with respect to their color and flavor quantum numbers, and a complete linearly independent set (up to Fierz transformations) of $U(N_f)_A \times U(N_f)_V$ symmetric four-quark interactions is given by

$$(V-A) = (\bar{\Psi}\gamma_\mu\Psi)^2 + (\bar{\Psi}\gamma_\mu\gamma_5\Psi)^2 \ , \tag{4.28}$$

$$(V+A) = (\bar{\Psi}\gamma_\mu\Psi)^2 - (\bar{\Psi}\gamma_\mu\gamma_5\Psi)^2 \ , \tag{4.29}$$

$$(S-P) = (\bar{\Psi}^i\Psi^j)^2 - (\bar{\Psi}^i\gamma_5\Psi^j)^2, \tag{4.30}$$

$$(V-A)^{adj} = (\bar{\Psi}\gamma_\mu T\Psi)^2 + (\bar{\Psi}\gamma_\mu\gamma_5 T\Psi)^2 \ , \tag{4.31}$$

where color $(a, b, \dots)$ and flavor $(i, j, \dots)$ indices are contracted pairwise. Note, however, that $U_A(1)$-breaking anomaly terms, in particular $\sim (\bar{\Psi}\Psi)^{N_f}$, are absent since they arise from topologically nontrivial gauge configurations [109]. The authors defined $(\bar{\Psi}^i\Psi^j)^2 = \bar{\Psi}^i\Psi^j\bar{\Psi}^j\Psi^i$, etc., and denote the generators of $SU(N_c)$ in the fundamental representation by $(T)_{ab}$. Then, the above assumptions lead to the following truncation [108, 109] for the effective action of QCD:

$$\Gamma = S_{gf} + \int d^4x \Bigg[\bar{\Psi}(i\gamma^\mu\partial_\mu + gT^a\gamma^\mu A^a_\mu - m_q)\Psi - \frac{1}{4}F^{\mu\nu}_a F^a_{\mu\nu}$$
$$+\frac{1}{2}\Bigg(\lambda_-(V-A) + \lambda_+(V+A) + \lambda_\sigma(S-P) + \lambda_{VA}[2(V-A)^{adj} + \frac{1}{N_c}(V-A)]\Bigg)\Bigg] , \tag{4.32}$$

where S_{gf} denotes gauge-fixing terms, and we have set wave-function renormalization factors to one for simplicity. An important remark in Ref. [109] concerns the axial anomaly. For $N_f = 2$ one can rewrite $(S-P)$ as follows:

$$(S-P) = \frac{1}{2}\left[(\bar{\Psi}\Psi)^2 - (\bar{\Psi}\vec{\tau}\gamma_5\Psi)^2\right] - \left[\det\bar{\Psi}(1+\gamma_5)\Psi + \det\bar{\Psi}(1-\gamma_5)\Psi\right] \ , \tag{4.33}$$

where $\vec{\tau} = (\sigma_1, \sigma_2, \sigma_3)$ denotes the Pauli matrices. Note that $\bar{\Psi}\Psi \equiv \bar{\Psi}_i \Psi_i$ with summation over i implied. Furthermore, for $N_f = 2$ the term involving the determinant is given by

$$\det \bar{\Psi}(1+\gamma_5)\Psi + \det \bar{\Psi}(1-\gamma_5)\Psi = \frac{1}{2}\left[(\bar{\Psi}\Psi)^2 - (\bar{\Psi}\vec{\tau}\gamma_5\Psi)^2\right] - \frac{1}{4}\left[(\bar{\Psi}\vec{\tau}\Psi)^2 - (\bar{\Psi}\vec{\tau}\gamma_5\Psi)^2\right] . \quad (4.34)$$

Whereas the first term on the right-hand side of Eq. (4.34) is not invariant under $U(1)_A$ transformations (A.17), the second term in Eq. (4.34), $(\bar{\Psi}\vec{\tau}\Psi)^2 - (\bar{\Psi}\vec{\tau}\gamma_5\Psi)^2$, is invariant (see Eq. (A.22)). Consequently the combination $(S-P)$ is invariant because the term $\frac{1}{2}\left[(\bar{\Psi}\Psi)^2 - (\bar{\Psi}\vec{\tau}\gamma_5\Psi)^2\right]$ is canceled by the appropriate contribution in the determinant term (4.34). Therefore, the $U(1)_A$ anomaly is absent in the truncation (4.32). Accordingly, one can take account of the anomaly by carrying out the substitution

$$\lambda_\sigma(S-P) \to G_1\left[(\bar{\Psi}\Psi)^2 - (\bar{\Psi}\vec{\tau}\gamma_5\Psi)^2\right] + (G_{\text{top}} - 2G_1)\left[\det \bar{\Psi}(1+\gamma_5)\Psi + \det \bar{\Psi}(1-\gamma_5)\Psi\right] \quad (4.35)$$

in expression (4.32), so that the anomaly is absent for $G_{\text{top}} = 0$ and present for $G_{\text{top}} \neq 0$. In Ref. [110] the authors applied the Wetterich equation to the above truncation (4.32). For different numbers of massless quark flavors and vanishing chemical potential, an estimate for the (pseudo)critical temperature of the chiral phase transition is obtained. Their estimates for $N_f = 2$ ($T_c \approx 186 \pm 33$ MeV) and $N_f = 3$ ($T_c \approx 161 \pm 31$ MeV) are found to be in good agreement with lattice results. The order of the phase transition is discussed in Ref. [109]. We want to note that the conclusion about the order of the two-flavor phase transition in Fig. 20 of Ref. [109] is premature. According to the sketch, the phase transition is of second order for $N_f = 2$. This result, however, was obtained taking into account only the sigma meson and the pions, which corresponds to an infinite anomaly strength (compare with Sec. 3.3.2).

In the following we restrict the discussion to the two-flavor case. We discuss the basic idea how to derive an effective action involving mesons by the method of (partial) bosonization. The nontrivial part of this approach is calculating the fermion determinant obtained after having integrated over the quarks. Since we are not aiming at performing this final step we keep the lightest scalar ($J^{PC} = 0^{++}$), pseudoscalar ($J^{PC} = 0^{-(+)}$), vector ($J^{PC} = 1^{-(-)}$), and axial-vector ($J^{PC} = 1^{+(+)}$) mesons for demonstrational purposes. In correspondence with the meson summary table of the Particle Data Group [74] we can identify the mesons with observed particle resonances. We note, however, that the stated mass values are not fully appropriate for a study with $N_f = 2$ because they involve contributions from heavier quarks. A better choice is given by the nonstrange contributions (Ref. [111] considers for example the nonstrange contribution of the eta meson). Also the assignment of the mesons to different particle resonances is still under debate [112, 113, 114]. In particular there are two scenarios how to identify the sigma and the a_0 meson with particle resonances. Either they correspond to $f_0(500)$ and $a_0(980)$, or to $f_0(1370)$ and $a_0(1450)$, respectively. The mesonic properties are summarized in Tab. A.1 of App. A.2, which in addition discusses the transformation properties under chiral symmetry.

Instead of starting from a complete set of linearly independent $U(2)_A \times U(2)_V$ symmetric four-quark interactions as in expression (4.32), we use the following $SU(2)_A \times SU(2)_V$-symmetric

ansatz (which involves $U(1)_A$ violation):

$$\Gamma' = S_{gf} + \int d^4x \Bigg[\bar{\Psi}(i\gamma^\mu \partial_\mu + gT^a \gamma^\mu A^a_\mu - m_q)\Psi - \frac{1}{4} F^{\mu\nu}_a F^a_{\mu\nu} + G_1 \left[(\bar{\Psi}\Psi)^2 - (\bar{\Psi}\vec{\tau}\gamma_5\Psi)^2 \right] + G_2 \left[(\bar{\Psi}\vec{\tau}\Psi)^2 - (\bar{\Psi}\gamma_5\Psi)^2 \right] + G_3 \left[(\bar{\Psi}\gamma_\mu\Psi)^2 + (\bar{\Psi}\gamma_\mu\gamma_5\Psi)^2 \right] + G_4 \left[(\bar{\Psi}\gamma_\mu\gamma_5\vec{\tau}\Psi)^2 + (\bar{\Psi}\gamma_\mu\vec{\tau}\Psi)^2 \right] \Bigg] . \tag{4.36}$$

The basis from which functional approaches, such as the FRG method, are derived is the path integral formalism. Since the average effective action at $k = \Lambda$ equals the classical action, we can write down the (Minkowskian) generating functional (which in the Euclidean and at finite temperature turns into the partition function):

$$Z = \int \mathcal{D}\bar{\Psi}\mathcal{D}\Psi\mathcal{D}A\, \mathrm{e}^{\mathrm{i}\,\Gamma'} \ . \tag{4.37}$$

Since the generating functional can be multiplied by an overall constant, bosonic degrees of freedom can be trivially introduced as follows:

$$Z = \mathcal{N} \int \mathcal{D}\bar{\Psi}\mathcal{D}\Psi\mathcal{D}A\mathcal{D}\sigma\mathcal{D}\vec{\pi}\mathcal{D}\eta\mathcal{D}\vec{a}_0\mathcal{D}\omega^\mu\mathcal{D}\vec{a}^\mu_1\mathcal{D}f^\mu_1\mathcal{D}\vec{\rho}^\mu \times \times \mathrm{e}^{\mathrm{i}\,\Gamma' - \mathrm{i}\int d^4x \left[m_1^2(\sigma^2+\vec{\pi}^2) + m_2^2(\eta^2+\vec{a}_0^2) + m_3^2(\omega_\mu\omega^\mu + f_{1,\mu}f_1^\mu) + m_4^2(\vec{\rho}_\mu\vec{\rho}^\mu + \vec{a}_{1,\mu}\vec{a}_1^\mu) \right]} \ . \tag{4.38}$$

Performing Hubbard-Stratonovich transformations (compare with Ref. [115]),

$$\sigma \to \sigma + \frac{\sqrt{G_1}}{m_1}\bar{\Psi}\Psi \ , \quad \vec{\pi} \to \vec{\pi} + \mathrm{i}\,\frac{\sqrt{G_1}}{m_1}\bar{\Psi}\vec{\tau}\gamma_5\Psi \ , \tag{4.39}$$

$$\eta \to \eta + \mathrm{i}\,\frac{\sqrt{G_2}}{m_2}\bar{\Psi}\gamma_5\Psi \ , \quad \vec{a}_0 \to \vec{a}_0 + \frac{\sqrt{G_2}}{m_2}\bar{\Psi}\vec{\tau}\Psi \ , \tag{4.40}$$

$$\omega^\mu \to \omega^\mu + \frac{\sqrt{G_3}}{m_3}\bar{\Psi}\gamma_\mu\Psi \ , \quad f_1^\mu \to f_1^\mu + \frac{\sqrt{G_3}}{m_3}\bar{\Psi}\gamma_\mu\gamma_5\Psi \ , \tag{4.41}$$

$$\vec{a}_1^\mu \to \vec{a}_1^\mu + \frac{\sqrt{G_4}}{m_4}\bar{\Psi}\gamma_\mu\gamma_5\vec{\tau}\Psi \ , \quad \vec{\rho}^\mu \to \vec{\rho}^\mu + \frac{\sqrt{G_4}}{m_4}\bar{\Psi}\gamma_\mu\vec{\tau}\Psi \ , \tag{4.42}$$

mesonic degrees of freedom are generated:

$$Z = \mathcal{N} \int \mathcal{D}\bar{\Psi}\mathcal{D}\Psi\mathcal{D}A\mathcal{D}\sigma\mathcal{D}\vec{\pi}\mathcal{D}\eta\mathcal{D}\vec{a}_0\mathcal{D}\omega^\mu\mathcal{D}\vec{a}^\mu_1\mathcal{D}f^\mu_1\mathcal{D}\vec{\rho}^\mu\, \mathrm{e}^{\mathrm{i}\,S_{gf} - \mathrm{i}\int d^4x \frac{1}{4}F^{\mu\nu}_a F^a_{\mu\nu}} \times \times \mathrm{e}^{-\mathrm{i}\int d^4x \left[m_1^2(\sigma^2+\vec{\pi}^2) + m_2^2(\eta^2+\vec{a}_0^2) + m_3^2(\omega_\mu\omega^\mu + f_{1,\mu}f_1^\mu) + m_4^2(\vec{\rho}_\mu\vec{\rho}^\mu + \vec{a}_{1,\mu}\vec{a}_1^\mu) \right]} \mathrm{e}^{\mathrm{i}\int d^4x \bar{\Psi}B\Psi} \ , \tag{4.43}$$

where we denoted

$$B = (i\gamma^\mu\partial_\mu + gT^a\gamma^\mu A^a_\mu - m_q - g_1\sigma - g_1\,\mathrm{i}\,\gamma_5\vec{\tau}\cdot\vec{\pi} - g_2\,\mathrm{i}\,\gamma_5\eta - g_2\vec{\tau}\cdot\vec{a}_0 - g_3\gamma_\mu\omega^\mu - g_3\gamma_\mu\gamma_5 f_1^\mu - g_4\gamma_\mu\vec{\tau}\cdot\vec{\rho}^\mu - g_4\gamma_\mu\gamma_5\vec{\tau}\cdot\vec{a}_1^\mu) \ , \tag{4.44}$$

with $g_i \equiv 2\sqrt{G_i}/m_i$. At this stage there are no kinetic terms for the mesons and no interactions between them. Such terms arise when carrying out the integration over the quark fields,

$$\int \mathcal{D}\bar{\Psi}\mathcal{D}\Psi\, \mathrm{e}^{\mathrm{i}\int d^4x \bar{\Psi}B\Psi} = \mathrm{e}^{\mathrm{i}\int d^4x [-\mathrm{i}\,\mathrm{Tr}\ln B]} \ , \tag{4.45}$$

and performing a derivative expansion of the fermion determinant in terms of the mesonic fields which have been introduced,

$$
\begin{aligned}
-\mathrm{i}\,\mathrm{Tr}\ln B = -\mathrm{i}\ln\det B \simeq \frac{1}{2}(\partial_\mu\sigma)^2 + \frac{1}{2}(\partial_\mu\vec{\pi})^2 + \frac{1}{2}(\partial_\eta\sigma)^2 + \frac{1}{2}(\partial_\mu\vec{a}_0)^2 \\
+\frac{1}{2}(\partial_\mu\omega^\mu)^2 + \frac{1}{2}(\partial_\mu\vec{a}_1^\mu)^2 + \frac{1}{2}(\partial_\mu f_1^\mu)^2 + \frac{1}{2}(\partial_\mu\vec{\rho}^\mu)^2 - U_{\mathrm{mes}}\ .
\end{aligned}
\tag{4.46}
$$

Instead of explicitly calculating the mesonic potential, U_{mes}, we can make an ansatz restricted by symmetry properties and experimental observations. Clearly, assuming $m_q = 0$, U_{mes} should be invariant under $G_{(c)} \equiv (S)U(2)_A \times U(2)_V$ (in the presence of the axial $U(1)_A$ anomaly). In Sec. 3.3.2 we discussed in detail how to construct the potential for scalar and pseudoscalar mesons using the eight-dimensional $[\bar{2},2]\oplus[2,\bar{2}]$ representation of $SU(2)\times SU(2)$. These mesons are presumably most important when investigating the phase transition. Nevertheless, vector and axial-vector mesons might have substantial influence. In Refs. [112, 116, 117] it has been discussed how to incorporate them in the mesonic potential taking account of vector meson dominance and the way in which the photon enters the effective theory. In this thesis we are not seriously concerned with vector and axial-vector mesons but we discuss a toy model based on the symmetry properties in Sec. 6.8.1.

In the following we want to discuss how the quark-meson model emerges from the above considerations. Completely integrating out the fermions corresponds to neglecting momentum fluctuations which are high enough to resolve the internal quark structure of the mesons. In other words, one imposes an UV cutoff at a compositeness scale, roughly estimated by $k_{\mathrm{comp}} \sim 600$ MeV [90], below which quarks can be predominantly assumed to be confined into mesons. The mesonic terms generated in the expansion (4.46) are the dominant degrees of freedom at low energy scales, $k \ll k_{\mathrm{comp}}$, whereas the Yukawa interaction term $\bar{\Psi}B\Psi$ becomes relevant around $k \sim k_{\mathrm{comp}}$. In a RG treatment it is rather natural to include both contributions in a truncation for the effective action. The Refs. [118, 119] demonstrate how to cope with the technical difficulties arising in such a joint treatment. In the standard version of the quark-meson model one only takes into account the sigma meson and the pions. One associates these four degrees of freedom with the four-dimensional representation $[\bar{2},2]$ of $SU(2)\times SU(2)$, which is identical to the defining representation of $O(4)$. The effective action reads

$$
\Gamma = \int d^4x \left[\frac{1}{2}(\partial_\mu\sigma)^2 + \frac{1}{2}(\partial_\mu\vec{\pi})^2 + \bar{\Psi}(i\gamma^\mu\partial_\mu - g\,[\sigma + \mathrm{i}\,\gamma_5\vec{\tau}\cdot\vec{\pi}])\Psi - U_{\mathrm{mes}}\right] , \tag{4.47}
$$

where U_{mes} is the most general $O(4)$ symmetric polynomial (in the fundamental representation of $O(4)$) constructed from the $O(4)$ invariant $\sigma^2 + \vec{\pi}^2$, which is given by

$$
U_{\mathrm{mes}} \equiv -\frac{m^2}{2}(\sigma^2 + \vec{\pi}^2) + \frac{\lambda}{4}(\sigma^2 + \vec{\pi}^2)^2 , \tag{4.48}
$$

where terms of naive scaling dimension larger than 4 are omitted. Note that neither the Yukawa interaction nor the potential (4.48) is invariant under $U(1)_A$, i.e., the axial anomaly is present. Gauge-field terms are neglected in the quark-meson model. This is a severe simplification since quarks should not only interact via the Yukawa coupling, but also via the quark-gluon vertex as soon as they are included. Below momentum scales $k < k_{\mathrm{comp}}$ it is consistent to neglect both quarks and gauge fields, but if one aims to set up a consistent theory with a cutoff larger than

$k_{\rm comp}$ one should include the gluon fields. A first step in this direction is represented by the Polyakov-loop extended quark-meson (PQM) model (see for instance Sec. I.4.5.6 in Ref. [4]). Work on keeping the terms

$$S_{gf} + \int d^4x \left[\bar{\Psi}(i\gamma^\mu \partial_\mu + gT^a \gamma^\mu A^a_\mu - m_q)\Psi - \frac{1}{4} F^{\mu\nu}_a F^a_{\mu\nu} \right] \tag{4.49}$$

is currently under progress in the FRG community (compare with Refs. [120, 121]). For a status report on the FRG approach towards the simultaneous treatment of the deconfinement and the chiral phase transition in case of physical quark masses we refer to Ref. [122]. For a fixed-point analysis in $d = 4$ dimensions we point to Ref. [123]. In its present form, however, the study tells nothing about the phase transition since it neglects mesonic degrees of freedom.
For a qualitative understanding of the influence of gauge fields on critical behavior we refer to Ref. [84] (see also [49, 124]). In the framework of a one-loop ϵ-expansion Ref. [84] investigated dimensionally reduced $O(N)$ and $SU(N)$ gauge theories, respectively, involving scalar fields transforming according to different tensor representations. No IR-stable fixed points exist in presence of an asymptotically free gauge-field coupling (indicating a first-order phase transition), whereas in the opposite case there are theories exhibiting such (and hence a second-order phase transition is implied). Nevertheless the following "rule of thumb" was stated, which is still a good guide today: "(one-loop) gauge effects act to drive a first-order transition."

Chapter 5

Constructing invariants

5.1 General remarks

As it has been discussed in Sec. 2.1 the construction of polynomial invariants for different representations of groups is of great importance for the investigation of phase transitions associated to a breaking of symmetry. It has been further demonstrated in chapter 2.4 that this task is a crucial ingredient in RG studies of second-order phase transitions. But the topic is actually of much more general importance as almost any physical theory is related, at least to some extent, to symmetry. Symmetry considerations therefore play a central role in the construction of models, for example in the determination of the Higgs potential in gauge theories [49, 124], in the model building of high-energy physics [125], molecular physics, atomic physics [126], etc. At this point it is worth noting that several elementary invariants have been derived which are of use for the construction of effective models within the standard model [127, 128, 129]. In conclusion, it is highly desirable to have systematic techniques at hand to derive the invariants.
Most groups relevant in physics are compact Lie groups. Since any compact Lie group is isomorphic to a closed subgroup of the orthogonal group [130] the latter subgroups are of particular importance. The group $U(2) \times U(2)$, for instance, is a soubgroup of $O(8)$ [125].
Methods for the construction of invariants comprise approaches restricted to finite groups [7, 21, 131] and techniques which are suited for continuous groups [48, 124, 132, 133, 134]. For the latter groups the practical determination of integrity bases is an open problem when considering the general case [48]. At least for any classical or exceptional Lie group L (but probably even for a much more general class of groups), in case of the adjoint representation a complete set of linearly independent basic invariants is given by $\{I_m\}$, where m takes values depending on L, and I_m is defined by

$$I_m = \mathrm{Tr}\left(\sum_i \varphi_i X_i\right)^m , \tag{5.1}$$

with X_i denoting the generators of L in an arbitrary representation, and φ_i denoting the components of the carrier space for the adjoint representation [132, 133]. The invariants are listed for the classical and exceptional Lie groups in Tab. I of Ref. [133]. For an explicit example consider the adjoint representation of $SU(2)$. According to the table cited above the only basic invariant

is given by I_2. We can choose the X_i as the generators in the fundamental representation (the Pauli matrices) so that we obtain

$$I_2 = 2(\varphi_1^2 + \varphi_2^2 + \varphi_3^2) \ , \tag{5.2}$$

which is indeed the correct result because the adjoint representation of $SU(2)$ equals the fundamental representation of $SO(3)$.
We note that there exist construction methods based on basic invariant tensors (see for example [135, 136, 137]). In particular, we observe a close relationship between the principal invariants stated in Ref. [136] and the most general invariant polynomials derived for $O(N)$, $SU(N)$, $O(N) \times O(M)$, $(S)U(N) \times U(M)$, and $U(N) \times SO(M)$ for various representations (compare with Refs. [49, 52] and expressions (3.16) and (3.18), respectively). Since this goes beyond the scope of this thesis we were not able to investigate this further. In Sec. 5.2 we give an example illustrating the projection operator method. In Sec. 5.3 we describe a new brute-force algorithm which we have developed using *Mathematica*. It turned out to be practical for continuous groups.

5.2 Method using projection operators

Refs. [7, 21] nicely explain how to construct the invariants for representations of finite groups in case the carrier space and the representation matrices are known. The method is explained at the example of the group C_{3v}, which characterizes the symmetry of an equilateral triangle. To give a second example, we consider here the two-dimensional irreducible representation of the group C_{4v}, which we denote as $\Gamma^{(5)}$ consistent with Ref. [138]. In the latter reference we find the matrices representing the eight group elements in $\Gamma^{(5)}$,

$$\Gamma^{(5)}(E) = \begin{pmatrix} 1 & 0 \\ 0 & 1 \end{pmatrix} \ , \quad \Gamma^{(5)}(C_4) = \begin{pmatrix} 0 & -1 \\ 1 & 0 \end{pmatrix} \ , \quad \Gamma^{(5)}(C_4^2) = \begin{pmatrix} -1 & 0 \\ 0 & -1 \end{pmatrix} \ , \quad \Gamma^{(5)}(C_4^3) = \begin{pmatrix} 0 & 1 \\ -1 & 0 \end{pmatrix} \ ,$$

$$\Gamma^{(5)}(m_x) = \begin{pmatrix} 1 & 0 \\ 0 & -1 \end{pmatrix} \ , \quad \Gamma^{(5)}(m_y) = \begin{pmatrix} -1 & 0 \\ 0 & 1 \end{pmatrix} \ , \quad \Gamma^{(5)}(\sigma_u) = \begin{pmatrix} 0 & -1 \\ -1 & 0 \end{pmatrix} \ , \quad \Gamma^{(5)}(\sigma_v) = \begin{pmatrix} 0 & 1 \\ 1 & 0 \end{pmatrix} \ ,$$

which act on the carrier space $(x, y)^T$. Polynomial invariants of order n are in some sense related to the n-th power of the representation, $[\Gamma^{(5)}]^n$, which is associated with an n-dimensional carrier space. In order to determine a set of linearly independent polynomial invariants of order n it is helpful to calculate their number, N_n, first. We can infer this number from the traces (also known as *characters*) of the matrices representing the group elements in the representations of powers up to n. These representations can be constructed from the original one, $\Gamma^{(5)}$. For instance, the carrier space of $[\Gamma^{(5)}]^2$ is given by $(x^2, xy, y^2)^T$. The matrix representing a group element in $[\Gamma^{(5)}]^2$ can be calculated from the transformation of x and y under the group element. For instance, under the action of the element C_4 the components transform as $x \to -y$ and $y \to x$. The matrix $[\Gamma^{(5)}]^2(C_4)$ representing the group element in the 2-nd power of the representation is then determined from

$$[\Gamma^{(5)}]^2(C_4) \begin{pmatrix} x^2 \\ xy \\ y^2 \end{pmatrix} = \begin{pmatrix} y^2 \\ -xy \\ x^2 \end{pmatrix}$$

as

$$[\Gamma^{(5)}]^2(C_4) = \begin{pmatrix} 0 & 0 & 1 \\ 0 & -1 & 0 \\ 1 & 0 & 0 \end{pmatrix} .$$

Instead of calculating all of the matrices, one can use iterative formulas for the characters,

$$\mathrm{Tr}\,[\Gamma^{(5)}]^2(g) = \frac{1}{2}\left[\mathrm{Tr}\,\Gamma^{(5)}(g^2) + (\mathrm{Tr}\,\Gamma^{(5)}(g))^2\right] , \tag{5.3}$$

$$\mathrm{Tr}\,[\Gamma^{(5)}]^3(g) = \frac{1}{3}\,\mathrm{Tr}\,\Gamma^{(5)}(g^3) + \frac{1}{2}\,\mathrm{Tr}\,\Gamma^{(5)}(g^2)\,\mathrm{Tr}\,\Gamma^{(5)}(g) + \frac{1}{6}(\mathrm{Tr}\,\Gamma^{(5)}(g))^3 , \tag{5.4}$$

$$\begin{aligned}\mathrm{Tr}\,[\Gamma^{(5)}]^4(g) &= \frac{1}{4}\,\mathrm{Tr}\,\Gamma^{(5)}(g^4) + \frac{1}{3}\,\mathrm{Tr}\,\Gamma^{(5)}(g^3)\,\mathrm{Tr}\,\Gamma^{(5)}(g) \\ &+\frac{1}{8}(\mathrm{Tr}\,\Gamma^{(5)}(g^2))^2 + \frac{1}{4}\,\mathrm{Tr}\,\Gamma^{(5)}(g^2)(\mathrm{Tr}\,\Gamma^{(5)}(g))^2 + \frac{1}{24}(\mathrm{Tr}\,\Gamma^{(5)}(g))^4 .\end{aligned} \tag{5.5}$$

As illustration, for $g = C_4$ one obtains

$$\mathrm{Tr}\,[\Gamma^{(5)}]^2(C_4) = \frac{1}{2}\left(\mathrm{Tr}\,\Gamma^{(5)}(C_4 \cdot C_4) + (\mathrm{Tr}\,\Gamma^{(5)}(C_4))^2\right) = \frac{1}{2}(-2+0) = -1 .$$

The number N_n can now be calculated from the formula

$$N_n = \frac{1}{d(C_{4v})} \sum_{i=1}^{d(C_{4v})} \mathrm{Tr}\,[\Gamma^{(5)}]^n(g_i) , \tag{5.6}$$

where $d(C_{4v}) = 8$ is the number of elements of the group. For example, we obtain for the number of linearly independent second-order invariants

$$N_2 = \frac{1}{8}(3\cdot 1 - 1\cdot 1 + 3\cdot 1 - 1\cdot 1 + 1\cdot 1 + 1\cdot 1 + 1\cdot 1 + 1\cdot 1) = 1 .$$

Furthermore, we calculate $N_1 = 0$, $N_3 = 0$, and $N_4 = 2$. Invariants can be constructed from properly defined projection operators (in addition to Refs. [7, 21] see also Ref. [139]). In our example it is sufficient to use the simplest one,

$$\mathcal{P}_{\Gamma^{(5)}} = \sum_{i=1}^{d(C_{4v})} \Gamma^{(5)}(g_i) . \tag{5.7}$$

Obviously, $\mathcal{P}$ is a matrix. One defines its action on monomials $x^k y^l$ from the transformation of x and y, respectively, under $\Gamma^{(5)}(g_i)$ acting on $(x,y)^T$. For instance, $\Gamma^{(5)}(C_4)(x,y)^T = (-y,x)^T$, and hence $\Gamma^{(5)}(C_4)x^k y^l = (-y)^k x^l$. Accordingly we obtain for instance

$$\mathcal{P}_{\Gamma^{(5)}} x^2 = 4\left(x^2+y^2\right) , \quad \mathcal{P}_{\Gamma^{(5)}} x^4 = 4\left(x^4+y^4\right) , \quad \mathcal{P}_{\Gamma^{(5)}} y^4 = 4\left(x^4+y^4\right) \tag{5.8}$$

$$\mathcal{P}_{\Gamma^{(5)}} x^2y^2 = 8x^2y^2 , \quad \mathcal{P}_{\Gamma^{(5)}} x^3y = 0 . \tag{5.9}$$

Since we know the number of linearly independent invariants for each polynomial order, we conclude that the most general C_{4v}-symmetric polynomial associated with the representation $\Gamma^{(5)}$ is given by

$$r(x^2+y^2) + g_1(x^4+y^4) + g_2x^2y^2 = r(x^2+y^2) + \frac{g_2}{2}(x^2+y^2)^2 + \left(g_1 - \frac{g_2}{2}\right)(x^4+y^4) . \tag{5.10}$$

This confirms the Landau potential stated in Eq. (2.40).
The above consideration was restricted to finite groups. We suspect, however, that the method can be generalized to continuous groups, at least in principle. Unfortunately, we were only able to confirm this for the fundamental representation of $O(N)$ with $N = 2, 3$. Our conjecture is based on the observation that for several formulas involving the sum over group elements, $\sum_{g_i}$, the sum turns into an integral over the Haar measure, $\int d\mu_G(g)$, when the relations are generalized to continuous groups G (see for instance Ref. [134]). On this basis we conjecture that the projectors known for finite groups can be generalized accordingly. For instance the projector (5.7) should give rise to its analogue

$$\mathcal{P}_{\Gamma(G)} = \int d\mu_{\Gamma(G)}(g)\Gamma(g) \ , \tag{5.11}$$

where $\Gamma(G)$ denotes a certain matrix representation of the continuous group G, and $\Gamma(g)$ denotes a group element in this representation. For the fundamental representation of $O(2)$ the matrix elements are two-dimensional rotation matrices acting on a real two-dimensional carrier space. We use the notation defined in Eq. (A.1). We obtain for instance

$$\mathcal{P}_{O(2)}x^2 = \int_0^{2\pi} (x\cos\alpha - y\sin\alpha)^2 \, d\alpha = \pi(x^2 + y^2) \ . \tag{5.12}$$

Similarly, we obtain $(i, j \geq 0)$

$$\mathcal{P}_{O(2)}x^i y^j = \begin{cases} 0 & \text{for } i + j \text{ odd} \ , \\ \pi(x^2 + y^2) & \text{for } i + j = 2 \ , \\ \frac{3}{4}\pi(x^2 + y^2)^2 & \text{for } i + j = 4 \ . \end{cases} \tag{5.13}$$

For the fundamental representation of $SO(3)$ the group elements can be parameterized by rotations of fixed radius in three-dimensional space (x, y, z),

$$R_z(\phi_2)R_x(\theta)R_z(\phi_1) \ , \tag{5.14}$$

with angles $\theta \in [0, \pi)$, $\phi_1, \phi_2 \in [0, 2\pi]$. The rotation matrices can be easily found in the literature. Then the Haar measure is given by [140]

$$d\mu_{SO(3)} = \frac{1}{8\pi^2}\sin\theta d\theta d\phi_1 d\phi_2 \ . \tag{5.15}$$

The integrals $\int_0^\pi \int_0^{2\pi} \int_0^{2\pi} d\mu_{SO(3)} R_z(\phi_2)R_x(\theta)R_z(\phi_1)x^i x^j x^k$ are easily calculated using *Mathematica*. We find again corresponding powers of the basic invariant $(x^2 + y^2 + z^2)$.

5.3 New brute-force algorithm

In the following we describe how to construct the $SU(2)_A \times SU(2)_V$ invariants for the $[\bar{2}, 2] \oplus [2, \bar{2}]$ representation using a brute-force algorithm implemented in *Mathematica*. The corresponding notebook is provided in Sec. B.2. We note that our method is not restricted to this special case, and we have checked that it can be successfully applied to other groups as well. However, one has to know the explicit form of the symmetry transformation for the representation of interest. As

a further example, in Sec. B.1 we provide a self-explanatory notebook confirming the invariants which have been derived in Sec. 5.2 for the two-dimensional irreducible representation $\Gamma^{(5)}$ of the group C_{4v}. The latter example demonstrates that a construction via brute force is not only extremely comprehensive in comparison to the mathematically involved projection operator method, but that it can be even more effective from a computational point of view. We note, however, that in case of large-dimensional order parameters there can easily occur problems with memory of *Mathematica* due to the rapidly increasing number of monomials. In such cases one either needs a powerful computer or a more sophisticated method to solve the (simple) system of linear equations. The following paragraphs have been taken from our publication [1].
The $[\bar{2},2]\oplus[2,\bar{2}]$ representation is 8-dimensional. Accordingly, the corresponding invariants of order N are polynomials in eight components which are in our notation the fields σ, $\vec{\pi}$, η, and $\vec{a}$, i.e., they are of the form

$$p = \sum_{m_i \in m} c_i m_i \ , \tag{5.16}$$

where m denotes the set of all possible monomials of order N,

$$m = \{\sigma^{n_1}\pi_1^{n_2}\pi_2^{n_3}\pi_3^{n_4}\eta^{n_5}a_1^{n_6}a_2^{n_7}a_3^{n_8}\} \ , \quad n_i \in \mathbb{N} \ , \quad \sum_i n_i = N \ , \tag{5.17}$$

and the coefficients c_i are expected to be rational multiples of each other.
Infinitesimal $SU(2)_A$ transformations for the above representation are inferred from Eqs. (A.23)-(A.26) (compare with Ref. [141]),

$$\sigma' = \sigma + \vec{\alpha}\cdot\vec{\pi} \ , \quad \pi_i' = \pi_i - \alpha_i\sigma \ , \quad \eta' = \eta - \vec{\alpha}\cdot\vec{a} \ , \quad a_i' = a_i + \alpha_i\eta \ , \tag{5.18}$$

where $\vec{\alpha} = (\alpha_1, \alpha_2, \alpha_3)$ consists of three infinitesimal angles. Infinitesimal $SU(2)_V$ transformations for the above representation are given by

$$\sigma' = \sigma \ , \quad \vec{\pi}' = \vec{\pi} + \vec{\beta}\times\vec{\pi} \ , \quad \eta' = \eta \ , \quad \vec{a}' = \vec{a} + \vec{\beta}\times\vec{a} \ , \tag{5.19}$$

where $\vec{\beta} = (\beta_1, \beta_2, \beta_3)$ consists of three infinitesimal angles.
Under the transformation (5.18), the polynomial p transforms as

$$p \to p' = \sum_{m_i \in m} c_i'(\vec{c}, \vec{\alpha}) m_i \ , \tag{5.20}$$

where the new coefficients, c_i', depend on the coefficients $\vec{c}$ and the angles $\vec{\alpha}$, and where we only keep terms linear in α_i. Since invariants are defined by $p = p'$, we obtain a system of equations,

$$c_i = c_i'(\vec{c}, \vec{\alpha}) \ , \tag{5.21}$$

determining all invariants of order N.
For $N = 2$, the sum in Eq. (5.16) runs from $i = 1$ to $i = 36$, since there are 36 different monomials of order $N = 2$. Using for example *Mathematica's* option *SolveAlways* [142], solutions for the coefficients c_i can be found, such that Eqs. (5.21) are fulfilled for arbitrary values of the angles α_i. Inserting the solution into the general ansatz (5.16), we obtain

$$p = c_1(\sigma^2 + \vec{\pi}^2) + c_2(\eta^2 + \vec{a}^2) + c_3(\sigma\eta - \vec{\pi}\cdot\vec{a}) \ . \tag{5.22}$$

Since the coefficients c_i are independent from each other, there exist exactly three linearly independent invariants of order $N = 2$:

$$\varphi_1 = \sigma^2 + \vec{\pi}^2 \ , \quad \varphi_2 = \eta^2 + \vec{a}^2 \ , \quad \varphi_3 = \sigma\eta - \vec{\pi}\cdot\vec{a} \ . \tag{5.23}$$

For $N = 4$, the sum in Eq. (5.16) runs from $i = 1$ to $i = 330$, since there are 330 different monomials of order $N = 4$. Again, using *Mathematica*, we find solutions for the coefficients c_i, such that Eqs. (5.21) are fulfilled for arbitrary values of the angles α_i. Inserting the solution into the general ansatz (5.16), we obtain

$$\begin{aligned} p = {} & c_1\left(\eta^2 + \vec{a}^2\right)^2 + c_2\left(\sigma^2 + \vec{\pi}^2\right)^2 + c_3\left(-\sigma\eta + \vec{\pi}\cdot\vec{a}\right)^2 + c_4\left(-\sigma\eta + \vec{\pi}\cdot\vec{a}\right)\left(\sigma^2 + \vec{\pi}^2\right) \\ & + c_5\left(\eta^2 + \vec{a}^2\right)\left(-\sigma\eta + \vec{\pi}\cdot\vec{a}\right) + c_6\left[\left(\eta^2 + \vec{a}^2\right)\left(\sigma^2 + \vec{\pi}^2\right) - \left(\sigma\eta - \vec{\pi}\cdot\vec{a}\right)^2\right] \ . \end{aligned} \tag{5.24}$$

Since the coefficients c_i are independent from each other, there exist exactly four linearly independent invariants of order $N = 4$:

$$\varphi_1^2 \ , \quad \varphi_2^2 \ , \quad \varphi_1\varphi_2 \ , \quad \gamma = \varphi_3^2 \ . \tag{5.25}$$

Note that the quadratic invariant φ_3 is not invariant under parity transformations

$$\sigma \to \sigma \ , \quad \vec{\pi} \to \vec{\pi} \ , \quad \eta \to -\eta \ , \quad \vec{a} \to -\vec{a} \ , \tag{5.26}$$

and therefore cannot appear in a theory without parity violation.
Note further that the invariants (5.23) and (5.25) are also invariant under $SU(2)_V$ transformations (5.19). Proceeding along the same lines described above one can derive several additional invariants for this symmetry. Since these are not $SU(2)_A$ symmetric, and hence no $SU(2)_A \times SU(2)_V$ invariants, we do not list them here.

Chapter 6

Fixed-point analysis of dimensionally reduced theories

In this chapter we study the fixed points for different dimensionally reduced scalar models calculated from the FRG equation in local-potential approximation (4.24). The method we use is described in Sec. 4.3.2. The stability properties of the fixed points are investigated in the framework discussed in Sec. 2.3. We note that the stability properties of fixed points depend on the spatial dimension, which is set to $D = 3$ for all our studies (although we keep D general in the expressions for the flow equations up to quartic order; it is fixed to $D = 3$ in the flow equations for higher-order couplings). We merely state the potentials but always assume a kinetic term of the form (2.23).

6.1 $O(N)$ model

In field theory, the $O(N)$ model for the N-dimensional vector representation of the orthogonal group $O(N)$ is defined by the potential

$$U = r\vec{\phi}\cdot\vec{\phi} + \frac{\lambda}{24}\left(\vec{\phi}\cdot\vec{\phi}\right)^2 \ , \tag{6.1}$$

where $\vec{\phi} = (\phi_1, ..., \phi_N)^T$ denotes a real N-component vector. The $O(N \leq 3)$ models are also known under the following names: Ising model ($N = 1$), XY-model ($N = 2$), Heisenberg model ($N = 3$). Including higher-order terms, $\sim \left(\vec{\phi}\cdot\vec{\phi}\right)^n$ with $n > 2$, the potential (6.1) is actually the most general $O(N)$-symmetric polynomial for the fundamental representation of $O(N)$.
For $N = 1$ we obtain

$$k\partial_k \bar{r}_k = -2\bar{r}_k - K_D \frac{\bar{\lambda}_k}{2(1+2\bar{r}_k)^2} \tag{6.2}$$

$$k\partial_k \bar{\lambda}_k = (D-4)\bar{\lambda}_k + K_D \frac{6\bar{\lambda}_k^{\,2}}{(1+2\bar{r}_k)^3} \ . \tag{6.3}$$

In Fig. 6.1 we show the solution of the above flow equations for $D = 3$ ($K_3 = 1/6\pi^2$) in the neighborhood of the Wilson-Fisher fixed point.

We note that for $\bar{r} = 0$ the results from the lowest-order ϵ-expansion are reproduced. For a derivation of the flow equations in the ϵ-expansion we refer to chapter 4.2.2 of Ref. [6] and simply cite the result:

$$k\partial_k \bar{r}_k = -2\bar{r}_k - \frac{1}{4}\frac{\bar{u_k}}{1+2\bar{r}_k} \tag{6.4}$$

$$k\partial_k \bar{u}_k = (D-4)\bar{u}_k + \frac{3}{2}\frac{{\bar{u_k}}^2}{(1+2\bar{r}_k)^2} \ . \tag{6.5}$$

Redefining $\bar{u} = 4K_D\bar{\lambda}$, we observe that Eq. (6.3) indeed equals Eq. (6.5) for $\bar{r} = 0$.

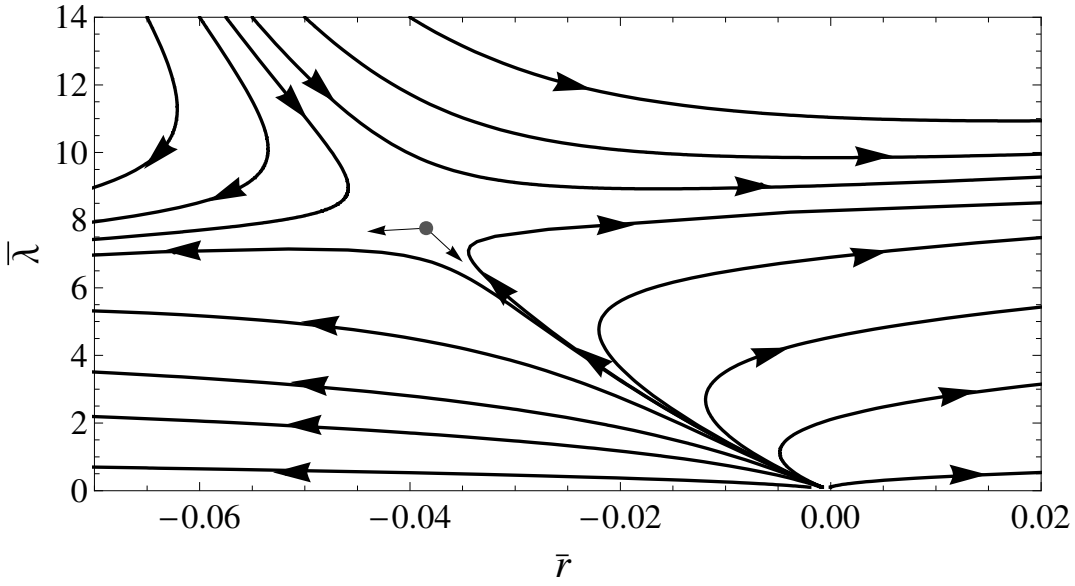

Figure 6.1: Solution of the flow equations in the neighborhood of the IR-stable Ising fixed point (grey point). Arrows point in IR direction. The eigenvectors plotted indicate the relevant and the irrelevant scaling direction, respectively.

For arbitrary N, the flow equations and the fixed points with their associated stability-matrix eigenvalues can be easily calculated using the *Mathematica* notebook provided in App. D. In Tab. 6.1 we list results for several values of N.

6.2 Models with two-component order parameter and a stable fixed point

In this section we present our FRG results for the potential (2.41).
Let us first consider the case $g_3 \equiv 0$, which corresponds to the most general C_{4v}-potential. We

Table 6.1: Stability-matrix eigenvalues, y_i, for the Wilson-Fisher fixed point of the $O(N)$ model, $d = 3$, FRG (in local-potential approximation), up to quartic coupling. The bar denotes rescaled quantities.

N	$\frac{1}{2}\bar{\mu}_*^2$	$\bar{\lambda}_{1*}$	$\nu = -1/y_1$	y_2
1	-0.03846	7.76271	0.54272=-1/-1.84256	1.1759
2	-0.04545	6.67366	0.55149=-1/-1.81327	1.21327
3	-0.05102	5.84682	0.55871=-1/-1.78985	1.24439
4	-0.05556	5.1988	0.564751=-1/-1.77069	1.27069
8	-0.06757	3.59143	0.581495=-1/-1.71971	1.34471

obtain the flow equations

$$k\partial_k \bar{r}_k = -2\bar{r}_k - 2K_D \frac{6\bar{g}_{1,k} + \bar{g}_{2,k}}{(1+2\bar{r}_k)^2} \tag{6.6}$$

$$k\partial_k \bar{g}_{1,k} = (D-4)\bar{g}_{1,k} + 4K_D \frac{36\bar{g}_{1,k}^2 + \bar{g}_{2,k}^2}{(1+2\bar{r}_k)^3} \tag{6.7}$$

$$k\partial_k \bar{g}_{2,k} = (D-4)\bar{g}_{2,k} + 32K_D \frac{(3\bar{g}_{1,k} + \bar{g}_{2,k})\,\bar{g}_{2,k}}{(1+2\bar{r}_k)^3} \ . \tag{6.8}$$

Apart from the IR-unstable Gaussian fixed point, $(\bar{r} = 0, \bar{g}_1 = 0, \bar{g}_2 = 0)$, we find two IR-unstable anisotropic fixed points,

$$(\bar{r} = -0.03846, \bar{g}_1 = 0.16172, \bar{g}_2 = 0.97034) \ ,$$
$$(\bar{r} = -0.03846, \bar{g}_1 = 0.32345, \bar{g}_2 = 0) \ ,$$

for both of which the stability-matrix eigenvalues read

$$\{-1.84256, 1.1759, -0.33334\} \ ,$$

and an IR-stable $O(2)$ fixed point,

$$(\bar{r} = -0.0454545, \bar{g}_1 = 0.278069, \bar{g}_2 = 0.556138) \ ,$$

for which the stability-matrix eigenvalues are given by

$$\{-1.81327, 1.21327, 0.2\} \ .$$

We also determined the flow equations for the most general C_4-invariant potential up to sixth order in the fields. The analysis, however, remains inconclusive due to the occurrence of marginal eigenvalues.

6.3 Cubic anisotropy model

The cubic anisotropy model (up to quartic order) is given by

$$U = r\sum_i^N \phi_i^2 + \frac{\lambda_1}{24}(\sum_i^N \phi_i^2)^2 + \frac{\lambda_2}{24}\sum_i^N \phi_i^4 \ . \tag{6.9}$$

The name is related to the group O constituted by all rotations (of the $N = 3$ components) which leave invariant the cube. For $N = 2$ cubic symmetry corresponds to the group C_{4v}, and for $N = 4$ to the group $\left(\frac{O}{D_2}; \frac{O}{D_2}\right)^*$. The model has been reviewed in section 11.3 of Ref. [14]. We restrict the discussion to $D = 3$. Apart from the trivial Gaussian one, there exist three different fixed points: the $O(N)$-symmetric fixed point, the fixed point with cubic symmetry, and a fixed point with Ising critical exponents (the quartic $O(N)$-symmetric coupling vanishes for this point). It has been pointed out that the $O(N)$ fixed point is IR stable for $N < N_c$, whereas it becomes unstable for $N > N_c$ where the fixed point with cubic symmetry is IR stable instead. The value of N_c, however, is still under debate. Studies in low order of the ϵ-expansion, as well as several complementary investigations, find $3 < N_c < 4$, whereas more recent 5-loop ϵ-expansion results indicate $2 < N_c < 3$. Therefore, in the following we consider the interesting case $N = 3$ from FRG in the local-potential approximation. We find the $O(3)$ fixed point to be IR stable, whereas the other fixed points (Gaussian, Ising-like, Cubic) are IR unstable. Again, the local-potential approximation is completely consistent with the one-loop ϵ-expansion.
We obtain the following flow equations for the rescaled couplings:

$$k\partial_k \bar{r}_k = -2\bar{r}_k - \frac{1}{6} K_D \frac{5\bar{\lambda}_{1,k} + 3\bar{\lambda}_{2,k}}{(1+2\bar{r}_k)^2} \ , \tag{6.10}$$

$$k\partial_k \bar{\lambda}_{1,k} = (D-4)\bar{\lambda}_{1,k} + \frac{2}{3} K_D \frac{\bar{\lambda}_{1,k}(11\bar{\lambda}_{1,k} + 6\bar{\lambda}_{2,k})}{(1+2\bar{r}_k)^3} \ , \tag{6.11}$$

$$k\partial_k \bar{\lambda}_{2,k} = (D-4)\bar{\lambda}_{2,k} + 2K_D \frac{\bar{\lambda}_{2,k}(4\bar{\lambda}_{1,k} + 3\bar{\lambda}_{2,k})}{(1+2\bar{r}_k)^3} \ . \tag{6.12}$$

Apart from the IR-unstable Gaussian fixed point, $(\bar{r} = 0, \bar{\lambda}_1 = 0, \bar{\lambda}_2 = 0)$, we find three fixed points.
The stability-matrix eigenvalues for the $O(3)$ fixed point, $(\bar{r} = -0.05102, \bar{\lambda}_1 = 5.84682, \bar{\lambda}_2 = 0)$, are given by $\{-1.78985, 1.24439, 0.09091\}$ and indicate that it is IR stable.
The cubic fixed point $(\bar{r} = -0.05, \bar{\lambda}_1 = 7.19494, \bar{\lambda}_2 = -2.39831)$ is associated with the stability-matrix eigenvalues $\{-1.79415, 1.23859, -0.11111\}$ indicating its IR instability.
Finally there is a Ising-like fixed point $(\bar{r} = -0.03846, \bar{\lambda}_1 = 0, \bar{\lambda}_2 = 7.76271)$ with stability-matrix eigenvalues $\{-1.84256, 1.1759, -0.33333\}$. The first two eigenvalues are characteristic of the Ising universality class (compare with Tab. 6.1) whereas the additional one indicates the IR instability of the fixed point.
One might suspect that the Ising-like fixed point is associated to eigenvalues distinguishable from the Ising universality class at higher truncation order. We checked this by including all linearly independent invariants of sixth order in the fields,

$$\lambda_3 (\sum_i^N \phi_i^2)^3 + \lambda_4 (\sum_i^N \phi_i^2)(\sum_j^N \phi_j^4) + \lambda_5 \sum_i^N \phi_i^6 \ . \tag{6.13}$$

We still find a Ising-like fixed point,

$$(\bar{r} = -0.07143, \bar{\lambda}_1 = 0, \bar{\lambda}_2 = 12.43052, \bar{\lambda}_3 = 0, \bar{\lambda}_4 = 0, \bar{\lambda}_5 = 0.75113) \ ,$$

associated with eigenvalues

$$\{12.2196, 5.21314, 2, -1.68572, 1.13275, -0.213137\} \ .$$

The eigenvalues $\{12.2196, -1.68572, 1.13275\}$ are indeed those found for the Ising model up to sixth order in the field.
The case $N = 4$, i.e. the most general $\left(\frac{O}{D_2}; \frac{O}{D_2}\right)^*$-potential, is discussed in Sec. 6.4. For the case $N = 2$, i.e., the most general C_{4v}-potential, we refer to Sec. 6.2.

6.4 Models with four-component order parameter and a stable fixed point

Table 6.2: Centralizers E_c (labeling a most general E_c-symmetric Landau potential) and the largest symmetry group leaving invariant the associated IR-stable fixed-point potential, E_c^*, called little group of E_c. $O(4)$ is called *isotropic*, $\left(\frac{Y}{C_2}; \frac{Y^*}{C_2}\right)^*$ is called *di-icosahedral*, $(D_\infty \times D_\infty)^*$ is called *dicylindrical*, and $\left(\frac{O}{D_2}; \frac{O}{D_2}\right)^*$ is called *cubic*.

E_c	E_c^*
$O(4)$	$O(4)$
$\left(\frac{Y}{C_2}; \frac{Y^*}{C_2}\right)^*$	$\left(\frac{Y}{C_2}; \frac{Y^*}{C_2}\right)^*$
$\left(\frac{O}{D_2}; \frac{O}{D_2}\right)^*$	$\left(\frac{O}{D_2}; \frac{O}{D_2}\right)^*$
$(D_\infty \times D_\infty)^*$	$(D_\infty \times D_\infty)^*$
$\left(\frac{D_4}{D_2}; \frac{D_4}{D_2}\right)^*$	$(D_\infty \times D_\infty)^*$
$\left(\frac{C_8}{C_4}; \frac{D_4}{D_2}\right)$	$(D_\infty \times D_\infty)^*$

In this section we discuss our FRG results for the most general potentials invariant under the anisotropic centralizers stated in Tab. 6.2. For the isotropic $O(4)$-symmetric potential we refer to Sec. 6.1.

6.4.1 $\left(\frac{Y}{C_2}; \frac{Y^*}{C_2}\right)^*$

The most general $\left(\frac{Y}{C_2}; \frac{Y^*}{C_2}\right)^*$-symmetric potential up to quartic order is given by

$$U = r\sum_{i=1}^{4}\phi_i^2 + \lambda_1\left(\sum_{i=1}^{4}\phi_i^2\right)^2 + \lambda_2\left[5(\phi_1^4+\phi_2^4+\phi_3^4)+\phi_4^4+\frac{60}{\sqrt{5}}\phi_1\phi_2\phi_3\phi_4+12\phi_4^2(\phi_1^2+\phi_2^2+\phi_3^2)\right] \quad (6.14)$$

We obtain the rescaled flow equations

$$k\partial_k\bar{r}_k = -2\bar{r}_k - 12K_D\frac{2\bar{\lambda}_{1,k}+7\bar{\lambda}_{2,k}}{(1+2\bar{r}_k)^2}\ , \quad (6.15)$$

$$k\partial_k\bar{\lambda}_{1,k} = (D-4)\bar{\lambda}_{1,k} + 48K_D\frac{4\bar{\lambda}_{1,k}^2+14\bar{\lambda}_{1,k}\bar{\lambda}_{2,k}+27\bar{\lambda}_{2,k}^2}{(1+2\bar{r}_k)^3}\ , \quad (6.16)$$

$$k\partial_k\bar{\lambda}_{2,k} = (D-4)\bar{\lambda}_{2,k} + 192K_D\frac{\bar{\lambda}_{2,k}(\bar{\lambda}_{1,k}+3\bar{\lambda}_{2,k})}{(1+2\bar{r}_k)^3}\ . \quad (6.17)$$

Again, we observe that the one-loop ϵ-expansion result (compare with Tab. III of Ref. [31]) is reproduced when setting $\bar{r}_k = 0$ and properly redefining the couplings. At this truncation order the $O(4)$ fixed point, $(\bar{r} = -0.05556, \bar{\lambda}_1 = 0.21662, \bar{\lambda}_2 = 0)$, is marginal as one infers from the stability-matrix eigenvalues $\{-1.77069, 1.27069, 0\}$, whereas the cubic fixed point, $(\bar{r} = -0.05319, \bar{\lambda}_1 = 0.28298, \bar{\lambda}_2 = -0.02096)$ is IR unstable as inferred from the eigenvalues $\{-1.78068, 1.25687, -0.047619\}$. The marginality of the isotropic fixed point indicates, however, that also the stability analysis of the anisotropic fixed point is inconclusive at quartic truncation order. We note that also in the one-loop ϵ-expansion a marginal eigenvalue occurs (compare with Tab. IV of Ref. [31]). In the framework of the ϵ-expansion one can get rid of the marginality at two-loop order (see Tab. V of Ref. [31]). In the local-potential approximation of FRG, taking into account the sixth-order invariants

$$\lambda_3 \left(\sum_{i=1}^{4} \phi_i^2\right)^3 + \lambda_4 \left(\sum_{i=1}^{4} \phi_i^2\right)\left[5(\phi_1^4 + \phi_2^4 + \phi_3^4) + \phi_4^4 + \frac{60}{\sqrt{5}}\phi_1\phi_2\phi_3\phi_4 + 12\phi_4^2(\phi_1^2 + \phi_2^2 + \phi_3^2)\right] \tag{6.18}$$

one can get also rid of the marginal eigenvalue (which should be the case for the one-loop ϵ-expansion as well). We note, however, that these are not all linearly independent sixth order invariants, and the remaining one(s) should be taken into account in a fully conclusive analysis. For simplicity we neglect them in our investigation and indeed find an IR-stable $\left(\frac{Y}{C_2}; \frac{Y^*}{C_2}\right)^*$-symmetric fixed point,

$$(\bar{r} = -0.12011, \bar{\lambda}_1 = 0.23417, \bar{\lambda}_2 = 0.03085, \bar{\lambda}_3 = 0.18003, \bar{\lambda}_4 = 0.0621996) \,,$$

for which the stability-matrix eigenvalues read

$$\{14.5934, 6.17205, 1.5506, 0.208268, -1.48923\} \,.$$

6.4.2 $\left(\frac{O}{D_2}; \frac{O}{D_2}\right)^*$

We proceed with the most general $\left(\frac{O}{D_2}; \frac{O}{D_2}\right)^*$-potential up to sixth polynomial order,

$$U = r\sum_i^4 \phi_i^2 + \frac{\lambda_1}{24}\left(\sum_i^4 \phi_i^2\right)^2 + \frac{\lambda_2}{24}\sum_i^4 \phi_i^4 + \lambda_3\left(\sum_i^4 \phi_i^2\right)^3 + \lambda_4\left(\sum_i^4 \phi_i^2\right)\left(\sum_j^4 \phi_j^4\right) + \lambda_5\left(\sum_i^4 \phi_i^6\right) \,. \tag{6.19}$$

We find the following flow equations:

$$k\partial_k \bar{r}_k = -2\bar{r}_k - \frac{K_D}{2}\frac{(2\bar{\lambda}_{1,k} + \bar{\lambda}_{2,k})}{(1+2\bar{r}_k)^2} \,, \tag{6.20}$$

$$k\partial_k \bar{\lambda}_{1,k} = (D-4)\bar{\lambda}_{1,k} + 4K_D \frac{\bar{\lambda}_{1,k}(2\bar{\lambda}_{1,k} + \bar{\lambda}_{2,k}) - 72(2\bar{r}_k+1)(4\bar{\lambda}_{3,k} + \bar{\lambda}_{4,k})}{(1+2\bar{r}_k)^3} \,, \tag{6.21}$$

$$k\partial_k \bar{\lambda}_{2,k} = (D-4)\bar{\lambda}_{2,k} + 2K_D \frac{\bar{\lambda}_{2,k}(4\bar{\lambda}_{1,k} + 3\bar{\lambda}_{2,k}) - 72(2\bar{r}_k+1)(4\bar{\lambda}_{4,k} + 5\bar{\lambda}_{5,k})}{(1+2\bar{r}_k)^3} \,, \tag{6.22}$$

$$k\partial_k \bar{\lambda}_{3,k} = \frac{K_3}{72}\frac{-10\bar{\lambda}_{1,k}^3 - 3\bar{\lambda}_{2,k}\bar{\lambda}_{1,k}^2 + 288(2\bar{r}_k+1)(9\bar{\lambda}_{3,k} + \bar{\lambda}_{4,k})\bar{\lambda}_{1,k} + 432(2\bar{r}_k+1)\bar{\lambda}_{2,k}\bar{\lambda}_{3,k}}{(1+2\bar{r}_k)^4} \,, \tag{6.23}$$

$$k\partial_k \bar{\lambda}_{4,k} = \frac{K_3}{24}\frac{-8\bar{\lambda}_{2,k}\bar{\lambda}_{1,k}^2 - 3(\bar{\lambda}_{2,k}^2 - 16(2\bar{r}_k+1)(14\bar{\lambda}_{4,k} + 5\bar{\lambda}_{5,k}))\bar{\lambda}_{1,k} + 48(2\bar{r}_k+1)\bar{\lambda}_{2,k}(12\bar{\lambda}_{3,k} + 7\bar{\lambda}_{4,k})}{(1+2\bar{r}_k)^4} \,, \tag{6.24}$$

$$k\partial_k \bar{\lambda}_{5,k} = \frac{K_3}{8}\frac{\bar{\lambda}_{2,k}(128\bar{\lambda}_{4,k}(2\bar{r}_k+1) - \bar{\lambda}_{2,k}(2\bar{\lambda}_{1,k} + \bar{\lambda}_{2,k})) + 80(2\bar{r}_k+1)(2\bar{\lambda}_{1,k} + 3\bar{\lambda}_{2,k})\bar{\lambda}_{5,k}}{(1+2\bar{r}_k)^4} \,. \tag{6.25}$$

At quartic truncation order ($\lambda_3 = \lambda_4 = \lambda_5$) we reproduce the ϵ-expansion result at one-loop order (compare with Eqs. (4) and (5) of Ref. [143]) when setting $\bar{r}_k = 0$ and properly redefining the

couplings. Whereas the cubic fixed point is IR unstable, the $O(4)$ fixed point is marginal, indicating that one has to go beyond quartic truncation order. To solve the fixed point equations at higher truncation order we applied an algorithm with randomized starting values in a reasonably large domain of parameter space, each of the starting values lying in the interval $[-10^4, 10^4]$. Using 10^5 different starting values, we checked that these should be the only solutions for given starting values in the above domain of parameter space. Apart from the Gaussian fixed point, we find six different fixed points. There are three IR-unstable $\left(\frac{O}{D_2}; \frac{O}{D_2}\right)^*$-symmetric fixed points, first

$$(\bar{r} = -0.02268, \bar{\lambda}_1 = -11.217, \bar{\lambda}_2 = 27.3307, \bar{\lambda}_3 = -0.05318, \bar{\lambda}_4 = 1.51546, \bar{\lambda}_5 = -0.30854) \ ,$$

for which the stability-matrix eigenvalues read

$$\{11.4536, -2.85698, -1.91474, -0.0671996 + 1.55317\,\mathrm{i}, -0.0671996 - 1.55317\,\mathrm{i}, 1.14137\} \ ,$$

second

$$(\bar{r} = -0.04685, \bar{\lambda}_1 = -4.22854, \bar{\lambda}_2 = 17.5725, \bar{\lambda}_3 = 0.23709, \bar{\lambda}_4 = -0.82491, \bar{\lambda}_5 = 1.40115) \ ,$$

for which the stability-matrix eigenvalues read

$$\{11.0574, 2.61531, -1.76448, 1.04669, -0.295782 + 0.790764\,\mathrm{i}, -0.295782 - 0.790764\,\mathrm{i}\} \ ,$$

and third

$$(\bar{r} = -0.10102, \bar{\lambda}_1 = 13.3721, \bar{\lambda}_2 = -11.5082, \bar{\lambda}_3 = 1.07211, \bar{\lambda}_4 = -2.49304, \bar{\lambda}_5 = 1.8374) \ ,$$

for which the stability-matrix eigenvalues read

$$\{13.761, 6.38171, -0.104173 + 2.54967\,\mathrm{i}, , -0.104173 - 2.54967\,\mathrm{i}, -1.52874, 1.36167\} \ .$$

Then there is the same Ising-like fixed point as for the cubic anisotropy model with $N = 3$,

$$(\bar{r} = -0.07143, \bar{\lambda}_1 = 0, \bar{\lambda}_2 = 12.43052, \bar{\lambda}_3 = 0, \bar{\lambda}_4 = 0, \bar{\lambda}_5 = 0.75113) \ ,$$

associated with the eigenvalues

$$\{12.2196, 5.21314, 2, -1.68572, 1.13275, -0.213137\} \ .$$

Also the $O(4)$ fixed point

$$(\bar{r} = -0.10976, \bar{\lambda}_1 = 7.91848, \bar{\lambda}_2 = 0, \bar{\lambda}_3 = 0.309944, \bar{\lambda}_4 = 0, \bar{\lambda}_5 = 0)$$

is unstable as one infers from its stability-matrix eigenvalues

$$\{12.9187, 9.24667, 5.625, -1.50401, 1.33533, -0.121665\} \ .$$

Finally, there is a fourth $\left(\frac{O}{D_2}; \frac{O}{D_2}\right)^*$-symmetric fixed point,

$$(\bar{r} = -0.10605, \bar{\lambda}_1 = 5.87836, \bar{\lambda}_2 = 3.83762, \bar{\lambda}_3 = 0.1598, \bar{\lambda}_4 = 0.22639, \bar{\lambda}_5 = 0.09684) \ ,$$

which is IR stable as one infers from the eigenvalues

$$\{13.1153, 9.56795, 5.17813, 1.31346, 0.0875986, -1.52192\} \ .$$

6.4.3 $(D_\infty \times D_\infty)^*$, $\left(\frac{D_4}{D_2};\frac{D_4}{D_2}\right)^*$, and $\left(\frac{C_8}{C_4};\frac{D_4}{D_2}\right)$

The most general $\left(\frac{C_8}{C_4};\frac{D_4}{D_2}\right)$-invariant Landau potential up to sixth polynomial order reads [40]

$$\begin{aligned}U = {} & r\sum_i^4 \phi_i^2 + g_1\left(\sum_i^4 \phi_i^2\right)^2 + g_2\left[(\phi_1^2+\phi_2^2)^2 + (\phi_3^2+\phi_4^2)^2\right] + g_3\left[\phi_1\phi_2(\phi_1^2-\phi_2^2) - \phi_3\phi_4(\phi_3^2-\phi_4^2)\right] \\ & + g_4\sum_i^4 \phi_i^4 + g_5\left(\sum_i^4 \phi_i^2\right)^3 + g_6\sum_i^4 \phi_i^6 + g_7\left[\phi_1\phi_2(\phi_1^4-\phi_2^4) - \phi_3\phi_4(\phi_3^4-\phi_4^4)\right] + g_8\left(\sum_i^4 \phi_i^2\right)\left(\sum_j^4 \phi_j^4\right) \\ & + g_9\left(\sum_i^4 \phi_i^2\right)\left[(\phi_1^2+\phi_2^2)^2 + (\phi_3^2+\phi_4^2)^2\right] + g_{10}\left(\sum_i^4 \phi_i^2\right)\left[\phi_1\phi_2(\phi_1^2-\phi_2^2) - \phi_3\phi_4(\phi_3^2-\phi_4^2)\right] \ . \end{aligned} \tag{6.26}$$

The special case $g_i = 0$, where $i \geq 3$, corresponds to the most general $(D_\infty \times D_\infty)^*$-symmetric Landau potential at quartic order. For $g_3 = 0$, $g_i = 0$, where $i \geq 5$, one obtains the most general $\left(\frac{D_4}{D_2};\frac{D_4}{D_2}\right)^*$-symmetric Landau potential at quartic order. At sixth order in the fields, however, the most general Landau potentials for the latter symmetries are not special cases of U.
We derived the flow equations for the full potential U. Since they are rather lengthy we do not state them here explicitly. We have solved them numerically by the method of randomized initial values. Unfortunately there exist fixed points exhibiting marginal eigenvalues. We suspect that this might have to do with the existence of lines of fixed points (compare with the discussion in Ref. [31]). Interestingly, we find two IR-stable fixed points of different symmetry, namely

$$A_1 \equiv (\bar{r} = -0.09655, \bar{g}_1 = 0.73696, \bar{g}_2 = -0.64010, \bar{g}_5 = 0.62921, \bar{g}_9 = -0.26343, \bar{g}_{3,4,6,7,8,10} = 0) \ , \tag{6.27}$$

which is associated to the stability-matrix eigenvalues

$$\begin{aligned}&\{13.7836, 8.1382, 8.1382, 0.246709 + 2.80159\,\mathrm{i}, 0.246709 - 2.80159\,\mathrm{i}, 0.156746 + 1.57142\,\mathrm{i}, \\ &0.156746 - 1.57142\,\mathrm{i}, 0.156746 + 1.57142\,\mathrm{i}, 0.156746 - 1.57142\,\mathrm{i}, 1.33844, -1.548\} \ , \end{aligned} \tag{6.28}$$

and

$$A_2 \equiv (\bar{r} = -0.08513, \bar{g}_1 = -0.01660, \bar{g}_2 = 0.45873, \bar{g}_5 = -0.28840, \bar{g}_9 = 0.83807, \bar{g}_{3,4,6,7,8,10} = 0) \ , \tag{6.29}$$

which is associated to the eigenvalues

$$\{12.4717, 9.7189, 9.7189, 5.43242, 3.21794, 3.21794, 1.19774, 0.1574, 0.1574, 0.000472, -1.62133\} \ . \tag{6.30}$$

We checked that the eigenvalue 0.000472 is really positive and not a marginal eigenvalue in insufficient numerical accuracy. If the stability analysis at this truncation order were not inconclusive due to the occurrence of marginal eigenvalues for other fixed points, the simultaneous existence of two different IR-stable fixed points would constitute a violation of the universality hypothesis. We therefore expect that either A_1 or A_2 becomes unstable at higher truncation order. Further investigations are necessary to clarify the situation.

6.5 $U(2)_A \times U(2)_V$ linear sigma model

We were pushed to a reinvestigation of the $U(2)_A \times U(2)_V$ linear sigma model from the FRG method during the final stage of our work where we became aware of the very recent publication [33] which confirms the existence of an IR-stable $U(2)_A \times U(2)_V$-symmetric fixed point from a field-theoretic RG approach. In this section we study the most general Landau potential up to sixth polynomial order invariant under $U(2)_A \times U(2)_V$ in the $[2,\bar{2}] \oplus [\bar{2},2]$-representation. Since the authors of Ref. [33] use a resummation procedure, we speculate that it might be necessary to go beyond the perturbatively renormalizable truncation order (four for $D = 3$) in order to reproduce their result from FRG. Whereas no IR-stable fixed points were found at quartic polynomial order [87], we find two IR-stable fixed points at sixth order, S_1 and S_2. This is a rather unexpected result because no marginal stability-matrix eigenvalues occur for the fixed points at quartic order. In the absence of marginal eigenvalues it is usually assumed that the utilized truncation order is sufficient, which does not seem to be justified in the given case at first glance. The occurrence of *two* IR-stable fixed points is critical with respect to the universality hypothesis. Although both of them seem to be $U(2)_A \times U(2)_V$-symmetric, they are associated with different values for ν. The results at this truncation order, however, are inconclusive because the Gaussian fixed point aquires marginal stability-matrix eigenvalues. We also investigated higher-order truncations (up to canonical scaling dimension ten) and found a single IR-unstable $U(2)_A \times U(2)_V$-symmetric at each of these truncation orders, while the Gaussian fixed-point remains marginal rendering our studies inconclusive. We believe that this is different beyond the local-potential approximation which assumes $\eta = 0$. In fact, the IR-stable $U(2)_A \times U(2)_V$-symmetric fixed point found in Ref. [33] is associated with an anomalous dimension of $\eta \sim 0.12$ indicating that it might be necessary to go beyond the local-potential approximation to confirm its existence. Investigations in this direction are in progress.

Using a similar algorithm to the one provided in App. B.2, we verify that the potential

$$\frac{1}{2}m_\Phi^2 \mathrm{Tr}\Phi^\dagger\Phi + \lambda_1(\mathrm{Tr}\Phi^\dagger\Phi)^2 + \lambda_2 \mathrm{Tr}(\Phi^\dagger\Phi)^2 + \lambda_3(\mathrm{Tr}\Phi^\dagger\Phi)^3 + \lambda_4\left(\mathrm{Tr}\Phi^\dagger\Phi\right)\mathrm{Tr}(\Phi^\dagger\Phi)^2 \ , \tag{6.31}$$

where Φ is defined in Eq. (3.15), and which can be rewritten as

$$\begin{aligned} U = {} & r\left(\sigma^2 + \vec{\pi}^2 + \eta^2 + \vec{a}_0^2\right) + g_1\left(\sigma^2 + \vec{\pi}^2 + \eta^2 + \vec{a}_0^2\right)^2 \\ & + g_2\left[\left(\sigma^2 + \vec{\pi}^2\right)\left(\eta^2 + \vec{a}_0^2\right) - \left(\sigma\eta - \vec{\pi}\cdot\vec{a}_0\right)^2\right] + g_3\left(\sigma^2 + \vec{\pi}^2 + \eta^2 + \vec{a}_0^2\right)^3 \\ & + g_4\left(\sigma^2 + \vec{\pi}^2 + \eta^2 + \vec{a}_0^2\right)\left[\left(\sigma^2 + \vec{\pi}^2\right)\left(\eta^2 + \vec{a}_0^2\right) - \left(\sigma\eta - \vec{\pi}\cdot\vec{a}_0\right)^2\right] \ , \end{aligned} \tag{6.32}$$

is the most general Landau potential at the given order. We obtain the following flow equations for the rescaled couplings:

$$k\frac{\partial \bar{r}_k}{\partial k} = -2\bar{r}_k - 2K_D\frac{20\bar{g}_{1,k}+3\bar{g}_{2,k}}{(1+2\bar{r}_k)^2} \ , \tag{6.33}$$

$$k\frac{\partial \bar{g}_{1,k}}{\partial k} = (D-4)\bar{g}_{1,k} + 2K_D\frac{128\bar{g}_{1,k}^2+24\bar{g}_{2,k}\bar{g}_{1,k}+6\bar{g}_{2,k}^2-3(1+2\bar{r}_k)(12\bar{g}_{3,k}+\bar{g}_{4,k})}{(1+2\bar{r}_k)^3} \ , \tag{6.34}$$

$$k\frac{\partial \bar{g}_{2,k}}{\partial k} = (D-4)\bar{g}_{2,k} + 16K_D\frac{\bar{g}_{2,k}^2+12\bar{g}_{1,k}\bar{g}_{2,k}-2\bar{g}_{4,k}(1+2\bar{r}_k)}{(1+2\bar{r}_k)^3} \ , \tag{6.35}$$

$$k\frac{\partial \bar{g}_{3,k}}{\partial k} = 8K_3\frac{-272\bar{g}_{1,k}^3-36\bar{g}_{2,k}\bar{g}_{1,k}^2-18\bar{g}_{2,k}^2\bar{g}_{1,k}-3\bar{g}_{2,k}^3+3(2\bar{r}_k+1)(\bar{g}_{2,k}(3\bar{g}_{3,k}+\bar{g}_{4,k})+2\bar{g}_{1,k}(22\bar{g}_{3,k}+\bar{g}_{4,k}))}{(1+2\bar{r}_k)^4} \ , \tag{6.36}$$

$$k\frac{\partial \bar{g}_{4,k}}{\partial k} = 8K_3\frac{(2\bar{r}_k+1)(72\bar{g}_{2,k}\bar{g}_{3,k}+92\bar{g}_{1,k}\bar{g}_{4,k}+19\bar{g}_{2,k}\bar{g}_{4,k})-3\bar{g}_{2,k}\left(192\bar{g}_{1,k}^2+44\bar{g}_{2,k}\bar{g}_{1,k}+\bar{g}_{2,k}^2\right)}{(1+2\bar{r}_k)^4} \ . \tag{6.37}$$

Apart from two complex-valued fixed points (which are not relevant for our purposes) and the Gaussian fixed point (exhibiting two marginal stability-matrix eigenvalues), we find the following fixed points.
First, there is the $O(8)$ fixed point,

$$(\bar{r} = -0.135468, \bar{g}_1 = 0.213201, \bar{g}_2 = 0, \bar{g}_3 = 0.128472, \bar{g}_4 = 0) \ ,$$

which is IR unstable as one infers from the stability-matrix eigenvalues

$$\{12.9247, 8.12499, 1.50915, -1.3798, -0.503366\} \ .$$

The interesting fixed points are the IR stable ones,

$$S_1 \equiv (\bar{r} = -0.131592, \bar{g}_1 = 0.0827324, \bar{g}_2 = 0.858639, \bar{g}_3 = 0.209119, \bar{g}_4 = 0.216127) \ , \tag{6.38}$$

which is associated with stability-matrix eigenvalues

$$\{15.6603, 0.624502 + 3.53423\,\mathrm{i}, 0.624502 - 3.53423\,\mathrm{i}, 1.63064, -1.37434\} \ , \tag{6.39}$$

and

$$S_2 \equiv (\bar{r} = -0.102993, \bar{g}_1 = 0.333416, \bar{g}_2 = -0.941056, \bar{g}_3 = 0.306972, \bar{g}_4 = -0.715374) \ , \tag{6.40}$$

which is associated with stability-matrix eigenvalues

$$\{13.2219, 1.18817 + 2.14805\,\mathrm{i}, 1.18817 - 2.14805\,\mathrm{i}, -1.51084, 1.37317\} \ . \tag{6.41}$$

We observe that the stability-matrix eigenvalues (6.39) and (6.41), respectively, are different but very similar.

6.6 $SU(2)_A \times U(2)_V$ linear sigma model

In this section (compare with our publication [1]) we investigate the FRG flow of the Lagrangian (3.22) in different parameterizations proceeding in analogy to Ref. [87]. We reproduce the result of Ref. [87] in the limit $c, y, z \to 0$. The fields Φ_i entering Eq. (4.20) are given by $\sigma, \vec{\pi}, \eta$, and $\vec{a}$. With the invariants

$$\varphi \equiv \sigma^2 + \vec{\pi}^2 + \eta^2 + \vec{a}^2 \ , \quad \xi = (\sigma^2 + \vec{\pi}^2)(\eta^2 + \vec{a}^2) - (\sigma\eta - \vec{\pi}\cdot\vec{a})^2 \ , \quad \alpha \equiv \sigma^2 - \eta^2 + \vec{\pi}^2 - \vec{a}^2 \ , \tag{6.42}$$

and the abbreviation

$$\beta \equiv \alpha^2 - \frac{\varphi^2}{2} + 2\xi = \frac{1}{2}\left(\eta^2 + \vec{a}^2 - \sigma^2 - \vec{\pi}^2 - 2\vec{a}\cdot\vec{\pi} + 2\eta\sigma\right)\left(\eta^2 + \vec{a}^2 - \sigma^2 - \vec{\pi}^2 + 2\vec{a}\cdot\vec{\pi} - 2\eta\sigma\right) \ ,$$

the bare potential (3.23) reads

$$U(\varphi, \xi, \alpha) = \frac{1}{2}\mu^2\varphi + \frac{1}{4!}\lambda_1\varphi^2 + \lambda_2\xi + c\alpha + y\alpha\varphi + z\beta \ . \tag{6.43}$$

Using relation (3.20) and a different notation,

$$\varphi_1 = \sigma^2 + \vec{\pi}^2 \ , \quad \varphi_2 = \eta^2 + \vec{a}^2 \ , \quad \gamma = (\sigma\eta - \vec{\pi}\cdot\vec{a})^2 \ , \tag{6.44}$$

we obtain

$$U(\varphi_1, \varphi_2, \gamma) = m_1^2\varphi_1 + m_2^2\varphi_2 + l_1\varphi_1^2 + l_2\varphi_2^2 + l_{12}\varphi_1\varphi_2 + l_3\gamma \ , \tag{6.45}$$

where we introduced new couplings,

$$m_1^2 = \frac{1}{2}\mu^2 + c \ , \quad m_2^2 = \frac{1}{2}\mu^2 - c \ , \tag{6.46}$$

$$l_1 = y + \frac{\lambda_1}{4!} + \frac{z}{2} \ , \quad l_2 = -y + \frac{\lambda_1}{4!} + \frac{z}{2} \ , \quad l_{12} = \frac{\lambda_1}{12} + \lambda_2 - z \ , \quad l_3 = -(\lambda_2 + 2z) \ . \tag{6.47}$$

Note that the number of linearly independent invariants is the same in expressions (6.43) and (6.45), respectively. When calculating the mass eigenvalues M_i, we have to simplify the computation by setting the values of several fields to zero after having performed the second derivatives in Eq. (4.20). Keeping all fields nonzero, we obtain complicated expressions for the eigenvalues because an 8×8 matrix has to be diagonalized. One can circumvent the diagonalization using the relation

$$\sum_i \frac{1}{k^2 + M_i^2} = Tr\mathcal{M}^{-1} \ , \quad \mathcal{M}_{ij} \equiv M_{ij} + k^2\delta_{ij} \ . \tag{6.48}$$

However, it still would take a symbolic computation program a long time to expand the r.h.s. of the FRG equation (4.24) in powers of the fields. Fortunately, the ϵ-expansion results from Ref. [85] can be reproduced by keeping nonzero values only for σ and one of the components of $\vec{a}$, say a_1 [87]. Note that this is not possible if we choose another field than a component of $\vec{a}$, since then $\xi = 0$ and we do not obtain a flow equation for λ_2.

6.6.1 Parameterization in terms of invariants

In this section we use the parameterization (6.45) for the potential. It is nontrivial to rewrite all fields ϕ_i in terms of the above invariants. Since we have three invariants, the rewriting can be performed unambiguously only if we keep at least three fields nonzero. Keeping η, σ, and a_1 nonzero, we obtain the unambiguous mapping

$$\sigma = \sqrt{\varphi_1} \ , \quad a_1 = \sqrt{\frac{\varphi_1\varphi_2 - \gamma}{\varphi_1}} \ , \quad \eta = \sqrt{\frac{\gamma}{\varphi_1}} \ . \tag{6.49}$$

We also repeated our analysis using π_1 instead of η and found identical results.
We express the mass eigenvalues M_i in terms of φ_1, φ_2, and γ and expand the r.h.s. of Eq. (4.24) in powers of these invariants. Then, inserting Eq. (6.45) on the l.h.s., we read off flow equations for the couplings by comparing coefficients. In order to calculate critical exponents we rescale quantities to obtain flow equations for dimensionless parameters. With

$$m_{i,k}^2 = k^2\bar{m}_{i,k}^2 \ , \quad l_{i,k} = k^{4-d}\bar{l}_{i,k} \ , \tag{6.50}$$

we obtain

$$k\frac{\partial\bar{m}_1^2}{\partial k} = -2\bar{m}_1^2 - \frac{1}{3\pi^2}\left(\frac{12\bar{l}_1}{\bar{\epsilon}_1^2} + \frac{\bar{l}_3 + 4\bar{l}_{12}}{\bar{\epsilon}_2^2}\right) , \tag{6.51}$$

$$k\frac{\partial\bar{m}_2^2}{\partial k} = -2\bar{m}_2^2 - \frac{1}{3\pi^2}\left(\frac{\bar{l}_3 + 4\bar{l}_{12}}{\bar{\epsilon}_1^2} + \frac{12\bar{l}_2}{\bar{\epsilon}_2^2}\right) , \tag{6.52}$$

$$k\frac{\partial\bar{l}_{12}}{\partial k} = -\bar{l}_{12} + \frac{2\left[4(\bar{l}_1\bar{\epsilon}_2^3 + \bar{l}_2\bar{\epsilon}_1^3)\left(\bar{l}_3 + 6\bar{l}_{12}\right) + \left(\bar{l}_3^2 + 4\bar{l}_{12}^2\right)(\bar{\epsilon}_1 + \bar{\epsilon}_2)\,\bar{\epsilon}_1\bar{\epsilon}_2\right]}{3\pi^2\bar{\epsilon}_1^3\bar{\epsilon}_2^3} , \tag{6.53}$$

$$k\frac{\partial\bar{l}_1}{\partial k} = -\bar{l}_1 + \frac{2}{3\pi^2}\left(\frac{48\bar{l}_1^2}{\bar{\epsilon}_1^3} + \frac{\bar{l}_3^2 + 2\bar{l}_3\bar{l}_{12} + 4\bar{l}_{12}^2}{\bar{\epsilon}_2^3}\right) , \tag{6.54}$$

$$k\frac{\partial\bar{l}_2}{\partial k} = -\bar{l}_2 + \frac{2}{3\pi^2}\left(\frac{48\bar{l}_2^2}{\bar{\epsilon}_2^3} + \frac{\bar{l}_3^2 + 2\bar{l}_3\bar{l}_{12} + 4\bar{l}_{12}^2}{\bar{\epsilon}_1^3}\right) , \tag{6.55}$$

$$k\frac{\partial\bar{l}_3}{\partial k} = -\bar{l}_3 + \frac{4\bar{l}_3\left[4\bar{l}_1\bar{\epsilon}_2^3 + 4\bar{l}_2\bar{\epsilon}_1^3 + \left(3\bar{l}_3 + 4\bar{l}_{12}\right)(\bar{\epsilon}_1 + \bar{\epsilon}_2)\,\bar{\epsilon}_1\bar{\epsilon}_2\right]}{3\pi^2\bar{\epsilon}_1^3\bar{\epsilon}_2^3} , \tag{6.56}$$

where we omitted the index k and used the abbreviation

$$\bar{\epsilon}_i = 1 + 2\bar{m}_i^2 . \tag{6.57}$$

In order to find the fixed points we have to set the left-hand sides to zero and solve the resulting system of equations. Since the equations are nonlinear, this has to be done numerically, using starting values for which a standard root-finding algorithm converges towards a solution. We applied an algorithm with randomized starting values in a reasonably large domain of parameter space, each of the starting values lying in the interval $[-10^4, 10^4]$. We found the nontrivial solutions given in Tab. 6.3 where they are listed together with the corresponding eigenvalues of the stability matrix. Using 10^6 different starting values, we checked that these are the only solutions for given starting values in the above domain of parameter space.

From comparison with the corresponding stability-matrix eigenvalues for the $O(N)$ models in the same approximation scheme (local-potential approximation, fourth-order truncation in the fields), see Tab. 6.1, we can unambiguously identify those fixed points in Tab. 6.3 with $O(N)$ critical exponents. Let us start our discussion with the fixed points FP_6 and FP_7. From the vanishing of the couplings in the upper part of Tab. 6.3 we see that for each of these fixed points the fixed-point potential is that of an $O(4)$ model. Fixed point FP_6 is that for the $O(4)$ representation $\Phi_1 = \sigma t_0 + i\vec{t}\cdot\vec{\pi}$, while FP_7 that for $\Phi_2 = i\eta t_0 + \vec{t}\cdot\vec{a}$. From the eigenvalues of the stability matrix in the lower part of Tab. 6.3 one observes that both fixed points have more than one negative eigenvalue, which means that they are unstable. Comparison of the second and third eigenvalue with the last two columns in Tab. 6.1 also tells us that they have one relevant $O(4)$ scaling direction.

For fixed point FP_5, the two masses $\bar{m}_i^2$ and the two coupling constants $\bar{l}_i$ are identical, while $\bar{l}_{12} = 0$. This means that the fixed-point potential is that of two independent, identical $O(4)$ models. From the lower part of Tab. 6.3 we see that this fixed point is a multicritical fixed point with two relevant $O(4)$ scaling directions. The third negative eigenvalue of the stability matrix renders this an unstable fixed point. Fixed point FP_8 is another unstable multicritical fixed point with a single $O(4)$ scaling direction.

From the vanishing of $\bar{l}_3$ and the fact that $\bar{l}_1 = \bar{l}_2 = \bar{l}_{12}/2$, the fixed-point potential for FP_9 is that

of an $O(8)$ model. The stability matrix indicates that this fixed point is unstable. Comparison of the eigenvalues of the stability matrix with Tab. 6.1 shows that it has one relevant $O(8)$ scaling direction. Since all eigenvalues of the stability matrix are negative, fixed points FP_{10} and FP_{11} are UV-stable fixed points. Fixed points FP_1 and FP_2 are unstable fixed points, none of them belonging to one of the $O(N)$ universality classes.
Finally, FP_3 and FP_4 are IR-stable fixed points. While for the other fixed points the (rescaled) eigenvalues of the (squared) mass matrix are always positive semi-definite, for FP_3 and FP_4 we find one negative eigenvalue in all minima of the (rescaled) fixed-point potential $\bar{U}(\bar{\sigma}, \bar{\eta}, \bar{a}_1)$, which corresponds to an unphysical situation. However, this could be an artifact of our fourth-order truncation of the potential (6.45), and the masses could be real-valued in higher order [144]. In that case, these IR-stable fixed points are in the $SU(2)\times U(2)$ universality class. Nevertheless, at quartic truncation order we have to reject them.
In the framework of the ϵ-expansion it is often assumed that negative (positive) eigenvalues remain negative (positive) at higher truncation order, also if marginal eigenvalues occur. As we found out in our studies, in the framework of FRG this is not necessarily the case (although, as a rule of thumb, it is rather unlikely that a large number of eigenvalues changes sign). An example is given in Sec. 6.4.2. At quartic truncation order there exists exactly one IR-unstable cubic fixed point, whose stability-matrix eigenvalues do not involve marginal eigenvalues. The stability matrix eigenvalues associated with the $O(4)$ fixed point, however, do involve a marginal eigenvalue. At sixth order in the truncation one finds four different cubic fixed points, of which exactly one is IR stable. This demonstrates that the stability properties of all other fixed points can change at higher truncation order if merely one of them contains a marginal eigenvalue. We therefore constructed also all sixth-order invariants, using a similar routine to the one provided in App. B.2, in order to verify that the most general $SU(2)_A \times U(2)_V$-symmetric and parity-invariant potential up to naive scaling dimension six is given by

$$U = m_1^2\varphi_1 + m_2^2\varphi_2 + l_1\varphi_1^2 + l_2\varphi_2^2 + l_{12}\varphi_1\varphi_2 + l_3\gamma + l_4\varphi_1^3 + l_5\varphi_1^2\varphi_2 + l_6\varphi_1\varphi_2^2 + l_7\varphi_1\gamma + l_8\varphi_2^3 + l_9\varphi_2\gamma \ . \tag{6.58}$$

We refrain from stating the lengthy flow equations and merely list some of the fixed points relevant for the discussion in Tab. 6.4, namely those which correspond to FP_3, FP_5, FP_6, and FP_8, respectively, at the given truncation order. We observe that, unfortunately, also at this truncation order there occur marginal eigenvalues, namely for the $O(4)$ fixed points FP_6 and FP_8. We speculate that this might have to do with the occurrence of a line of (unstable) $O(4)$ fixed points, since we encountered a similar situation in Sec. 6.4.3. Further investigations are necessary to understand the exact fixed-point structure. We further observe that the unphysical IR-stable fixed points (FP_3 and FP_4) also exist at sixth order. They are still associated with negative mass-matrix eigenvalues rendering these fixed points unphysical.

6.6.2 Parameterization in terms of original fields

In this section, in contrast to the previous one, we keep the potential parameterized in terms of the original fields ϕ_i. This avoids the use of the chain rule together with tedious rewriting procedures and serves as a check of our results. As in the previous section, we expand the r.h.s. of Eq. (4.24) and read off flow equations for the couplings by comparison of coefficients, but now

Table 6.3: Fixed points in the presence of nonzero anomaly strength, in $D = 3$ dimension, in the FRG analysis in the local-potential approximation, with couplings up to quartic order. The bar denotes rescaled quantities.

FP	$\bar{m}_1^2$	$\bar{m}_2^2$	$\bar{l}_1$	$\bar{l}_2$	$\bar{l}_{12}$	$\bar{l}_3$
FP_1	-3.80278	-0.197224	-355.58	0.273944	29.6088	0
FP_2	-0.197224	-3.80278	0.273944	-355.58	29.6088	0
FP_3	-1.34694	-0.333929	-17.0334	0.128417	5.64724	-5.93079
FP_4	-0.333929	-1.34694	0.128417	-17.0334	5.64724	-5.93079
FP_5	-0.0555556	-0.0555556	0.216617	0.216617	0	0
FP_6	-0.0555556	0	0.216617	0	0	0
FP_7	0	-0.0555556	0	0.216617	0	0
FP_8	-0.0555556	-0.0555556	0.108308	0.108308	0.216617	0.433234
FP_9	-0.0675676	-0.0675676	0.149643	0.149643	0.299286	0
FP_{10}	0.609013	-1.18037	-34.5716	7.9826	-9.98504	129.304
FP_{11}	-1.18037	0.609013	7.9826	-34.5716	-9.98504	129.304
FP	stability-matrix eigenvalues					
FP_1	{9.64793,-5.66667,-0.585909+4.07239 i,-0.585909-4.07239 i,3.83241,-1.30852}					
FP_2	{9.64793,-5.66667,-0.585909+4.07239 i,-0.585909-4.07239 i,3.83241,-1.30852}					
FP_3	{29.6235,14.0524 +4.23653 i,14.0524 -4.23653 i,0.917927 +9.64911 i,0.917927 -9.64911 i,-1.17232}					
FP_4	{29.6235,14.0524 +4.23653 i,14.0524 -4.23653 i,0.917927 +9.64911 i,0.917927 -9.64911 i,-1.17232}					
FP_5	{-1.77069,-1.77069,1.27069,1.27069,-0.666667,0 }					
FP_6	{-2.,-1.77069,1.27069,-1.,-0.833333,-0.5}					
FP_7	{-2.,-1.77069,1.27069,-1.,-0.833333,-0.5}					
FP_8	{-2.,-1.77069,1.27069,-0.666667,0,0}					
FP_9	{-1.98804,-1.71971,1.34471,0.613041,-0.25,-0.25}					
FP_{10}	{-28.9145,-16.865,-10.9156,-3.11604+5.87462 i,-3.11604-5.87462 i,-1.28288}					
FP_{11}	{-28.9145,-16.865,-10.9156,-3.11604+5.87462 i,-3.11604-5.87462 i,-1.28288}					

Table 6.4: Fixed points in the presence of nonzero anomaly strength, in $D = 3$ dimension, in the FRG analysis in the local-potential approximation, with couplings up to naive scaling dimension six. The bar denotes rescaled quantities.

FP_i	$\bar{m}_1^2$	$\bar{m}_2^2$	$\bar{l}_1$	$\bar{l}_2$	$\bar{l}_{12}$	$\bar{l}_3$	$\bar{l}_4$	$\bar{l}_5$	$\bar{l}_6$	$\bar{l}_7$	$\bar{l}_8$	$\bar{l}_9$
3	-0.7774	-0.428	-0.938	0.034	0.618	-0.767	-7.898	6.728	-0.234	-7.573	0.022	0.116
5	-0.1098	-0.1098	0.3299	0.3299	0	0	0.3099	0	0	0	0.3099	0
6	-0.1098	0	0.3299	0	0	0	0.3099	0	0	0	0	0
8	-0.1098	-0.1098	0.165	0.165	0.3299	0.6599	0.0775	0.232	0.232	0.9298	0.0775	0.9298

FP_i	stability-matrix eigenvalues
3	$\{211.68, 114.7, 88.9892, 74.9107, 19.4627 + 53.8263\,\mathrm{i}, 19.4627 - 53.8263\,\mathrm{i}, 40.3879, 5.84219 + 22.4579\,\mathrm{i}, 5.84219 - 22.4579\,\mathrm{i}, 15.2941 + 6.09425\,\mathrm{i}, 15.2941 - 6.09425\,\mathrm{i}, -0.751575\}$
5	$\{12.9187, 12.9187, 6.53046, 5.625, 4.625, 4.125, -1.50401, -1.50401, 1.33533, 1.33533, -0.75, 0.344539\}$
6	$\{12.9187, 4.99126, 4.01279, -2, -1.50401, 1.33533, 1.125, -1, -0.887787, 0.375, -0.366265, 0\}$
8	$\{12.9187, 8, 6.53046, 4.625, 4.5, 2.25, -2, -1.50401, 1.33533, -0.75, 0.344539, 0\}$

the expansion is in powers of the original fields ϕ_i instead of the invariants φ_i, γ. Again, in order to obtain the correct flow equations, accounting for all three anomaly terms, we have to keep at least three fields nonzero after having performed the second derivatives in Eq. (4.20).
For checking purposes we keep an additional field nonzero, say π_1, and set π_2, π_3, a_2, and a_3 to zero after having computed the second derivatives. This means that the comparison of coefficients is carried out using the potential (3.23) for $\pi_2 = \pi_3 = a_2 = a_3 = 0$ on the l.h.s. of the flow equation (4.24). In this case the (scale-dependent) potential (3.23) reads

$$\begin{aligned} U_k = {} & a_1^2 m_{2,k}^2 + \eta^2 m_{2,k}^2 + \sigma^2 m_{1,k}^2 + \pi_1^2 m_{1,k}^2 + \lambda_{a\eta}\left(a_1^4 + \eta^4\right) + \lambda_{\sigma\pi}\left(\sigma^4 + \pi_1^4\right) \\ & + \delta_1\left(\pi_1^2 a_1^2 + \eta^2\sigma^2\right) + \delta_2 a_1^2\eta^2 + \delta_0\left(a_1^2\sigma^2 + \pi_1^2\eta^2\right) + \kappa\pi_1 a_1\eta\sigma + \delta_3\pi_1^2\sigma^2 \ , \end{aligned} \tag{6.59}$$

with

$$\lambda_{a\eta} \equiv \frac{\lambda_1}{24} - y + \frac{z}{2} \ , \quad \lambda_{\sigma\pi} \equiv \frac{\lambda_1}{24} + y + \frac{z}{2} \ , \quad \delta_0 \equiv \frac{\lambda_1}{12} + \lambda_2 - z \ ,$$
$$\delta_1 \equiv \frac{\lambda_1}{12} - 3z \ , \quad \delta_2 \equiv \frac{\lambda_1}{12} + z - 2y \ , \quad \delta_3 \equiv \frac{\lambda_1}{12} + z + 2y \ , \quad \kappa \equiv 4z + 2\lambda_2 \ .$$

Note that

$$\delta_3 = 2\lambda_{\sigma\pi} \ , \quad \delta_2 = 2\lambda_{a\eta} \ , \quad \delta_0 = \delta_1 + \frac{\kappa}{2} \ , \quad y = \frac{\lambda_{\sigma\pi}}{2} - \frac{\lambda_{a\eta}}{2} \ ,$$
$$z = -\frac{\delta_1}{4} + \frac{\lambda_{\sigma\pi}}{4} + \frac{\lambda_{a\eta}}{4} \ , \quad \lambda_1 = 3\delta_1 + 9\lambda_{a\eta} + 9\lambda_{\sigma\pi} \ , \quad \lambda_2 = \frac{\delta_1}{2} + \frac{\kappa}{2} - \frac{\lambda_{\sigma\pi}}{2} - \frac{\lambda_{a\eta}}{2} \ .$$

We verified that we obtain unambiguous flow equations for $m_{1,k}^2$, $m_{2,k}^2$, $\lambda_{1,k}$, $\lambda_{2,k}$, y_k, and z_k, no matter from which of the coefficients in Eq. (6.59) we extract them (which is a freedom we have

due to the additional field we have kept nonzero). We do not state the flow equations and fixed points again; we have checked that they are equivalent to those found in Sec. 6.6.1.

6.6.3 Physical anomaly strength

So far we have considered only a finite anomaly strength. According to Ref. [98], however, the limit $c \to -\infty$ should be closer to reality: in order to reproduce the correct vacuum mass of the eta meson in the two-flavor quark-meson model at tree-level, one has to choose a value for the anomaly strength ($|c| \sim (958\ \mathrm{MeV})^2$) which exceeds a physically reasonable UV cut-off scale for the RG flow ($k \sim 600$ MeV). Therefore, on all scales relevant for the RG flow, effectively $c \to -\infty$. More precisely, instead of this limit, we should rather consider the limit

$$m_{2,k}^2 = \frac{1}{2}\mu_k^2 - c_k \to \infty \ , \tag{6.60}$$

otherwise $m_{1,k}^2 \equiv \frac{1}{2}\mu_k^2 + c_k \to -\infty$ would impose severe constraints on the RG flow in order to finally obtain positive-definite masses for σ and $\vec{\pi}$.
In the limit $m_{2,k}^2 \to \infty$ the flow equations (6.51)–(6.56) simplify to

$$k\frac{\partial \bar{m}_1^2}{\partial k} = -2\bar{m}_1^2 - \frac{4\bar{l}_1}{\pi^2 \bar{\epsilon}_1^2} \ , \tag{6.61}$$

$$k\frac{\partial \bar{l}_{12}}{\partial k} = -\bar{l}_{12} + \frac{8\bar{l}_1\left(\bar{l}_3 + 6\bar{l}_{12}\right)}{3\pi^2 \bar{\epsilon}_1^3} \ , \tag{6.62}$$

$$k\frac{\partial \bar{l}_1}{\partial k} = -\bar{l}_1 + \frac{32\bar{l}_1^2}{\pi^2 \bar{\epsilon}_1^3} \ , \tag{6.63}$$

$$k\frac{\partial \bar{l}_2}{\partial k} = -\bar{l}_2 + \frac{2}{3\pi^2}\frac{\bar{l}_3^2 + 2\bar{l}_3\bar{l}_{12} + 4\bar{l}_{12}^2}{\bar{\epsilon}_1^3} \ , \tag{6.64}$$

$$k\frac{\partial \bar{l}_3}{\partial k} = -\bar{l}_3 + \frac{16\bar{l}_3\bar{l}_1}{3\pi^2 \bar{\epsilon}_1^3} \ . \tag{6.65}$$

The above flow equations have only one nontrivial fixed point, namely the $O(4)$ fixed point,

$$\left(\bar{m}_1^2 = -0.0555556, \bar{l}_1 = 0.216617, \bar{l}_2 = 0, \bar{l}_{12} = 0, \bar{l}_3 = 0\right) \ . \tag{6.66}$$

Calculating its stability-matrix eigenvalues,

$$\{-1.77069, 1.27069, -1, -0.83334, -0.5\} \ , \tag{6.67}$$

we find that it is IR unstable. According to standard rules one would, erroneously, conclude that the phase transition cannot be of second order. According to common sense, however, this cannot be true since the fields η and $\vec{a}$ are infinitely heavy, so that fluctuations of these fields are completely suppressed and cannot affect the critical behavior. In Sec. 6.7 we explain, using a simpler model as an example, why we have to neglect the spurious negative eigenvalues when inferring the order of the phase transition. From the discussion in Sec. 6.7, we conclude that couplings occurring only in front of terms involving infinitely heavy fields have to be neglected in the stability analysis of fixed points. This can be also understood from the fact that the

fluctuations represented by infinitely heavy fields are zero.
Inserting the fixed-point solution (6.66) into the rescaled potential (6.45), we obtain

$$\bar{U}_{k=0} = -0.0555556\left(\bar{\sigma}^2 + \bar{\vec{\pi}}^2\right) + 0.216617\left(\bar{\sigma}^2 + \bar{\vec{\pi}}^2\right)^2 \ . \tag{6.68}$$

Since the fixed-point potential is $O(4)$ symmetric, we can choose $\bar{\vec{\pi}}_0 = 0$ in the vacuum state. Then, the rescaled vacuum is given by

$$(\bar{\sigma}_0 = 0.358099, \bar{\vec{\pi}}_0 = 0) \ . \tag{6.69}$$

Using these vacuum expectation values we calculate the rescaled mass eigenvalues (i.e., the rescaled physical masses):

$$\bar{M}_\sigma^2 = 2/9 \ , \quad \bar{M}_{\pi_i}^2 = 0 \ , \quad \bar{M}_\eta^2 \to \infty \ , \quad \bar{M}_{a_i}^2 \to \infty \ . \tag{6.70}$$

We see that, as expected, we have three Goldstone bosons, the three pions $\vec{\pi}$, whereas η and $\vec{a}$ are infinitely heavy and thus decouple. Considering Eq. (6.45), we conclude that the couplings $\bar{l}_2$, $\bar{l}_{12}$, and $\bar{l}_3$ appear only in front of terms involving infinitely heavy fields and must not be included in the stability analysis. Including only $\bar{m}_1^2$ and $\bar{l}_1$, we find the stability-matrix eigenvalues

$$\{-1.77069, 1.27069\} \ , \tag{6.71}$$

from which we finally conclude that there exists a stable $O(4)$ fixed point in case of infinite anomaly strength. We also note that we verified that above the critical dimension, $d \geq 4$, the Gaussian fixed point becomes IR stable with mean-field critical exponent $\nu = 1/2$, as expected.

6.7 Coupled vector model

The most general potential (up to quartic order) invariant under $O(N_1) \oplus O(N_2)$, with $O(N_i)$ in the fundamental representation, is given by [14]

$$U = m_1^2\vec{\phi}_1^2 + m_2^2\vec{\phi}_2^2 + \frac{\lambda_{11}}{24}\left(\vec{\phi}_1^2\right)^2 + \frac{\lambda_{12}}{12}\vec{\phi}_1^2\vec{\phi}_2^2 + \frac{\lambda_{22}}{24}\left(\vec{\phi}_2^2\right)^2 \ , \tag{6.72}$$

where $\vec{\phi}_i$ is a N_i-component vector. It is also known as coupled vector model. We focus on the simplest case $N_1 = N_2 = 1$, i.e.,

$$U = m_1^2\phi_1^2 + m_2^2\phi_2^2 + \frac{\lambda_{11}}{24}\phi_1^4 + \frac{\lambda_{12}}{12}\phi_1^2\phi_2^2 + \frac{\lambda_{22}}{24}\phi_2^4 \ . \tag{6.73}$$

The following discussion has been taken from our publication [1]. For a mean-field analysis of the model we refer to Ref. [145], for a leading-order ϵ-expansion to Ref. [146].
Using the method of Taylor expansion and comparison of coefficients, we find the following flow equations:

$$k\frac{\partial\bar{m}_1^2}{\partial k} = -2\bar{m}_1^2 - \frac{1}{36\pi^2}\left(\frac{3\bar{\lambda}_{11}}{\bar{\epsilon}_1^2} + \frac{\bar{\lambda}_{12}}{\bar{\epsilon}_2^2}\right) \ , \quad k\frac{\partial\bar{m}_2^2}{\partial k} = -2\bar{m}_2^2 - \frac{1}{36\pi^2}\left(\frac{3\bar{\lambda}_{22}}{\bar{\epsilon}_2^2} + \frac{\bar{\lambda}_{12}}{\bar{\epsilon}_1^2}\right) \ , \tag{6.74}$$

$$k\frac{\partial\bar{\lambda}_{11}}{\partial k} = -\bar{\lambda}_{11} + \frac{1}{\pi^2}\left(\frac{\bar{\lambda}_{11}^2}{\bar{\epsilon}_1^3} + \frac{\bar{\lambda}_{12}^2}{9\bar{\epsilon}_2^3}\right) \ , \quad k\frac{\partial\bar{\lambda}_{22}}{\partial k} = -\bar{\lambda}_{22} + \frac{1}{\pi^2}\left(\frac{\bar{\lambda}_{22}^2}{\bar{\epsilon}_2^3} + \frac{\bar{\lambda}_{12}^2}{9\bar{\epsilon}_1^3}\right) \ , \tag{6.75}$$

$$k\frac{\partial\bar{\lambda}_{12}}{\partial k} = -\bar{\lambda}_{12} + \frac{\bar{\lambda}_{12}}{9\pi^2\bar{\epsilon}_1^3\bar{\epsilon}_2^3}\left[2\bar{\lambda}_{12}\left(\bar{\epsilon}_1 + \bar{\epsilon}_2\right)\bar{\epsilon}_2\bar{\epsilon}_1 + 3\bar{\lambda}_{22}\bar{\epsilon}_1^3 + 3\bar{\lambda}_{11}\bar{\epsilon}_2^3\right] \ , \tag{6.76}$$

where we again used the abbreviation (6.57).
In this work we are only interested in the Ising fixed point,

$$(\bar{m}_1^2 = -0.03846, \bar{m}_2^2 = 0, \bar{\lambda}_{11} = 7.76271, \bar{\lambda}_{12} = 0, \bar{\lambda}_{22} = 0) \ , \tag{6.77}$$

the stability-matrix eigenvalues of which,

$$\{-2, -1.84256, 1.1759, -1, -0.666667\} \ , \tag{6.78}$$

indicate that it appears to be unstable in the $\bar{m}_2^2$, $\bar{\lambda}_{12}$, and $\bar{\lambda}_{22}$ directions.
Examining the above flow equations in the limit $\bar{m}_2^2 \to \infty$,

$$k\frac{\partial \bar{m}_1^2}{\partial k} = -2\bar{m}_1^2 - \frac{1}{12\pi^2}\frac{\bar{\lambda}_{11}}{\bar{\epsilon}_1^2} \ , \quad k\frac{\partial \bar{\lambda}_{11}}{\partial k} = -\bar{\lambda}_{11} + \frac{1}{\pi^2}\frac{\bar{\lambda}_{11}^2}{\bar{\epsilon}_1^3} \ , \tag{6.79}$$

$$k\frac{\partial \bar{\lambda}_{22}}{\partial k} = -\bar{\lambda}_{22} + \frac{1}{9\pi^2}\frac{\bar{\lambda}_{12}^2}{\bar{\epsilon}_1^3} \ , \quad k\frac{\partial \bar{\lambda}_{12}}{\partial k} = -\bar{\lambda}_{12} + \frac{1}{3\pi^2}\frac{\bar{\lambda}_{12}\bar{\lambda}_{11}}{\bar{\epsilon}_1^3} \ , \tag{6.80}$$

we still find negative eigenvalues corresponding to the unstable $\bar{\lambda}_{12}$ and $\bar{\lambda}_{22}$ directions, respectively. We obviously have the same situation as in Sec. 6.6.3. Formally, the negative eigenvalues would indicate that the Ising fixed point is IR unstable. In this particular case, however, one cannot conclude from this that the phase transition is fluctuation-induced first order. Fluctuations in $\bar{\lambda}_{12}$ and $\bar{\lambda}_{22}$ direction are completely suppressed due to the infinitely heavy ϕ_2 field and cannot affect the critical behavior. To prove this, we investigate in detail the scale evolution of the dimensionful potential for different initial values for the parameters in the UV. Using the invariants

$$\varphi_1 = \phi_1^2 \ , \quad \varphi_2 = \phi_2^2 \ , \tag{6.81}$$

we make the following ansatz for the potential running under the RG flow:

$$U_k = V_k(\varphi_1) + W_k(\varphi_1)\varphi_2 + X_k(\varphi_1)\varphi_2^2 \ . \tag{6.82}$$

Having expressed the mass eigenvalues M_i^2 in terms of φ_1 and φ_2, we expand the r.h.s. of Eq. (4.24) and read off flow equations for $V_k(\varphi_1)$, $W_k(\varphi_1)$, and $X_k(\varphi_1)$ by comparison of coefficients. We solve the resulting system of three partial differential equations together with the initial conditions

$$V_{k=\Lambda}(\varphi_1) = m_{1,\Lambda}^2\varphi_1 + \frac{\lambda_{11,\Lambda}}{24}\varphi_1^2 \ , \quad W_{k=\Lambda}(\varphi_1) = m_{2,\Lambda}^2 + \frac{\lambda_{12,\Lambda}}{12}\varphi_1 \ , \quad X_{k=\Lambda}(\varphi_1) = \frac{\lambda_{22,\Lambda}}{24} \ . \tag{6.83}$$

Fig. 6.2 illustrates the potential for various values of the RG-flow parameter k for various values of $m_{2,\Lambda}^2$ and $\lambda_{12,\Lambda}$ for fixed values of $m_{1,\Lambda}^2$, $\lambda_{11,\Lambda}$, and $\lambda_{22,\Lambda} = 0$. We observe that the influence of the coupling $\bar{\lambda}_{12}$ on the shape of the potential becomes smaller for larger values of m_2^2. We have checked that the same is true for nonzero values of the coupling $\bar{\lambda}_{22}$. We also observe that the RG-evolved potential exhibits the typical shape for a (fluctuation-induced) first-order phase transition in the case of a light φ_2 field (upper panels), while the transition remains of second order for a heavy φ_2 field (lower panels).

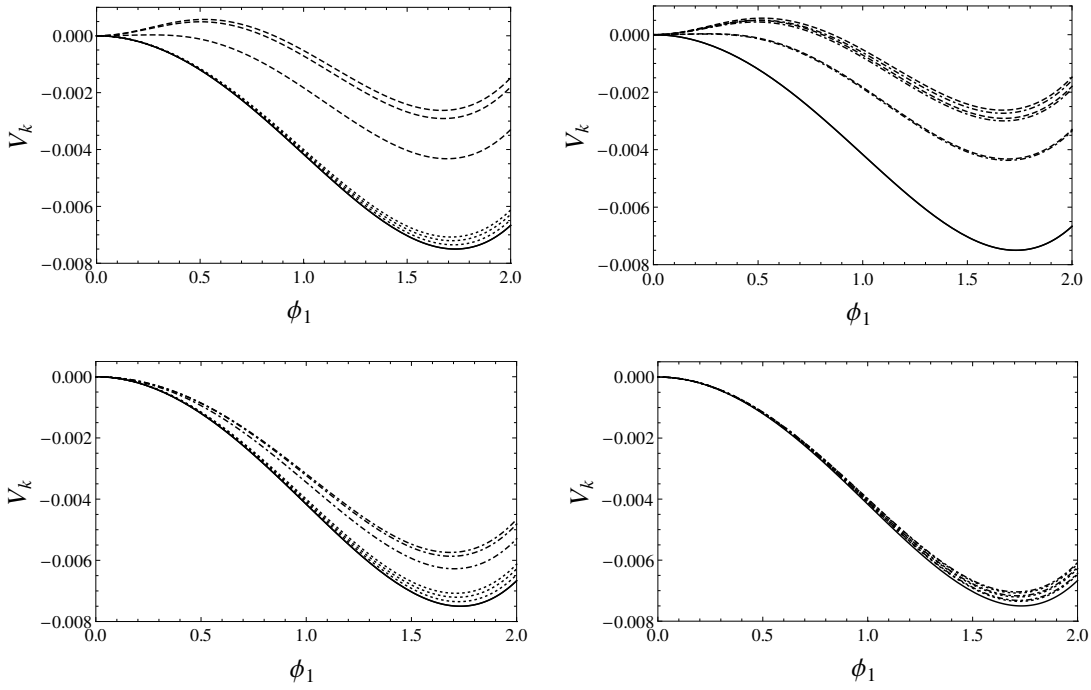

Figure 6.2: Scale evolution of the potential V_k. In each panel, the solid line is the same and corresponds to the start of the evolution in the UV ($k/\Lambda = 1$). Furthermore, in each panel there are two sets of three curves (drawn with identical line mode). These three curves correspond to the RG potentials at the scales $k/\Lambda = 0.7$, $k/\Lambda = 0.4$, and $k/\Lambda = 0.12$ respectively. For all panels, $m^2_{1,\Lambda} = -0.005\Lambda^2$, $\lambda_{11,\Lambda} = 0.02\Lambda$, $\lambda_{22,\Lambda} = 0$. In the upper left, the lower left, and the lower right panel, the dotted curves correspond to $m^2_{2,\Lambda} = 0$, $\lambda_{12,\Lambda} = 0$ (and therefore coincide with solutions for the Ising model). In the upper left and upper right panel, the dashed curves are for $m^2_{2,\Lambda} = 0$, $\lambda_{12,\Lambda} = 8\Lambda$. In the lower left panel, the dot-dashed curves are for $m^2_{2,\Lambda} = 0.5\Lambda^2$ and $\lambda_{12,\Lambda} = 8\Lambda$. In the lower right panel, the dot-dashed curves are for $m^2_{2,\Lambda} = 8\Lambda^2$ and $\lambda_{12,\Lambda} = 8\Lambda$.

6.8 Toy models

6.8.1 Toy model involving vector and axial-vector mesons defining a novel universality class

In this section we introduce the most general parity and $SU(2)_V \times SU(2)_A$ symmetric potential for the representation $[3,1]\oplus[1,3]$ which involves six real field components. In models concerned with vector meson dominance these six fields have been identified with the rho and the a_1 triplets, which are chiral partners. Alternatively, we could reinterpret one of the vectors as the pion field, yielding a toy model for the pion and, say, the rho meson. The six fields, denoted by $\vec{\rho}^{\mu}$ and $\vec{a}_1^{\mu}$, transform as stated in Eqs. (A.27) and (A.28), respectively. In the framework of our toy model we neglect the Lorentz indices. Whereas these mesons play for example an important role for the phase transition in models with hidden local symmetry [147, 148], we do not want to overrate the physical implications of our toy model. We regard it as a first step towards a more accurate treatment and we merely report on the infrared stable fixed point found under the RG flow. Its existence is made possible since only the combination $\vec{\rho}^2+\vec{a}_1^2$ is invariant, whereas the individual terms $\vec{\rho}^2$ and $\vec{a}_1^2$, respectively, are not. Including in addition the omega and the f_1 mesons by using a $[2,\bar{2}]\oplus[\bar{2},2]$-representation, we found no stable IR-fixed point due to the additional invariants ω^2 and f_1^2.

Using a similar algorithm to the one provided in App. B.2, we derived the following most general potential (up to quartic order) invariant under $SU(2)_V \times SU(2)_A$ in the representation $[3,1]\oplus[1,3]$ and under parity:

$$U = r(\vec{\rho}^2+\vec{a}_1^2) + g_1(\vec{\rho}^2+\vec{a}_1^2)^2 + g_2(\vec{\rho}\cdot\vec{a}_1)^2 \ , \tag{6.84}$$

where $\vec{\rho}\equiv(\rho_1,\rho_2,\rho_3)^T$, and $\vec{a}_1\equiv(a_1,a_2,a_3)^T$. Using the notation of Tab. II in Ref. [42], we can rewrite the potential as

$$U = rI_0 + g_1 I_0^2 + g_2(I_2^{(4)} + 2I_3^{(4)}) \ ,$$

which is not listed in Ref. [42] as a Landau potential exhibiting a stable IR fixed point (apparently because it is not associated with a representation of a point group).

We obtain the following flow equations for the rescaled couplings:

$$k\frac{\partial\bar{r}_k}{\partial k} = -2\bar{r}_k - 2K_D\frac{16\bar{g}_{1,k}+\bar{g}_{2,k}}{(1+2\bar{r}_k)^2} \ , \tag{6.85}$$

$$k\frac{\partial\bar{g}_{1,k}}{\partial k} = (D-4)\bar{g}_{1,k} + 4K_D\frac{56\bar{g}_{1,k}^2+4\bar{g}_{2,k}\bar{g}_{1,k}+\bar{g}_{2,k}^2}{(1+2\bar{r}_k)^3} \ , \tag{6.86}$$

$$k\frac{\partial\bar{g}_{2,k}}{\partial k} = (D-4)\bar{g}_{2,k} + 8K_D\frac{(24\bar{g}_{1,k}+5\bar{g}_{2,k})\,\bar{g}_{2,k}}{(1+2\bar{r}_k)^3} \ . \tag{6.87}$$

Apart from the IR-unstable Gaussian fixed point we find three different fixed points. The $O(6)$ fixed point

$$(\bar{r}=-0.0625, \bar{g}_1=0.177103, \bar{g}_2=0)$$

is associated with stability-matrix eigenvalues

$$\{-1.74125, 1.31268, -0.142857\} \ ,$$

which indicate its IR instability.
The second fixed point,

$$(\bar{r} = -0.0510204, \bar{g}_1 = 0.121809, \bar{g}_2 = 0.487235) \ ,$$

is associated with stability-matrix eigenvalues

$$\{-1.78985, 1.24439, -0.0909091\} \ ,$$

and is hence IR unstable, too. Note that for this fixed point $\bar{g}_2 = 4\bar{g}_1$, which characterizes its symmetry.
The third fixed point,

$$(\bar{r} = -0.0584416, \bar{g}_1 = 0.149947, \bar{g}_2 = 0.299893) \ ,$$

is IR stable as one infers from its stability-matrix eigenvalues

$$\{-1.75847, 1.28788, 0.0588235\} \ .$$

Note that the symmetry of the IR-stable fixed point is characterized by $\bar{g}_2 = 2\bar{g}_1$.

6.8.2 Toy model involving vector mesons, axial-vector mesons, and pions

In this section we extend the toy model discussed in Sec. 6.8.1 by including in addition the three pions, which completes the particle content taken into account in Refs. [147, 148]. Again we neglect the Lorentz indices of the vector and axial-vector mesons. From the local isomorphism $SU(2) \simeq SO(3)$ we conclude that

$$SU(2)_L \times SU(2)_R \simeq SO(3)_L \times SO(3)_R \ . \tag{6.88}$$

The most general $SO(3)$-invariant polynomial coincides with the most general $O(3)$-invariant polynomial. Accordingly, also the most general polynomial invariant under $SO(3)_L \otimes SO(3)_R$ is the same as that invariant under $O(3)_L \otimes O(3)_R$, which, taking both of the $SO(3)$ groups in the product (6.88) in the fundamental representation, is given (up to quartic order) by [88]

$$U = r\mathrm{Tr}\Phi^T\Phi + g_1(\mathrm{Tr}\Phi^T\Phi)^2 + g_2\mathrm{Tr}(\Phi^T\Phi)^2 \ , \tag{6.89}$$

where Φ is a real-valued 3×3 matrix,

$$\Phi = \begin{pmatrix} \phi_1 & \phi_2 & \phi_3 \\ \phi_4 & \phi_5 & \phi_6 \\ \phi_7 & \phi_8 & \phi_9 \end{pmatrix} \ , \tag{6.90}$$

which transforms under $(S)O(3)_L \times (S)O(3)_R$ according to

$$\Phi \to L\Phi R \ , \tag{6.91}$$

where L and R, respectively, denote arbitrary elements of $(S)O(3)$ in the fundamental representation, $L \in (S)O(3)$ and $R \in (S)O(3)$.
We checked that the potential (6.89) can indeed be rewritten as [14]

$$U = r\sum_{i=1}^{9}\phi_i^2 + \lambda_1\left(\sum_{i=1}^{9}\phi_i^2\right)^2 + \lambda_2\left[(\vec{\rho}\times\vec{a}_1)^2 + (\vec{\pi}\times\vec{a}_1)^2 + (\vec{\pi}\times\vec{\rho})^2\right] , \tag{6.92}$$

where the vectors

$$\vec{\pi} \equiv (\phi_1,\phi_2,\phi_3)^T , \quad \vec{\rho} \equiv (\phi_4,\phi_5,\phi_6)^T , \quad \vec{a}_1 \equiv (\phi_7,\phi_8,\phi_9)^T , \tag{6.93}$$

can be interpreted as the pion, the rho meson, and the a_1 meson fields, respectively.
We obtain the following flow equations for the rescaled couplings:

$$k\frac{\partial\bar{r}_k}{\partial k} = -2\bar{r}_k - 4K_D\frac{11\bar{\lambda}_{1,k}+2\bar{\lambda}_{2,k}}{(1+2\bar{r}_k)^2} , \tag{6.94}$$

$$k\frac{\partial\bar{\lambda}_{1,k}}{\partial k} = (D-4)\bar{\lambda}_{1,k} + 16K_D\frac{17\bar{\lambda}_{1,k}^2+4\bar{\lambda}_{2,k}\bar{\lambda}_{1,k}+\bar{\lambda}_{2,k}^2}{(1+2\bar{r}_k)^3} , \tag{6.95}$$

$$k\frac{\partial\bar{\lambda}_{2,k}}{\partial k} = (D-4)\bar{\lambda}_{2,k} + 16K_D\frac{\left(12\bar{\lambda}_{1,k}+\bar{\lambda}_{2,k}\right)\bar{\lambda}_{2,k}}{(1+2\bar{r}_k)^3} . \tag{6.96}$$

Apart from two complex-valued fixed points (which have to be rejected in our context) and the IR-unstable Gaussian fixed point, the only nontrivial fixed point is the $O(9)$ fixed point

$$(\bar{r} = -0.06962, \bar{\lambda}_1 = 0.13884, \bar{\lambda}_2 = 0) ,$$

for which the stability-matrix eigenvalues

$$\{-1.71096, 1.35802, -0.294118\}$$

indicate its IR instability (in consistence with Ref. [88]). We note that the equivalence of our flow equations with those inferred from the one-loop ϵ-expansion in Ref. [88] can be shown by appropriately redefining the coupling constants and setting $\bar{r}_k = 0$.

6.8.3 Novel IR-stable fixed point for an eight-component order parameter

Apart from the $U(2)_A \times U(2)_V$ model (see Ref. [33] and Sec. 6.5) and the $SU(2)_A \times U(2)_V$ model (at inconclusive truncation order, however), both in the $[2,\bar{2}] \oplus [\bar{2},2]$-representation, we are not aware of other Landau potentials involving an eight-component order parameter and exhibiting an IR-stable fixed point. Also a systematic investigation for point groups did not reveal any [44]. We therefore report on a novel universality class associated with an eight-component order parameter.
Extending the vectors involved in the potential (6.84) to general N-component vectors, $\vec{\rho} \to \vec{\phi} \equiv (\phi_1,\ldots,\phi_N)^T$, $\vec{a}_1 \to \vec{\varphi} \equiv (\varphi_1,\ldots,\varphi_N)^T$, we obtain a Landau potential involving a $2N$-component order parameter,

$$U = r(\vec{\phi}^2+\vec{\varphi}^2) + g_1(\vec{\phi}^2+\vec{\varphi}^2)^2 + g_2(\vec{\phi}\cdot\vec{\varphi})^2 + g_3(\vec{\phi}^2+\vec{\varphi}^2)^3 + g_4(\vec{\phi}^2+\vec{\varphi}^2)(\vec{\phi}\cdot\vec{\varphi})^2 , \tag{6.97}$$

where we also included higher-order terms since marginal eigenvalues occur at quartic order. In the following we focus on the case $N = 4$. Before considering the general case, one should first clarify to which centralizer the potential corresponds in order to decide about its physical relevance. For $N = 4$ we obtain the following flow equations for the rescaled couplings:

$$k\frac{\partial \bar{r}_k}{\partial k} = -2\bar{r}_k - 2K_D \frac{20\bar{g}_{1,k}+\bar{g}_{2,k}}{(1+2\bar{r}_k)^2} \ , \tag{6.98}$$

$$k\frac{\partial \bar{g}_{1,k}}{\partial k} = (D-4)\bar{g}_{1,k} + 2K_D \frac{128\bar{g}_{1,k}^2+8\bar{g}_{2,k}\bar{g}_{1,k}+2\bar{g}_{2,k}^2-(2\bar{r}_k+1)(36\bar{g}_{3,k}+\bar{g}_{4,k})}{(1+2\bar{r}_k)^3} \ , \tag{6.99}$$

$$k\frac{\partial \bar{g}_{2,k}}{\partial k} = (D-4)\bar{g}_{2,k} + 16K_D \frac{3\bar{g}_{2,k}(4\bar{g}_{1,k}+\bar{g}_{2,k})-2\bar{g}_{4,k}(1+2\bar{r}_k)}{(1+2\bar{r}_k)^3} \ , \tag{6.100}$$

$$k\frac{\partial \bar{g}_{3,k}}{\partial k} = 8K_3 \left(\frac{\bar{g}_{2,k}(3\bar{g}_{3,k}+\bar{g}_{4,k})+2\bar{g}_{1,k}(66\bar{g}_{3,k}+\bar{g}_{4,k})}{(1+2\bar{r}_k)^3} - \frac{272\bar{g}_{1,k}^3+12\bar{g}_{2,k}\bar{g}_{1,k}^2+6\bar{g}_{2,k}^2\bar{g}_{1,k}+\bar{g}_{2,k}^3}{(1+2\bar{r}_k)^4} \right) , \tag{6.101}$$

$$k\frac{\partial \bar{g}_{4,k}}{\partial k} = 8K_3 \left(\frac{72\bar{g}_{2,k}\bar{g}_{3,k}+92\bar{g}_{1,k}\bar{g}_{4,k}+25\bar{g}_{2,k}\bar{g}_{4,k}}{(1+2\bar{r}_k)^3} - \frac{9\bar{g}_{2,k}(4\bar{g}_{1,k}+\bar{g}_{2,k})(16\bar{g}_{1,k}+\bar{g}_{2,k})}{(1+2\bar{r}_k)^4} \right) . \tag{6.102}$$

Apart from several IR-unstable fixed points, we find the following IR-stable fixed point:

$$(\bar{r} = -0.10976, \bar{g}_1 = 0.16497, \bar{g}_2 = 0.65987, \bar{g}_3 = 0.07749, \bar{g}_4 = 0.92983) \ .$$

The associated stability-matrix eigenvalues read

$$\{12.9187, 6.53046, 1.33533, 0.344539, -1.50401\} \ .$$

Chapter 7

Effective Models for QCD at nonzero temperature

7.1 General remarks

As we have pointed out earlier, a study in the framework of dimensional reduction is limited in several respects calling for a finite-temperature approach where temperature is a tunable variable (see the discussion in Secs. 4.3.2 and 4.3.1, respectively). A fixed-point study, in particular, can merely either rule out or confirm the possible existence of a second-order phase transition and predict its universality class. As we observed in our fixed-point studies, however, several predictions remain inconclusive and require a crosscheck from a complementary approach. Extending the study to finite temperature is a first step towards clarification, which remains incomplete up to date. Further investigations are required particularly concerning the truncation dependence of results.
We successively improved our numerical routines by comparing to results stated in the literature. Having started with simple differential equations, we proceeded with FRG-flow equations. For example, we reproduced Fig. 5.3 of Ref. [149]. We also reproduced the results for the quark-meson model of Ref. [150], which we present in Sec. 7.3. We are currently crosschecking our numerical results for the linear sigma model (see Sec. 7.2) with those of other collaborations. First comparison of our routines provided in App. C with an independent code has been successful for certain initial values. We hope that this will be also the case for the rest of our results. We emphasize, however, the preliminary character of the numerical studies presented in section 7.2.

7.2 Linear sigma model

In this chapter we discuss preliminary numerical results for the linear sigma model at nonzero temperature in presence ($SU(2)_A \times U(2)_V$) and in absence ($U(2)_A \times U(2)_V$) of the axial anomaly. The FRG flow is inferred from Eq. (4.21) and is hence of nonperturbative nature. The dimensionally reduced theories are discussed in Secs. 6.6 and 6.5, respectively. In the presence of the

anomaly we use the truncation

$$U_p = V(\varphi_1) + W(\varphi_1)\varphi_2 + A(\varphi_1)\varphi_2^2 + B(\varphi_1)\gamma \ . \tag{7.1}$$

where the fields are defined in Eq. (6.44). The functions $V(\varphi_1)$, $W(\varphi_1)$, $A(\varphi_1)$, and $B(\varphi_1)$, respectively, will be fixed in the UV such that certain physical values are produced in the IR. We note that the functions are therefore not hampered by any expansion in the variable φ_1. Since only the sigma field, σ, is expected to acquire a nonvanishing vacuum expectation value, the expansion in φ_2 and γ, respectively, is reasonable. We do not claim, however, that the truncation order is sufficient. Further investigations are desirable. In the absence of the anomaly we use the truncation (compare with Ref. [87])

$$U_a = V(\varphi) + W(\varphi)\xi \ , \tag{7.2}$$

where the fields are defined in Eq. (6.42). Again, $V(\varphi)$ and $W(\varphi)$ are arbitrary functions which will be appropriately fitted in the UV.

Since we work in terms of the invariants defined in Eqs. (6.44) and (6.42), respectively, we have to apply the chain rule in order to bring the mass matrix (4.20), entering the flow equation via its eigenvalues, into a form suited for our numerical approach. For example,

$$\frac{\partial U_a}{\partial \phi_i} = (V'(\varphi) + W'(\varphi)\xi)\,\frac{\partial \varphi}{\partial \phi_i} + W(\varphi)\frac{\partial \xi}{\partial \phi_i} \ ,$$

and similar for the second derivative and for U_p, respectively. As in Secs. 6.5 and 6.6, respectively, we need to keep only some of the fields ϕ_i nonzero after having calculated the mass matrix. In the absence of the anomaly we can for instance keep σ and a_1, whereas in the presence of the anomaly we can keep in addition η.

Our preliminary results in the presence of the anomaly can be summarized as follows. In the UV we use functions of the form

$$V_{k=\Lambda}(\varphi_1) = r(\varphi_1 - \phi_0^2)^2 \ , \quad W_{k=\Lambda}(\varphi_1) = \sum_n w_n \varphi_1^n \ , \quad A_{k=\Lambda}(\varphi_1) = \sum_n a_n \varphi_1^n \ , \quad B_{k=\Lambda}(\varphi_1) = \sum_n b_n \varphi_1^n \ .$$

We investigate the scale evolution of U_k with k and evaluate the result in φ_1-direction, i.e., at $\varphi_2 = \xi = 0$ (since only the sigma field is assumed to take a nonzero vacuum expectation value). Note that we take account of $\varphi_2 \neq 0$ and $\xi \neq 0$ during the evolution, of course. Whereas a local maximum evolves near the origin under the evolution of the potential for some UV parameters, we do not find one for others. This indicates that the phase transition (which occurs when tuning the temperature T towards a critical value) is of first order for some UV parameters, whereas it is of second order for others. As already mentioned, different UV parameters yield different physical observables (in this case the meson masses and the pion decay constant) in the IR limit. We checked that all the masses are positive semidefinite in the IR but we did not adjust them to their physical values, yet, because we wanted to understand the variable order of the phase transition first. In order to further investigate this issue we studied the evolution of the potential for different values of ϕ_0 and T. We stopped the integration at a certain $k = k_0$ below which the position of the nontrivial local minimum, $\phi_{0,k}$, does not change significantly anymore. For each ϕ_0 and T we adjusted r such that both local minima are at the same height in the IR limit, $U_{k=k_0}(\phi = \phi_{0,k_0}) \approx U_{k=k_0}(\phi = 0)$. For simplicity we used a relatively small cutoff of $\Lambda = 500$

MeV. Typical evolutions are shown for $T = 30$ MeV and varying ϕ_0 in Figs. 7.1–7.5. In Fig. 7.1 we observe a pronounced local maximum which is characteristic for a first-order phase transition, and we find that the nontrivial minimum does not change significantly below $k_0 \sim 2$ MeV. Decreasing ϕ_0, in Figs. 7.2 and 7.3 we observe that the local maximum becomes less and less pronounced. Furthermore, ϕ_{0,k_0} decreases and settles for smaller k_0. Finally, for $\phi_0 \sim 174 - 179$ MeV we reach the restored phase (see Figs. 7.3 and 7.5). Interestingly, for $\phi_0 < 179$ MeV we can obtain an evolution where no local maximum occurs by choosing r only a little bit larger than described above. In this way it seems that we can turn an evolution characteristic for a first-order transition (Fig. 7.3) into one characteristic of a second-order transition (Fig. 7.4). We note that we were not able to reach lower values than $k \sim 6.36$ MeV in Fig. 7.4 due to numerical problems. Accordingly, we cannot be sure that the potential becomes flat in the IR limit. This is the case, however, for the parameter set in Fig. 7.6 where we show a second-order (or extremely weak first-order) transition occuring at roughly $T_c \sim 125$ MeV. We note that such transitions might occur only for unphysical ratios $T_c/\Lambda > 1/7$[1]. More elaborated parameter studies are necessary to decide for which regime of UV values the phase transition is of second-order or, respectively, a very weak first-order.

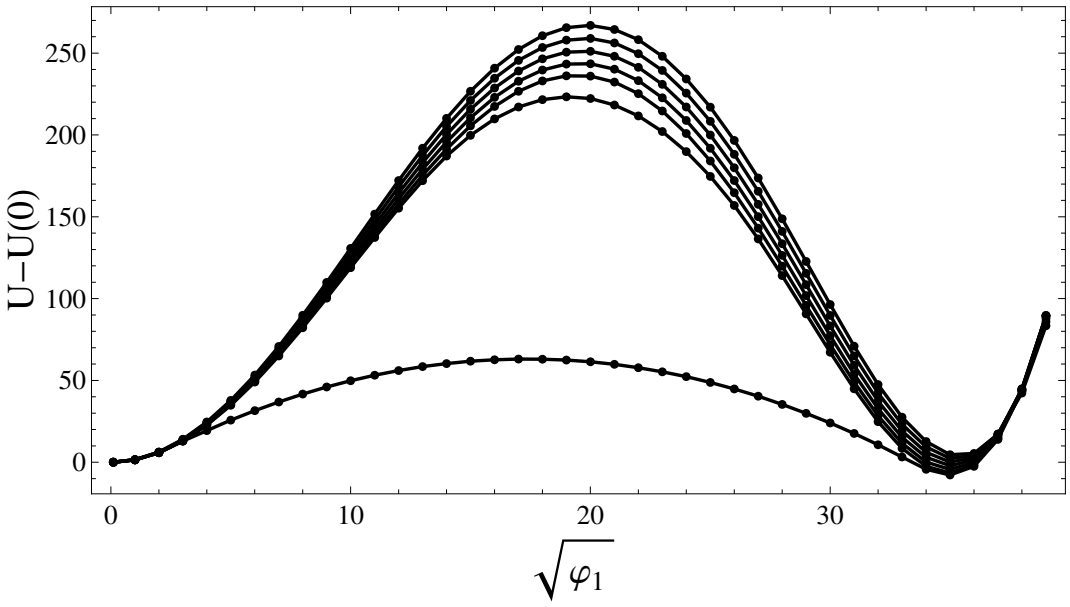

Figure 7.1: $SU(2)_A \times U(2)_V$-model. $W_{k=\Lambda} = 10$, $A_{k=\Lambda} = 0$, $B_{k=\Lambda} = 0.8$. $\Lambda = 500$ MeV. $T = 30$ MeV, $\phi_0 = 191$ MeV, $r = 0.0125594$. Evolution from $k = 6.7$ MeV to $k = 0.7$ MeV. $\Delta k = 1$ MeV between each line.

If we had found an IR-stable fixed point associated to physical masses in the dimensionally reduced theory, the occurence of a second-order phase transition at finite temperature would be easily understood as follows. UV parameters yielding a first-order transition should be associ-

[1] We thank Mario Mitter, Jan M. Pawlowski, and Bernd-Jochen Schaefer for discussions about this issue, and for pointing out the existence of a maximal temperature above which the predictions of the dimensionally reduced theory could fail.

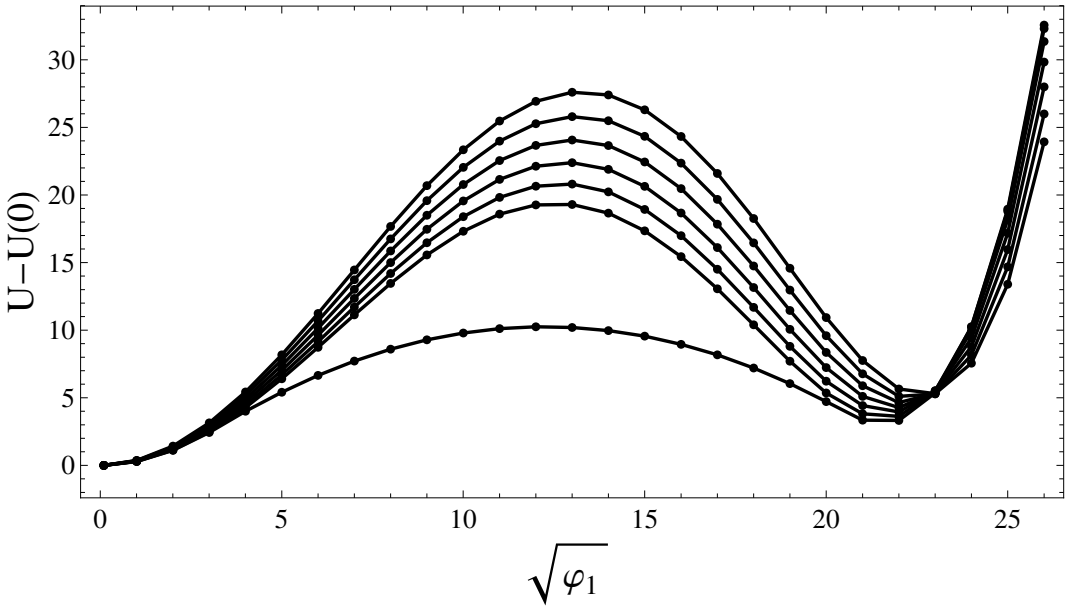

Figure 7.2: $SU(2)_A \times U(2)_V$-model. $W_{k=\Lambda}$ = 10, $A_{k=\Lambda}$ = 0, $B_{k=\Lambda}$ = 0.8. Λ = 500 MeV, T = 30 MeV, ϕ_0 = 183 MeV, r = 0.0139854. Evolution from k = 6.43 MeV to k = 0.43 MeV. Δk = 1 MeV between each line.

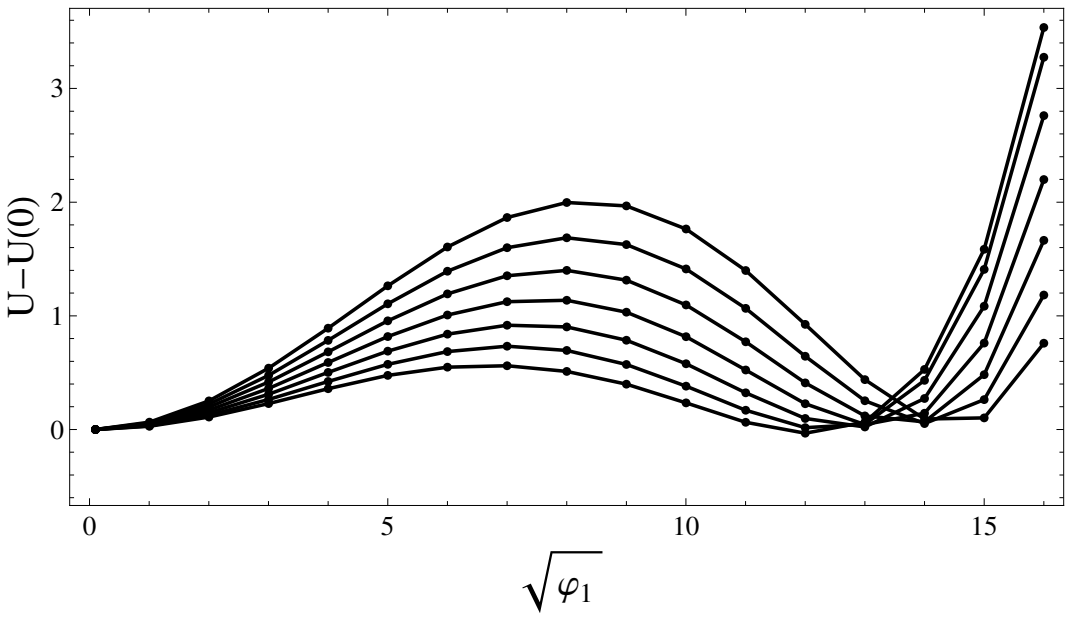

Figure 7.3: $SU(2)_A \times U(2)_V$-model. $W_{k=\Lambda}$ = 10, $A_{k=\Lambda}$ = 0, $B_{k=\Lambda}$ = 0.8. Λ = 500 MeV, T = 30 MeV, ϕ_0 = 179 MeV, r = 0.0147909. Evolution from k = 6.26 MeV to k = 0.26 MeV. Δk = 1 MeV between each line.

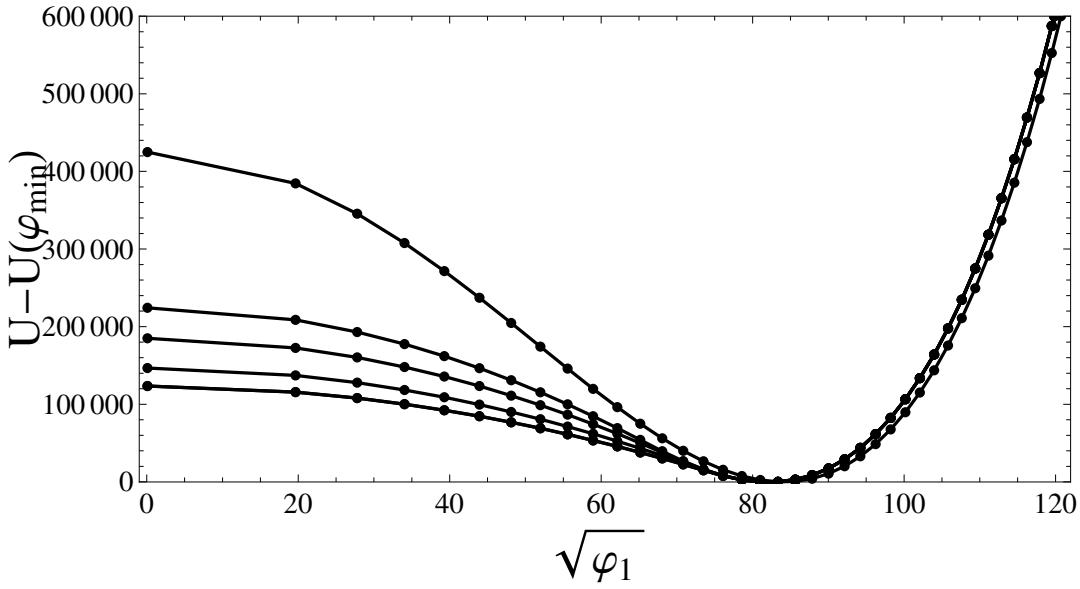

Figure 7.4: $SU(2)_A \times U(2)_V$-model. $W_{k=\Lambda}$ = 10, $A_{k=\Lambda}$ = 0, $B_{k=\Lambda}$ = 0.8. Λ = 500 MeV, T = 30 MeV, ϕ_0 = 179 MeV, r = 1/60. Curves correspond to k = 70 MeV, k = 9 MeV, k = 8 MeV, k = 7 MeV, and k = 6.36 MeV, respectively

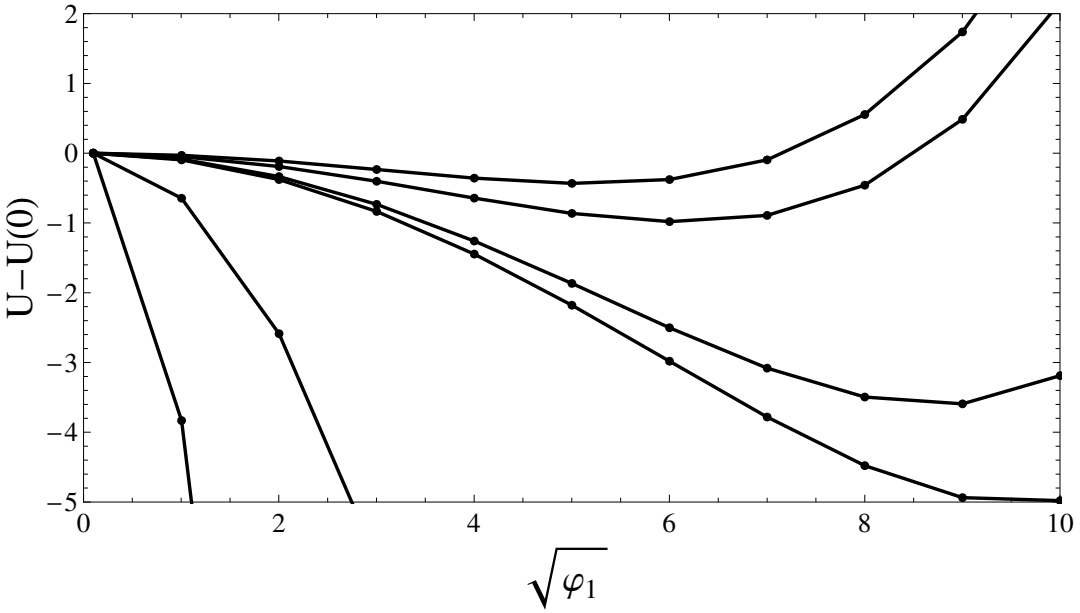

Figure 7.5: $SU(2)_A \times U(2)_V$-model. $W_{k=\Lambda}$ = 10, $A_{k=\Lambda}$ = 0, $B_{k=\Lambda}$ = 0.8. Λ = 500 MeV, T = 30 MeV, ϕ_0 = 174 MeV, r = 0.0159019. Curves correspond to k = 50 MeV, k = 30 MeV, k = 10 MeV, k = 8 MeV, k = 2.28 MeV, and k = 0.28 MeV, respectively

ated with UV parameters in the dimensionally reduced theory which do not lie in the basin of attraction for the IR-stable fixed point. Since we were not able to confirm the existence of such a physically stable IR fixed point (see Sec. 6.6), the possibility of a second-order transition is somehow unexpected.

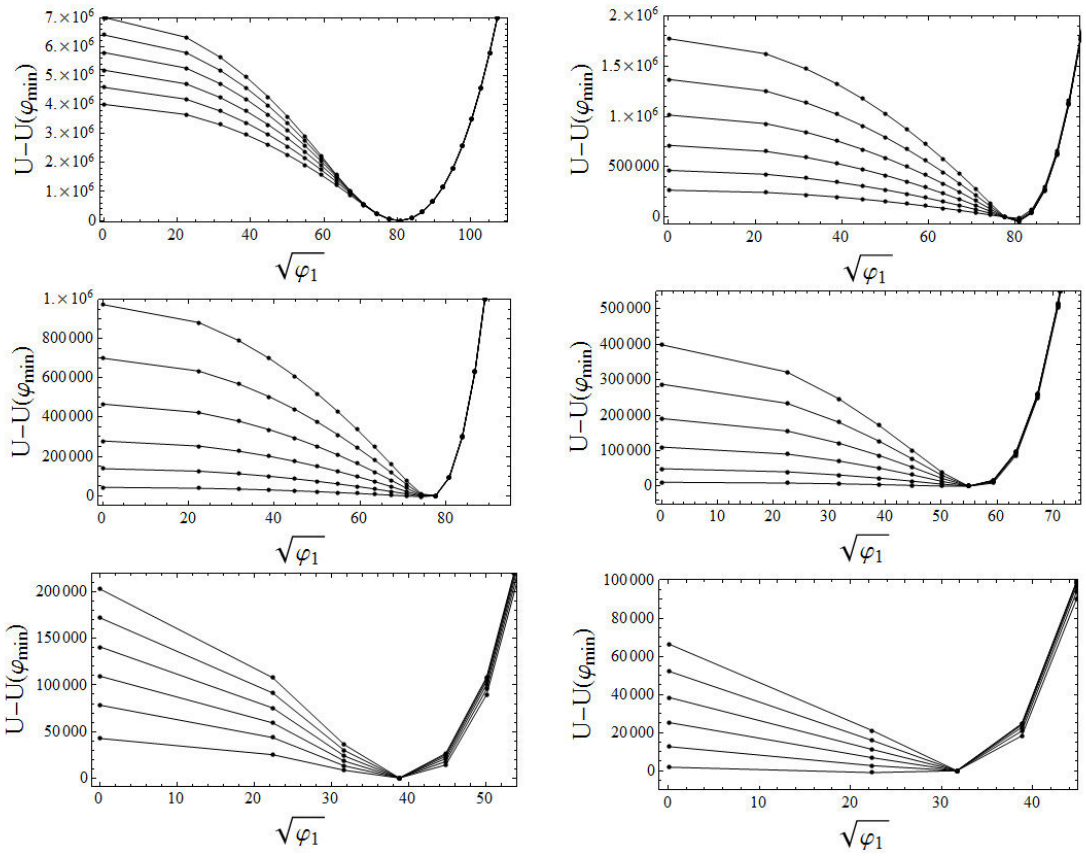

Figure 7.6: $SU(2)_A \times U(2)_V$-model. $W_{k=\Lambda} = 12992$, $A_{k=\Lambda} = 0$, $B_{k=\Lambda} = 0.2$. $\Lambda = 500$ MeV, $\phi_0 = 110$ MeV, $r = 1/3$. From left to right, top to bottom: $T = 0.1$ MeV, evolution from $k = 52.3$ MeV to $k = 37.3$ MeV; $T = 10$ MeV, evolution from $k = 24.45$ MeV to 9.45 MeV; $T = 50$ MeV, evolution from $k = 19.2$ MeV to 4.2 MeV; $T = 100$ MeV, evolution from $k = 18$ MeV to 3 MeV; $T = 120$ MeV, evolution from $k = 24.92$ MeV to 9.92 MeV; $T = 125$ MeV, evolution from $k = 18.6$ MeV to 3.6 MeV. $\Delta k = 3$ MeV between each line.

Before dialing up the cutoff and fitting the UV potential to physical observables we would like to clarify the above issue. For this purpose we went one step back to the $U(2)_A \times U(2)_V$-model. A similar situation is observed in this case (we refrain from showing the preliminary results here). Further work is in progress. Finally, we want to point out the strategy[2] for further investigations in presence of the anomaly. We plan to fit our UV parameters such that at $T = 0$ the nonstrange contributions to the meson masses (with focus on eta and sigma), as well as the pion decay constant in vacuum, are reproduced in the IR. From this one can determine the instanton density

[2]We thank Rob Pisarski for pointing out the possibility of fitting to the instanton density.

in dependence of T, the quark masses, and the instanton scale size ρ [compare with Eq. (3.8)]. Since the anomaly strength is proportional to the instanton density, one can now use this as input in the UV for studies at nonzero temperature.

7.3 Quark-meson model

In Sec. 4.4 we discussed how the quark-meson model, defined in Eq. (4.47), arises as an effective theory for QCD. We focus on the two-flavor case, take into account the sigma meson and the pions, and assume three colors. Neglecting the flow for the Yukawa coupling g and assuming that only the sigma field acquires a nonzero vacuum expectation value, the derivation of a flow equation within the proper-time RG approach has been discussed in Ref. [150]. The result reads

$$\frac{\partial U}{\partial k} = \frac{k^4}{12\pi^2}\left[\frac{3}{E_\pi}\coth\left(\frac{E_\pi}{2T}\right) + \frac{1}{E_\sigma}\coth\left(\frac{E_\sigma}{2T}\right) - \frac{12}{E_q}\left\{\tanh\left(\frac{E_q-\mu}{2T}\right) + \tanh\left(\frac{E_q+\mu}{2T}\right)\right\}\right], \quad (7.3)$$

where $E_\pi = \sqrt{k^2 + 2U'(\varphi)}$, the prime denotes the derivative with respect to $\varphi = \sigma^2 + \vec{\pi}^2$, $E_\sigma = \sqrt{k^2 + 2U'(\varphi) + 4\varphi U''(\varphi)}$, and $E_q = \sqrt{k^2 + g^2\varphi}$. It turns out that the result can be obtained as well using the FRG method (for details we refer to Ref. [151]).

The UV potential, $U_{k=\Lambda}$, should be chosen such that one obtains the following physical values in the IR limit $k = 0$. The position of the minimum in the IR and for $T = \mu = 0$ shall be equal to the pion decay constant in the vacuum, $\sqrt{\varphi_0} = f_\pi \sim 90$ MeV. The mass of the sigma field in the IR and for $T = \mu = 0$ shall be equal to the vacuum mass of the sigma particle, $M_\sigma = \sqrt{2U'(\varphi_0) + 4\varphi U''(\varphi_0)} \sim 500$ MeV. The Yukawa coupling shall be chosen such that one obtains a meaningful constituent quark mass, $m_q = g\sqrt{\varphi_0}$. Consistent with Ref. [150] we choose $U_{k=\Lambda} = \frac{5}{2}\varphi^2$, $\Lambda = 500$ MeV, and $g = 3.2$. In Fig. 7.7 we show the evolution of the potential for $T = \mu = 0$ in the regime where the position of the minimum settles. The evolution can be stopped as soon as the position of the minimum does not change anymore. We infer from the potential at

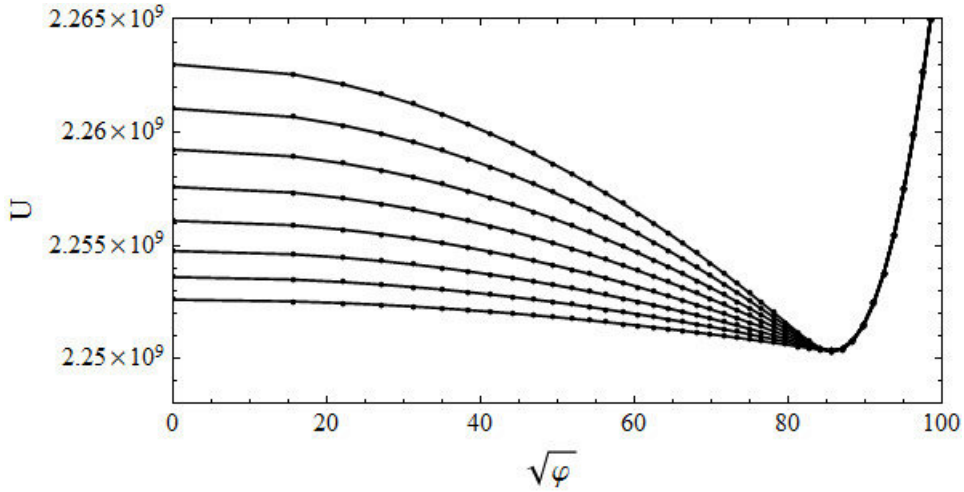

Figure 7.7: $T = 0$ MeV, $\mu = 0$ MeV. Evolution from $k = 60$ MeV to $k = 25$ MeV. $\Delta k = 5$ MeV between each line.

$k = 25$ MeV: $\sqrt{\varphi_0} \sim 85.5$ MeV, $M_\sigma \sim 265$ MeV, $m_q \sim 273.5$ MeV. The phase diagram as inferred from the evolution at different values for T and μ has been presented in Fig. 1 of Ref. [150]. We reproduced Figs. 3 and 4 of Ref. [150] using a similar routine to the ones provided in App. C. Fig. 3 of Ref. [150] corresponds to our Fig. 7.9, whereas Fig. 4 of Ref. [150] corresponds to our Figs. 7.11 and 7.13. In order to illustrate the evolution of the potential at larger k, we include Figs. 7.8, 7.10, and 7.12, showing the regime 200 MeV$> k >$ 60.

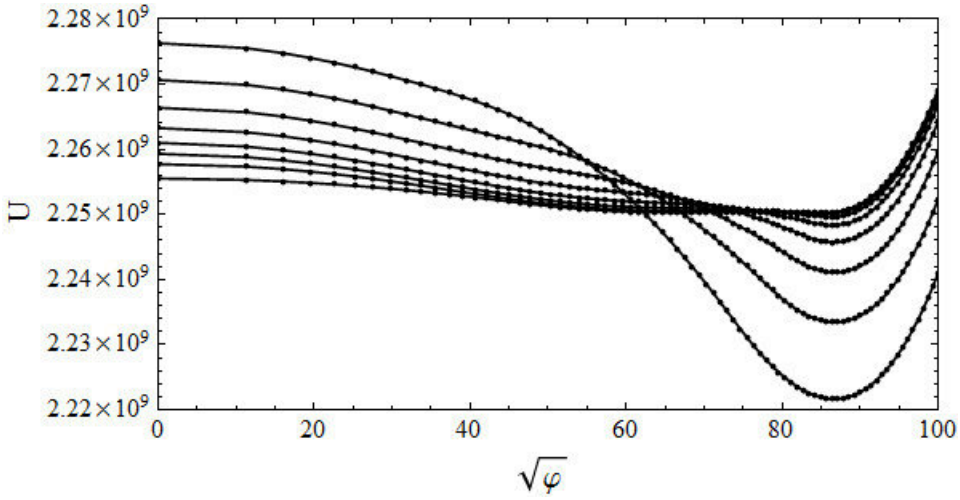

Figure 7.8: $T = 6$ MeV, $\mu = 254$ MeV. Evolution from $k = 200$ MeV to $k = 60$ MeV. $\Delta k = 20$ MeV between each line.

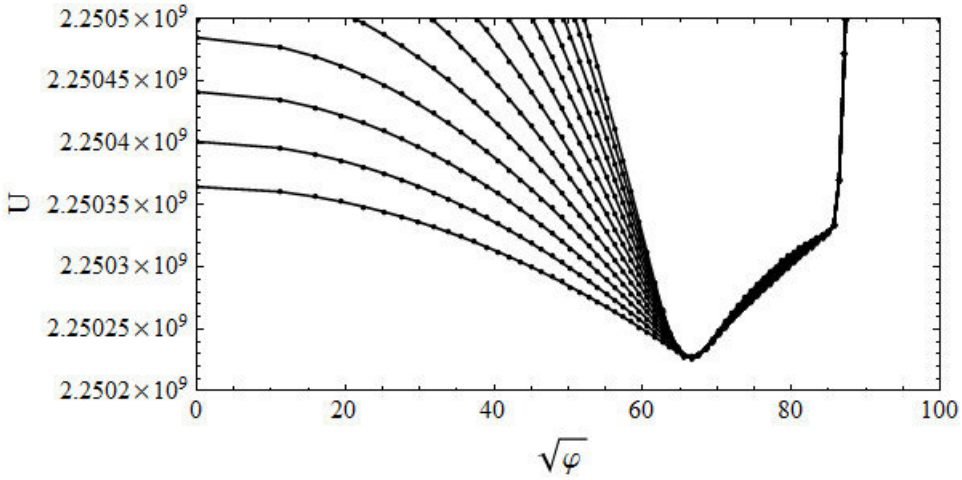

Figure 7.9: $T = 6$ MeV, $\mu = 254$ MeV. Lowest line $k = 8$ MeV, highest line $k = 20$ MeV, $\Delta k = 1$ MeV between each line.

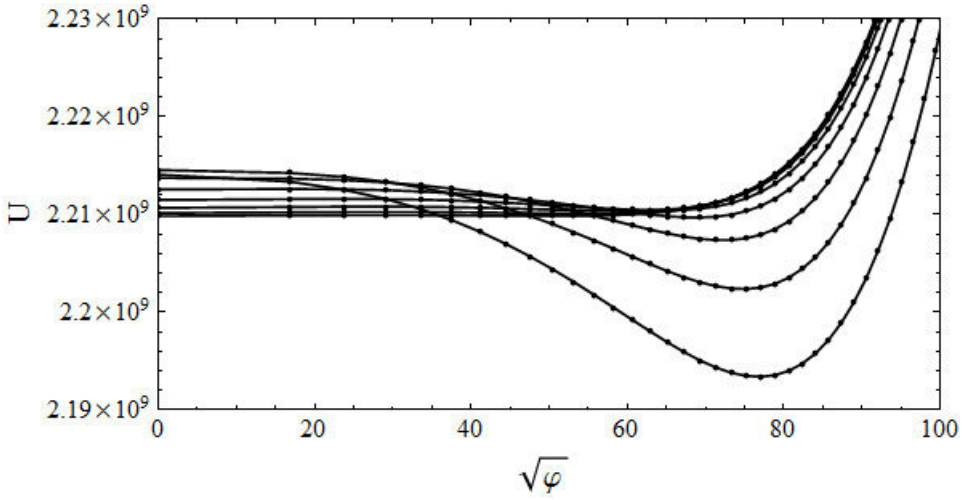

Figure 7.10: T = 45.1 MeV, μ = 253.9 MeV. Evolution from k = 200 MeV to k = 60 MeV. Δk = 20 MeV between each line.

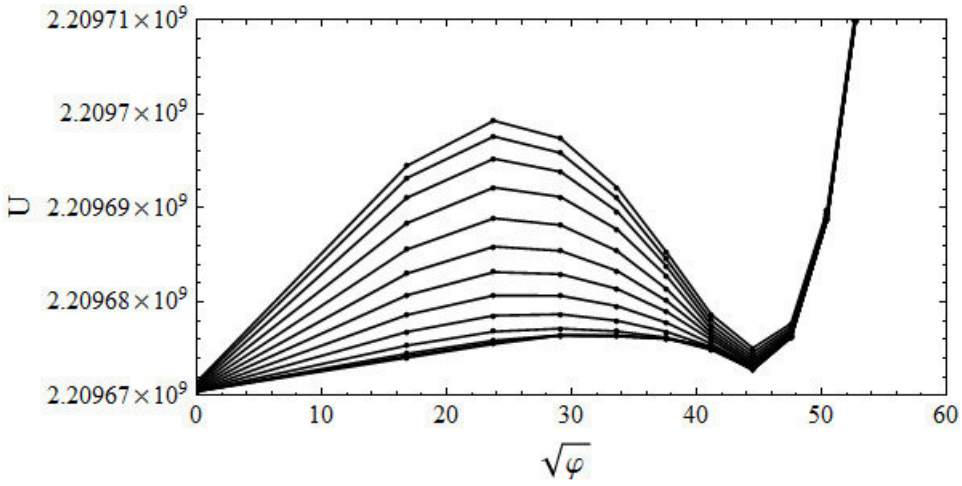

Figure 7.11: T = 45.1 MeV, μ = 253.9 MeV. Lowest line k = 2 MeV, highest line k = 14 MeV, Δk = 1 MeV between each line.

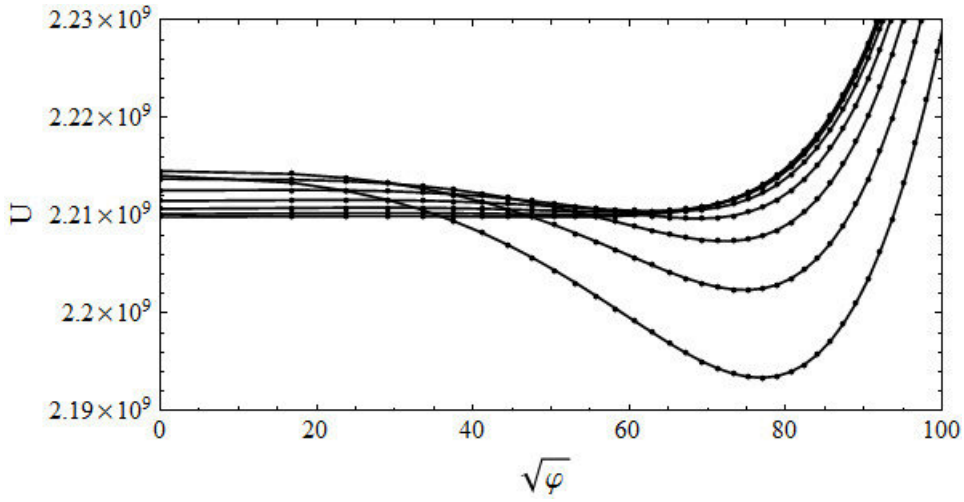

Figure 7.12: T = 100 MeV, μ = 0 MeV. Evolution from k = 200 MeV to k = 60 MeV. Δk = 20 MeV between each line.

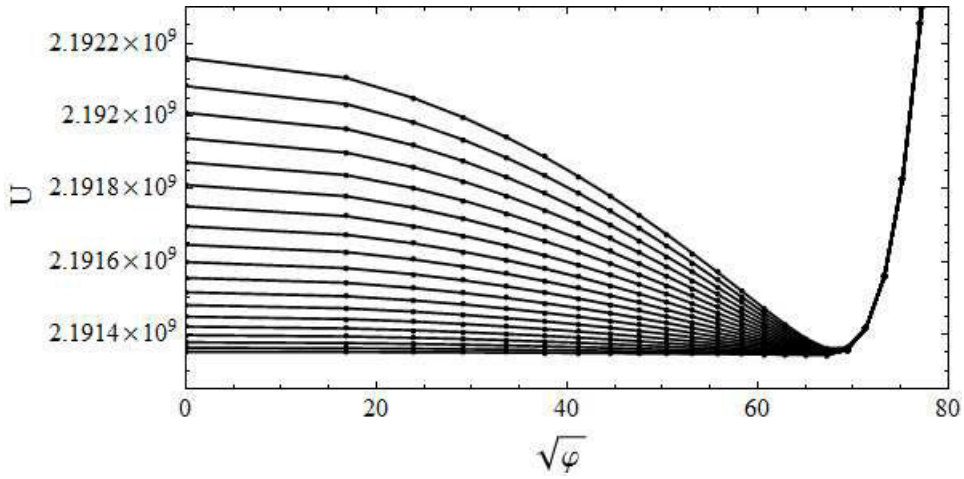

Figure 7.13: T = 100 MeV, μ = 0 MeV. Lowest line k = 2 MeV, highest line k = 20 MeV, Δk = 1 MeV between each line.

Mit dem Wissen wächst der Zweifel
(Johann Wolfgang von Goethe)

Chapter 8

Conclusions and Outlook

With our work we address the question of which order the chiral phase transition of two-flavor QCD is. The framework of our studies is that of effective models for the order parameter and the functional renormalization group (FRG) method. A crucial ingredient substantiating the meaning behind our approach is the universality hypothesis, the validity of which is therefore another central topic of our thesis. In this context we systematically reinvestigated a large amount of most general Landau potentials invariant under certain symmetries from the FRG approach in local-potential approximation (LPA), which enabled us to obtain a deeper understanding of the method and to point out several limitations of effective approaches towards QCD.
Whereas there is not much room for speculation about the symmetry of the effective theory for the order parameter (which necessarily corresponds to a subgroup $G \subseteq U(2)_A \times U(2)_V$), the identification of the components of the order parameter with the relevant mesonic degrees of freedom is highly nontrivial. This choice, which corresponds to the choice of the representation of G, cannot be definitely inferred from QCD at the moment and has to be made a priori. It is, however, guided by observations in collider experiments, lattice calculations, and plausibility considerations. Nevertheless, it is indispensable to test out several possible choices. A well-known choice consists in assigning the pion and its chiral partner, the sigma meson, to the $O(4)$ representation of $SU(2)_A \times SU(2)_V$, which allows for a second-order phase transition. This scenario is meaningful only if all other mesons remain heavy near the critical temperature. Considering the two-flavor case this requires the axial anomaly to be sufficiently strong. At intermediate anomaly strength, taking into account the eta and the a_0 meson in addition, our FRG fixed-point study of the dimensionally reduced theory for the order parameter cannot confirm the existence of a second-order phase transition. Our results favor a fluctuation-induced first-order scenario. In general, the existence of a second-order phase transition is unlikely due to the existence of two quadratic invariants, which rule out a second-order phase transition at mean-field level. There is, however, still a hypothetical chance that the unphysical IR-stable $SU(2)_A \times U(2)_V$-symmetric fixed point, encountered in the truncation up to naive scaling dimension six, could become physical at higher truncation order. This leads us to our (preliminary) FRG studies at nonzero temperature, which are dicussed next.
Whereas a fixed-point analysis of the dimensionally reduced theory (where temperature is not an explicit parameter anymore) is of great value to predict or to rule out, respectively, a second-order

chiral phase transition, it is not practical to judge the strength of a first-order chiral phase transition since the latter depends on the observables (meson masses and the pion decay constant in vacuum) to which one has to fit at zero temperature. Our (preliminary) FRG studies at nonzero temperature allow for both, either an extremely weak first-order transition, or a pronounced one, respectively, depending on the chosen value for the cutoff and on the above mentioned parameters. There is even evidence for a second-order phase transition for certain parameter choices, but it might be as well an extremely weak first-order phase transition. It is not clear, yet, if these parameter values are consistent with the region of validity for the dimensionally reduced theory, and if they are in some way related to the occurence of the unphysical IR-stable $SU(2)_A \times U(2)_V$-symmetric fixed point. Before we can draw reliable conclusions further investigations are required.

Very recently (end of September 2013) the existence of a $U(2)_A \times U(2)_V$-symmetric stable IR fixed point (associated with an anomalous dimension $\eta \sim 0.12$) has been stated in the literature by Pelissetto and Vicari. This result is very surprising since the first-order nature of the two-flavor case has been widely accepted and verified. Apparently, one- and higher-loop ϵ-expansions failed because for $D = 3$ ($\epsilon = 1$) only fixed points can be found which also exist near $D = 4$ (small ϵ). The RG approach of the above mentioned authors circumvents the ϵ-expansion and works directly in $D = 3$. Inspired by their important finding, we performed an FRG calculation taking into account invariants up to naive scaling dimension ten. At sixth order we find two $U(2)_A \times U(2)_V$-symmetric fixed points, and a single $U(2)_A \times U(2)_V$-symmetric fixed point at eighth and tenth order, respectively. The stability analysis remains inconclusive because the Gaussian fixed point aquires marginal eigenvalues. We believe that this is different beyond the local-potential approximation which assumes $\eta = 0$. Investigations in this direction are in progress.

In any case, the current results point out the limitations of both the local-potential approximation and the ϵ-expansion, on which most fixed-point studies (and investigations of the universality hypothesis) are based. In case of a sufficiently large value for the anomalous dimension the fixed-point structure can change significantly, and with it the conclusion whether a second-order phase transition can exist and to which universality class it belongs. Systematic investigations of the fixed-point structure for models with $N \leq 8$ order-parameter components were performed in the literature in the framework of the ϵ-expansion. We were able to verify most of their predictions from FRG in the local-potential approximation. Some of them, however, are questioned by the occurence of marginal stability-matrix eigenvalues. The former predictions are reliable, if η is sufficiently small in the corresponding experiment. The latter ones call for additional investigations taking η properly into account. Such studies would also be relevant to refine the current version of the universality hypothesis. Apart from (possible) violations reported in the literature, we presented our own studies which give cause for serious concern. We plan further investigations in this direction.

In our conclusions concerning the linear sigma model corresponding to the representation $[\bar{2}, 2] \oplus [2, \bar{2}]$ we only took into account the lightest scalar and pseudoscalar mesons, so far. We also investigated, however, the $[3, 1] \oplus [1, 3]$ representation as well as the $SO(3) \otimes SO(3)$ representation. In the first case we found an IR-stable fixed point (defining, to our knowledge, a new universality class) indicating the existence of a second-order phase transition, whereas in the second case the phase transition is predicted to be of first order. Neglecting the Lorentz indices of the vector and

axial-vector mesons in the framework of a toy model, we can consider the following scenarios. If the rho and the a_1 meson fields are the components of the order parameter we can assign them to the $[3,1] \oplus [1,3]$ representation concluding that the phase transition is of second order. This scenario is very unlikely since the pion as the (approximate) Goldstone boson should be part of the order-parameter field. Alternatively one could exchange one of the mesons with the pion. One can simultaneously account for all three mesons (which play the central role in several studies featuring hidden local symmetry) by assigning them to the $SO(3) \otimes SO(3)$ representation. That is, if the pion, the rho, and the a_1 meson fields are components of the order parameter the phase transition is of first order. Although we neglected the Lorentz indices, our results can be regarded as a first estimate and hopefully serve as a guide for more refined studies. We also emphasize that the new $[3,1] \oplus [1,3]$ universality class might be relevant in other areas of physics. We also pointed out that the coupling between the order parameter and other degrees of freedom can affect the order of the phase transition. In QCD the inclusion of gauge-field fluctuations should lead to a fluctuation-induced first-order transition. It would be therefore interesting to investigate the linear sigma model coupled to gauge fields from FRG. Fermions, on the other hand, should not affect universality since their lowest Matsubara mode acts like a thermal mass rendering them heavy.

In total, the existence of two new universality classes is proposed in this thesis: (i) the class characterized by the $[3,1] \oplus [1,3]$ representation of $SU(2)_A \times SU(2)_V$, (ii) a class (or maybe classes) of yet undetermined symmetry arising from a generalization of the Landau potential associated to the first mentioned class. Furthermore we discussed the existence of the $U(2)_A \times U(2)_V$ universality class in the framework of the FRG method. Speculations concerning the existence of a $SU(2)_A \times U(2)_V$ universality class are inconclusive, yet.

Furthermore, we developed a practical brute-force algorithm for the systematic construction of all linearly independent polynomial invariants of a given order using *Mathematica*. The knowledge of such complete sets is of crucial importance for model building and RG fixed-point studies.

Appendix A

Group-theoretical details

In this appendix we outline our understanding of certain group-theoretical issues relevant for our work.

A.1 Aspects of representation theory

In the following we summarize certain aspects of representation theory as inferred from Refs. [152, 153]. In general, for a group G one can distinguish the following kinds of matrix representations $\Gamma(G)$ involving N order-parameter components $\Phi_i \in \mathbb{R}$. In the following, summation over identical indices is implied.

- A *vector representation* is given by $p \times p$ matrices acting on the carrier space $\varphi^{\cdot} = (\varphi^1, \ldots, \varphi^p)^T$ as $\varphi'^i = U^i{}_j \varphi^j$. Short: $\varphi'^{\cdot} = U\varphi^{\cdot}$. By a tiny upper (lower) dot we indicate column (row) tuples involving components with upper (lower) indices. Note that the matrices form a matrix representation which acts on vectors and is therefore called vector representation. In general, U depends on a set of parameters $\vec{\alpha}$, and the components φ^i consist of algebraic combinations of the order-parameter components Φ_k. For faithful representations of continuous groups, for example, the matrices are in one-to-one correspondence with the (infinite set of) group elements, so that $\vec{\alpha}$ is a continuous variable unambiguously labeling the group elements. Rotations in two-dimensional space, for instance, can be described by a 2×2-matrix $U(\alpha)$ involving an angle α, acting on a two-dimensional vector $(x, y)^T$,

$$\begin{pmatrix} x' \\ y' \end{pmatrix} = \begin{pmatrix} \cos\alpha & -\sin\alpha \\ \sin\alpha & \cos\alpha \end{pmatrix} \begin{pmatrix} x \\ y \end{pmatrix} , \tag{A.1}$$

  forming a faithful representation of the group $O(2)$. For finite representations of finite groups, on the other hand, the parameters are not continuous. Regarding the ambiguous dependence of the φ^i on the components of physical space (here the spatial coordinates) consider for example the equivalent representation

$$\begin{pmatrix} x' + y' \\ x' - y' \end{pmatrix} = \begin{pmatrix} \cos\alpha & \sin\alpha \\ -\sin\alpha & \cos\alpha \end{pmatrix} \begin{pmatrix} x + y \\ x - y \end{pmatrix} . \tag{A.2}$$

Equivalent representations are related by a change of basis, i.e., a similarity transformation, and they are usually defined to be identical. Inequivalent representations are given for example by

$$\begin{pmatrix} x' \\ y' \\ z' \end{pmatrix} = \begin{pmatrix} \cos\alpha & -\sin\alpha & 0 \\ \sin\alpha & \cos\alpha & 0 \\ 0 & 0 & 1 \end{pmatrix} \begin{pmatrix} x \\ y \\ z \end{pmatrix} \tag{A.3}$$

and

$$\begin{pmatrix} x' + \mathrm{i}\, y' \\ z' \\ x' - \mathrm{i}\, y' \end{pmatrix} = \begin{pmatrix} \mathrm{e}^{\mathrm{i}\,\alpha} & 0 & 0 \\ 0 & 1 & 0 \\ 0 & 0 & \mathrm{e}^{-\mathrm{i}\,\alpha} \end{pmatrix} \begin{pmatrix} x + \mathrm{i}\, y \\ z \\ x - \mathrm{i}\, y \end{pmatrix} , \tag{A.4}$$

respectively.
If $\varphi^i \in \mathbb{C}$ the matrices are usually also complex-valued and one has a complex vector representation. Then one obtains another representation by taking the complex conjugate of the above equation, i.e., $\varphi'^{i*} = \left(U^i{}_j\right)^* \varphi^{j*} = \left(U^\dagger\right)^j{}_i \varphi^{j*}$. By convention we can distinguish between upper (covariant) indices and lower (contravariant) indices defining $\varphi_j \equiv \varphi^{j*}$. Accordingly, $\varphi'_i = \left(U^\dagger\right)^j{}_i \varphi_j$. Short: $(\varphi'_\cdot)^\dagger = (\varphi_\cdot)^\dagger U^\dagger$, which can be rewritten as $\varphi'_\cdot = \varphi_\cdot U^\dagger$ denoting $\varphi_\cdot = (\varphi_1, \ldots, \varphi_p)$. The matrices $U^\dagger$ define the *conjugate vector representation* associated with the carrier space $\varphi_\cdot$.

- *Tensor representations* can be constructed by forming outer tensor products,

$$\varphi_{i_1} \cdots \varphi_{i_N} \varphi^{j_1} \cdots \varphi^{j_M} \equiv \varphi^{j_1 \cdots j_M}_{i_1 \cdots i_N} ,$$

which are consequently tensors transforming as

$$\varphi'^{j_1 \cdots j_M}_{i_1 \cdots i_N} = \left(U^\dagger\right)^{k_1}_{i_1} \cdots \left(U^\dagger\right)^{k_N}_{i_N} U^{j_1}_{l_1} \cdots U^{j_M}_{l_M} \varphi^{l_1 \cdots l_M}_{k_1 \cdots k_N} . \tag{A.5}$$

We note that Eq. (A.5) can be rewritten in terms of the Kronecker product $\otimes$ defined for matrices. Consider for example a transformation of the form

$$c'_{ij} = A_{ik} B_{jl} c_{kl} . \tag{A.6}$$

Eq. (A.6) is equivalent to each of the following relations. Denoting

$$A \equiv \begin{pmatrix} A_{11} & A_{12} \\ A_{21} & A_{22} \end{pmatrix} \text{ and } B \equiv \begin{pmatrix} B_{11} & B_{12} \\ B_{21} & B_{22} \end{pmatrix} , \tag{A.7}$$

we can rewrite

$$\begin{pmatrix} c'_1 \\ c'_2 \end{pmatrix} \otimes \begin{pmatrix} c'_3 \\ c'_4 \end{pmatrix} = A \otimes B \begin{pmatrix} c_1 \\ c_2 \end{pmatrix} \otimes \begin{pmatrix} c_3 \\ c_4 \end{pmatrix} , \tag{A.8}$$

where we introduced components c_i via

$$\begin{pmatrix} c_1 \\ c_2 \end{pmatrix} \otimes \begin{pmatrix} c_3 \\ c_4 \end{pmatrix} = \begin{pmatrix} c_1 c_3 \\ c_1 c_4 \\ c_2 c_3 \\ c_2 c_4 \end{pmatrix} \equiv \begin{pmatrix} c_{11} \\ c_{12} \\ c_{21} \\ c_{22} \end{pmatrix} . \tag{A.9}$$

Alternatively we can introduce the matrix

$$c \equiv \begin{pmatrix} c_{11} & c_{12} \\ c_{21} & c_{22} \end{pmatrix} \tag{A.10}$$

and obtain

$$c' = AcB^T \ . \tag{A.11}$$

Furthermore:

$$\begin{pmatrix} c_1' \\ c_2' \end{pmatrix} = A \begin{pmatrix} c_1 \\ c_2 \end{pmatrix} \ , \quad \begin{pmatrix} c_3' \\ c_4' \end{pmatrix} = B \begin{pmatrix} c_3 \\ c_4 \end{pmatrix} \ . \tag{A.12}$$

A.2 Chiral symmetry

Quark fields Ψ consist of components $\Psi_{c,f,\sigma}$ carrying N_c color indices, N_f flavor indices, and four Dirac indices. Accordingly they are Kronecker products of tuples in color space, Ψ_C, tuples in flavor space (the subspace for $N_f = 2$ is called strong isospin), Ψ_F, and tuples in Dirac (i.e., spin) space, Ψ_D. Namely

$$\Psi = \Psi_C \otimes \Psi_F \otimes \Psi_D \ , \tag{A.13}$$

where $\otimes$ denotes the Kronecker product. Quark fields Ψ_F belong to the irreducible representation $[N_f]$ of $SU(N_f)$, antiquark fields $\bar{\Psi}_F$ to the irreducible representation $[\bar{N_f}]$. For $N_f = 2$, the generators of $SU(2)$ in the representation $[2]$ are given by half the Pauli matrices. Hence, from (3.4) we obtain the following infinitesimal transformations for this representation:

$$SU(2)_V : \ \Psi \to \left(1 + \mathrm{i} \sum_{a=1}^{3} \alpha_V^a \frac{\sigma_a}{2}\right) \Psi \ , \tag{A.14}$$

$$SU(2)_A : \ \Psi \to \left(1 + \mathrm{i}\,\gamma_5 \sum_{a=1}^{3} \alpha_A^a \frac{\sigma_a}{2}\right) \Psi \ , \tag{A.15}$$

$$U(1)_V : \ \Psi \to \left(1 + \mathrm{i}\,\alpha_V^0 \frac{\mathbf{1}_2}{2}\right) \Psi \ , \tag{A.16}$$

$$U(1)_A : \ \Psi \to \left(1 + \mathrm{i}\,\gamma_5 \alpha_A^0 \frac{\mathbf{1}_2}{2}\right) \Psi \ . \tag{A.17}$$

QCD describes mesons as quark-antiquark pairs. The mesonic fields can be identified with currents

$$\bar{\Psi} \mathcal{O} \Psi \ , \tag{A.18}$$

where the operator $\mathcal{O}$ determines their transformation properties under spin (J), parity (P), strong isospin (I), and Lorentz symmetry (see Tab. A.1). We can derive the behavior of the mesonic fields under infinitesimal continuous transformations (A.14)–(A.17) by plugging in the respective transformation into the expressions of Tab. A.1 , keeping only terms up to linear order

Table A.1:

J^{PC}	I	$\mathcal{O}$	resonance	abbreviation for $\bar{\Psi}\mathcal{O}\Psi$	transforms as Lorentz...
0^{++}	0	1	$f_0(500)$ or $f_0(1370)$	σ	scalar
0^{++}	1	$\vec{\tau}$	$a_0(980)$ or $a_0(1450)$	$\vec{a}_0 = (a_1, a_2, a_3)$	scalar
0^{-+}	0	$\mathrm{i}\gamma_5$	η	η	pseudoscalar
$0^{-(+)}$	1	$\mathrm{i}\gamma_5\vec{\tau}$	$\pi^0, \pi^\pm$	$\vec{\pi} = (\pi_1, \pi_2, \pi_3)$	pseudoscalar
$1^{-(-)}$	0	γ^μ	$\omega(782)$	ω^μ	vector
$1^{-(-)}$	1	$\gamma^\mu\vec{\tau}$	$\rho(770)$	$\vec{\rho}^\mu = (\rho_1^\mu, \rho_2^\mu, \rho_3^\mu)$	vector
$1^{+(+)}$	0	$\gamma^\mu\gamma_5$	$f_1(1285)$	f_1^μ	axial vector
$1^{+(+)}$	1	$\gamma^\mu\gamma_5\vec{\tau}$	$a_1(1260)$	$\vec{a}_1^\mu = (a_{1,1}^\mu, a_{1,2}^\mu, a_{1,3}^\mu)$	axial vector

in the angles $\alpha_{A,V}^a$, and rearranging matrices according to the relations

$$\gamma_\mu\gamma_5 = -\gamma_5\gamma_\mu \ , \tag{A.19}$$

$$[\sigma_i, \sigma_j] = \sigma_i\sigma_j - \sigma_j\sigma_i = 2\,\mathrm{i}\sum_{k=1}^{3}\epsilon_{ijk}\sigma_k \ , \quad i,j = 1,2,3 \ , \tag{A.20}$$

$$\{\sigma_i, \sigma_j\} = \sigma_i\sigma_j + \sigma_j\sigma_i = 2\delta_{ij}\mathbf{1}_2 \ , \quad i,j = 1,2,3 \ . \tag{A.21}$$

Also note that the gamma matrices commute with the Pauli matrices $\vec{\tau} \equiv (\sigma_1, \sigma_2, \sigma_3)$ for the trivial reason that they act on distinct subspaces, Dirac space Ψ_D and flavor space Ψ_F, respectively, As an example consider the invariance of the combination $(\bar{\Psi}\vec{\tau}\Psi)^2 - (\bar{\Psi}\vec{\tau}\gamma_5\Psi)^2$ under $U(1)_A$ transformations (A.17). Denoting for simplicity $\alpha_A^0\frac{\mathbf{1}_2}{2} \equiv \alpha_A$, one obtains

$$\begin{aligned}
(\bar{\Psi}\vec{\tau}\Psi)^2 - (\bar{\Psi}\vec{\tau}\gamma_5\Psi)^2 \xrightarrow{U(1)_A} &\sum_i \big[\bar{\Psi}(1+\mathrm{i}\alpha_A\gamma_5)\tau_i(1+\mathrm{i}\alpha_A\gamma_5)\Psi\big]\big[\bar{\Psi}(1+\mathrm{i}\alpha_A\gamma_5)\tau_i(1+\mathrm{i}\alpha_A\gamma_5)\Psi\big] \\
&- \sum_i \big[\bar{\Psi}(1+\mathrm{i}\alpha_A\gamma_5)\tau_i\gamma_5(1+\mathrm{i}\alpha_A\gamma_5)\Psi\big]\big[\bar{\Psi}(1+\mathrm{i}\alpha_A\gamma_5)\tau_i\gamma_5(1+\mathrm{i}\alpha_A\gamma_5)\Psi\big] \\
&= \sum_i \big[\bar{\Psi}\tau_i\Psi\bar{\Psi}\tau_i\Psi + \bar{\Psi}\tau_i\Psi\bar{\Psi}2\,\mathrm{i}\alpha_A\gamma_5\tau_i\Psi + \bar{\Psi}2\,\mathrm{i}\alpha_A\gamma_5\tau_i\Psi\bar{\Psi}\tau_i\Psi\big] \\
&- \sum_i \big[\bar{\Psi}\tau_i\gamma_5\Psi\bar{\Psi}\tau_i\gamma_5\Psi + \bar{\Psi}\tau_i\gamma_5\Psi\bar{\Psi}2\,\mathrm{i}\alpha_A\tau_i\Psi + \bar{\Psi}2\,\mathrm{i}\alpha_A\tau_i\Psi\bar{\Psi}\tau_i\gamma_5\Psi\big] \\
&= (\bar{\Psi}\vec{\tau}\Psi)^2 - (\bar{\Psi}\vec{\tau}\gamma_5\Psi)^2 \ ,
\end{aligned} \tag{A.22}$$

where terms of order α_A^2 have been dropped in the calculation. Similarly one derives the following transformation rules under infinitesimal vector and axial-vector transformations:

$$\sigma \xrightarrow{SU(2)_V} \sigma \ , \quad \sigma \xrightarrow{SU(2)_A} \sigma + \vec{\alpha}_A\cdot\vec{\pi} \ , \quad \sigma \xrightarrow{U(1)_V} \sigma \ , \quad \sigma \xrightarrow{U(1)_A} \sigma + \alpha_A^0\eta \ , \tag{A.23}$$

$$\eta \xrightarrow{SU(2)_V} \eta \ , \quad \eta \xrightarrow{SU(2)_A} \eta - \vec{\alpha}_A\cdot\vec{a}_0 \ , \quad \eta \xrightarrow{U(1)_V} \eta \ , \quad \eta \xrightarrow{U(1)_A} \eta - \alpha_A^0\sigma \ , \tag{A.24}$$

$$\vec{\pi} \xrightarrow{SU(2)_V} \vec{\pi} + \vec{\alpha}_V\times\vec{\pi} \ , \quad \vec{\pi} \xrightarrow{SU(2)_A} \vec{\pi} - \vec{\alpha}_A\sigma \ , \quad \vec{\pi} \xrightarrow{U(1)_V} \vec{\pi} \ , \quad \vec{\pi} \xrightarrow{U(1)_A} \vec{\pi} - \alpha_A^0\vec{a}_0 \ , \tag{A.25}$$

$$\vec{a}_0 \xrightarrow{SU(2)_V} \vec{a}_0 + \vec{\alpha}_V\times\vec{a}_0 \ , \quad \vec{a}_0 \xrightarrow{SU(2)_A} \vec{a}_0 + \vec{\alpha}_A\eta \ , \quad \vec{a}_0 \xrightarrow{U(1)_V} \vec{a}_0 \ , \quad \vec{a} \xrightarrow{U(1)_A} \vec{a} + \alpha_A^0\vec{\pi} \ , \tag{A.26}$$

$$\vec{\rho}^{\,\mu} \xrightarrow{SU(2)_V} \vec{\rho}^{\,\mu} - \vec{\alpha}_V \times \vec{\rho}^{\,\mu} \ , \quad \vec{\rho}^{\,\mu} \xrightarrow{SU(2)_A} \vec{\rho}^{\,\mu} - \vec{\alpha}_A \times \vec{a}_1^{\,\mu} \ , \quad \vec{\rho}^{\,\mu} \xrightarrow{U(1)_V} \vec{\rho}^{\,\mu} \ , \quad \vec{\rho}^{\,\mu} \xrightarrow{U(1)_A} \vec{\rho}^{\,\mu} \ , \tag{A.27}$$

$$\vec{a}_1^{\,\mu} \xrightarrow{SU(2)_V} \vec{a}_1^{\,\mu} - \vec{\alpha}_V \times \vec{a}_1^{\,\mu} \ , \quad \vec{a}_1^{\,\mu} \xrightarrow{SU(2)_A} \vec{a}_1^{\,\mu} - \vec{\alpha}_A \times \vec{\rho}^{\,\mu} \ , \quad \vec{a}_1^{\,\mu} \xrightarrow{U(1)_V} \vec{a}_1^{\,\mu} \ , \quad \vec{a}_1^{\,\mu} \xrightarrow{U(1)_A} \vec{a}_1^{\,\mu} \ , \tag{A.28}$$

$$\omega^\mu \xrightarrow{SU(2)_V} \omega_\mu \ , \quad \omega^\mu \xrightarrow{SU(2)_A} \omega_\mu \ , \quad \omega^\mu \xrightarrow{U(1)_V} \omega_\mu \ , \quad \omega^\mu \xrightarrow{U(1)_A} \omega_\mu \ , \tag{A.29}$$

$$f_1^\mu \xrightarrow{SU(2)_V} f_1^\mu \ , \quad f_1^\mu \xrightarrow{SU(2)_A} f_1^\mu \ , \quad f_1^\mu \xrightarrow{U(1)_V} f_1^\mu \ , \quad f_1^\mu \xrightarrow{U(1)_A} f_1^\mu \ . \tag{A.30}$$

We proceed with further group-theoretical aspects. More details can be found for example in Refs. [97, 141, 154, 155] Irreducible representations of $SU(2)$ can be labeled by $[2j+1]$, where $j = 0, \frac{1}{2}, 1, \ldots$, or in a different notation by $[j]$. Each of them is in one-to-one correspondence with a multiplet consisting of $2j+1$ states, and the generators of $SU(2)$ in the representation $[2j+1]$ are (generally complex-valued) $(2j+1)\times(2j+1)$-matrices. Hence, the elements of the group in the representation $[2j+1]$ are (generally complex-valued) $(2j+1)\times(2j+1)$-matrices acting on a carrier space of the representation, which is spanned by a (generally complex-valued) $(2j+1)$-dimensional tuple. For instance, the carrier space of the representation $[2]$ is given by a two-dimensional, complex-valued spinor $\psi = (u,d)^T$. Conjugate irreducible representations are labeled by $[\overline{2j+1}]$ (or $[\overline{j}]$, respectively). The carrier space of the representation $[\overline{2}]$ is given by a two-dimensional, complex-valued spinor $\psi^\dagger = (u^*, d^*)$.
Consistent with Eq. (A.5) the spinor ψ transforms according to

$$\psi'^i = U^i{}_j \psi^j \ , \tag{A.31}$$

where $\psi^1 = u$, $\psi^2 = d$, and U is an arbitrary unitary 2×2 matrix with determinant 1, i.e., an arbitrary element of $SU(2)$ in the fundamental representation. The spinor $\psi^\dagger$ transforms according to

$$\psi'_i = \left(U^\dagger\right)^j{}_i \psi_j \ , \tag{A.32}$$

where $\psi_1 = u^*$, $\psi_2 = d^*$. Accordingly, the outer tensor product $\psi_i^j = \psi_i \psi^j$ transforms as

$$\psi'^i{}_k = U^i{}_j \left(U^\dagger\right)^l{}_k \psi_l^j \ , \tag{A.33}$$

where $\psi_1^1 = uu^*$, $\psi_2^1 = ud^*$, $\psi_1^2 = du^*$, $\psi_2^2 = dd^*$. With Eq. (A.11), for $A = B^* = U$, we can rewrite the transformation (A.33) as

$$\underline{\Psi}' = U \underline{\Psi} U^\dagger \ , \tag{A.34}$$

where $\underline{\Psi} = \begin{pmatrix} \psi_1^1 & \psi_2^1 \\ \psi_1^2 & \psi_2^2 \end{pmatrix}$, $U = \begin{pmatrix} U^1{}_1 & U^1{}_2 \\ U^2{}_1 & U^2{}_2 \end{pmatrix}$, and $U^\dagger = \begin{pmatrix} \left(U^\dagger\right)^1{}_1 & \left(U^\dagger\right)^1{}_2 \\ \left(U^\dagger\right)^2{}_1 & \left(U^\dagger\right)^2{}_2 \end{pmatrix}$. Alternatively, according to Eq. (A.8):

$$\begin{pmatrix} u' \\ d' \end{pmatrix} \otimes \begin{pmatrix} u'^* \\ d'^* \end{pmatrix} = \begin{pmatrix} U^1{}_1 & U^1{}_2 \\ U^2{}_1 & U^2{}_2 \end{pmatrix} \otimes \begin{pmatrix} \left(U^1{}_1\right)^* & \left(U^1{}_2\right)^* \\ \left(U^2{}_1\right)^* & \left(U^2{}_2\right)^* \end{pmatrix} \begin{pmatrix} u \\ d \end{pmatrix} \otimes \begin{pmatrix} u^* \\ d^* \end{pmatrix} \ . \tag{A.35}$$

The above defined representation associated with $\underline{\Psi}$ relates to the fundamental representation of $O(4)$, which can seen as follows. All invariants under the transformation (A.34) which can be

constructed from $\underline{\Psi}$ are given, up to quartic order in the fields, by

$$\sqrt{\mathrm{Tr}\,\underline{\Psi}\;\underline{\Psi}^\dagger} = (\mathrm{Re}\,u)^2 + (\mathrm{Im}\,u)^2 + (\mathrm{Re}\,d)^2 + (\mathrm{Im}\,d)^2 \ , \tag{A.36}$$

$$\mathrm{Tr}\,\underline{\Psi}\;\underline{\Psi}^\dagger = \sqrt{\mathrm{Tr}\left(\underline{\Psi}\;\underline{\Psi}^\dagger\right)^2} = \left((\mathrm{Re}\,u)^2 + (\mathrm{Im}\,u)^2 + (\mathrm{Re}\,d)^2 + (\mathrm{Im}\,d)^2\right)^2 \ . \tag{A.37}$$

Identifying $\phi_1 \equiv \mathrm{Re}\,u$, $\phi_2 = \mathrm{Im}\,u$, $\phi_3 = \mathrm{Re}\,d$, and $\phi_4 = \mathrm{Im}\,d$, we recognize that the basic invariant is that of $O(4)$ in the fundamental representation, $\phi_1^2 + \phi_2^2 + \phi_3^2 + \phi_4^2$.
Taking account of their flavor content, mesonic fields can be identified with linear combinations of the components ψ_j^i as follows.

$$\sigma \equiv \frac{1}{\sqrt{2}}(uu^* + dd^*) \ , \quad a_0^+ \equiv ud^* \equiv \frac{1}{\sqrt{2}}(a_1 - \mathrm{i}\,a_2) \ , \tag{A.38}$$

$$a_0^- \equiv du^* \equiv \frac{1}{\sqrt{2}}(a_1 + \mathrm{i}\,a_2) \ , \quad a_0^0 \equiv \frac{1}{\sqrt{2}}(uu^* - dd^*) \equiv a_3 \ , \tag{A.39}$$

where σ denotes the sigma-meson field, and (a_0^+, a_0^-, a_0^0) denotes the a_0-meson field ($\vec{a}_0 = (a_1, a_2, a_3)$ denotes an equivalent parameterization).

$$\eta \equiv \frac{1}{\sqrt{2}}(uu^* + dd^*) \ , \quad \pi^+ \equiv ud^* \equiv \frac{1}{\sqrt{2}}(\pi_1 - \mathrm{i}\,\pi_2) \ , \tag{A.40}$$

$$\pi^- \equiv du^* \equiv \frac{1}{\sqrt{2}}(\pi_1 + \mathrm{i}\,\pi_2) \ , \quad \pi^0 \equiv \frac{1}{\sqrt{2}}(uu^* - dd^*) \equiv \pi_3 \ , \tag{A.41}$$

where η denotes the eta-meson field, and (π^+, π^-, π^0) denotes the pion field ($\vec{\pi} = (\pi_1, \pi_2, \pi_3)$ denotes an equivalent parameterization).

$$\omega^\mu \equiv \frac{1}{\sqrt{2}}(uu^* + dd^*) \ , \quad \rho^{+,\mu} \equiv ud^* \equiv \frac{1}{\sqrt{2}}(\rho_1^\mu - \mathrm{i}\,\rho_2^\mu) \ , \tag{A.42}$$

$$\rho^{-,\mu} \equiv du^* \equiv \frac{1}{\sqrt{2}}(\rho_1^\mu + \mathrm{i}\,\rho_2^\mu) \ , \quad \rho^{0,\mu} \equiv \frac{1}{\sqrt{2}}(uu^* - dd^*) \equiv \rho_3^\mu \ , \tag{A.43}$$

where ω denotes the omega-meson field, and $(\rho^{+,\mu}, \rho^{-,\mu}, \rho^{0,\mu})$ denotes the rho-meson field ($\vec{\rho}^\mu = (\rho_1^\mu, \rho_2^\mu, \rho_3^\mu)$ denotes an equivalent parameterization).

$$f_1^\mu \equiv \frac{1}{\sqrt{2}}(uu^* + dd^*) \ , \quad a_1^{+,\mu} \equiv ud^* \equiv \frac{1}{\sqrt{2}}(a_{1,1}^\mu - \mathrm{i}\,a_{1,2}^\mu) \ , \tag{A.44}$$

$$a_1^{-,\mu} \equiv du^* \equiv \frac{1}{\sqrt{2}}(a_{1,1}^\mu + \mathrm{i}\,a_{1,2}^\mu) \ , \quad a_1^{0,\mu} \equiv \frac{1}{\sqrt{2}}(uu^* - dd^*) \equiv a_{1,3}^\mu \ , \tag{A.45}$$

where f_1^μ denotes the f_1-meson field, and $(a_1^{+,\mu}, a_1^{-,\mu}, a_1^{0,\mu})$ denotes the a_1-meson field ($\vec{a}_1^\mu = (a_{1,1}^\mu, a_{1,2}^\mu, a_{1,3}^\mu)$ denotes an equivalent parameterization).
$\underline{\Psi}$ can now be parameterized in terms of the mesonic fields. We can either use the scalar fields,

$$\underline{\Psi} \equiv S \equiv \frac{1}{\sqrt{2}}\left(\sigma \mathbf{1}_2 + \vec{a}_0 \cdot \vec{\tau}\right) = \frac{1}{\sqrt{2}}\begin{pmatrix} \sigma + a_3 & a_1 - \mathrm{i}\,a_2 \\ a_1 + \mathrm{i}\,a_2 & \sigma - a_3 \end{pmatrix} \ , \tag{A.46}$$

the pseudoscalar fields,

$$\underline{\Psi} \equiv P \equiv \frac{1}{\sqrt{2}}\left(\eta \mathbf{1}_2 + \vec{\pi} \cdot \vec{\tau}\right) = \frac{1}{\sqrt{2}}\begin{pmatrix} \eta + \pi_3 & \pi_1 - \mathrm{i}\,\pi_2 \\ \pi_1 + \mathrm{i}\,\pi_2 & \eta - \pi_3 \end{pmatrix} \ , \tag{A.47}$$

the vector-meson fields,

$$\underline{\Psi} \equiv V^\mu = \frac{1}{\sqrt{2}} \left(\omega^\mu \mathbf{1}_2 + \vec{\rho}^\mu \cdot \vec{\tau} \right) \ , \tag{A.48}$$

or the axial-vector meson fields,

$$\underline{\Psi} \equiv A^\mu = \frac{1}{\sqrt{2}} \left(f_1^\mu \mathbf{1}_2 + \vec{a}_1^\mu \cdot \vec{\tau} \right) \ . \tag{A.49}$$

We can now consider a representation associated with the direct sum $S \oplus P$, which can be identified with

$$\Phi \equiv S + \mathrm{i}\, P \ , \tag{A.50}$$

taking account of scalar and pseudoscalar mesons. From Eqs. (A.23)-(A.30) we can verify the transformation laws for the different fields under axial and axial-vector transformations:

$$\Phi \xrightarrow{SU(2)_V} \mathcal{U}_V \Phi \mathcal{U}_V^\dagger \ , \quad \Phi \xrightarrow{SU(2)_A} \mathcal{U}_A \Phi \mathcal{U}_A \ , \quad \Phi \xrightarrow{U(1)_V} \mathcal{U}_V^0 \Phi \mathcal{U}_V^{0\,\dagger} \ , \quad \Phi \xrightarrow{U(1)_A} \mathcal{U}_A^0 \Phi \mathcal{U}_A{}^0 \ , \tag{A.51}$$

$$R^\mu \xrightarrow{SU(2)_V} \mathcal{U}_V R^\mu \mathcal{U}_V^\dagger \ , \quad L^\mu \xrightarrow{SU(2)_V} \mathcal{U}_V L^\mu \mathcal{U}_V^\dagger \ , \quad R^\mu \xrightarrow{U(1)_V} \mathcal{U}_V^0 R^\mu \mathcal{U}_V^{0\,\dagger} \ , \quad L^\mu \xrightarrow{U(1)_V} \mathcal{U}_V^0 L^\mu \mathcal{U}_V^{0\,\dagger} \ , \tag{A.52}$$

$$R^\mu \xrightarrow{SU(2)_A} \mathcal{U}_A R^\mu \mathcal{U}_A^\dagger \ , \quad L^\mu \xrightarrow{SU(2)_A} \mathcal{U}_A^\dagger L^\mu \mathcal{U}_A \ , \quad R^\mu \xrightarrow{U(1)_A} \mathcal{U}_A^0 R^\mu \mathcal{U}_A^{0\,\dagger} \ , \quad L^\mu \xrightarrow{U(1)_A} \mathcal{U}_A^{0\,\dagger} L^\mu \mathcal{U}_A^0 \ , \tag{A.53}$$

where we defined

$$R^\mu = V^\mu + A^\mu \ , \quad L^\mu = V^\mu - A^\mu \ , \tag{A.54}$$

$$\mathcal{U}_{V/A} = \exp\left(\frac{\mathrm{i}}{2} \vec{\alpha}_{V/A} \cdot \vec{\tau} \right) \in SU(2) \tag{A.55}$$

denotes an arbitrary element of $SU(2)$ (in the fundamental representation), and

$$\mathcal{U}_{V/A}^0 = \exp\left(\frac{\mathrm{i}}{2} \alpha_{V/A} \mathbf{1}_2 \right) \in U(1) \tag{A.56}$$

denotes an arbitrary element of $U(1)$ (in two-dimensional representation).
The representation associated with (A.50) is known as $[2, \overline{2}] \oplus [\overline{2}, 2]$ representation of $SU(2) \times SU(2)$. Similarly, matrix fields associated with the three-dimensional irreducible representations $[3, 1]$ and $[1, 3]$, respectively, are for instance given by

$$\mathcal{V}^\mu = \frac{1}{\sqrt{2}} \left(\vec{\rho}^\mu \cdot \vec{\tau} \right) \ , \quad \mathcal{A}^\mu = \frac{1}{\sqrt{2}} \left(\vec{a}_1^\mu \cdot \vec{\tau} \right) \ . \tag{A.57}$$

Appendix B

Brute-force algorithms for the construction of invariants

In this appendix we provide *Mathematica* notebooks implementing a straightforward construction of polynomial invariants for a given order. As example for a finite group we choose the representation $\Gamma^{(5)}(C_{4v})$, for which we already constructed the invariants from the projection operator method in Sec. 5.2. As example for a continuous group we choose $SU(2)_A \times SU(2)_V$ in the $[\bar{2},2] \oplus [2,\bar{2}]$ representation and consider infinitesimal $SU(2)_A$ transformations.
In contrast to output and comments, input is set in boldface.

B.1 Two-dimensional irreducible representation of C_{4v}

$$\boldsymbol{M_1} = \begin{pmatrix} 1 & 0 \\ 0 & 1 \end{pmatrix}$$
$$\boldsymbol{M_2} = \begin{pmatrix} 0 & -1 \\ 1 & 0 \end{pmatrix}$$
$$\boldsymbol{M_3} = \begin{pmatrix} -1 & 0 \\ 0 & -1 \end{pmatrix}$$
$$\boldsymbol{M_4} = \begin{pmatrix} 0 & 1 \\ -1 & 0 \end{pmatrix}$$
$$\boldsymbol{M_5} = \begin{pmatrix} 1 & 0 \\ 0 & -1 \end{pmatrix}$$
$$\boldsymbol{M_6} = \begin{pmatrix} -1 & 0 \\ 0 & 1 \end{pmatrix}$$
$$\boldsymbol{M_7} = \begin{pmatrix} 0 & -1 \\ -1 & 0 \end{pmatrix}$$
$$\boldsymbol{M_8} = \begin{pmatrix} 0 & 1 \\ 1 & 0 \end{pmatrix}$$

```
Do[vp_i = Dot[M_i, ( x )
                   ( y )], {i, 1, 8}]
Do[xp_i = vp_i[[1, 1]]; yp_i = vp_i[[2, 1]], {i, 1, 8}]

sys =
Table[a * x^2 + b * y^2 + c * x * y == a * xp_i^2 + b * yp_i^2 + c * xp_i * yp_i,
{i, 1, 8}]

SolveAlways[sys, {x, y}]
{{a → b, c → 0}}

sys = Table[a * x^4 + b * x^3 * y + c * x^2 * y^2 + d * x * y^3 + f * y^4 ==
a * xp_i^4 + b * xp_i^3 * yp_i + c * xp_i^2 * yp_i^2 + d * xp_i * yp_i^3 + f * yp_i^4,
{i, 1, 8}]

sol = SolveAlways[sys, {x, y}]
{{b → 0, d → 0, a → f}}
a * x^4 + b * x^3 * y + c * x^2 * y^2 + d * x * y^3 + f * y^4 /. sol
{f x^4 + c x^2 y^2 + f y^4}
```

B.2 Two-flavor linear sigma model

• Infinitesimal $SU(2)_A$ transformations are given by:

```
σp = σ + α1 * pi_1 + α2 * pi_2 + α3 * pi_3
pi1p = pi_1 - α1 * σ
pi2p = pi_2 - α2 * σ
pi3p = pi_3 - α3 * σ
ηp = η - α1 * a1 - α2 * a2 - α3 * a3
a1p = a1 + α1 * η
a2p = a2 + α2 * η
a3p = a3 + α3 * η
```

• Terms of order $\mathcal{O}(\vec{\alpha}^2)$ will be set to zero:

```
alsq = Expand[(α1 + α2 + α3)^2]
v1 = Table[alsq[[i]] / (alsq[[i]] /. {α1→1, α2→1, α3→1}) → 0, {i, 1, Length[alsq]}]
alsq = Expand[(α1 + α2 + α3)^3]
v2 = Table[alsq[[i]] / (alsq[[i]] /. {α1→1, α2→1, α3→1}) → 0, {i, 1, Length[alsq]}]
alsq = Expand[(α1 + α2 + α3)^4]
v3 = Table[alsq[[i]] / (alsq[[i]] /. {α1→1, α2→1, α3→1}) → 0, {i, 1, Length[alsq]}]
```

• Construction of the quartic invariants:

```
qua = Expand[(a1 + a2 + a3 + η + σ + pi_1 + pi_2 + pi_3)^4]

mon =
Table[
```

```
qua[[i]]/
(qua[[i]]/.{a1 → 1, a2 → 1, a3 → 1, η → 1, σ → 1,
 pi1 → 1, pi2 → 1, pi3 → 1}), {i, 1, Length[qua]}]

monp =
Table[FullSimplify[
Expand[
(qua[[i]]/.{a1 → a1p, a2 → a2p, a3 → a3p,
η → ηp, σ → σp, pi1 → pi1p, pi2 → pi2p,
 pi3 → pi3p})/
(qua[[i]]/.{a1 → 1, a2 → 1, a3 → 1, η → 1,
 σ → 1, pi1 → 1, pi2 → 1, pi3 → 1})] /.v1/.v2/.
v3], {i, 1, Length[qua]}]

Do[
eqj = Sum [Coefficient [ci * monp[[i]],
σ^Exponent[mon[[j]],σ] * pi1^Exponent[mon[[j]],pi1] *
pi2^Exponent[mon[[j]],pi2] * pi3^Exponent[mon[[j]],pi3] *
η^Exponent[mon[[j]],η] * a1^Exponent[mon[[j]],a1] *
a2^Exponent[mon[[j]],a2] * a3^Exponent[mon[[j]],a3]],
{i, 1, Length[monp]}]
, {j, 1, Length[mon]}]

sys = Table [eqi == ci, {i, 1, Length[mon]}]

solal = SolveAlways[sys, {α1, α2, α3}]

in = Expand [Sum [ci * mon[[i]]/.{solal[[1]]},
{i, 1, Length[mon]}]]
```

$$a1^4 c_{35} + 2a1^2 a2^2 c_{35} + a2^4 c_{35} + 2a1^2 a3^2 c_{35} + 2a2^2 a3^2 c_{35} + a3^4 c_{35} + 2a1^2 \eta^2 c_{35} + 2a2^2 \eta^2 c_{35} + 2a3^2 \eta^2 c_{35} + \eta^4 c_{35} - a1^2 \eta\sigma c_{229} - a2^2 \eta\sigma c_{229} - a3^2 \eta\sigma c_{229} - \eta^3 \sigma c_{229} + \eta^2 \sigma^2 c_{300} + a1^2 \sigma^2 c_{304} + a2^2 \sigma^2 c_{304} + a3^2 \sigma^2 c_{304} - \eta\sigma^3 c_{325} + \sigma^4 c_{330} + a1^3 c_{229} pi_1 + a1a2^2 c_{229} pi_1 + a1a3^2 c_{229} pi_1 + a1\eta^2 c_{229} pi_1 - 2a1\eta\sigma c_{300} pi_1 + 2a1\eta\sigma c_{304} pi_1 + a1\sigma^2 c_{325} pi_1 + a1^2 c_{300} pi_1^2 + a2^2 c_{304} pi_1^2 + a3^2 c_{304} pi_1^2 + \eta^2 c_{304} pi_1^2 - \eta\sigma c_{325} pi_1^2 + 2\sigma^2 c_{330} pi_1^2 + a1 c_{325} pi_1^3 + c_{330} pi_1^4 + a1^2 a2 c_{229} pi_2 + a2^3 c_{229} pi_2 + a2a3^2 c_{229} pi_2 + a2\eta^2 c_{229} pi_2 - 2a2\eta\sigma c_{300} pi_2 + 2a2\eta\sigma c_{304} pi_2 + a2\sigma^2 c_{325} pi_2 + 2a1a2 c_{300} pi_1 pi_2 - 2a1a2 c_{304} pi_1 pi_2 + a2 c_{325} pi_1^2 pi_2 + a2^2 c_{300} pi_2^2 + a1^2 c_{304} pi_2^2 + a3^2 c_{304} pi_2^2 + \eta^2 c_{304} pi_2^2 - \eta\sigma c_{325} pi_2^2 + 2\sigma^2 c_{330} pi_2^2 + a1 c_{325} pi_1 pi_2^2 + 2 c_{330} pi_1^2 pi_2^2 + a2 c_{325} pi_2^3 + c_{330} pi_2^4 + a1^2 a3 c_{229} pi_3 + a2^2 a3 c_{229} pi_3 + a3^3 c_{229} pi_3 + a3\eta^2 c_{229} pi_3 - 2a3\eta\sigma c_{300} pi_3 + 2a3\eta\sigma c_{304} pi_3 + a3\sigma^2 c_{325} pi_3 + 2a1a3 c_{300} pi_1 pi_3 - 2a1a3 c_{304} pi_1 pi_3 + a3 c_{325} pi_1^2 pi_3 + 2a2a3 c_{300} pi_2 pi_3 - 2a2a3 c_{304} pi_2 pi_3 + a3 c_{325} pi_2^2 pi_3 + a3^2 c_{300} pi_3^2 + a1^2 c_{304} pi_3^2 + a2^2 c_{304} pi_3^2 + \eta^2 c_{304} pi_3^2 - \eta\sigma c_{325} pi_3^2 + 2\sigma^2 c_{330} pi_3^2 + a1 c_{325} pi_1 pi_3^2 + 2 c_{330} pi_1^2 pi_3^2 + a2 c_{325} pi_2 pi_3^2 + 2 c_{330} pi_2^2 pi_3^2 + a3 c_{325} pi_3^3 + c_{330} pi_3^4$$

```
inv1 = Coefficient [in[[1]], c35]
```

$$a1^4 + 2a1^2 a2^2 + a2^4 + 2a1^2 a3^2 + 2a2^2 a3^2 + a3^4 + 2a1^2 \eta^2 + 2a2^2 \eta^2 + 2a3^2 \eta^2 + \eta^4$$

```
inv2 = Coefficient [in[[1]], c229]
```

$$-a1^2 \eta\sigma - a2^2 \eta\sigma - a3^2 \eta\sigma - \eta^3 \sigma + a1^3 pi_1 + a1a2^2 pi_1 + a1a3^2 pi_1 + a1\eta^2 pi_1 + a1^2 a2 pi_2 + a2^3 pi_2 + a2a3^2 pi_2 + a2\eta^2 pi_2 + a1^2 a3 pi_3 + a2^2 a3 pi_3 + a3^3 pi_3 + a3\eta^2 pi_3$$

```
inv3 = Coefficient [in[[1]], c300]
```

$\eta^2\sigma^2 - 2a1\eta\sigma pi_1 + a1^2 pi_1^2 - 2a2\eta\sigma pi_2 + 2a1a2 pi_1 pi_2 + a2^2 pi_2^2 - 2a3\eta\sigma pi_3 + 2a1a3 pi_1 pi_3 + 2a2a3 pi_2 pi_3 + a3^2 pi_3^2$

inv4 = Coefficient [in[[1]], c_{304}]

$a1^2\sigma^2 + a2^2\sigma^2 + a3^2\sigma^2 + 2a1\eta\sigma pi_1 + a2^2 pi_1^2 + a3^2 pi_1^2 + \eta^2 pi_1^2 + 2a2\eta\sigma pi_2 - 2a1a2 pi_1 pi_2 + a1^2 pi_2^2 + a3^2 pi_2^2 + \eta^2 pi_2^2 + 2a3\eta\sigma pi_3 - 2a1a3 pi_1 pi_3 - 2a2a3 pi_2 pi_3 + a1^2 pi_3^2 + a2^2 pi_3^2 + \eta^2 pi_3^2$

inv5 = Coefficient [in[[1]], c_{325}]

$-\eta\sigma^3 + a1\sigma^2 pi_1 - \eta\sigma pi_1^2 + a1 pi_1^3 + a2\sigma^2 pi_2 + a2 pi_1^2 pi_2 - \eta\sigma pi_2^2 + a1 pi_1 pi_2^2 + a2 pi_2^3 + a3\sigma^2 pi_3 + a3 pi_1^2 pi_3 + a3 pi_2^2 pi_3 - \eta\sigma pi_3^2 + a1 pi_1 pi_3^2 + a2 pi_2 pi_3^2 + a3 pi_3^3$

inv6 = Coefficient [in[[1]], c_{330}]

$\sigma^4 + 2\sigma^2 pi_1^2 + pi_1^4 + 2\sigma^2 pi_2^2 + 2 pi_1^2 pi_2^2 + pi_2^4 + 2\sigma^2 pi_3^2 + 2 pi_1^2 pi_3^2 + 2 pi_2^2 pi_3^2 + pi_3^4$

known1 = $\left(\sigma^2 + pi_1^2 + pi_2^2 + pi_3^2\right)$

known2 = $\left(\eta^2 + a1^2 + a2^2 + a3^2\right)$

known3 = $(\sigma * \eta - pi_1 * a1 - pi_2 * a2 - pi_3 * a3)^2$

known4 = $\sigma * \eta - pi_1 * a1 - pi_2 * a2 - pi_3 * a3$

FullSimplify[inv1]

$\left(a1^2 + a2^2 + a3^2 + \eta^2\right)^2$

FullSimplify[inv2]

$\left(a1^2 + a2^2 + a3^2 + \eta^2\right)(-\eta\sigma + a1 pi_1 + a2 pi_2 + a3 pi_3)$

FullSimplify[inv3]

$(-\eta\sigma + a1 pi_1 + a2 pi_2 + a3 pi_3)^2$

FullSimplify[inv4]

$\left(a1^2 + a2^2 + a3^2\right)\sigma^2 + \left(a2^2 + a3^2 + \eta^2\right) pi_1^2 + \left(a1^2 + a3^2 + \eta^2\right) pi_2^2 + 2a3\eta\sigma pi_3 + \left(a1^2 + a2^2 + \eta^2\right) pi_3^2 + 2a2 pi_2 (\eta\sigma - a3 pi_3) + 2a1 pi_1 (\eta\sigma - a2 pi_2 - a3 pi_3)$

SolveAlways[

c1 * known1^2 + c2 * known2^2 + c3 * known4^2+

c4 * known1 * known2 + c5 * known1 * known4+

c6 * known2 * known4 == inv4,

{$\sigma, \eta, pi_1, pi_2, pi_3$, a1, a2, a3}]

$\{\{c1 \to 0, c2 \to 0, c3 \to -1, c4 \to 1, c5 \to 0, c6 \to 0\}\}$

FullSimplify[−1 * known4^2 + 1 * known1 * known2 − inv4]

0

FullSimplify[inv5]

$-(\eta\sigma - a1 pi_1 - a2 pi_2 - a3 pi_3)\left(\sigma^2 + pi_1^2 + pi_2^2 + pi_3^2\right)$

FullSimplify[inv6]

$\left(\sigma^2 + pi_1^2 + pi_2^2 + pi_3^2\right)^2$

• Construction of the quadratic invariants:

qua = Expand $\left[(a1 + a2 + a3 + \eta + \sigma + pi_1 + pi_2 + pi_3)^2\right]$

```
mon =
Table[
qua[[i]]/
(qua[[i]]/.{a1 → 1, a2 → 1, a3 → 1, η → 1, σ → 1,
 pi1 → 1, pi2 → 1, pi3 → 1}), {i, 1, Length[qua]}]

monp =
Table[FullSimplify[
Expand[
(qua[[i]]/.{a1 → a1p, a2 → a2p, a3 → a3p,
η → ηp, σ → σp, pi1 → pi1p, pi2 → pi2p,
 pi3 → pi3p})/
(qua[[i]]/.{a1 → 1, a2 → 1, a3 → 1, η → 1,
 σ → 1, pi1 → 1, pi2 → 1, pi3 → 1})] /.v1/.v2/.
v3], {i, 1, Length[qua]}]

Do[
eqj = Sum [Coefficient [ci * monp[[i]],
σ^Exponent[mon[[j]],σ] * pi1^Exponent[mon[[j]],pi1] *
pi2^Exponent[mon[[j]],pi2] * pi3^Exponent[mon[[j]],pi3] *
η^Exponent[mon[[j]],η] * a1^Exponent[mon[[j]],a1] *
a2^Exponent[mon[[j]],a2] * a3^Exponent[mon[[j]],a3]],
{i, 1, Length[monp]}]
, {j, 1, Length[mon]}]

sys = Table [eqi == ci, {i, 1, Length[mon]}]

solal = SolveAlways[sys, {α1, α2, α3}]

in = Expand [Sum [ci * mon[[i]]/.{solal[[1]]},
{i, 1, Length[mon]}]]
{a1^2 c6 + a2^2 c6 + a3^2 c6 + η^2 c6 − ησ c31 + σ^2 c36 + a1 c31 pi1 + c36 pi1^2 + a2 c31 pi2 + c36 pi2^2 + a3 c31 pi3 + c36 pi3^2}

inv1 = Coefficient [in[[1]], c6]
a1^2 + a2^2 + a3^2 + η^2
inv2 = Coefficient [in[[1]], c36]
σ^2 + pi1^2 + pi2^2 + pi3^2
inv3 = Coefficient [in[[1]], c31]
−ησ + a1 pi1 + a2 pi2 + a3 pi3
```

Appendix C

Numerical methods

We basically use two independent numerical approaches for our calculations at finite temperature. Both are based on discretizing the field variable $x \equiv \varphi$ (in the usual terminology of differential equations we refer to it as spatial variable in the following, which should not be confused with the spatial dimension D) on a one-dimensional grid. The first one is based on approximating the spatial derivatives $U^{(n)}(\varphi) \equiv U(n)x$ by appropriate finite-difference formulas (usually 4th order turns out to be good enough, sometimes we use higher-order ones, however). In the following we refer to this method as *Finite-Difference Method*. We became aware of its practical use by the master thesis of Eirik Eik Svanes who kindly provides a *Mathlab* code within his work [149]. We decided to use this method, since it is well documented by Eirik Eik Svanes in his master thesis. Our implementation, however, is different. The second method is what we refer to as *Taylor Method*. It is described on page 5 in Ref. [156]. We thank Mario Mitter for pointing out this reference to us. We also want to thank him and Bernd-Jochen Schaefer for useful discussions about certain numerical details.
Applying either of the above methods yields a system of coupled ordinary differential equations in the RG scale k. We solve this systems using different versions of the Runge-Kutta method. Preferable is the Cash-Karp method with adaptive stepsize control (which is described in Ref. [157]). We also made good experiences with the built-in option IDA of *Mathematica's* NDSolve. All of the methods described can be implemented in *Mathematica*. We provide notebooks for the Finite-Difference Method as well as for the Taylor method. For both cases we choose the FRG-flow equation (in LPA) of the $U(2) \times U(2)$ model in the truncation (7.2).

C.1 Finite-Difference Method

```
T = 1576/10;
diff = 5;
sqxmin = 230;
amp = 4/240;
xmin = sqxmin^2;
```

$$\text{vv}[\text{x\_}] = \text{amp} * (x - \text{xmin})\text{^}2$$
$$\text{ww}[\text{x\_}] = \frac{13}{100}$$

$$\text{fv}[\text{k\_}, \varphi\_, \text{v\_}, \text{vx\_}, \text{vxx\_}, \text{w\_}, \text{wx\_}, \text{wxx\_}] =$$
$$\frac{k^4 \text{Coth}\left[\frac{\sqrt{k^2+2\text{vx}}}{2T}\right]}{3\pi^2\sqrt{k^2+2\text{vx}}} + \frac{k^4 \text{Coth}\left[\frac{\sqrt{k^2+2\text{vx}+2w\varphi}}{2T}\right]}{6\pi^2\sqrt{k^2+2\text{vx}+2w\varphi}} +$$
$$\frac{k^4 \text{Coth}\left[\frac{\sqrt{k^2+2\text{vx}+2\text{vxx}\varphi+w\varphi-\sqrt{(2\text{vxx}-w)^2\varphi^2}}}{2T}\right]}{12\pi^2\sqrt{k^2+2\text{vx}+2\text{vxx}\varphi+w\varphi-\sqrt{(2\text{vxx}-w)^2\varphi^2}}} +$$
$$\frac{k^4 \text{Coth}\left[\frac{\sqrt{k^2+2\text{vx}+2\text{vxx}\varphi+w\varphi+\sqrt{(2\text{vxx}-w)^2\varphi^2}}}{2T}\right]}{12\pi^2\sqrt{k^2+2\text{vx}+2\text{vxx}\varphi+w\varphi+\sqrt{(2\text{vxx}-w)^2\varphi^2}}};$$
$$\text{fw}[\text{k\_}, \varphi\_, \text{v\_}, \text{vx\_}, \text{vxx\_}, \text{w\_}, \text{wx\_}, \text{wxx\_}] =$$
$$\left(k^4 \text{Csch}\left[\frac{\sqrt{k^2+2\text{vx}}}{2T}\right]^3\right.$$
$$\left(\left(\left(2k^2 - 3T^2 + 4\text{vx}\right)w^2 + 2T^2\left(k^2 + 2\text{vx}\right)\text{wx}\right)\right.$$
$$\text{Cosh}\left[\frac{\sqrt{k^2+2\text{vx}}}{2T}\right] +$$
$$T\left(3w^2 - 2\left(k^2 + 2\text{vx}\right)\text{wx}\right)$$
$$\left(T\text{Cosh}\left[\frac{3\sqrt{k^2+2\text{vx}}}{2T}\right] +\right.$$
$$\left.\left.\left.2\sqrt{k^2 + 2\text{vx}}\text{Sinh}\left[\frac{\sqrt{k^2+2\text{vx}}}{2T}\right]\right)\right)\right)\Big/$$
$$\left(48\pi^2T^2\left(k^2 + 2\text{vx}\right)^{5/2}\right) -$$
$$\left(k^4(w + \text{wx}\varphi)\text{Csch}\left[\frac{\sqrt{k^2+2\text{vx}}}{2T}\right]^2\right.$$
$$\left.\left.\left(\sqrt{k^2 + 2\text{vx}} + T\text{Sinh}\left[\frac{\sqrt{k^2+2\text{vx}}}{T}\right]\right)\right)\right)\Big/$$
$$\left(12\pi^2T\left(k^2 + 2\text{vx}\right)^{3/2}\varphi\right) +$$
$$\left(k^4(w - \text{wx}\varphi)\text{Csch}\left[\frac{\sqrt{k^2+2\text{vx}+2w\varphi}}{2T}\right]^2\right.$$
$$\left.\left.\left(\sqrt{k^2 + 2(\text{vx} + w\varphi)} + T\text{Sinh}\left[\frac{\sqrt{k^2+2\text{vx}+2w\varphi}}{T}\right]\right)\right)\right)\Big/$$
$$\left(12\pi^2T\varphi\left(k^2 + 2(\text{vx} + w\varphi)\right)^{3/2}\right) +$$
$$\left(k^4\left(3w^2 + 4\text{wx}^2\varphi^2 - 5\text{wx}\sqrt{(-2\text{vxx} + w)^2\varphi^2} -\right.\right.$$
$$\text{wxx}\varphi\sqrt{(-2\text{vxx} + w)^2\varphi^2} + w\varphi(8\text{wx} - \text{wxx}\varphi) +$$
$$\left.2\text{vxx}(6w + \varphi(4\text{wx} + \text{wxx}\varphi))\right)$$
$$\text{Csch}\left[\frac{\sqrt{k^2+2\text{vx}+2\text{vxx}\varphi+w\varphi-\sqrt{(-2\text{vxx}+w)^2\varphi^2}}}{2T}\right]^2$$
$$\left(\sqrt{k^2 + 2\text{vx} + 2\text{vxx}\varphi + w\varphi - \sqrt{(-2\text{vxx} + w)^2\varphi^2}} +\right.$$
$$T$$
$$\text{Sinh}[$$
$$\left.\left.\frac{\sqrt{k^2+2\text{vx}+2\text{vxx}\varphi+w\varphi-\sqrt{(-2\text{vxx}+w)^2\varphi^2}}}{T}\right]\right)\Big/$$

$$\Big(24\pi^2 T\sqrt{(-2\text{vxx}+w)^2\varphi^2}$$
$$\Big(k^2+2\text{vx}+2\text{vxx}\varphi+w\varphi-\sqrt{(-2\text{vxx}+w)^2\varphi^2}\Big)^{3/2}\Big)-$$
$$\Big(k^4\Big(3w^2+4\text{wx}^2\varphi^2+5\text{wx}\sqrt{(-2\text{vxx}+w)^2\varphi^2}+$$
$$\text{wxx}\varphi\sqrt{(-2\text{vxx}+w)^2\varphi^2}+w\varphi(8\text{wx}-\text{wxx}\varphi)+$$
$$2\text{vxx}(6w+\varphi(4\text{wx}+\text{wxx}\varphi))\Big)$$
$$\text{Csch}\left[\frac{\sqrt{k^2+2\text{vx}+2\text{vxx}\varphi+w\varphi+\sqrt{(-2\text{vxx}+w)^2\varphi^2}}}{2T}\right]^2$$
$$\Big(\sqrt{k^2+2\text{vx}+2\text{vxx}\varphi+w\varphi+\sqrt{(-2\text{vxx}+w)^2\varphi^2}}+$$
$$T$$
$$\text{Sinh}\Big[$$
$$\frac{\sqrt{k^2+2\text{vx}+2\text{vxx}\varphi+w\varphi+\sqrt{(-2\text{vxx}+w)^2\varphi^2}}}{T}\Big]\Big)\Big)\Big/$$
$$\Big(24\pi^2 T\sqrt{(-2\text{vxx}+w)^2\varphi^2}$$
$$\Big(k^2+2\text{vx}+2\text{vxx}\varphi+w\varphi+\sqrt{(-2\text{vxx}+w)^2\varphi^2}\Big)^{3/2}\Big);$$

kL = 500;
kR = 5;

nx = 180;
nfine = 80;
dx = $\frac{3*\text{xmin}-x_{\text{nfine}}}{\text{nx}-1}$;
Do$\left[x_i = \left(\frac{1}{10}\right)\text{^}2 + (i-1)\text{^}2, \{i, 1, \text{nfine}\}\right]$
Do[
$x_{i+1} = x_i + \text{dx}$
, $\{i, \text{nfine}, \text{nx}-1, 1\}$]

grid:=Table$[x_j, \{j, 1, \text{nx}\}]$

(*FiniteDifferenceFormulaforspatialderivativesvx,
vxxatthespatialgridpoints*)

vhelp[k_] = Table$[v_j[k], \{j, 1, \text{nx}\}]$;
(* derivatives for left boundary and middle points *)
D1v = NDSolve`FiniteDifferenceDerivative[1, grid,
vhelp[k], "DifferenceOrder" → diff];
D2v = NDSolve`FiniteDifferenceDerivative[2, grid,
vhelp[k], "DifferenceOrder" → diff];
(*computeboundaryconditions,
note : D1[[nx]]islastpoint*)

```
Do[vx_j = D1v[[j]], {j, 1, nx}];
Do[vxx_j = D2v[[j]], {j, 1, nx}];

whelp[k_] = Table[w_j[k], {j, 1, nx}];
(* derivatives for left boundary and middle points *)
D1w = NDSolve`FiniteDifferenceDerivative[1, grid,
whelp[k], "DifferenceOrder" → diff];
D2w = NDSolve`FiniteDifferenceDerivative[2, grid,
whelp[k], "DifferenceOrder" → diff];
(*computeboundaryconditions,
note : D1[[nx]]islastpoint*)
Do[wx_j = D1w[[j]], {j, 1, nx}];
Do[wxx_j = D2w[[j]], {j, 1, nx}];

sys =
Join[
Table[D[v_j[k], k] == fv[k, x_j, v_j[k], vx_j, vxx_j,
 w_j[k], wx_j, wxx_j], {j, 1, nx}],
Table[D[w_j[k], k] == fw[k, x_j, v_j[k], vx_j, vxx_j,
 w_j[k], wx_j, wxx_j], {j, 1, nx}]];

initc = Join[Table[v_j[kL] == vv[x_j], {j, 1, nx}],
 Table[w_j[kL] == ww[x_j], {j, 1, nx}]];

sysin = Join[sys, initc];
vars = Join[Table[v_j, {j, 1, nx}], Table[w_j, {j, 1, nx}]]

sol = NDSolve[sysin, vars, {k, kL, kR}]

ListPlot[Table[{√x_j, Re[sol[[1, j, 2]][t]]}, {j, 1, 39}] /. t → 16, PlotStyle → Black]
```

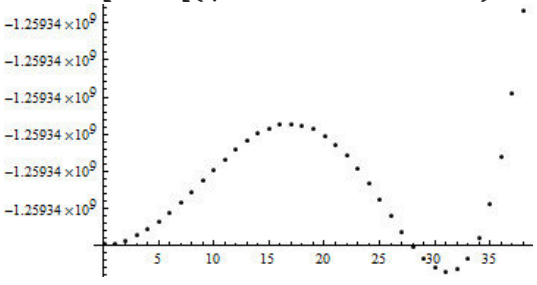

C.2 Taylor Method

```
T = 1576/10;
```

$$\mathrm{fv}[\mathrm{k\_}, \varphi\_, \mathrm{v\_}, \mathrm{vx\_}, \mathrm{vxx\_}, \mathrm{w\_}, \mathrm{wx\_}, \mathrm{wxx\_}] =$$
$$\frac{k^4 \mathrm{Coth}\left[\frac{\sqrt{k^2+2\mathrm{vx}}}{2T}\right]}{3\pi^2\sqrt{k^2+2\mathrm{vx}}} + \frac{k^4 \mathrm{Coth}\left[\frac{\sqrt{k^2+2\mathrm{vx}+2w\varphi}}{2T}\right]}{6\pi^2\sqrt{k^2+2\mathrm{vx}+2w\varphi}} +$$
$$\frac{k^4 \mathrm{Coth}\left[\frac{\sqrt{k^2+2\mathrm{vx}+2\mathrm{vxx}\varphi+w\varphi-\sqrt{(2\mathrm{vxx}-w)^2\varphi^2}}}{2T}\right]}{12\pi^2\sqrt{k^2+2\mathrm{vx}+2\mathrm{vxx}\varphi+w\varphi-\sqrt{(2\mathrm{vxx}-w)^2\varphi^2}}} +$$
$$\frac{k^4 \mathrm{Coth}\left[\frac{\sqrt{k^2+2\mathrm{vx}+2\mathrm{vxx}\varphi+w\varphi+\sqrt{(2\mathrm{vxx}-w)^2\varphi^2}}}{2T}\right]}{12\pi^2\sqrt{k^2+2\mathrm{vx}+2\mathrm{vxx}\varphi+w\varphi+\sqrt{(2\mathrm{vxx}-w)^2\varphi^2}}};$$
$$\mathrm{fw}[\mathrm{k\_}, \varphi\_, \mathrm{v\_}, \mathrm{vx\_}, \mathrm{vxx\_}, \mathrm{w\_}, \mathrm{wx\_}, \mathrm{wxx\_}] =$$
$$\left(k^4 \mathrm{Csch}\left[\frac{\sqrt{k^2+2\mathrm{vx}}}{2T}\right]^3\right.$$
$$\left(\left(\left(2k^2 - 3T^2 + 4\mathrm{vx}\right)w^2 + 2T^2\left(k^2 + 2\mathrm{vx}\right)\mathrm{wx}\right)\right.$$
$$\mathrm{Cosh}\left[\frac{\sqrt{k^2+2\mathrm{vx}}}{2T}\right] +$$
$$T\left(3w^2 - 2\left(k^2 + 2\mathrm{vx}\right)\mathrm{wx}\right)$$
$$\left(T\mathrm{Cosh}\left[\frac{3\sqrt{k^2+2\mathrm{vx}}}{2T}\right] +\right.$$
$$\left.\left.\left.2\sqrt{k^2 + 2\mathrm{vx}}\mathrm{Sinh}\left[\frac{\sqrt{k^2+2\mathrm{vx}}}{2T}\right]\right)\right)\right)\Big/$$
$$\left(48\pi^2T^2\left(k^2 + 2\mathrm{vx}\right)^{5/2}\right) -$$
$$\left(k^4(w + \mathrm{wx}\varphi)\mathrm{Csch}\left[\frac{\sqrt{k^2+2\mathrm{vx}}}{2T}\right]^2\right.$$
$$\left.\left(\sqrt{k^2 + 2\mathrm{vx}} + T\mathrm{Sinh}\left[\frac{\sqrt{k^2+2\mathrm{vx}}}{T}\right]\right)\right)\Big/$$
$$\left(12\pi^2T\left(k^2 + 2\mathrm{vx}\right)^{3/2}\varphi\right) +$$
$$\left(k^4(w - \mathrm{wx}\varphi)\mathrm{Csch}\left[\frac{\sqrt{k^2+2\mathrm{vx}+2w\varphi}}{2T}\right]^2\right.$$
$$\left.\left(\sqrt{k^2 + 2(\mathrm{vx} + w\varphi)} + T\mathrm{Sinh}\left[\frac{\sqrt{k^2+2\mathrm{vx}+2w\varphi}}{T}\right]\right)\right)\Big/$$
$$\left(12\pi^2T\varphi\left(k^2 + 2(\mathrm{vx} + w\varphi)\right)^{3/2}\right) +$$
$$\left(k^4\left(3w^2 + 4\mathrm{wx}^2\varphi^2 - 5\mathrm{wx}\sqrt{(-2\mathrm{vxx} + w)^2\varphi^2} -\right.\right.$$
$$\mathrm{wxx}\varphi\sqrt{(-2\mathrm{vxx} + w)^2\varphi^2} + w\varphi(8\mathrm{wx} - \mathrm{wxx}\varphi) +$$
$$2\mathrm{vxx}(6w + \varphi(4\mathrm{wx} + \mathrm{wxx}\varphi)))$$
$$\mathrm{Csch}\left[\frac{\sqrt{k^2+2\mathrm{vx}+2\mathrm{vxx}\varphi+w\varphi-\sqrt{(-2\mathrm{vxx}+w)^2\varphi^2}}}{2T}\right]^2$$
$$\left(\sqrt{k^2 + 2\mathrm{vx} + 2\mathrm{vxx}\varphi + w\varphi - \sqrt{(-2\mathrm{vxx} + w)^2\varphi^2}} +\right.$$
$$T$$
$$\mathrm{Sinh}[$$
$$\left.\left.\frac{\sqrt{k^2+2\mathrm{vx}+2\mathrm{vxx}\varphi+w\varphi-\sqrt{(-2\mathrm{vxx}+w)^2\varphi^2}}}{T}\right]\right)\Big/$$
$$\left(24\pi^2T\sqrt{(-2\mathrm{vxx} + w)^2\varphi^2}\right.$$
$$\left.\left(k^2 + 2\mathrm{vx} + 2\mathrm{vxx}\varphi + w\varphi - \sqrt{(-2\mathrm{vxx} + w)^2\varphi^2}\right)^{3/2}\right) -$$
$$\left(k^4\left(3w^2 + 4\mathrm{wx}^2\varphi^2 + 5\mathrm{wx}\sqrt{(-2\mathrm{vxx} + w)^2\varphi^2} +\right.\right.$$
$$\mathrm{wxx}\varphi\sqrt{(-2\mathrm{vxx} + w)^2\varphi^2} + w\varphi(8\mathrm{wx} - \mathrm{wxx}\varphi) +$$

$$2\text{vxx}(6w+\varphi(4\text{wx}+\text{wxx}\varphi)))$$
$$\text{Csch}\left[\frac{\sqrt{k^2+2\text{vx}+2\text{vxx}\varphi+w\varphi+\sqrt{(-2\text{vxx}+w)^2\varphi^2}}}{2T}\right]^2$$
$$\left(\sqrt{k^2+2\text{vx}+2\text{vxx}\varphi+w\varphi+\sqrt{(-2\text{vxx}+w)^2\varphi^2}}+\right.$$
$$T$$
$$\left.\text{Sinh}\left[\frac{\sqrt{k^2+2\text{vx}+2\text{vxx}\varphi+w\varphi+\sqrt{(-2\text{vxx}+w)^2\varphi^2}}}{T}\right]\right)\Big/$$
$$\left(24\pi^2T\sqrt{(-2\text{vxx}+w)^2\varphi^2}\right.$$
$$\left.\left(k^2+2\text{vx}+2\text{vxx}\varphi+w\varphi+\sqrt{(-2\text{vxx}+w)^2\varphi^2}\right)^{3/2}\right);$$

$$\text{nx} = 22;$$

$$\text{Do}\left[x_i = \left(\frac{1}{10}\right)\text{^}2+\left(\frac{1950}{100}*(i-1)\right)\text{^}2,\{i,1,\text{nx}\}\right];$$

$$\text{list1} =$$
$$\text{Table}\left[\text{vp}_i+\text{vpp}_i*\frac{x_{i+1}-x_i}{2.}+\text{vppp}_i*\frac{(x_{i+1}-x_i)\text{^}2}{8.}+\right.$$
$$\left.\text{vpppp}_i*\frac{(x_{i+1}-x_i)\text{^}3}{48.}==\right.$$
$$\text{vp}_{i+1}-\text{vpp}_{i+1}*\frac{x_{i+1}-x_i}{2.}+\text{vppp}_{i+1}*\frac{(x_{i+1}-x_i)\text{^}2}{8.}-$$
$$\left.\text{vpppp}_{i+1}*\frac{(x_{i+1}-x_i)\text{^}3}{48.},\{i,1,\text{nx}-1\}\right];$$
$$\text{list2} = \text{Table}\left[\text{vpp}_i+\text{vppp}_i*\frac{x_{i+1}-x_i}{2.}+\text{vpppp}_i*\frac{(x_{i+1}-x_i)\text{^}2}{8.}==\right.$$
$$\left.\text{vpp}_{i+1}-\text{vppp}_{i+1}*\frac{x_{i+1}-x_i}{2.}+\text{vpppp}_{i+1}*\frac{(x_{i+1}-x_i)\text{^}2}{8.},\right.$$
$$\{i,1,\text{nx}-1\}];$$
$$\text{list3} = \left\{\text{vppp}_1+\text{vpppp}_1*\frac{x_2-x_1}{2.}==\text{vppp}_2+\text{vpppp}_2*\frac{x_1-x_2}{2.},\right.$$
$$\text{vppp}_{\text{nx}-1}+\text{vpppp}_{\text{nx}-1}*\frac{x_{\text{nx}}-x_{\text{nx}-1}}{2.}==$$
$$\left.\text{vppp}_{\text{nx}}+\text{vpppp}_{\text{nx}}*\frac{x_{\text{nx}-1}-x_{\text{nx}}}{2.}\right\};$$
$$\text{alg} = \text{Join}[\text{list1},\text{list2},\text{list3}];$$
$$\text{va} = \text{Join}\left[\text{Table}\left[\text{vppp}_i,\{i,1,\text{nx}\}\right],\right.$$
$$\left.\text{Table}\left[\text{vpppp}_i,\{i,1,\text{nx}\}\right]\right];$$
$$\text{truncv} = \text{Solve}[\text{alg},\text{va}][[1]];$$

$$\text{list1} =$$
$$\text{Table}\left[\text{wp}_i+\text{wpp}_i*\frac{x_{i+1}-x_i}{2.}+\text{wppp}_i*\frac{(x_{i+1}-x_i)\text{^}2}{8.}+\right.$$
$$\left.\text{wpppp}_i*\frac{(x_{i+1}-x_i)\text{^}3}{48.}==\right.$$
$$\text{wp}_{i+1}-\text{wpp}_{i+1}*\frac{x_{i+1}-x_i}{2.}+\text{wppp}_{i+1}*\frac{(x_{i+1}-x_i)\text{^}2}{8.}-$$
$$\left.\text{wpppp}_{i+1}*\frac{(x_{i+1}-x_i)\text{^}3}{48.},\{i,1,\text{nx}-1\}\right];$$
$$\text{list2} = \text{Table}\left[\text{wpp}_i+\text{wppp}_i*\frac{x_{i+1}-x_i}{2.}+\text{wpppp}_i*\frac{(x_{i+1}-x_i)\text{^}2}{8.}==\right.$$
$$\left.\text{wpp}_{i+1}-\text{wppp}_{i+1}*\frac{x_{i+1}-x_i}{2.}+\text{wpppp}_{i+1}*\frac{(x_{i+1}-x_i)\text{^}2}{8.},\right.$$
$$\{i,1,\text{nx}-1\}];$$

```
list3 = {wppp1 + wpppp1 * (x2 - x1)/2. == wppp2 + wpppp2 * (x1 - x2)/2.,
wpppnx-1 + wppppnx-1 * (xnx - xnx-1)/2. ==
 wpppnx + wppppnx * (xnx-1 - xnx)/2.};
alg = Join[list1, list2, list3];
wa = Join[Table[wpppi, {i, 1, nx}],
 Table[wppppi, {i, 1, nx}]];
truncw = Solve[alg, wa][[1]];


trunc = Join[truncv, truncw]


Do[fj = fv[k, xj, vj, vpj, vppj, wj, wpj, wppj], {j, 1, nx}];


Do[
fj+nx =
(D[fv[k, x, v[x], v'[x], v"[x], w[x], w'[x], w"[x]],
x]/.{v[x] → vj, v'[x] → vpj, v"[x] → vppj,
v(3)[x] → vpppj, v(4)[x] → vppppj, w[x] → wj,
w'[x] → wpj, w"[x] → wppj, w(3)[x] → wpppj,
 w(4)[x] → wppppj, x → xj}) /.trunc, {j, 1, nx}];

Do[
fj+2*nx =
(D[D[fv[k, x, v[x], v'[x], v"[x], w[x], w'[x],
w"[x]], x], x]/.
{v[x] → vj, v'[x] → vpj, v"[x] → vppj,
v(3)[x] → vpppj, v(4)[x] → vppppj, w[x] → wj,
w'[x] → wpj, w"[x] → wppj, w(3)[x] → wpppj,
 w(4)[x] → wppppj, x → xj}) /.trunc, {j, 1, nx}];

(*f1 = D[v1, s], ..., fnx = D[vnx, s], fnx+1 = D[vp1, s], ...,
f2nx = D[vpnx, s], f2nx+1 = D[vpp1, s], ..., f3nx = D[vppnx, s]*)

Do[fj+3*nx = fw[k, xj, vj, vpj, vppj, wj, wpj, wppj],
{j, 1, nx}];


Do[
fj+4*nx =
(D[fw[k, x, v[x], v'[x], v"[x], w[x], w'[x], w"[x]],
x]/.{v[x] → vj, v'[x] → vpj, v"[x] → vppj,
```

```
v^(3)[x] → vppp_j, v^(4)[x] → vpppp_j, w[x] → w_j,
w'[x] → wp_j, w"[x] → wpp_j, w^(3)[x] → wppp_j,
 w^(4)[x] → wpppp_j, x → x_j}) /.trunc, {j, 1, nx}];

Do[
f_(j+5*nx) =
(D[D[fw[k, x, v[x], v'[x], v"[x], w[x], w'[x],
w"[x]], x], x]/.
{v[x] → v_j, v'[x] → vp_j, v"[x] → vpp_j,
v^(3)[x] → vppp_j, v^(4)[x] → vpppp_j, w[x] → w_j,
w'[x] → wp_j, w"[x] → wpp_j, w^(3)[x] → wppp_j,
 w^(4)[x] → wpppp_j, x → x_j}) /.trunc, {j, 1, nx}];

(*f_(3nx+1) = D[w1, s], ..., f_(4nx) = D[wnx, s], f_(4nx+1) = D[wp1, s], ...,
f_(5nx) = D[wpnx, s], f_(5nx+1) = D[wpp1, s], ..., f_(6nx) = D[wppnx, s]*)


(*Cash – KarpCoefficients : *)

a2 = 1/5; a3 = 3/10; a4 = 3/5; a5 = 1; a6 = 7/8;
b21 = 1/5; b31 = 3/40; b41 = 3/10; b51 = -11/54;
b61 = 1631/55296; b32 = 9/40; b42 = -9/10; b52 = 5/2;
b62 = 175/512; b43 = 6/5; b53 = -70/27; b63 = 575/13824;
b54 = 35/27; b64 = 44275/110592; b65 = 253/4096; c1 = 37/378;
c2 = 0; c3 = 250/621; c4 = 125/594; c5 = 0; c6 = 512/1771;
cS1 = 2825/27648; cS2 = 0; cS3 = 18575/48384; cS4 = 13525/55296
cS5 = 277/14336; cS6 = 1/4;


helpp = Join[Table[v[j, i + 1], {j, 1, nx}],
Table[vp[j, i + 1], {j, 1, nx}],
Table[vpp[j, i + 1], {j, 1, nx}],
Table[w[j, i + 1], {j, 1, nx}],
Table[wp[j, i + 1], {j, 1, nx}],
Table[wpp[j, i + 1], {j, 1, nx}]]

help = Join[Table[v[j, i], {j, 1, nx}],
Table[vp[j, i], {j, 1, nx}], Table[vpp[j, i], {j, 1, nx}],
Table[w[j, i], {j, 1, nx}], Table[wp[j, i], {j, 1, nx}],
Table[wpp[j, i], {j, 1, nx}]]

helppS = Join[Table[vS[j, i + 1], {j, 1, nx}],
Table[vpS[j, i + 1], {j, 1, nx}],
```

```
Table[vppS[j, i + 1], {j, 1, nx}],
Table[wS[j, i + 1], {j, 1, nx}],
Table[wpS[j, i + 1], {j, 1, nx}],
Table[wppS[j, i + 1], {j, 1, nx}]]


vv[x_] = 4/240 * (x - 230^2)^2;
vvx[x_] = D[vv[x], x];
vvxx[x_] = D[vvx[x], x];
Do[v[j, 1] = vv[x_j], {j, 1, nx}];
Do[vp[j, 1] = vvx[x_j], {j, 1, nx}];
Do[vpp[j, 1] = vvxx[x_j], {j, 1, nx}];


ww[x_] = 13/100;
wwx[x_] = D[ww[x], x];
wwxx[x_] = D[wwx[x], x];
Do[w[j, 1] = ww[x_j], {j, 1, nx}];
Do[wp[j, 1] = wwx[x_j], {j, 1, nx}];
Do[wpp[j, 1] = wwxx[x_j], {j, 1, nx}];

adaptivestepsizeCashKarp :

Join[{k}, Table[v_j, {j, 1, nx}], Table[vp_j, {j, 1, nx}],
Table[vpp_j, {j, 1, nx}], Table[w_j, {j, 1, nx}],
Table[wp_j, {j, 1, nx}], Table[wpp_j, {j, 1, nx}]]
Withorwithout(dependsonwhichblockcommentedout)
Adaptivestep - size, takeonlyv, vp, vpp,
wforerrorintoaccount :

eps = 8

kh_1 = 500
h = -0.05


com = Join[{{k, _Real}}, Table[{v_j, _Real}, {j, 1, nx}],
Table[{vp_j, _Real}, {j, 1, nx}],
Table[{vpp_j, _Real}, {j, 1, nx}],
Table[{w_j, _Real}, {j, 1, nx}],
Table[{wp_j, _Real}, {j, 1, nx}],
Table[{wpp_j, _Real}, {j, 1, nx}]]
```

```
Do[fcp_j = Compile[Evaluate[com], Evaluate[f_j]],
{j, 1, 6 * nx}]

i = 1
Do[
k = kh_i; Do[v_j = v[j, i], {j, 1, nx}];
Do[vp_j = vp[j, i], {j, 1, nx}];
Do[vpp_j = vpp[j, i], {j, 1, nx}];
Do[w_j = w[j, i], {j, 1, nx}]; Do[wp_j = wp[j, i], {j, 1, nx}];
Do[wpp_j = wpp[j, i], {j, 1, nx}];
Do[
k1_j = h * fcp_j[k, v_1, v_2, v_3, v_4, v_5, v_6, v_7, v_8, v_9,
v_10, v_11, v_12, v_13, v_14, v_15, v_16, v_17, v_18, v_19, v_20,
v_21, v_22, vp_1, vp_2, vp_3, vp_4, vp_5, vp_6, vp_7, vp_8,
vp_9, vp_10, vp_11, vp_12, vp_13, vp_14, vp_15, vp_16, vp_17,
vp_18, vp_19, vp_20, vp_21, vp_22, vpp_1, vpp_2, vpp_3,
vpp_4, vpp_5, vpp_6, vpp_7, vpp_8, vpp_9, vpp_10, vpp_11,
vpp_12, vpp_13, vpp_14, vpp_15, vpp_16, vpp_17, vpp_18,
vpp_19, vpp_20, vpp_21, vpp_22, w_1, w_2, w_3, w_4, w_5, w_6,
w_7, w_8, w_9, w_10, w_11, w_12, w_13, w_14, w_15, w_16, w_17, w_18,
w_19, w_20, w_21, w_22, wp_1, wp_2, wp_3, wp_4, wp_5, wp_6, wp_7,
wp_8, wp_9, wp_10, wp_11, wp_12, wp_13, wp_14, wp_15, wp_16,
wp_17, wp_18, wp_19, wp_20, wp_21, wp_22, wpp_1, wpp_2, wpp_3,
wpp_4, wpp_5, wpp_6, wpp_7, wpp_8, wpp_9, wpp_10, wpp_11,
wpp_12, wpp_13, wpp_14, wpp_15, wpp_16, wpp_17, wpp_18,
 wpp_19, wpp_20, wpp_21, wpp_22], {j, 1, 6 * nx}];
k = kh_i + a2 * h; Do[v_j = v[j, i] + b21 * k1_j, {j, 1, nx}];
Do[vp_j = vp[j, i] + b21 * k1_{j+nx}, {j, 1, nx}];
Do[vpp_j = vpp[j, i] + b21 * k1_{j+2*nx}, {j, 1, nx}];
Do[w_j = w[j, i] + b21 * k1_{j+3*nx}, {j, 1, nx}];
Do[wp_j = wp[j, i] + b21 * k1_{j+4*nx}, {j, 1, nx}];
Do[wpp_j = wpp[j, i] + b21 * k1_{j+5*nx}, {j, 1, nx}];
Do[
k2_j = h * fcp_j[k, v_1, v_2, v_3, v_4, v_5, v_6, v_7, v_8, v_9,
v_10, v_11, v_12, v_13, v_14, v_15, v_16, v_17, v_18, v_19, v_20,
v_21, v_22, vp_1, vp_2, vp_3, vp_4, vp_5, vp_6, vp_7, vp_8,
vp_9, vp_10, vp_11, vp_12, vp_13, vp_14, vp_15, vp_16, vp_17,
vp_18, vp_19, vp_20, vp_21, vp_22, vpp_1, vpp_2, vpp_3,
vpp_4, vpp_5, vpp_6, vpp_7, vpp_8, vpp_9, vpp_10, vpp_11,
vpp_12, vpp_13, vpp_14, vpp_15, vpp_16, vpp_17, vpp_18,
vpp_19, vpp_20, vpp_21, vpp_22, w_1, w_2, w_3, w_4, w_5, w_6,
w_7, w_8, w_9, w_10, w_11, w_12, w_13, w_14, w_15, w_16, w_17, w_18,
w_19, w_20, w_21, w_22, wp_1, wp_2, wp_3, wp_4, wp_5, wp_6, wp_7,
```

$$\mathrm{wp}_8, \mathrm{wp}_9, \mathrm{wp}_{10}, \mathrm{wp}_{11}, \mathrm{wp}_{12}, \mathrm{wp}_{13}, \mathrm{wp}_{14}, \mathrm{wp}_{15}, \mathrm{wp}_{16},$$
$$\mathrm{wp}_{17}, \mathrm{wp}_{18}, \mathrm{wp}_{19}, \mathrm{wp}_{20}, \mathrm{wp}_{21}, \mathrm{wp}_{22}, \mathrm{wpp}_1, \mathrm{wpp}_2, \mathrm{wpp}_3,$$
$$\mathrm{wpp}_4, \mathrm{wpp}_5, \mathrm{wpp}_6, \mathrm{wpp}_7, \mathrm{wpp}_8, \mathrm{wpp}_9, \mathrm{wpp}_{10}, \mathrm{wpp}_{11},$$
$$\mathrm{wpp}_{12}, \mathrm{wpp}_{13}, \mathrm{wpp}_{14}, \mathrm{wpp}_{15}, \mathrm{wpp}_{16}, \mathrm{wpp}_{17}, \mathrm{wpp}_{18},$$
$$\mathrm{wpp}_{19}, \mathrm{wpp}_{20}, \mathrm{wpp}_{21}, \mathrm{wpp}_{22}], \{j, 1, 6 * \mathrm{nx}\}];$$
$$k = \mathrm{kh}_i + \mathrm{a3} * h; \mathrm{Do}[v_j = v[j, i] + \mathrm{b31} * \mathrm{k1}_j + \mathrm{b32} * \mathrm{k2}_j,$$
$$\{j, 1, \mathrm{nx}\}]; \mathrm{Do}[\mathrm{vp}_j = \mathrm{vp}[j, i] + \mathrm{b31} * \mathrm{k1}_{j+\mathrm{nx}} + \mathrm{b32} * \mathrm{k2}_{j+\mathrm{nx}},$$
$$\{j, 1, \mathrm{nx}\}];$$
$$\mathrm{Do}[\mathrm{vpp}_j = \mathrm{vpp}[j, i] + \mathrm{b31} * \mathrm{k1}_{j+2*\mathrm{nx}} + \mathrm{b32} * \mathrm{k2}_{j+2*\mathrm{nx}}, \{j, 1, \mathrm{nx}\}];$$
$$\mathrm{Do}[w_j = w[j, i] + \mathrm{b31} * \mathrm{k1}_{j+3*\mathrm{nx}} + \mathrm{b32} * \mathrm{k2}_{j+3*\mathrm{nx}}, \{j, 1, \mathrm{nx}\}];$$
$$\mathrm{Do}[\mathrm{wp}_j = \mathrm{wp}[j, i] + \mathrm{b31} * \mathrm{k1}_{j+4*\mathrm{nx}} + \mathrm{b32} * \mathrm{k2}_{j+4*\mathrm{nx}}, \{j, 1, \mathrm{nx}\}];$$
$$\mathrm{Do}[\mathrm{wpp}_j = \mathrm{wpp}[j, i] + \mathrm{b31} * \mathrm{k1}_{j+5*\mathrm{nx}} + \mathrm{b32} * \mathrm{k2}_{j+5*\mathrm{nx}}, \{j, 1, \mathrm{nx}\}];$$
$$\mathrm{Do}[$$
$$\mathrm{k3}_j = h * \mathrm{fcp}_j [k, v_1, v_2, v_3, v_4, v_5, v_6, v_7, v_8, v_9,$$
$$v_{10}, v_{11}, v_{12}, v_{13}, v_{14}, v_{15}, v_{16}, v_{17}, v_{18}, v_{19}, v_{20},$$
$$v_{21}, v_{22}, \mathrm{vp}_1, \mathrm{vp}_2, \mathrm{vp}_3, \mathrm{vp}_4, \mathrm{vp}_5, \mathrm{vp}_6, \mathrm{vp}_7, \mathrm{vp}_8,$$
$$\mathrm{vp}_9, \mathrm{vp}_{10}, \mathrm{vp}_{11}, \mathrm{vp}_{12}, \mathrm{vp}_{13}, \mathrm{vp}_{14}, \mathrm{vp}_{15}, \mathrm{vp}_{16}, \mathrm{vp}_{17},$$
$$\mathrm{vp}_{18}, \mathrm{vp}_{19}, \mathrm{vp}_{20}, \mathrm{vp}_{21}, \mathrm{vp}_{22}, \mathrm{vpp}_1, \mathrm{vpp}_2, \mathrm{vpp}_3,$$
$$\mathrm{vpp}_4, \mathrm{vpp}_5, \mathrm{vpp}_6, \mathrm{vpp}_7, \mathrm{vpp}_8, \mathrm{vpp}_9, \mathrm{vpp}_{10}, \mathrm{vpp}_{11},$$
$$\mathrm{vpp}_{12}, \mathrm{vpp}_{13}, \mathrm{vpp}_{14}, \mathrm{vpp}_{15}, \mathrm{vpp}_{16}, \mathrm{vpp}_{17}, \mathrm{vpp}_{18},$$
$$\mathrm{vpp}_{19}, \mathrm{vpp}_{20}, \mathrm{vpp}_{21}, \mathrm{vpp}_{22}, w_1, w_2, w_3, w_4, w_5, w_6,$$
$$w_7, w_8, w_9, w_{10}, w_{11}, w_{12}, w_{13}, w_{14}, w_{15}, w_{16}, w_{17}, w_{18},$$
$$w_{19}, w_{20}, w_{21}, w_{22}, \mathrm{wp}_1, \mathrm{wp}_2, \mathrm{wp}_3, \mathrm{wp}_4, \mathrm{wp}_5, \mathrm{wp}_6, \mathrm{wp}_7,$$
$$\mathrm{wp}_8, \mathrm{wp}_9, \mathrm{wp}_{10}, \mathrm{wp}_{11}, \mathrm{wp}_{12}, \mathrm{wp}_{13}, \mathrm{wp}_{14}, \mathrm{wp}_{15}, \mathrm{wp}_{16},$$
$$\mathrm{wp}_{17}, \mathrm{wp}_{18}, \mathrm{wp}_{19}, \mathrm{wp}_{20}, \mathrm{wp}_{21}, \mathrm{wp}_{22}, \mathrm{wpp}_1, \mathrm{wpp}_2, \mathrm{wpp}_3,$$
$$\mathrm{wpp}_4, \mathrm{wpp}_5, \mathrm{wpp}_6, \mathrm{wpp}_7, \mathrm{wpp}_8, \mathrm{wpp}_9, \mathrm{wpp}_{10}, \mathrm{wpp}_{11},$$
$$\mathrm{wpp}_{12}, \mathrm{wpp}_{13}, \mathrm{wpp}_{14}, \mathrm{wpp}_{15}, \mathrm{wpp}_{16}, \mathrm{wpp}_{17}, \mathrm{wpp}_{18},$$
$$\mathrm{wpp}_{19}, \mathrm{wpp}_{20}, \mathrm{wpp}_{21}, \mathrm{wpp}_{22}], \{j, 1, 6 * \mathrm{nx}\}];$$
$$k = \mathrm{kh}_i + \mathrm{a4} * h; \mathrm{Do}[v_j = v[j, i] + \mathrm{b41} * \mathrm{k1}_j + \mathrm{b42} * \mathrm{k2}_j + \mathrm{b43} * \mathrm{k3}_j,$$
$$\{j, 1, \mathrm{nx}\}];$$
$$\mathrm{Do}[\mathrm{vp}_j = \mathrm{vp}[j, i] + \mathrm{b41} * \mathrm{k1}_{j+\mathrm{nx}} + \mathrm{b42} * \mathrm{k2}_{j+\mathrm{nx}} + \mathrm{b43} * \mathrm{k3}_{j+\mathrm{nx}},$$
$$\{j, 1, \mathrm{nx}\}];$$
$$\mathrm{Do}[\mathrm{vpp}_j = \mathrm{vpp}[j, i] + \mathrm{b41} * \mathrm{k1}_{j+2*\mathrm{nx}} + \mathrm{b42} * \mathrm{k2}_{j+2*\mathrm{nx}} +$$
$$\mathrm{b43} * \mathrm{k3}_{j+2*\mathrm{nx}}, \{j, 1, \mathrm{nx}\}];$$
$$\mathrm{Do}[w_j = w[j, i] + \mathrm{b41} * \mathrm{k1}_{j+3*\mathrm{nx}} + \mathrm{b42} * \mathrm{k2}_{j+3*\mathrm{nx}} + \mathrm{b43} * \mathrm{k3}_{j+3*\mathrm{nx}},$$
$$\{j, 1, \mathrm{nx}\}];$$
$$\mathrm{Do}[\mathrm{wp}_j = \mathrm{wp}[j, i] + \mathrm{b41} * \mathrm{k1}_{j+4*\mathrm{nx}} + \mathrm{b42} * \mathrm{k2}_{j+4*\mathrm{nx}} + \mathrm{b43} * \mathrm{k3}_{j+4*\mathrm{nx}},$$
$$\{j, 1, \mathrm{nx}\}];$$
$$\mathrm{Do}[\mathrm{wpp}_j = \mathrm{wpp}[j, i] + \mathrm{b41} * \mathrm{k1}_{j+5*\mathrm{nx}} + \mathrm{b42} * \mathrm{k2}_{j+5*\mathrm{nx}} + \mathrm{b43} * \mathrm{k3}_{j+5*\mathrm{nx}},$$
$$\{j, 1, \mathrm{nx}\}];$$
$$\mathrm{Do}[$$
$$\mathrm{k4}_j = h * \mathrm{fcp}_j [k, v_1, v_2, v_3, v_4, v_5, v_6, v_7, v_8, v_9,$$
$$v_{10}, v_{11}, v_{12}, v_{13}, v_{14}, v_{15}, v_{16}, v_{17}, v_{18}, v_{19}, v_{20},$$

$v_{21}, v_{22}, \mathrm{vp}_1, \mathrm{vp}_2, \mathrm{vp}_3, \mathrm{vp}_4, \mathrm{vp}_5, \mathrm{vp}_6, \mathrm{vp}_7, \mathrm{vp}_8,$
$\mathrm{vp}_9, \mathrm{vp}_{10}, \mathrm{vp}_{11}, \mathrm{vp}_{12}, \mathrm{vp}_{13}, \mathrm{vp}_{14}, \mathrm{vp}_{15}, \mathrm{vp}_{16}, \mathrm{vp}_{17},$
$\mathrm{vp}_{18}, \mathrm{vp}_{19}, \mathrm{vp}_{20}, \mathrm{vp}_{21}, \mathrm{vp}_{22}, \mathrm{vpp}_1, \mathrm{vpp}_2, \mathrm{vpp}_3,$
$\mathrm{vpp}_4, \mathrm{vpp}_5, \mathrm{vpp}_6, \mathrm{vpp}_7, \mathrm{vpp}_8, \mathrm{vpp}_9, \mathrm{vpp}_{10}, \mathrm{vpp}_{11},$
$\mathrm{vpp}_{12}, \mathrm{vpp}_{13}, \mathrm{vpp}_{14}, \mathrm{vpp}_{15}, \mathrm{vpp}_{16}, \mathrm{vpp}_{17}, \mathrm{vpp}_{18},$
$\mathrm{vpp}_{19}, \mathrm{vpp}_{20}, \mathrm{vpp}_{21}, \mathrm{vpp}_{22}, w_1, w_2, w_3, w_4, w_5, w_6,$
$w_7, w_8, w_9, w_{10}, w_{11}, w_{12}, w_{13}, w_{14}, w_{15}, w_{16}, w_{17}, w_{18},$
$w_{19}, w_{20}, w_{21}, w_{22}, \mathrm{wp}_1, \mathrm{wp}_2, \mathrm{wp}_3, \mathrm{wp}_4, \mathrm{wp}_5, \mathrm{wp}_6, \mathrm{wp}_7,$
$\mathrm{wp}_8, \mathrm{wp}_9, \mathrm{wp}_{10}, \mathrm{wp}_{11}, \mathrm{wp}_{12}, \mathrm{wp}_{13}, \mathrm{wp}_{14}, \mathrm{wp}_{15}, \mathrm{wp}_{16},$
$\mathrm{wp}_{17}, \mathrm{wp}_{18}, \mathrm{wp}_{19}, \mathrm{wp}_{20}, \mathrm{wp}_{21}, \mathrm{wp}_{22}, \mathrm{wpp}_1, \mathrm{wpp}_2, \mathrm{wpp}_3,$
$\mathrm{wpp}_4, \mathrm{wpp}_5, \mathrm{wpp}_6, \mathrm{wpp}_7, \mathrm{wpp}_8, \mathrm{wpp}_9, \mathrm{wpp}_{10}, \mathrm{wpp}_{11},$
$\mathrm{wpp}_{12}, \mathrm{wpp}_{13}, \mathrm{wpp}_{14}, \mathrm{wpp}_{15}, \mathrm{wpp}_{16}, \mathrm{wpp}_{17}, \mathrm{wpp}_{18},$
$\mathrm{wpp}_{19}, \mathrm{wpp}_{20}, \mathrm{wpp}_{21}, \mathrm{wpp}_{22}], \{j, 1, 6 * \mathrm{nx}\}];$
$k = \mathrm{kh}_i + \mathrm{a5} * h;$
$\mathrm{Do}[v_j = v[j, i] + \mathrm{b51} * \mathrm{k1}_j + \mathrm{b52} * \mathrm{k2}_j + \mathrm{b53} * \mathrm{k3}_j + \mathrm{b54} * \mathrm{k4}_j,$
$\{j, 1, \mathrm{nx}\}];$
$\mathrm{Do}[\mathrm{vp}_j = \mathrm{vp}[j, i] + \mathrm{b51} * \mathrm{k1}_{j+\mathrm{nx}} + \mathrm{b52} * \mathrm{k2}_{j+\mathrm{nx}} + \mathrm{b53} * \mathrm{k3}_{j+\mathrm{nx}} +$
$\mathrm{b54} * \mathrm{k4}_{j+\mathrm{nx}}, \{j, 1, \mathrm{nx}\}];$
$\mathrm{Do}[\mathrm{vpp}_j = \mathrm{vpp}[j, i] + \mathrm{b51} * \mathrm{k1}_{j+2*\mathrm{nx}} + \mathrm{b52} * \mathrm{k2}_{j+2*\mathrm{nx}} +$
$\mathrm{b53} * \mathrm{k3}_{j+2*\mathrm{nx}} + \mathrm{b54} * \mathrm{k4}_{j+2*\mathrm{nx}}, \{j, 1, \mathrm{nx}\}];$
$\mathrm{Do}[w_j = w[j, i] + \mathrm{b51} * \mathrm{k1}_{j+3*\mathrm{nx}} + \mathrm{b52} * \mathrm{k2}_{j+3*\mathrm{nx}} + \mathrm{b53} * \mathrm{k3}_{j+3*\mathrm{nx}} +$
$\mathrm{b54} * \mathrm{k4}_{j+3*\mathrm{nx}}, \{j, 1, \mathrm{nx}\}];$
$\mathrm{Do}[\mathrm{wp}_j = \mathrm{wp}[j, i] + \mathrm{b51} * \mathrm{k1}_{j+4*\mathrm{nx}} + \mathrm{b52} * \mathrm{k2}_{j+4*\mathrm{nx}} +$
$\mathrm{b53} * \mathrm{k3}_{j+4*\mathrm{nx}} + \mathrm{b54} * \mathrm{k4}_{j+4*\mathrm{nx}}, \{j, 1, \mathrm{nx}\}];$
$\mathrm{Do}[\mathrm{wpp}_j = \mathrm{wpp}[j, i] + \mathrm{b51} * \mathrm{k1}_{j+5*\mathrm{nx}} + \mathrm{b52} * \mathrm{k2}_{j+5*\mathrm{nx}} +$
$\mathrm{b53} * \mathrm{k3}_{j+5*\mathrm{nx}} + \mathrm{b54} * \mathrm{k4}_{j+5*\mathrm{nx}}, \{j, 1, \mathrm{nx}\}];$
$\mathrm{Do}[$
$\mathrm{k5}_j = h * \mathrm{fcp}_j[k, v_1, v_2, v_3, v_4, v_5, v_6, v_7, v_8, v_9,$
$v_{10}, v_{11}, v_{12}, v_{13}, v_{14}, v_{15}, v_{16}, v_{17}, v_{18}, v_{19}, v_{20},$
$v_{21}, v_{22}, \mathrm{vp}_1, \mathrm{vp}_2, \mathrm{vp}_3, \mathrm{vp}_4, \mathrm{vp}_5, \mathrm{vp}_6, \mathrm{vp}_7, \mathrm{vp}_8,$
$\mathrm{vp}_9, \mathrm{vp}_{10}, \mathrm{vp}_{11}, \mathrm{vp}_{12}, \mathrm{vp}_{13}, \mathrm{vp}_{14}, \mathrm{vp}_{15}, \mathrm{vp}_{16}, \mathrm{vp}_{17},$
$\mathrm{vp}_{18}, \mathrm{vp}_{19}, \mathrm{vp}_{20}, \mathrm{vp}_{21}, \mathrm{vp}_{22}, \mathrm{vpp}_1, \mathrm{vpp}_2, \mathrm{vpp}_3,$
$\mathrm{vpp}_4, \mathrm{vpp}_5, \mathrm{vpp}_6, \mathrm{vpp}_7, \mathrm{vpp}_8, \mathrm{vpp}_9, \mathrm{vpp}_{10}, \mathrm{vpp}_{11},$
$\mathrm{vpp}_{12}, \mathrm{vpp}_{13}, \mathrm{vpp}_{14}, \mathrm{vpp}_{15}, \mathrm{vpp}_{16}, \mathrm{vpp}_{17}, \mathrm{vpp}_{18},$
$\mathrm{vpp}_{19}, \mathrm{vpp}_{20}, \mathrm{vpp}_{21}, \mathrm{vpp}_{22}, w_1, w_2, w_3, w_4, w_5, w_6,$
$w_7, w_8, w_9, w_{10}, w_{11}, w_{12}, w_{13}, w_{14}, w_{15}, w_{16}, w_{17}, w_{18},$
$w_{19}, w_{20}, w_{21}, w_{22}, \mathrm{wp}_1, \mathrm{wp}_2, \mathrm{wp}_3, \mathrm{wp}_4, \mathrm{wp}_5, \mathrm{wp}_6, \mathrm{wp}_7,$
$\mathrm{wp}_8, \mathrm{wp}_9, \mathrm{wp}_{10}, \mathrm{wp}_{11}, \mathrm{wp}_{12}, \mathrm{wp}_{13}, \mathrm{wp}_{14}, \mathrm{wp}_{15}, \mathrm{wp}_{16},$
$\mathrm{wp}_{17}, \mathrm{wp}_{18}, \mathrm{wp}_{19}, \mathrm{wp}_{20}, \mathrm{wp}_{21}, \mathrm{wp}_{22}, \mathrm{wpp}_1, \mathrm{wpp}_2, \mathrm{wpp}_3,$
$\mathrm{wpp}_4, \mathrm{wpp}_5, \mathrm{wpp}_6, \mathrm{wpp}_7, \mathrm{wpp}_8, \mathrm{wpp}_9, \mathrm{wpp}_{10}, \mathrm{wpp}_{11},$
$\mathrm{wpp}_{12}, \mathrm{wpp}_{13}, \mathrm{wpp}_{14}, \mathrm{wpp}_{15}, \mathrm{wpp}_{16}, \mathrm{wpp}_{17}, \mathrm{wpp}_{18},$
$\mathrm{wpp}_{19}, \mathrm{wpp}_{20}, \mathrm{wpp}_{21}, \mathrm{wpp}_{22}], \{j, 1, 6 * \mathrm{nx}\}];$
$k = \mathrm{kh}_i + \mathrm{a6} * h;$

```
Do[v_j = v[j,i] + b61*k1_j + b62*k2_j + b63*k3_j + b64*k4_j +
 b65*k5_j, {j,1,nx}];
Do[vp_j = vp[j,i] + b61*k1_{j+nx} + b62*k2_{j+nx} + b63*k3_{j+nx} +
 b64*k4_{j+nx} + b65*k5_{j+nx}, {j,1,nx}];
Do[vpp_j = vpp[j,i] + b61*k1_{j+2*nx} + b62*k2_{j+2*nx} +
 b63*k3_{j+2*nx} + b64*k4_{j+2*nx} + b65*k5_{j+2*nx}, {j,1,nx}];
Do[w_j = w[j,i] + b61*k1_{j+3*nx} + b62*k2_{j+3*nx} + b63*k3_{j+3*nx} +
 b64*k4_{j+3*nx} + b65*k5_{j+3*nx}, {j,1,nx}];
Do[wp_j = wp[j,i] + b61*k1_{j+4*nx} + b62*k2_{j+4*nx} +
 b63*k3_{j+4*nx} + b64*k4_{j+4*nx} + b65*k5_{j+4*nx}, {j,1,nx}];
Do[wpp_j = wpp[j,i] + b61*k1_{j+5*nx} + b62*k2_{j+5*nx} +
 b63*k3_{j+5*nx} + b64*k4_{j+5*nx} + b65*k5_{j+5*nx}, {j,1,nx}];
Do[
k6_j = h*fcp_j[k, v_1, v_2, v_3, v_4, v_5, v_6, v_7, v_8, v_9,
v_10, v_11, v_12, v_13, v_14, v_15, v_16, v_17, v_18, v_19, v_20,
v_21, v_22, vp_1, vp_2, vp_3, vp_4, vp_5, vp_6, vp_7, vp_8,
vp_9, vp_10, vp_11, vp_12, vp_13, vp_14, vp_15, vp_16, vp_17,
vp_18, vp_19, vp_20, vp_21, vp_22, vpp_1, vpp_2, vpp_3,
vpp_4, vpp_5, vpp_6, vpp_7, vpp_8, vpp_9, vpp_10, vpp_11,
vpp_12, vpp_13, vpp_14, vpp_15, vpp_16, vpp_17, vpp_18,
vpp_19, vpp_20, vpp_21, vpp_22, w_1, w_2, w_3, w_4, w_5, w_6,
w_7, w_8, w_9, w_10, w_11, w_12, w_13, w_14, w_15, w_16, w_17, w_18,
w_19, w_20, w_21, w_22, wp_1, wp_2, wp_3, wp_4, wp_5, wp_6, wp_7,
wp_8, wp_9, wp_10, wp_11, wp_12, wp_13, wp_14, wp_15, wp_16,
wp_17, wp_18, wp_19, wp_20, wp_21, wp_22, wpp_1, wpp_2, wpp_3,
wpp_4, wpp_5, wpp_6, wpp_7, wpp_8, wpp_9, wpp_10, wpp_11,
wpp_12, wpp_13, wpp_14, wpp_15, wpp_16, wpp_17, wpp_18,
 wpp_19, wpp_20, wpp_21, wpp_22], {j,1,6*nx}];
Do[Evaluate[helpp[[j]]] =
(Evaluate[help[[j]]] + c1*k1_j + c2*k2_j + c3*k3_j +
 c4*k4_j + c5*k5_j + c6*k6_j), {j,1,6*nx}];


Do[Evaluate[helppS[[j]]] =
(Evaluate[help[[j]]] + cS1*k1_j + cS2*k2_j + cS3*k3_j +
 cS4*k4_j + cS5*k5_j + cS6*k6_j), {j,1,6*nx}];
(*trickdescribedbelow(16.2.8)inNumerical
Recipes*)
(*Δ0 : desirederrorforcurrentstep,
Δ1 : errorestimateforcurrentstep*)
(*Δ1_j = Abs[helpp[[j]] - helppS[[j]]],
Δ0_j = 10^-eps * yscal_j*)
```

```
Do[yscal_j = Abs[help[[j]]] + Abs[helpp[[j]] - help[[j]]],
{j, 1, 6 * nx}];
(*Do[yscal_j = Abs[helpp[[j]] - help[[j]]], {j, 1, 6 * nx}];*)

(*If[i == 1, Print[Table[yscal_j, {j, 1, 6 * nx}]]];*)

err = Max[Table[Abs[Abs[helpp[[j]] - helppS[[j]]] / (10^-eps * yscal_j)],
{j, 1, 4 * nx}]];


(* Adaptive step size BEGIN*)

pos =
Position[Table[Abs[Abs[helpp[[j]] - helppS[[j]]] / (10^-eps * yscal_j)],
{j, 1, 4 * nx}], err][[1, 1]];
worstdiff = Abs[helpp[[pos]] - helppS[[pos]]];
worstscal = yscal_pos;
worst2 = Abs[Abs[helpp[[pos]] - helppS[[pos]]] / (10^-eps * yscal_pos)];


(*(16.2.10)stepsizeadjustment*)


If[err > 1
, Do[v[j, i + 1] =., {j, 1, nx}];
Do[vp[j, i + 1] =., {j, 1, nx}];
Do[vpp[j, i + 1] =., {j, 1, nx}];
Do[w[j, i + 1] =., {j, 1, nx}];
Do[wp[j, i + 1] =., {j, 1, nx}];
Do[wpp[j, i + 1] =., {j, 1, nx}];
Do[vS[j, i + 1] =., {j, 1, nx}];
Do[vpS[j, i + 1] =., {j, 1, nx}];
Do[vppS[j, i + 1] =., {j, 1, nx}];
Do[wS[j, i + 1] =., {j, 1, nx}];
Do[wpS[j, i + 1] =., {j, 1, nx}];
Do[wppS[j, i + 1] =., {j, 1, nx}]; mess = "do again";
Print[i, err, mess]; h = 0.9 * h * err^-1/4
, i = i + 1; kh_i = kh_i-1 + h; mess = "accepted";
Print[{i - 1, kh_i-1, h, err, mess, pos, worstdiff,
worstscal, worst2}]; h = 0.9 * h * err^-1/5];


(*Adaptive step size END*)
```

```
(*
(*Fixed Stepsize BEGIN*)
i = i + 1; kh_i = kh_{i-1} + h; mess = "accepted";
Print[{i - 1, kh_{i-1}, h, err, mess}];
(*Fixed Stepsize END*)
*)

If[kh_i < 9, Break[]];


, {ih, 1, 100000}]
ListPlot[Table[{√x_j, v[j, 700]}, {j, 1, 20}]]
```

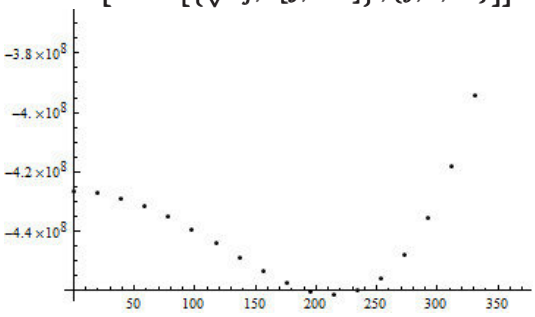

Appendix D

$O(N)$ fixed points

For convenience we provide a simple *Mathematica* notebook which allows for a quick calculation of the stability-matrix eigenvalues for the $O(n)$ models (up to quartic coupling) from FRG in local-potential approximation. n can be chosen arbitrarily without further modifications.

```
n = 8;
phi = Sum[a_i^2, {i, 1, n}];
U = r1 * (phi) + 1/24 * λ1 * (phi)^2;
v = Table[a_i → 0, {i, 2, n}];
Do[
M_ih,ih = With[{i = ih, j = ih}, FullSimplify[D[D[U, a_i], a_j]/.v]]
, {ih, 1, n}];
diag = Table[M_ih,ih + k^2, {ih, 1, n}];
SUM = Tr[FullSimplify[Inverse[DiagonalMatrix[diag]]]];
RHSr1 = SeriesCoefficient[SUM, {a_1, 0, 2}];
RHSr1s = FullSimplify[RHSr1/.{r1 → r1s * k^2, λ1 → k^(4-d) * λ1s}];
βr1s = -2 * r1s + K * (FullSimplify[RHSr1s * k^d]);
RHSλ1 = 24 * SeriesCoefficient[SUM, {a_1, 0, 4}];
RHSλ1s = FullSimplify[RHSλ1/.{r1 → r1s * k^2, λ1 → k^(4-d) * λ1s}];
βλ1s = (d - 4) * λ1s + K * (FullSimplify[RHSλ1s * k^(2d-2)]);

d = 3;
K = (2*π^(d/2))/(d*Gamma[d/2]) * 1/(2*π)^d;
sol = NSolve[{βr1s == 0, βλ1s == 0}, {r1s, λ1s}];
Table[{sol[[i]], Eigenvalues[({D[βr1s, r1s] D[βr1s, λ1s]
                               D[βλ1s, r1s] D[βλ1s, λ1s]}/.sol[[i]])]}, {i, 1, Length[sol]}]
```

$$\{\{\{r1s \to -0.0675676, \lambda 1s \to 3.59143\}, \{-1.71971, 1.34471\}\}, \{\{r1s \to 0., \lambda 1s \to 0.\}, \{-2., -1.\}\}\}$$

Appendix E

Fixed-point planes, $SU(2)_A \times U(2)_V$

For illustrational purposes we show here the flow in the vicinity of some of the fixed points of Tab. 6.3. Note the change in notation ($l_i \equiv g_i$, $r_i \equiv m_i^2$).
The following graphs comprise all fixed-point planes for one of the IR-unstable $O(4)$ fixed points (FP_6). Note that in each plane the remaining couplings are set to their fixed-point values.

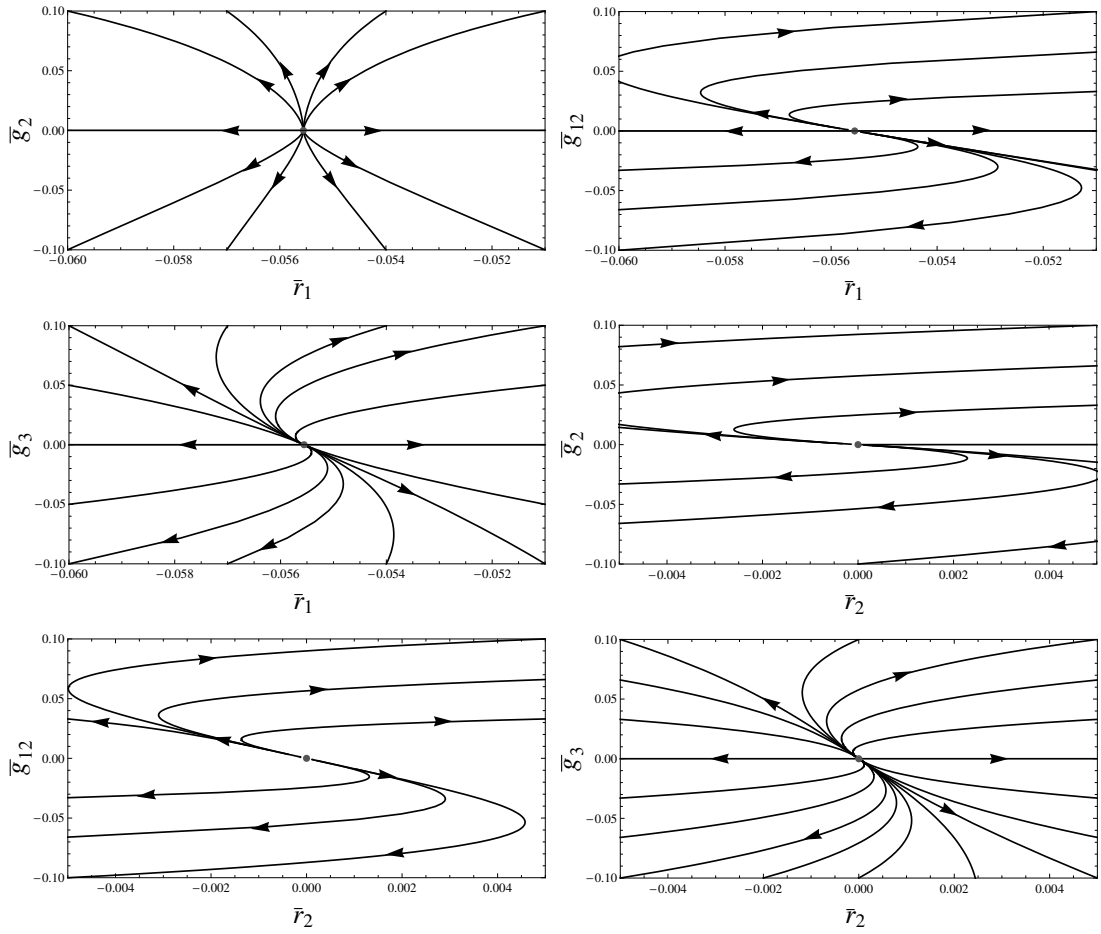

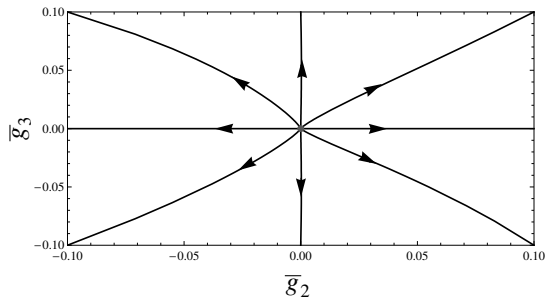
$\overline{g}_3$
$\overline{g}_2$

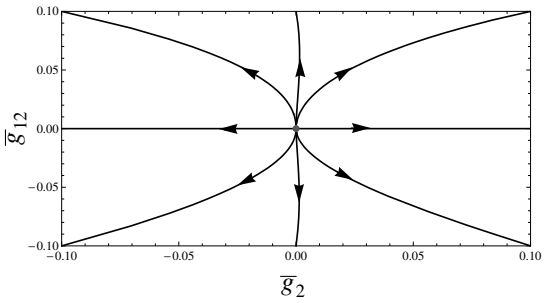
$\overline{g}_{12}$
$\overline{g}_2$

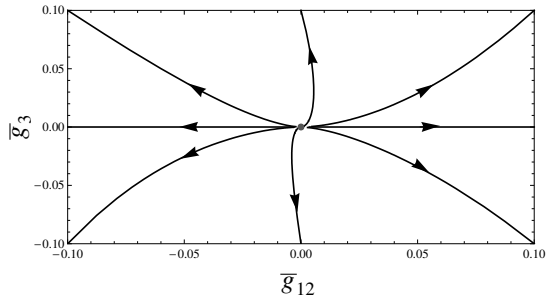
$\overline{g}_3$
$\overline{g}_{12}$

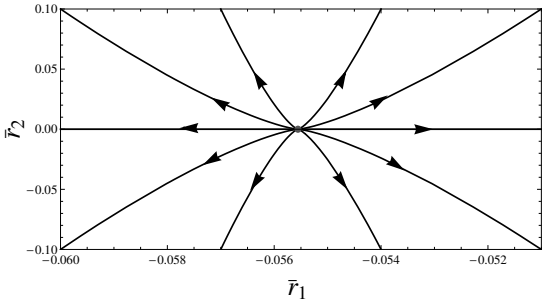
$\overline{r}_2$
$\overline{r}_1$

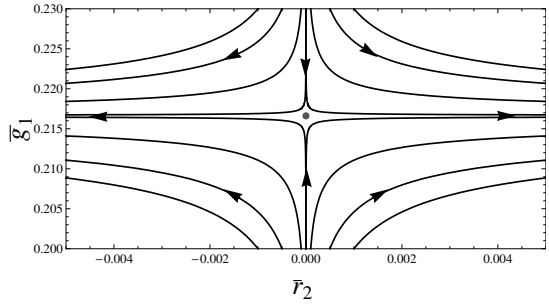
$\overline{g}_1$
$\overline{r}_2$

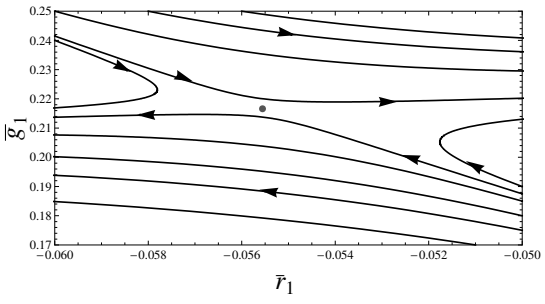
$\overline{g}_1$
$\overline{r}_1$

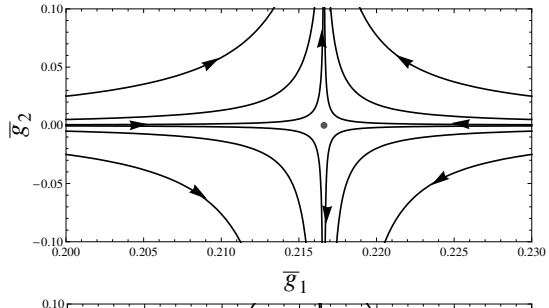
$\overline{g}_2$
$\overline{g}_1$

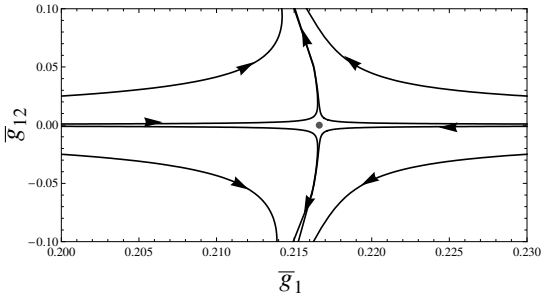
$\overline{g}_{12}$
$\overline{g}_1$

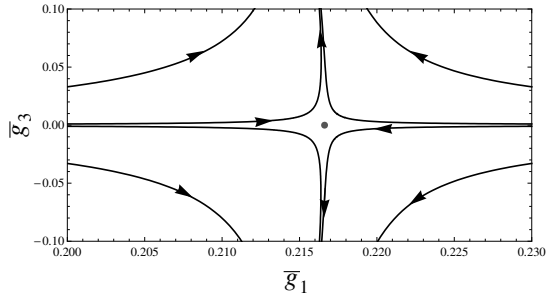
$\overline{g}_3$
$\overline{g}_1$

The following graphs show all fixed-point planes involving a relevant direction for one of the unphysical IR-stable fixed points (FP_4).

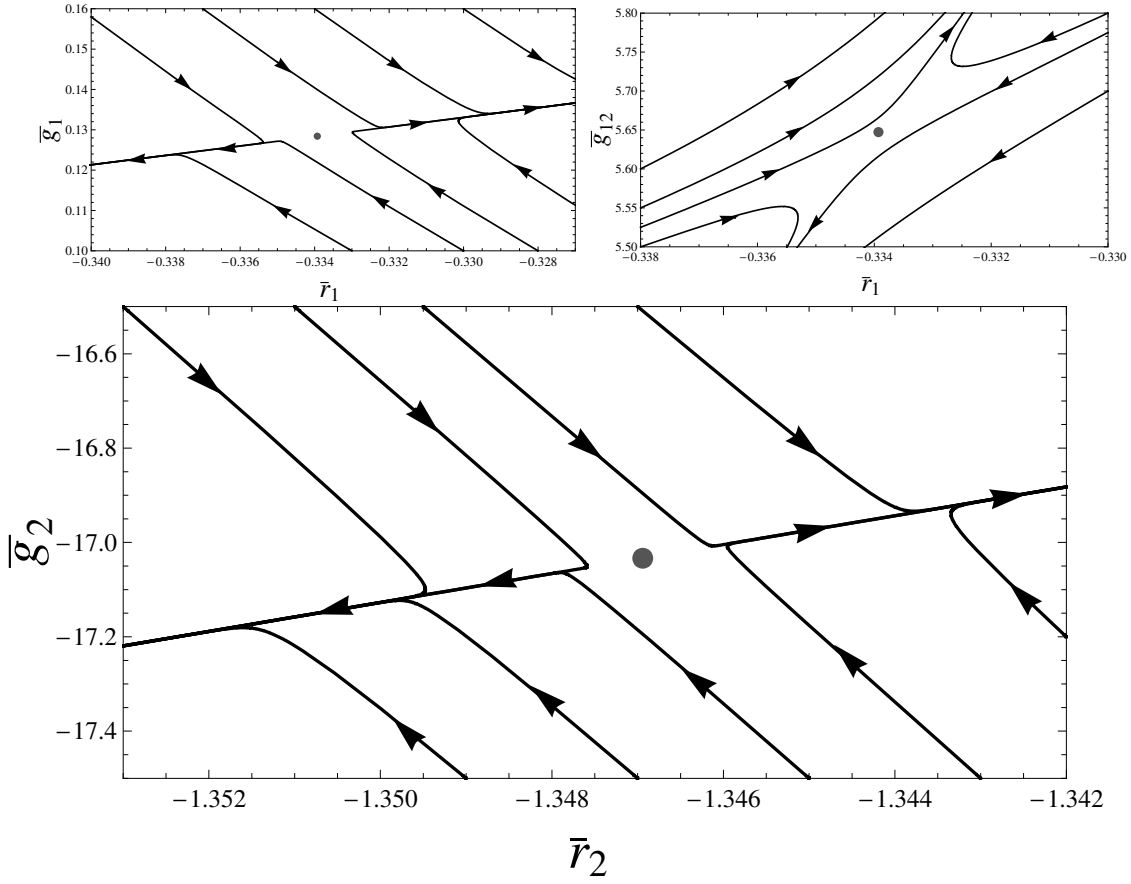

Deutschsprachige Zusammenfassung

Die Untersuchung der Natur auf extrem kleinen und extrem grossen Längenskalen hat seit jeher zu bahnbrechenden wissenschaftlichen Einsichten und Innovationen geführt. Insbesondere zu unserem heutigen Verständnis, dass Nukleonen (Protonen und Neutronen) aus Quarks zusammengesetzt sind, die infolge der starken Wechselwirkung, vermittelt durch Gluonenaustausch, gebunden sind. Mit dem Aufkommen des Quarkmodells von Gell-Mann wurde bald die Quantenchromodynamik (QCD) erfolgreich in der Beschreibung vieler Eigenschaften der starken Wechselwirkung, die im Experiment gemessen wurden. Um es mit Goethe zu sagen: mit den modernen Hochenergie-Beschleuniger-Experimenten versuchen Physiker auf dem ganzen Globus unser Verständnis davon zu verbessern, was die Welt im Innersten zusammenhält. Am Large Hadron Collider (LHC) werden beispielsweise Protonen derart beschleunigt und miteinander zur Kollision gebracht, dass bislang unerreichte Energiedichten auftreten. Während die höchste erreichbare Kollisionsenergie von 14 TeV lediglich der Energie entspricht, die beim In-die-Hände-Klatschen auftritt, sind die erzeugten Energiedichten unglaublich hoch verglichen mit denen des Alltags. Infolge der enormen Energiedichte nehmen Temperatur, T, und baryochemisches Potential, μ_B, Werte an, die mit denen des frühen Universums vergleichbar sind. Es gibt sowohl theoretische als auch experimentelle Hinweise darauf, dass hadronische Materie mit zunehmendem T und/oder μ_B einen Phasenübergang durchläuft, hin zu einem exotischen Zustand, der als Quark-Gluon-Plasma bekannt ist. Dieser Übergang wird begleitet von einem sogenannten chiralen Übergang. Es ist eine wichtige Frage, ob bei diesem chiralen Übergang latente Wärme auftritt oder nicht, d.h., ob es sich um einen echten Phasenübergang (von erster bzw. zweiter Ordnung) handelt oder ob ein sogenannter crossover vorliegt. Einige Resultate deuten auf einen crossover für $\mu_B = 0$ und einen Phasenübergang erster Ordnung für $T = 0$ hin, lassen jedoch noch keinen endgültigen Schluss zu, ob dies tatsächlich der Realität entspricht. Wenn ja, so liegt die Annahme nahe, dass ein kritischer Endpunkt, $(T_c \neq 0, \mu_B \neq 0)$, existiert, an dem der chirale Übergang von zweiter Ordnung ist, was als Grenzfall zwischen einem Phasenübergang erster Ordnung und einem kontinuierlichen crossover angesehen werden kann. In der Tat existiert ein kritischer Endpunkt in einigen theoretischen Zugängen zur Beschreibung des chiralen Phasenübergangs, deren Aussagekraft seit jeher lebhaft diskutiert wird. Ein zentrales Ziel des zukünftigen CBM-Experiments an der GSI in Darmstadt ist es, die Existenz im Experiment zu überprüfen.

In der Nähe des QCD-(Phasen)übergangs ist es die Abwesenheit jeglicher perturbativer Entwicklungsparameter (infolge der Stärke der Wechselwirkung), die exakte analytische Berechnungen so

gut wie unmöglich macht. Das gleiche gilt für realistische effektive Modelle für QCD. Nichtperturbative Methoden sind daher unverzichtbar für die Untersuchung des QCD-Phasendiagramms. Zu den populärsten dieser Zugänge gehören Gitter-QCD, Resummierungsverfahren, der Dyson-Schwinger-Formalismus, sowie die Funktionale Renormierungsgruppe (FRG). All diese Methoden ergänzen sich gegenseitig und werden zum Teil auch miteinander kombiniert. Eine der Stärken der FRG-Methode ist, dass sie nicht nur erfolgreich auf effektive Modelle angewendet werden kann, sondern auch auf QCD selbst. Für letztere Ab-Initio-Rechnungen sind die aus effektiven Modellen für QCD gewonnenen Resultate von grossem Wert.
Der Schwerpunkt der vorliegenden Arbeit liegt auf der Fragestellung von welcher Ordnung der chirale QCD-Phasenübergang im Fall von genau zwei leichten Quarksorten (up und down) ist. Problemstellungen wie die Suche nach einer Antwort auf die Frage nach den Bedingungen für die Existenz eines Phasenübergangs zweiter Ordnung, die Bestimmung der Universalitätsklasse in diesem Fall etc. erfordern Wissen und Techniken aus verschiedenen Gebieten.
Kapitel 1 besteht aus einer allgemeinen Einleitung, welche (gemeinsam mit Kapitel 8, in dem unsere Resultate diskutiert werden) zugleich Grundlage dieser Zusammenfassung ist.
In Kapitel 2 werden wir zunächst einige allgemeine Aspekte von Phasenübergängen darstellen, die von besonderer Relevanz für das Verständnis des Renormierungsgruppen-Zugangs zu ebendiesen sind. Unser Fokus liegt hierbei auf einer kritischen Diskussion der Universalitätshypothese, einem entscheidenden Baustein bei der Konstruktion effektiver Theorien für Ordnungsparameter, deren Glaubwürdigkeit häufig stark von Universalitätsbetrachtungen abhängt. Insbesondere die Rechtfertigung des linearen Sigma-Modells als effektive Theorie für den chiralen Ordnungsparameter beruht auf der Gültigkeit der Universalitätshypothese. Wir diskutieren ausführlich verschiedene Formulierungen letzterer, angefangen bei einer Aufzählung derjenigen Eigenschaften einer Theorie, von denen die kritischen Exponenten maßgeblich abhängen, hin zu Versuchen, die Universalitätshypothese präziser zu formulieren als dies üblicherweise erfolgt, nämlich durch Angabe hinreichender Bedingungen für die Zugehörigkeit zu einer bestimmten Universalitätsklasse. In diesem Zusammenhang weisen wir auch auf solche Resultate hin, welche die uneingeschränkte Gültigkeit der Universalitätshypothese in Frage stellen.
Kapitel 3 beschäftigt sich mit dem chiralen Phasenübergang von einem allgemeinen Standpunkt aus. Wir ergänzen wohlbekannte Fakten durch eine detaillierte Diskussion der sogenannten $O(4)$-Hypothese, die ihren Ursprung ebenfalls in Universalitätsbetrachtungen hat. Die Überprüfung der Gültigkeit selbiger wird schließlich in Kapitel 6 und 7 in Angriff genommen.
In Kapitel 4 stellen wir die von uns benutzte nichtperturbative Methode vor, die oben bereits erwähnte FRG-Methode. Im Rahmen dieser Arbeit beschränken wir uns auf die sogenannte lokale Potential-Näherung (LPA). Außerdem diskutieren wir den Zusammenhang zwischen effektiven Theorien für QCD und der zugrundeliegenden fundamentalen Theorie unter Ausnutzung der FRG-eigenen Perspektive.
Kapitel 5 behandelt ein mathematisches Thema, das für alle unserer Untersuchungen unabdingbar ist, nämlich die systematische Konstruktion polynomialer Invarianten zu einer gegebenen Symmetrie. An dieser Stelle sei betont, dass diese Thematik von sehr allgemeinem Interesse ist und in all jenen Forschungsgebieten Relevanz besitzt, in denen Symmetriebetrachtungen eine Rolle spielen. Im Rahmen dieser Arbeit weisen wir auf die Bedeutung im Kontext der Hochenergie-Physik hin und hoffen, das Interesse in systematische Methoden zur Ableitung von

Invarianten für kontinuierliche Symmetriegruppen zu verstärken. Wir präsentieren einen einfachen, jedoch neuartigen, Algorithmus für die praktische Konstruktion von Invarianten einer gegebenen polynomialen Ordnung.
Kapitel 6 widmet sich Renormierungsgruppen-Studien einer Reihe dimensional reduzierter Theorien, welche das Potential besitzen, die mögliche Existenz eines Phasenübergangs zweiter Ordnung vorherzusagen bzw. auszuschließen. Von zentralem Interesse ist hierbei das lineare Sigma-Modell, insbesondere in Anwesenheit der axialen Anomalie. Es stellt sich heraus, dass die Fixpunkt-Struktur des letzteren vergleichsweise kompliziert ist und ein tieferes Verständnis der zugrundeliegenden Methode sowie ihrer Annahmen erfordert. Dies führt uns zu einer sorgfältigen Analyse der Fixpunkt-Struktur verschiedener Modelle (jeweils definiert durch das allgemeinste Landau-Potential invariant unter einer gegebenen Symmetriegruppe) in lokaler Potential-Näherung, was wiederum unserer Diskussion der Universalitätshypothese zugutekommt und darüberhinaus weitere Spin-off-Effekte hat. Im Zusammenhang mit der Untersuchung des Einflusses von Vektor- und Axial-Vektor-Mesonen beispielsweise stoßen wir auf eine neue Universalitätsklasse, die eventuell in anderen Bereichen, in denen Chiralität eine Rolle spielt, von Relevanz sein könnte.
Während wenig Spielraum für die Wahl der Symmetriegruppe der effektiven Theorie für den chiralen Ordnungsparameter besteht (die Symmetriegruppe ist notwendigerweise eine Untergruppe $G \subseteq U(2)_A \times U(2)_V$), ist die Identifizierung der Ordnungsparameter-Komponenten mit den relevanten mesonischen Freiheitsgraden hochgradig nichttrivial. Diese Wahl entspricht der Wahl einer Darstellung der Gruppe G und kann zur Zeit nicht eindeutig aus der QCD hergeleitet werden. Die Entscheidung muss auf der Grundlage von Beschleuniger-Experimenten, Gitter-QCD-Rechnungen und Plausibilitätsbetrachtungen getroffen werden. Es ist daher unerlässlich, verschiedene Möglichkeiten auszutesten. Eine wohlbekannte Wahl besteht darin, das Pion und seinen chiralen Partner, das Sigma-Meson, der $O(4)$-Darstellung für $SU(2)_A \times SU(2)_V$ zuzuordnen, welche einen Phasenübergang zweiter Ordnung erlaubt. Dieses Szenario ist jedoch nur dann sinnvoll, wenn nahe der kritischen Temperatur alle anderen Mesonen entsprechend schwer sind. Im Fall von genau zwei leichten Quarkmassen ($N_f = 2$) erfordert dies eine hinreichend große Anomaliestärke. Berücksichtigt man zusätzlich zum Pion und Sigma-Meson auch das Eta-Meson und das a_0-Meson (mittels Wahl der $[\bar{2}, 2] \oplus [2, \bar{2}]$-Darstellung für $SU(2)_A \times SU(2)_V$), liefern unsere derzeitigen expliziten Rechnungen keinen Nachweis für die Existenz eines Phasenübergang zweiter Ordnung. Stattdessen spricht die Abwesenheit eines physikalischen (hinsichtlich der Massen) infrarot-stabilen Fixpunktes für einen fluktuationsinduzierten Phasenübergang erster Ordnung. Dieses Ergebnis ist auch zu erwarten (jedoch nicht impliziert), allein durch die Existenz zweier quadratischer Invarianten. Es besteht jedoch immer noch eine hypothetische Chance auf einen Phasenübergang zweiter Ordnung in der $SU(2)_A \times U(2)_V$-Universalitätsklasse. Dies wäre der Fall, wenn der entsprechende von uns gefundene unphysikalische infrarot-stabile Fixpunkt physikalisch werden sollte in höherer Trunkierungsordnung. Interessanterweise finden wir bei endlicher Temperatur (siehe unten) für gewisse Parameter einen Phasenübergang zweiter Ordnung. Es ist noch unklar, ob diese Wahl der Parameter in den Gültigkeitsbereich der dimensional reduzierten Theorie fällt. Möglicherweise handelt es sich aber auch lediglich um einen extrem schwachen Phasenübergang erster Ordnung. Es erfordert weitere Untersuchungen, um die korrekte Erklärung zu finden. Abgesehen davon basieren unsere Resultate auf einer FRG-

Fixpunkt-Studie der dimensional reduzierten Theorie, die keine Fixpunkte mit zu grosser anomaler Dimension erfasst, was ebenfalls aufbauende Studien motiviert (vgl. unten).
Neben der $[\bar{2},2]\oplus[2,\bar{2}]$-Darstellung werden auch die $[3,1]\oplus[1,3]$-Darstellung und die $SO(3)\otimes SO(3)$-Darstellung untersucht. Im Falle von $[3,1]\oplus[1,3]$ finden wir einen infrarot-stabilen Fixpunkt, der einen Phasenübergang zweiter Ordnung erlaubt und, soweit wir wissen, eine neue Universalitätsklasse definiert. Im Falle von $SO(3)\otimes SO(3)$ existiert kein infrarot-stabilen Fixpunkt, also auch kein Phasenübergang zweiter Ordnung. Vernachlässigt man die Lorentz-Indizes der Felder für Vektor- und Axial-Vektor-Mesonen im Rahmen eines vereinfachten Modells, so können wir zwischen folgenden Szenarien unterscheiden. Falls die Felder des Rho- und des a_1-Mesons als Komponenten des Ordnungsparameters angenommen werden, so können wir diese der $[3,1]\oplus[1,3]$-Darstellung zuweisen und die Existenz eines Phasenübergangs zweiter Ordnung folgern. Dieses Szenario ist jedoch wenig realistisch, da das Pion als (näherungsweises) Goldstone-Boson Teil des Ordnungsparameters sein sollte. Alternativ könnte man eines der Mesonen durch das Pion austauschen. Alle drei Mesonen gemeinsam kann man hingegen berücksichtigen, indem man sie der $SO(3)\otimes SO(3)$-Darstellung zuweist, was einen Phasenübergang erster Ordnung zur Folge hat. Diese Wahl macht schon mehr Sinn, da jene drei Mesonen eine zentrale Rolle in einigen Studien zu versteckter lokaler Symmetrie spielen. Obwohl wir mit der Vernachlässigung der Lorentz-Indizes eine starke Vereinfachung vorgenommen haben, stellen unsere Resultate einen ersten Schritt hin zu adäquateren Studien dar.
Erst vor kurzem (Ende September 2013) wurde die Existenz eines infrarot-stabilen $U(2)_A\times U(2)_V$-symmetrischen Fixpunkts durch Pelissetto und Vicari verifiziert (die zugehörige anomale Dimension ist mit $\eta\sim 0.12$ angegeben). Dieses Resultat war sehr überraschend, da für $N_f=2$ und abwesende Anomalie ein Phasenübergang erster Ordnung relativ gesichert erschien, insbesondere durch die ϵ-Entwicklung. Offensichtlich versagt letztere jedoch im Limes $\epsilon=1$, also für $D=3$ räumliche Dimensionen, da lediglich Fixpunkte gefunden werden können, die auch für kleines ϵ (also nahe $D=4$) existieren. Das von den oben genannten Autoren verwendete Resummierungsschema hingegen verzichtet auf eine herkömmliche ϵ-Entwicklung und arbeitet direkt in $D=3$. Inspiriert durch diesen wichtigen Fund führen wir eine FRG-Fixpunktstudie in lokaler Potential-Näherung und hoher Trunkierungsordnung (bis zu zehnter Ordnung in den Feldern) durch. Für die Trunkierung in sechster Ordnung finden wir zwei $U(2)_A\times U(2)_V$-symmetrische Fixpunkte, sowie einen einzigen solchen bei achter bzw. zehnter Ordnung. Die Stabilitätsanalyse besitzt jedoch leider keine Aussagekraft, da die Stabilitätsmatrix für den Gaußschen Fixpunkt marginale Eigenwerte besitzt. Wir sind überzeugt davon, dass dies nicht mehr der Fall ist, wenn man über die lokale Potential-Näherung hinausgeht und eine nichtverschwindende anomale Dimension, $\eta\neq 0$, zulässt. Untersuchungen in dieser Richtung sind im Gange. Die bisherigen Resultate verdeutlichen die Limitierungen der lokalen Potential-Näherung und der ϵ-Entwicklung, auf denen unsere Untersuchungen zur Universalitätshypothese in weiten Teilen beruhen. Im Falle einer entsprechend großen anomalen Dimension kann sich die Fixpunktstruktur entscheidend ändern und somit die Schlußfolgerung, ob ein Phasenübergang zweiter Ordnung existiert bzw. welcher Universalitätsklasse letzterer angehört (auch dann, wenn unter Vernachlässigung des Einflusses der anomalen Dimension keine marginalen Stabilitätsmatrix-Eigenwerte auftauchen). Systematische Untersuchungen der Fixpunktstruktur von Modellen mit $N\leq 8$ Ordnungsparameter-Komponenten wurden in der Literatur im Rahmen der ϵ-Entwicklung in Ein-Schleifen-Näherung

durchgeführt und im Rahmen dieser Dissertation innerhalb der lokalen Potential-Näherung. Die meisten der Vorhersagen der ϵ-Entwicklung konnten bestätigt werden, einige hingegen werden in Frage gestellt durch das Auftauchen marginaler Stabilitätsmatrix-Eigenwerte. Erstere sind zuverlässig lediglich dann, wenn η im Experiment tatsächlich hinreichend klein ist. Letztere motivieren aufbauende Untersuchungen, die mit dem Hinausgehen über die lokale Potential-Näherung bereits im Gange sind.

Einige wichtige Fragestellungen können nicht im Rahmen einer dimensional reduzierten Theorie behandelt werden, da die explizite Temperaturabhängigkeit in diesem Fall eliminiert wurde. Insbesondere ist es in diesem Fall nicht möglich, die Stärke eines Phasenübergangs erster Ordnung vorherzusagen, da diese von Observablen (Meson-Massen und die Pion-Zerfallskonstante im Vakuum) abhängen, an die man bei verschwindender Temperatur fitten muss. Dieser Umstand führt uns zu solchen FRG-Studien, in denen die Temperatur als expliziter Parameter verbleibt. Ein beträchtlicher Teil der für die vorliegende Dissertation zur Verfügung stehenden Arbeitszeit wurde darauf verwendet, eigene Implementierungen geeigneter Algorithmen zur numerischen Lösung der auftretenden partiellen Differentialgleichungen zu finden. Exemplarische Routinen (welche ausschließlich wohlbekannte Methoden nutzen) sind in einem Anhang zur Verfügung gestellt. Das Hauptziel der vorliegenden Arbeit, die Anwendung auf effektive Modelle für QCD, wird in Kapitel 7 präsentiert. Unsere (vorläufigen) FRG-Studien des linearen Sigma-Modells mit axialer Anomalie bei nichtverschwindender Temperatur erlauben verschiedene Szenarien. Sowohl einen extrem schwach ausgeprägten, als auch einen sehr deutlichen Phasenübergang erster Ordnung, ganz abhängig von der Wahl der Ultraviolett-Abschneideskala und oben genannter Parameter. Sogar ein Phasenübergang zweiter Ordnung scheint möglich für gewisse Parameterwerte. Um verlässliche Schlussfolgerungen zu ziehen, sind weitere Untersuchungen nötig und bereits im Gange. In Kapitel 7 verifizieren wir außerdem bereits bekannte numerische Resultate für das Quark-Meson-Modell, was zugleich einen guten Test der von uns verwandten Routinen darstellt. In den Anhängen A-D stellen wir verschiedene Routinen zur Verfügung, die im Rahmen der vorliegenden Dissertation benutzt wurden. Außerdem enthalten diese Anhänge Material auf das wir uns in den Hauptkapiteln beziehen.

Anhang A erklärt einige gruppentheoretische Aspekte, sowohl allgemeiner Art als auch in Bezug auf die chirale Symmetrie. Anhang B enthält zwei voll funktionsfähige *Mathematica*-Routinen, die unser Rezept zur systematischen Konstruktion polynomialer Invarianten in der Praxis verdeutlichen. Anhang C enthält ebenfalls zwei voll funktionsfähige *Mathematica*-Routinen. Diese sind Implementierungen zweier unterschiedlicher (wohlbekannter) Methoden zur Lösung typischer FRG-Flussgleichungen für eine RG-Skala-abhängige Funktion (in unserem Fall das effektive Potential) einer skalaren Feldvariablen. Die Finite-Differenzen-Methode basiert darauf, die partiellen Ableitungen nach der Feldvariablen durch geeignete Finite-Differenzen zu ersetzen. Die Taylor-Methode hingegen nutzt eine Taylor-Entwicklung der RG-Skala-abhängigen Funktion um verschiedene Feld-Gitterpunkte. Die Flussgleichungen für die Entwicklungskoeffizienten erhält man durch entsprechendes Ableiten der Flussgleichung für die Funktion nach dem Feld. Mit geeigneter Wahl der Entwicklungspunkte resultiert, wie auch im Fall der Finite-Differenzen-Methode, ein geschlossenes Gleichungssystem gewöhnlicher Differentialgleichungen in der RG-Skala, welches man mittels Runge-Kutta-Verfahren lösen kann. Anhang D stellt eine zweckdienliche *Mathematica*-Routine zur Verfügung, welche die Stabilitätsmatrix-Eigenwerte des

$O(N)$-symmetrischen Fixpunkts des $O(N)$-Modells für frei wählbares N berechnet. Es verdeutlicht zugleich am einfachstmöglichen Beispiel die Herleitung von Flussgleichungen in der lokalen Potential-Näherung.

Bibliography

[1] Mara Grahl and Dirk H. Rischke. Functional renormalization group study of the two-flavor linear sigma model in the presence of the axial anomaly. *Phys.Rev.*, D88:056014, 2013.

[2] Mara Grahl, Elina Seel, Francesco Giacosa, and Dirk H. Rischke. The O(2) model in polar coordinates at nonzero temperature. *Phys.Rev.*, D87:096014, 2013.

[3] Cern Communication Group. *LHC, the guide*. Cern Brochure, 2008.

[4] B. Friman, C. Höhne, J. Knoll, S. Leupold, J. Randrup, and R. Rapp. *The CBM Physics Book: Compressed Baryonic Matter in Laboratory Experiments*. Lecture Notes in Physics. Springer, 2011.

[5] H. Kleinert. Gauge fields in condensed matter. Vol. 1: Superflow and vortex lines. Disorder fields, phase transitions. 1989.

[6] Peter Kopietz, Lorenz Bartosch, and Florian Schuetz. *Introduction to the functional renormalization group*. Lecture Notes in Physics. Springer, Berlin, 2010.

[7] P. Tolédano and V. Dmitriev. *Reconstructive phase transitions: in crystals and quasicrystals*. World Scientific Publishing Company, Incorporated, 1996.

[8] Franz J. Wegner and Anthony Houghton. Renormalization group equation for critical phenomena. *Phys.Rev.*, A8:401–412, 1973.

[9] K.G. Wilson and John B. Kogut. The Renormalization group and the epsilon expansion. *Phys.Rept.*, 12:75–200, 1974.

[10] Christof Wetterich. Exact evolution equation for the effective potential. *Phys.Lett.*, B301:90–94, 1993.

[11] Tim R. Morris. The Exact renormalization group and approximate solutions. *Int.J.Mod.Phys.*, A9:2411–2450, 1994.

[12] Kenneth G. Wilson and Michael E. Fisher. Critical exponents in 3.99 dimensions. *Phys.Rev.Lett.*, 28:240–243, 1972.

[13] Hildegard Meyer-Ortmanns. Phase transitions in quantum chromodynamics. *Rev.Mod.Phys.*, 68:473–598, 1996.

[14] Andrea Pelissetto and Ettore Vicari. Critical phenomena and renormalization group theory. *Phys.Rept.*, 368:549–727, 2002.

[15] Yoshitaka Hatta and Takashi Ikeda. Universality, the qcd critical and tricritical point, and the quark number susceptibility. *Phys. Rev. D*, 67:014028, 2003.

[16] P.C. Hohenberg and B.I. Halperin. Theory of dynamic critical phenomena. *Rev.Mod.Phys.*, 49:435, 1977.

[17] Thomas Appelquist and Robert D. Pisarski. High-Temperature Yang-Mills Theories and Three-Dimensional Quantum Chromodynamics. *Phys.Rev.*, D23:2305, 1981.

[18] Thomas Appelquist and J. Carazzone. Infrared Singularities and Massive Fields. *Phys.Rev.*, D11:2856, 1975.

[19] S. Bornholdt, N. Tetradis, and C. Wetterich. High temperature phase transition in two scalar theories. *Phys.Rev.*, D53:4552–4569, 1996.

[20] L.D. Landau and E.M. Lifshitz. *Statistical physics, Part 1.* Vol.5 of Course of theoretical physics. Pergamon Press, 1980.

[21] J.C. Tolédano and P. Tolédano. *The Landau Theory of Phase Transitions: Application to Structural, Incommesurate, Magnetic and Liquid Crystal Systems.* World Scientific Lecture Notes in Physics. World Scientific, 1987.

[22] D.A. Lavis and G.M. Bell. *Statistical Mechanics of Lattice Systems Vol.2: Exact, Series and Renormalization Group Methods.* Springer, 1999.

[23] D. S. Ritchie and D. D. Betts. Extended universality of the ising model. *Phys. Rev. B*, 11:2559–2563, 1975.

[24] R. J. Baxter. *Exactly solved models in statistical mechanics.* Academic Press, 3rd edition, 1989.

[25] T. Sowiński, R. W. Chhajlany, O. Dutta, L. Tagliacozzo, and M. Lewenstein. Violation of the universality hypothesis in ultra-cold atomic systems. arXiv:1304.4835S. 2013.

[26] B. Sutherland. Critical Exponents of the Eight-Vertex Model in Any Dimension. *Phys.Rev.Lett.*, 32:379, 1974.

[27] R.V. Ditzian. Universality And A $3d$ Ising Model Whose Critical Exponent γ Varies Continuously With A Parameter. *Phys.Rev.Lett.*, 76:4380, 1996.

[28] Alastair D. Bruce. Structural phase transitions. II. Static critical behavior. *Advances In Physics*, 29:111–217, 1980.

[29] Robert B. Griffiths. Dependence of critical indices on a parameter. *Phys. Rev. Lett.*, 24(26):1479–1482, Jun 1970.

[30] M.N. Barber. An Introduction To The Fundamentals Of The Renormalization Group In Critical Phenomena. *Phys.Rep.*, 29:1, 1977.

[31] J.-C. Toledano, L. Michel, P. Toledano, and E. Brezin. Renormalization-group study of the fixed points and of their stability for phase transitions with four-component order parameters. *Phys.Rev.*, B31:7171, 1985.

[32] H. Kleinert and V. Schulte-Frohlinde. Critical properties of ϕ^4-theories. (World Scientific, 2001, River Edge, USA).

[33] A. Pelissetto and E. Vicari. Relevance of the axial anomaly at the finite-temperature chiral transition in QCD. arXiv:1309.5446v2 (25 Sep 2013).

[34] D. Mukamel and S. Krinsky. Physical realizations of $n \geq 4$-component vector models. i. derivation of the landau-ginzburg-wilson hamiltonians. *Phys. Rev. B*, 13:5065–5077, Jun 1976.

[35] P. Bak, S. Krinsky, and D. Mukamel. First-Order Transitions, Symmetry, and the ϵ Expansion. *Phys.Rev.Lett*, 36:52, 1976.

[36] G. Grinstein and D. Mukamel. Stable fixed points in models with many coupling constants. *J.Phys.*, A15:233, 1981.

[37] C. Rottman. Symmetry classification of continuous phase transitions in two dimensions. *Phys.Rev.*, B24:1482, 1981.

[38] J. Przystawa. Symmetry And Phase Transitions. *Physica*, A114:557, 1982.

[39] Y.M. Gufan and V.P. Sakhnenko. Features of phase transitions associated with two- and three-component order parameters. *Sov.Phys. JETP*, 36:1009, 1973.

[40] J.S. Kim, D.M. Hatch, and H.T. Stokes. Classification of continuous phase transitions and stable phases. II. Four-dimensional order parameters. *Phys.Rev.*, B33:6210, 1986.

[41] L. Michel, J.-C. Toledano, and P. Toledano. Landau free energies for $n = 4$ and the subgroups of $O(4)$. In: Symmetries and Broken Symmetries in Condensed Matter Physics: Proceedings of the Colloque Pierre Curie Held at the Ecole Supérieure de Physique Et de Chimie Industrielles de la Ville de Paris. Idset:263, 1981.

[42] D.M. Hatch, J.S. Kim, H.T. Stokes, and J.W. Felix. Renormalization-group classification of continuous structural phase transitions induced by six-component order parameters. *Phys.Rev.*, B33:6196, 1986.

[43] J.S. Kim, D.M. Hatch, and H.T. Stokes. Classification of continuous phase transitions and stable phases. I. Six-dimensional order parameters. *Phys.Rev.*, B33:1774, 1986.

[44] H.T. Stokes, J.S. Kim, and D.M. Hatch. Continuous solid-solid phase transitions driven by an eight-component order parameter: Hamiltonian densities and renormalization-group theory. *Phys.Rev.*, B35:388, 1987.

[45] E. Brezin, J.C. Le Guillou, and Jean Zinn-Justin. Discussion of critical phenomena for general n-vector models. *Phys.Rev.*, B10:892–900, 1974.

[46] L. Michel. Renormalization-group fixed points of general n-vector models. *Phys.Rev.*, B29:2777, 1984.

[47] Harold T. Stokes, Branton J. Campbell, and Ryan Cordes. Tabulation of irreducible representations of the crystallographic space groups and their superspace extensions. *Acta Crystallographica Section A*, 69(4):388–395, 2013.

[48] G. Sartori and V. Talamini. Orbit spaces of compact coregular simple lie groups with 2, 3 and 4 basic polynomial invariants: Effective tools in the analysis of invariant potentials. *J.Math.Phys.*, 39:2367, 1998.

[49] Ling-Fong Li. Group Theory of the Spontaneously Broken Gauge Symmetries. *Phys.Rev.*, D9:1723–1739, 1974.

[50] R.G. Priest and T.C. Lubensky. Critical properties of two tensor models with application to the percolation problem. *Phys.Rev.*, B13:4159–4171, 1976.

[51] L. Radzihovsky and T.C. Lubensky. Fluctuation-driven 1st-order isotropic-to-tetrahedratic phase transition. *Europhys.Lett.*, 54:206, 2001.

[52] Tomas Brauner. Spontaneous Symmetry Breaking and Nambu-Goldstone Bosons in Quantum Many-Body Systems. *Symmetry*, 2:609–657, 2010.

[53] N.V. Antonov, M.V. Kompaniets, and N.M. Lebedev. Critical behaviour of the $O(n) - \phi^4$ model with an antisymmetric tensor order parameter. *J.Phys.*, A46:405002, 2013.

[54] D. Mukamel. Notes on the Statistical Mechanics of Systems with Long-Range Interactions. arXiv:0905.1457. 2009.

[55] Roberto Franzosi, Marco Pettini, and Lionel Spinelli. Topology and phase transitions. II. Theorem on a necessary relation. *Nucl.Phys.*, B782:219–240, 2007.

[56] Siddhartha Sen. Symmetry, symmetry breaking and topology. *Symmetry*, 2:1401–1422, 2010.

[57] J. Brad Marston and Ian Affleck. Symplectic Landau-Ginzburg Fixed Points And The Localization Problem. *Nucl.Phys.*, B290:137, 1987.

[58] A. Falicov and A. Nihat Berker. Tricritical and Critical End-Point Phenomena under Random Bonds. *Phys.Rev.Lett.*, 76:4380, 1996.

[59] A. Kocić and J. Kogut. Can Sigma Models Describe Finite Temperature Chiral Transitions? *Phys.Rev.Lett.*, 74:3109, 1995.

[60] P.D. Morley and M.B. Kislinger. Relativistic Many Body Theory, Quantum Chromodynamics and Neutron Stars/Supernova. *Phys.Rept.*, 51:63, 1979.

[61] B. Povh, K. Rith, C. Scholz, and F. Zetsche. *Teilchen und Kerne: Eine Einfuhrung in Die Physikalischen Konzepte*. Springer London, Limited, 2008.

[62] John C. Collins and M.J. Perry. Superdense Matter: Neutrons Or Asymptotically Free Quarks? *Phys.Rev.Lett.*, 34:1353, 1975.

[63] Joseph I. Kapusta. Quantum Chromodynamics at High Temperature. *Nucl.Phys.*, B148:461–498, 1979.

[64] Alexander M. Polyakov. Thermal Properties of Gauge Fields and Quark Liberation. *Phys.Lett.*, B72:477–480, 1978.

[65] Agostino Butti, Andrea Pelissetto, and Ettore Vicari. On the nature of the finite-temperature transition in QCD. *JHEP*, 08:029, 2003.

[66] Mei Huang. QCD Phase Diagram at High Temperature and Density. hep-ph/1001.3216, 2010.

[67] Frank R. Brown, Frank P. Butler, Hong Chen, Norman H. Christ, Zhi-hua Dong, et al. On the existence of a phase transition for QCD with three light quarks. *Phys.Rev.Lett.*, 65:2491–2494, 1990.

[68] Edwin Laermann and Owe Philipsen. The Status of lattice QCD at finite temperature. *Ann.Rev.Nucl.Part.Sci.*, 53:163–198, 2003.

[69] M. Kaku. *Quantum field theory: a modern introduction*. Oxford University Press, Incorporated, 1993.

[70] A.A. Belavin, A.M. Polyakov, A.S. Schwartz, and Yu.S. Tyupkin. Pseudoparticle solutions of the yang-mills equations. *Physics Letters B*, 59:85 – 87, 1975.

[71] Gerard 't Hooft. How Instantons Solve the U(1) Problem. *Phys.Rept.*, 142:357–387, 1986.

[72] Michael Creutz. Anomalies and chiral symmetry in QCD. *Annals Phys.*, 324:1573–1584, 2009.

[73] David J. Gross, Robert D. Pisarski, and Laurence G. Yaffe. QCD and Instantons at Finite Temperature. *Rev.Mod.Phys.*, 53:43, 1981.

[74] C. Amsler et al. (Particle Data Group). *Physics Letters B*, 667:1, 2008.

[75] Sean Gavin, Andreas Gocksch, and Robert D. Pisarski. QCD and the chiral critical point. *Phys.Rev.*, D49:3079–3082, 1994.

[76] O. Kiriyama, M. Maruyama, and F. Takagi. Chiral phase transition at high temperature and density in the QCD - like theory. *Phys.Rev.*, D62:105008, 2000.

[77] A. Parola and L. Reatto. Liquid state theories and critical phenomena. *Adv.Phys.*, 44:211, 1995.

[78] M. Asakawa and K. Yazaki. Chiral Restoration At Finite Density And Temperature. *Nucl.Phys.*, A504:668–684, 1989.

[79] Boris A. Arbuzov, Mikhail K. Volkov, and Ivan V. Zaitsev. NJL model derived from QCD. *Int.J.Mod.Phys.*, A21:5721–5742, 2006.

[80] H. Fujii. Scalar density fluctuation at critical end point in NJL model. *Phys.Rev.*, D67:094018, 2003.

[81] M. Ohtani and H. Fujii. Sigma and hydrodynamic modes near the critical end point. *Prog.Theor.Phys.Suppl.*, 156:167–168, 2004.

[82] O. Scavenius, A. Mocsy, I.N. Mishustin, and D.H. Rischke. Chiral phase transition within effective models with constituent quarks. *Phys.Rev.*, C64:045202, 2001.

[83] Z. Fodor and S.D. Katz. Lattice determination of the critical point of QCD at finite T and mu. *JHEP*, 0203:014, 2002.

[84] Paul H. Ginsparg. First Order and Second Order Phase Transitions in Gauge Theories at Finite Temperature. *Nucl.Phys.*, B170:388, 1980.

[85] Robert D. Pisarski and Frank Wilczek. Remarks on the Chiral Phase Transition in Chromodynamics. *Phys. Rev.*, D29:338–341, 1984.

[86] J.M. Pawlowski. Exact flow equations and the U(1) problem. *Phys.Rev.*, D58:045011, 1998.

[87] Kenji Fukushima, Kazuhiko Kamikado, and Bertram Klein. Second-order and Fluctuation-induced First-order Phase Transitions with Functional Renormalization Group Equations. 2010.

[88] R. D. Pisarski and D. L. Stein. Critical Behavior Of Linear ϕ^4 models with G x G' symmetry. *Phys. Rev.*, B23:3549–3552, 1981.

[89] D. Espriu, V. Koulovassilopoulos, and A. Travesset. The phase diagram of the U(2) x U(2) sigma model. *Nucl. Phys. Proc. Suppl.*, 63:572–574, 1998.

[90] J. Berges, D. U. Jungnickel, and C. Wetterich. Two flavor chiral phase transition from nonperturbative flow equations. *Phys. Rev.*, D59:034010, 1999.

[91] Juergen Berges, Dirk-Uwe Jungnickel, and Christof Wetterich. The chiral phase transition at high baryon density from nonperturbative flow equations. *Eur. Phys. J.*, C13:323–329, 2000.

[92] J. Wirstam, J.T. Lenaghan, and K. Splittorff. Melting the diquark condensate in two color QCD: A Renormalization group analysis. *Phys.Rev.*, D67:034021, 2003.

[93] B.-J. Schaefer and M. Wagner. Three-flavor chiral phase structure in hot and dense qcd matter. *Phys.Rev.*, D79:014018, 2009.

[94] Yin Jiang and Pengfei Zhuang. Functional Renormalization for Chiral and $U_A(1)$ Symmetries at Finite Temperature. *Phys.Rev.*, D86:105016, 2012.

[95] A. Patkos. Invariant formulation of the Functional Renormalisation Group method for $U(n) \times U(n)$ symmetric matrix models. *Mod.Phys.Lett.*, A27:1250212, 2012.

[96] Mario Mitter and Bernd-Jochen Schaefer. Fluctuations and the axial anomaly with three quark flavors. arXiv:1308.3176 (14 Aug 2013).

[97] A. J. Paterson. Coleman-Weinberg Symmetry Breaking In The Chiral SU(n) x SU(n) Linear σ Model. *Nucl. Phys.*, B190:188, 1981.

[98] D. U. Jungnickel and C. Wetterich. Effective action for the chiral quark-meson model. *Phys. Rev.*, D53:5142–5175, 1996.

[99] Gerard 't Hooft. How Instantons Solve the U(1) Problem. *Phys. Rept.*, 142:357–387, 1986.

[100] K. Yagi, T. Hatsuda, and Y. Miake. Quark-gluon plasma: From big bang to little bang. *Camb. Monogr. Part. Phys. Nucl. Phys. Cosmol.*, 23:1–446, 2005.

[101] Boris Berdnikov and Krishna Rajagopal. Slowing out-of-equilibrium near the QCD critical point. *Phys.Rev.*, D61:105017, 2000.

[102] CBM collaboration. *Compressed Baryonic Matter Experiment (Technical Status Report).* GSI Darmstadt, 2005.

[103] Tamas Csorgo. Correlation Probes of a QCD Critical Point. *PoS*, HIGH-PTLHC08:027, 2008.

[104] Krishna Rajagopal and Frank Wilczek. Static and dynamic critical phenomena at a second order QCD phase transition. *Nucl.Phys.*, B399:395–425, 1993.

[105] W. Greiner and J. Reinhardt. Field quantization. 1996.

[106] Daniel F. Litim. Optimized renormalization group flows. *Phys.Rev.*, D64:105007, 2001.

[107] Holger Gies. Introduction to the functional RG and applications to gauge theories. *Lect.Notes Phys.*, 852:287–348, 2012.

[108] Holger Gies, Joerg Jaeckel, and Christof Wetterich. Towards a renormalizable standard model without fundamental Higgs scalar. *Phys.Rev.*, D69:105008, 2004.

[109] Jens Braun. Fermion Interactions and Universal Behavior in Strongly Interacting Theories. *J.Phys.*, G39:033001, 2012.

[110] Jens Braun and Holger Gies. Chiral phase boundary of QCD at finite temperature. *JHEP*, 0606:024, 2006.

[111] Denis Parganlija, Peter Kovacs, Gy"orgy Wolf, Francesco Giacosa, and Dirk H. Rischke. Eta, Eta' and eLSM. *PoS*, ConfinementX:117, 2012.

[112] Denis Parganlija, Francesco Giacosa, and Dirk H. Rischke. Vacuum Properties of Mesons in a Linear Sigma Model with Vector Mesons and Global Chiral Invariance. *Phys.Rev.*, D82:054024, 2010.

[113] Denis Parganlija, Francesco Giacosa, and Dirk H. Rischke. Structure of Scalar Mesons f(0)(600), a(0)(980), f(0)(1370) and a(0)(1450). *Acta Phys.Polon.Supp.*, 3:963–968, 2010.

[114] D. Parganlija. *Quarkonium Phenomenology in Vacuum*. PhD thesis, Goethe-University Frankfurt, 2011.

[115] U. Vogl and W. Weise. The Nambu and Jona Lasinio model: Its implications for hadrons and nuclei. *Prog.Part.Nucl.Phys.*, 27:195–272, 1991.

[116] S. Gasiorowicz and D.A. Geffen. Effective Lagrangians and field algebras with chiral symmetry. *Rev.Mod.Phys.*, 41:531–573, 1969.

[117] Stefan Struber and Dirk H. Rischke. Vector and axialvector mesons at nonzero temperature within a gauged linear sigma model. *Phys.Rev.*, D77:085004, 2008.

[118] U. Ellwanger and C. Wetterich. Evolution equations for the quark - meson transition. *Nucl.Phys.*, B423:137–170, 1994.

[119] Holger Gies and Christof Wetterich. Renormalization flow of bound states. *Phys.Rev.*, D65:065001, 2002.

[120] L. M. Haas. *On the QCD Phase Diagram with the Renormalisation Group*. Diploma thesis, University of Heidelberg, 2008.

[121] L. M. Haas. *On the phase diagram of QCD*. PhD thesis, University of Heidelberg, 2012.

[122] Jan M. Pawlowski. The QCD phase diagram: Results and challenges. *AIP Conf.Proc.*, 1343:75–80, 2011.

[123] Ming-Fan Li and Mingxing Luo. Functional renormalization flow and dynamical chiral symmetry breaking of QCD. *Phys.Rev.*, D85:085027, 2012.

[124] L. O'Raifeartaigh. *Group Structure of Gauge Theories*. Cambridge Monographs on Mathematical Physics. Cambridge University Press, 1988.

[125] R. Slansky. Group Theory for Unified Model Building. *Phys.Rept.*, 79:1–128, 1981.

[126] L. Michel (ed.). Symmetry, invariants, topology. *Phys.Rep.*, 341:3–396, 2001.

[127] Chung Ngoc Leung, S.T. Love, and S. Rao. Low-Energy Manifestations of a New Interaction Scale: Operator Analysis. *Z.Phys.*, C31:433, 1986.

[128] W. Buchmüller and D. Wyler. Effective Lagrangian Analysis of New Interactions and Flavor Conservation. *Nucl.Phys.*, B268:621, 1986.

[129] Uwe Müller. Basis invariants in nonAbelian gauge theories. arXiv:hep-th/9701124. 1996.

[130] Y. Félix, J. Oprea, and D. Tanré. *Algebraic Models in Geometry*. Oxford University Press, Oxford, 2008.

[131] R.P. Stanley. Invariants Of Finite Groups And The Applications To Combinatorics. *Bull.Am.Math.Soc.*, 1:475, 1979.

[132] B. Gruber and L. O'Raifeartaigh. S theorem and construction of the invariants of the semisimple compact lie algebras. *J.Math.Phys.*, 5:1796, 1964.

[133] Jai Sam Kim. Orbit Spaces of Low Dimensional Representations of Simple Compact Connected Lie Groups and Extrema of a Group Invariant Scalar Potential. *J.Math.Phys.*, 25:1694, 1984.

[134] Michael Forger. Invariant polynomials and Molien functions. *J.Math.Phys.*, 39:1107, 1998.

[135] J. Fuchs and C. Schweigert. *Symmetries, Lie Algebras and Representations.* Cambridge University Press, 1997.

[136] C. Truesdell and W. Noll. *The Non-Linear Field Theories of Mechanics (third edition).* Springer, 2004.

[137] J.A. Harvey. Patterns Of Symmetry Breaking In The Exceptional Groups. *Nucl.Phys.*, B163:254, 1980.

[138] A.W. Joshi. *Elements of Group Theory for Physicists.* New Age International, 1997.

[139] M. Hamermesh. *Group Theory and Its Application to Physical Problems.* Dover Books on Physics Series. Dover Publications, 1989.

[140] S. Širca and M. Horvat. *Computational Methods for Physicists: Compendium for Students.* Graduate Texts in Physics. Springer London, Limited, 2012.

[141] A. Hosaka and H. Toki. *Quarks, baryons and chiral symmetry.* World Scientific Publishing Company, Incorporated, 2001.

[142] Wolfram Research Inc. Mathematica, version 6.0. 2007.

[143] A. Aharony. Critical Behavior of Anisotropic Cubic Systems. *Phys.Rev.*, B8:4270, 1973.

[144] Mara Grahl, Mario Mitter, Dirk H. Rischke, and Bernd-Jochen Schaefer. In preparation.

[145] S. Galam. Multicritical behavior, irrelevant variables, and Landau theory. *Phys.Lett.*, A133:245, 1988.

[146] A. Aharony. Dependence of Universal Critical Behavior on Symmetry and Range of Interaction, In Phase Transitions and Critical Phenomena, Vol.6. 1976.

[147] Masayasu Harada and Chihiro Sasaki. Dropping ρ and A_1 meson masses at the chiral phase transition in the generalized hidden local symmetry. *Phys. Rev. D*, 73:036001, 2006.

[148] Yoshimasa Hidaka, Osamu Morimatsu, and Munehisa Ohtani. Renormalization group equations in a model of generalized hidden local symmetry and restoration of chiral symmetry. *Phys. Rev. D*, 73:036004, 2006.

[149] E.E. Svanes. *The Non-Perturbative Renormalization Group with Applications.* Master thesis, Norwegian University of Science and Technology, 2010.

[150] Bernd-Jochen Schaefer and Jochen Wambach. The Phase diagram of the quark meson model. *Nucl.Phys.*, A757:479–492, 2005.

[151] B. Stokić. *Renormalization Group Approach to Hot and Dense Matter*. PhD thesis, TU Darmstadt, 2008.

[152] A. Zee. *Quantum Field Theory In A Nutshell*. Princeton University Press, 2003.

[153] Nai-Chang Yeh. *Special Topics for Quantum Field Theory in Condensed Matter, Supplement 2: Continuous Groups of $O(N)$, $SO(N)$, and $SU(N)$*. Lecture notes NTU-222D5220, 2007.

[154] W. Greiner and B. Müller. *Quantum Mechanics: Symmetries*. Number Bd. 2 in Theoretical Physics. Springer-Verlag, 1994.

[155] Eef van Beveren. *Some notes on group theory*. Lecture notes. Departamento de Fisica, 1998.

[156] Jennifer A. Adams, J. Berges, S. Bornholdt, F. Freire, N. Tetradis, et al. Solving nonperturbative flow equations. *Mod.Phys.Lett.*, A10:2367–2380, 1995.

[157] W.H. Press, S.A. Teukolsky, W.T. Vetterling, and B.P. Flannery. *Numerical Recipes. The Art of Scientific Computing. Third Edition.* Cambridge University Press, 2008.